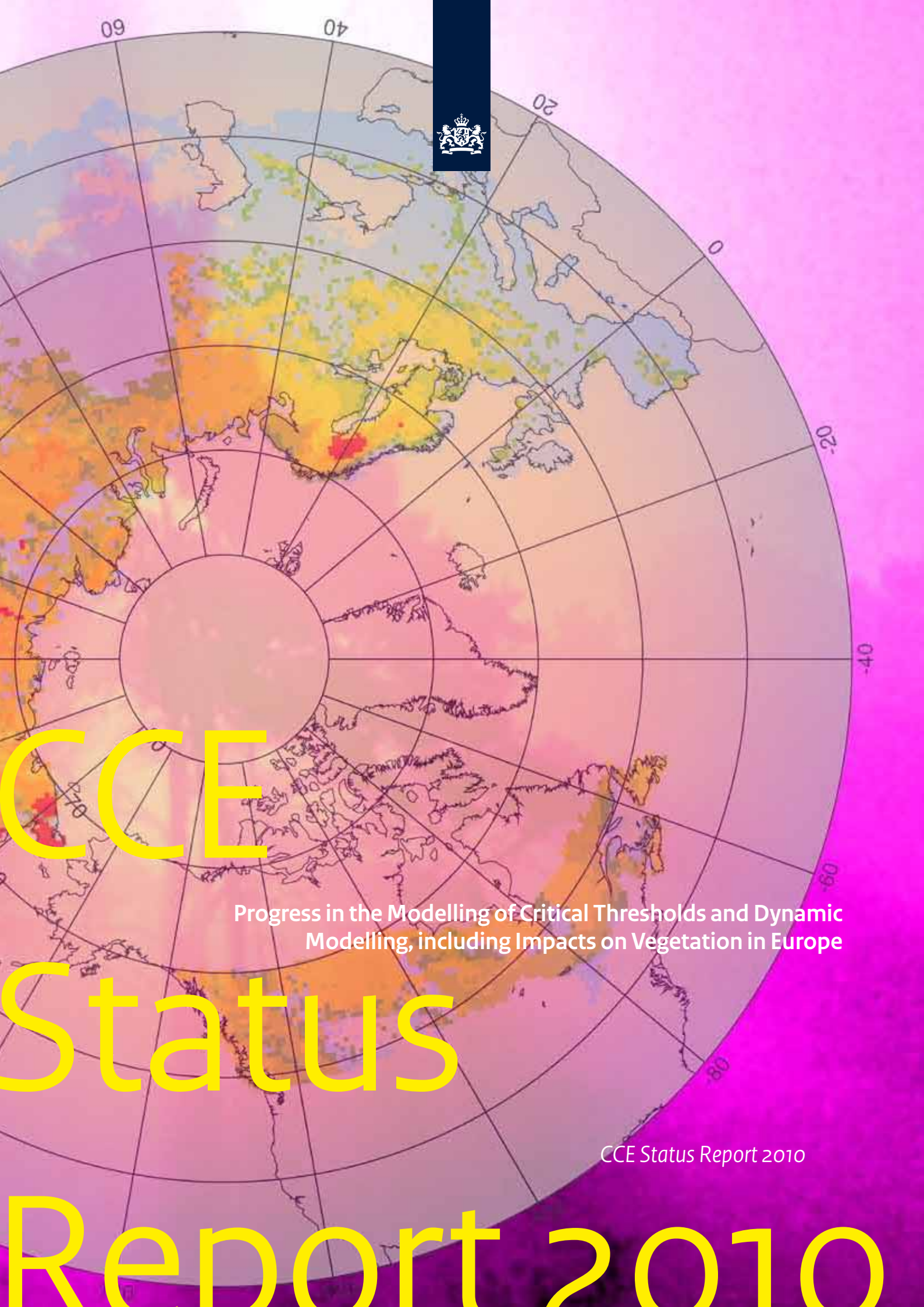

CCE Status Report 2010

Progress in the Modelling of Critical Thresholds and Dynamic Modelling, including Impacts on Vegetation in Europe

CCE Status Report 2010

Progress in the Modelling of Critical Thresholds and Dynamic Modelling, including Impacts on Vegetation in Europe

CCE Status Report 2010

J. Slootweg, M. Posch, J.-P. Hettelingh (eds)

This research has been performed by order and for the account of the Directorate for Climate and Air Quality of the Dutch Ministry of Infrastructure and the Environment; for the account of the European Commission LIFE III Programme within the framework “European Consortium for Modelling Air Pollution and Climate Strategies (EC4MACS)” and for the account of (the Working Group on Effects within) the trust fund for the effect-oriented activities under the Convention on Long-range Transboundary Air Pollution.

Report-report 680359001
ISBN 978-90-6960-249-3

Acknowledgements

The methods and results presented in this report are the product of close collaboration within the Effects Programme of the UNECE Convention on Long-range Transboundary Air Pollution, involving many institutions and individuals throughout Europe. Participants in the Effects Programme and National Focal Centres of the ICP Modelling and Mapping are acknowledged for their commitment and contributions to the work of the Coordination Centre for Effects (CCE).
In particular, the CCE acknowledges:

- The Ministry of Infrastructure and the Environment, and Mr J. Sliggers and Mr J.M. Prins in particular, for their continued support,
- The Working Group on Effects and the Task Force of the International Co-operative Programme on Modelling and Mapping of Critical Levels and Loads and Air Pollution Effects, Risks and Trends, in particular, for their collaboration and assistance,
- The EMEP Meteorological Synthesizing Centres East and West and the EMEP Centre for Integrated Assessment at the International Institute for Applied Systems Analysis, for their collaboration in the field of atmospheric dispersion and integrated assessment modelling,
- The UNECE secretariat of the Convention on Long-range Transboundary Air Pollution, for its valuable support, including the preparation of official documentations,
- The European Commission's LIFE III Programme, for co-funding the participation of the CCE in the European Consortium for Modelling Air pollution and Climate Strategies (EC4MACS),
- Gert Boer and Martin Middelburg (RIVM) for the design, lay-out and printing of this report.

Summary

This report describes the status of the impact assessment of nitrogen, sulphur and heavy metal depositions in Europe and the progress made regarding the relation between nitrogen deposition and loss of biodiversity.

Part 1 Progress CCE

The Centre for Integrated Assessment Modelling (CIAM) prepared Baseline (BL) and Maximum Feasible Reduction (MFR) scenarios with resulting nitrogen and sulphur depositions. Chapter 1 reports the impacts regarding exceedances of acidification and nitrogen critical loads, including results of the so-called "ex-post analysis". In addition, results from dynamic modelling were used to analyse the delays in responses of soil chemistry to changes in depositions.
Conclusions include that 'environmental improvements' achieved under MFR in comparison to BL are considerable for all indicators. However, it should also be noted that MFR does not lead to non-exceedance of critical loads and requirements for sustainable soil chemistry (i.e. non-violation of the chemical criterion) for all ecosystem areas in Europe.

Knowledge on nitrogen impacts has been further extended within the effects community by assessing the interaction between N and carbon (C). This is also reflected in an extension of the widely-used VSD model to include interactions between N- and C-pools and -fluxes, in a new model version, named VSD+. VSD+ has been applied by National Focal Centres (NFCs) of the International Collaborative Programme Modelling and Mapping (ICP M&M) on sites for which measurements are available. Another step forward in the assessment of impacts is the use of models that predict the abundance of species, based on abiotic conditions. NFCs were urged to familiarize themselves with one of them, the VEG model. Also data on species abundance in combination with abiotic data to feed vegetation models has been requested from NFCs for assimilation into a European database. These issues have been bundled into the 2009-2010 call for data of the CCE, of which the results are discussed in Chapter 2. In total 14 NFCs have responded to (part of) the call.

A workshop on the review and revision of empirical critical loads and dose-response relationships was held under the Convention on Long-range Transboundary Air Pollution, in Noordwijkerhout, from 23-25 June 2010. The newly agreed critical loads and recommendations on their use are summarized in Chapter 3.

Part 2 Indicators and Assessment of Change of Plant Species Diversity

This part elaborates the progress in the model development to link soil chemistry to vegetation effects. This is in line with the long-term strategy of the Convention which includes the encouragement of the assessment of air pollution effects with respect to the change of biodiversity. For this the VSD+ model has been linked to the VEG model. Results of this model combination have been evaluated and compared to results of the ForSAFE-VEG model combination. An important aspect for vegetation modelling that was missing in VSD+ is the modelling of the light that plants receive below the forest canopy. How this and the model coupling have been implemented together with results of the comparison can be found in Chapter 4.

In recent years, discussions took place on selecting an appropriate effect indicator to quantify changes in biodiversity with respect to (nitrogen) deposition. The arguments and proposed approaches are brought together in a framework which can help to focus this discussion. The reader can find this rationale and the framework in Chapter 5.

Part 3. Heavy Metals

The Protocol on Heavy Metals (HM) was signed in 1998 and entered into force in 2003. Currently the process for the revision of the Heavy Metals Protocol is underway. To support additional information to the negotiations on the proposed amendments on the HM Protocol, a research project has been commissioned by the Netherlands to TNO, EMEP MSC-E and the CCE. In this project four scenarios were compared for which emissions, costs of emission reductions, depositions and exceedances of critical loads have been calculated. The description of the emission scenarios, including the potential measures and their costs can be found in Chapter 6. The depositions that result from the emissions are reported and discussed in Chapter 7, including the estimation of re-suspension of metals from soils into the air. Chapter 8 gives the exceedances of the critical loads for the given scenarios and discusses the implications of re-suspension on the critical load concept. In chapter 9 the toxicological effects of metal concentrations in the soil solution on soil micro-organisms, plants and invertebrates are tentatively addressed using the CCE background database of a European ecosystem.

Conclusions of Part 3 include that the costs of revision of the HM protocol for UNECE Europe are estimated to be 1.3 and 11.6 billion € for Option 2 and Option 1, respectively.

The reduction of emissions is not only beneficial regarding heavy metal pollution, the measures taken in Option 2 and Option 1 may also bring about considerable reductions of $PM_{2.5}$ emissions in Europe. For the additional Hg emission reduction measures another 2.6 billion € should be added for both options.
Depositions of heavy metals are reduced, but not to the same extend as the reductions in emissions, due to the process of re-suspension. While the emission reductions are reflected in the lowering of critical load exceedances everywhere, still large parts of Europe's nature remain at risk. Uncertainty analysis requires further assessment of the state of implementation of the current protocol and of the origins of re-suspended deposition.

PART 4, finally, consists of the national reports sent by the NFCs describing their submissions to the 2009-2010 call for data, which was adopted by the Working Group on Effects at its 28th session (Geneva, 23-25 September 2009).

Key words: Acidification, air pollution effects, biodiversity, critical loads, dose–response relationships, dynamic modelling, ecosystem services, eutrophication, exceedance, LRTAP Convention, heavy metals

Rapport in het kort

Wat weten we over de relatie tussen stikstofdepositie en biodiversiteit? Dit rapport laat zien hoe de huidige kennis het Europese luchtbeleid op dit terrein kan ondersteunen. In Europa staat de biodiversiteit onder druk door onder andere een te hoge stikstofdepositie. De opstellers gaan in op de invloed van stikstofdepositie op de bodem en relevante chemische bodemprocessen. De bodem heeft invloed op de diversiteit van plantensoorten. Het kwantificeren van het verlies aan biodiversiteit zoals dat in dit rapport staat ondersteunt het Europese milieubeleid.

Voorts beschrijft het rapport de effecten van de verschillende scenario's die zijn opgesteld om emissies terug te brengen. Het gaat om het reduceren van emissies voor verzuring, vermesting en zware metalen. Deze emissies zijn destijds internationaal vastgelegd in protocollen (LRTAP Conventie Gotenburg, 1999, en Aarhus, 1998).

De scenario's zijn gemaakt door het Coordination Centre for Effects (CCE) in samenwerking met haar internationale partners. Deze scenario's geven inzicht in de effecten van luchtverontreiniging op de gezondheid en het milieu. Inzichten die zowel door de verenigde naties als de Europese commissie worden gebruikt voor haar beleid.

Contents

Part 1
Progress CCE

1 Analysis of Environmental Impacts Caused by the Baseline and Maximum Feasible Reduction Scenarios

Jean-Paul Hettelingh, Maximilian Posch, Jaap Slootweg, Anne-Christine Le Gall[a]

[a] Chair, ICP Modelling & Mapping, INERIS, France, anne-christine.le-gall@ineris.fr

1.1 Introduction

The Centre for Integrated Assessment Modelling (CIAM) of EMEP compiled a Baseline (BL) scenario based on national emission reporting (representing current legislation) and one simulating the implementation of best available technology ("Maximum Feasible Reductions", MFR) as described in Amann et al. (2010). These scenarios are used in this chapter to describe results of a country-specific analysis of the environmental effects in terms of eutrophication, acidification and change of biodiversity in 2000 and 2020.

Work was conducted in collaboration with EMEP/CIAM and EMEP/MSC-W, who provided the scenario-specific emission and deposition data, respectively. Depositions were computed with the source-receptor relationships implemented in the GAINS model, to ensure consistency between assessments of EMEP and the Working Group on Effects (WGE) for the Task Force on Integrated Assessment Modelling (TFIAM) and its reporting to the Working Group on Strategies and Review (WGSR).

Results include tables listing the percentage of a country's ecosystem area that is at risk due to the exceedance of critical loads of acidification or eutrophication, as well as the magnitudes of the Average Accumulated Exceedance (AAE, see Posch et al. 2001 for definitions) for each country. Maps are provided to illustrate the location and magnitude of these areas in each 50×50 km^2 EMEP grid cell. Tentative results are also reported of areas where the "change of biodiversity" caused by excessive N-deposition is significant, i.e. exceeds 5%. Finally, the status of recovery before, and after 2050 with respect to the BL in comparison to the MFR scenario are described. In addition, a new indicator "environmental improvement" is introduced[1] to measure scenario-specific progress in time.

[1] A "draft revised annex I on critical loads and levels", as part of the revision of the Gothenburg Protocol, includes a reference to a "Draft Guidance document V on recovery of ecosystems and environmental improvement". This guidance document lists a number of indicators to quantify "environmental improvement" to be reported by the WGE, including those by the ICP Modelling and Mapping presented here.

This new indicator has been proposed by the WGE in its preparation of a revised Annex I as part of the currently ongoing process to revise the 1999 Gothenburg Protocol to the LRTAP Convention.

1.2 The risk of eutrophication in 2000 and 2020

Figure 1.1 shows the location in Europe and magnitude of the AAE of nutrient N critical loads in 2000 and in 2020 for the BL and MFR scenarios. An improvement is visible in two ways. Firstly, the size of the European area where N critical loads are exceeded is reduced between 2000 and 2020. Secondly, the magnitude of the exceedances diminishes in this period. This is especially obvious under the MFR scenario which leads to non-exceedance in broad areas in Scandinavian and southern European countries as well as in Russia. Also countries with the highest exceedances (>1200 eq $ha^{-1}yr^{-1}$) in 2000, such as in western France, along the border-area between Germany and The Netherlands, in Denmark and in northern Italy, clearly benefit from reductions computed for 2020 under the BL and MFR scenarios.

Tables 1.1 and 1.2 express these results in numbers. The area at risk of eutrophication in Europe in 2000 and 2020 under the Baseline scenario is computed to be 52% and 38%, respectively (Table 1.1). In the EU27 these numbers are 74% and 61%, respectively. This implies an environmental improvement of 14% in Europe as a whole and 13% in the EU27. No change between 2000 and BL2020 of the area at risk can be noted in the Czech Republic, Denmark, Hungary, Liechtenstein, Lithuania, Macedonia, Slovakia and the Ukraine. However, the magnitude of the AAE in these countries does improve between 2000 and BL2020 (see Table 1.1) with 36% (CZ), 42% (DK), 38% (HU), 35% (LI), 20% (LT), 39% (SK) and 27% (UA). For Europe and the EU27 the AAE improvement is 45% and 46%, respectively.

The improvements achieved with MFR are given in Table 1.2. The area at risk in 2020 in Europe and the EU27 are computed to be 18% and 24%, respectively, implying an increase of protected area compared to 2000 of 38% and 50%. The improvement of AAE is 90% in ecosystem areas of both European regions. However, while the application of MFR leads to a significant decrease in AAE, it can be seen from Table 1.2 that MFR cannot prevent some risk of eutrophication to natural areas in any of the European countries.

Figure 1.1 Average Accumulated Exceedance (AAE) of critical loads for eutrophication in 2000 (left), and in 2020 under the BL (middle) and MFR (right) scenarios. The areas with peaks of exceedances in 2000 (red shading) are markedly decreased in 2020. However, area at risk of nutrient nitrogen (size of shades indicates relative area coverage) remain widely distributed over Europe in 2020, even under MFR.

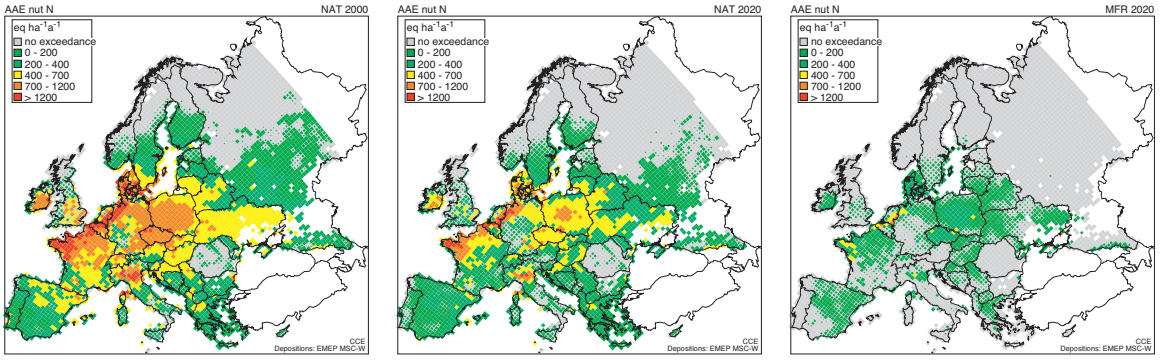

Table 1.1 Area at risk of **nutrient nitrogen** in 2000 (col. II) and in 2020 (col. IV) and the reduction of area at risk (col. VI) under the **Baseline** (BL) scenario based on national reports. Also shown is the exceedance (AAE) in 2000 and 2020, implying (col. VII) a reduction under BL of about 45% over Europe (see Figure 1.1)

		2000 National data		2020 BL National data		Environmental Improvements	
Nutrient N		Area@risk (%) II	AAE (eq $ha^{-1}a^{-1}$) III	Area@risk (%) IV	AAE (eq $ha^{-1}a^{-1}$) V	Area (%) VI (II-IV)	AAE (%) VII (III-V as %)
Albania	AL	99	285	99	240	1	16
Austria	AT	100	432	74	145	26	66
Bosnia-Herzegovina	BA	88	262	74	144	14	45
Belgium	BE	100	946	90	443	10	53
Bulgaria	BG	94	217	61	76	33	65
Belarus	BY	100	385	97	326	3	15
Switzerland	CH	99	644	95	345	4	46
Cyprus	CY	64	101	66	123	-3	-22
Czech Republic	CZ	100	1066	100	680	0	36
Germany	DE	85	642	66	324	19	50
Denmark	DK	100	1098	100	634	0	42
Estonia	EE	69	89	36	30	34	67
Spain	ES	95	327	89	184	6	44
Finland	FI	48	58	29	20	19	65
France	FR	98	581	87	284	11	51
United Kingdom	GB	26	147	18	60	8	59
Greece	GR	98	251	98	192	-1	24
Croatia	HR	100	520	99	346	1	34
Hungary	HU	100	545	100	339	0	38
Ireland	IE	89	676	81	443	8	34
Italy	IT	70	354	53	166	16	53
Liechtenstein	LI	100	635	100	411	0	35
Lithuania	LT	100	494	100	397	0	20
Luxembourg	LU	100	1109	99	690	1	38
Latvia	LV	99	273	93	163	6	40
Moldova	MD	96	312	92	263	4	16
Macedonia	MK	100	314	100	193	0	39
Netherlands	NL	93	1444	87	968	6	33
Norway	NO	22	31	10	8	12	75
Poland	PL	100	747	99	521	1	30
Portugal	PT	96	166	63	55	33	67
Romania	RO	21	24	13	9	8	64
Russia	RU	28	31	12	13	16	59
Sweden	SE	56	136	38	64	18	53
Slovenia	SI	98	365	69	88	29	76
Slovak Republic	SK	100	680	100	412	0	39
Ukraine	UA	100	506	100	367	0	27
Serbia and Montenegro	YU	96	284	84	151	13	47
EU27		74	333	61	179	13	46
All		52	185	38	102	14	45

Table 1.2[a] Area at risk of **nutrient nitrogen** in 2000 (col. II) and in 2020 (col. IV) and the reduction of area at risk (col. VI) under the **Maximum Feasible Reductions** (MFR) scenario. Also shown is the exceedance (AAE) in 2000 and 2020, implying (col. VII) a reduction under MFR of about 90 % over Europe (see Figure 1.1)

	2000 National data		2020 MFR		Environmental Improvements	
Nutrient N	Area@risk (%) II	AAE (eq $ha^{-1}a^{-1}$) III	Area@risk (%) IV	AAE (eq $ha^{-1}a^{-1}$) V	Area (%) VI (II-IV)	AAE (%) VII (III-V as %)
AL	99	285	33	27	67	91
AT	100	432	4	5	96	99
BA	88	262	26	11	63	96
BE	100	946	37	124	63	87
BG	94	217	3	2	91	99
BY	100	385	55	49	45	87
CH	99	644	30	30	69	95
CY	64	101	2	0	62	100
CZ	100	1066	99	333	1	69
DE	85	642	29	59	56	91
DK	100	1098	99	231	1	79
EE	69	89	4	1	65	99
ES	95	327	42	36	52	89
FI	48	58	2	0	47	99
FR	98	581	32	38	66	93
GB	26	147	3	3	23	98
GR	98	251	33	22	65	91
HR	100	520	43	32	57	94
HU	100	545	53	70	47	87
IE	89	676	52	76	37	89
IT	70	354	7	6	63	98
LI	100	635	99	136	1	79
LT	100	494	73	76	27	85
LU	100	1109	98	289	2	74
LV	99	273	33	17	67	94
MD	96	312	52	58	44	81
MK	100	314	51	32	49	90
NL	93	1444	74	459	19	68
NO	22	31	0	0	22	100
PL	100	747	80	154	20	79
PT	96	166	3	1	93	100
RO	21	24	0	0	21	100
RU	28	31	1	2	26	95
SE	56	136	10	6	47	96
SI	98	365	0	0	97	100
SK	100	680	86	100	14	85
UA	100	506	55	52	45	90
YU	96	284	28	24	68	92
EU27	74	333	24	35	50	90
All	52	185	14	18	38	90

[a] By ISO 3166 country codes. Country names can be found in Table 1.1

1.3 The risk of acidification in 2000 and 2020

Figure 1.2 shows the location in Europe and magnitude of the AAE of acidity critical loads in 2000 and in 2020 for the BL and MFR scenarios. An improvement is when the area at risk is compared between 2000 and 2020 under MFR. In the latter case a peak exceedance of between 700 and 1200 eq $ha^{-1}yr^{-1}$ occurs in the Netherlands and Poland, while extended areas in Europe are found to suffer from exceedances below 200 eq $ha^{-1}yr^{-1}$

Country specific details regarding the area at risk as well as exceedance magnitudes are provided in Table 1.3 (Base line) and in Table 1.4 (MFR). As shown in the last row of Table 1.3, the area at risk in Europe in 2000 (col II) and 2020 (col IV) is about 10 % and 4 % respectively.Under MFR (Table 1.4) the area at risk in 2020 is reduced to 1%. This can also be seen from the magnitudes of the AAE. For example, the AAE in the Netherlands, where we see from Figure 1.2 that lower exceedances occur in comparison to 2000, is 523 eq $ha^{-1}yr^{-1}$.

Figure 1.2 Average Accumulated Exceedance (AAE) of critical loads for acidification in 2000 (left) and 2020 under the BL (middle) and MFR (right) scenarios. Peaks of exceedances in 2000 on the Dutch-German border and in Poland (red shading) are reduced in 2020, as is the area at risk in general (size of coloured area in grid cells).

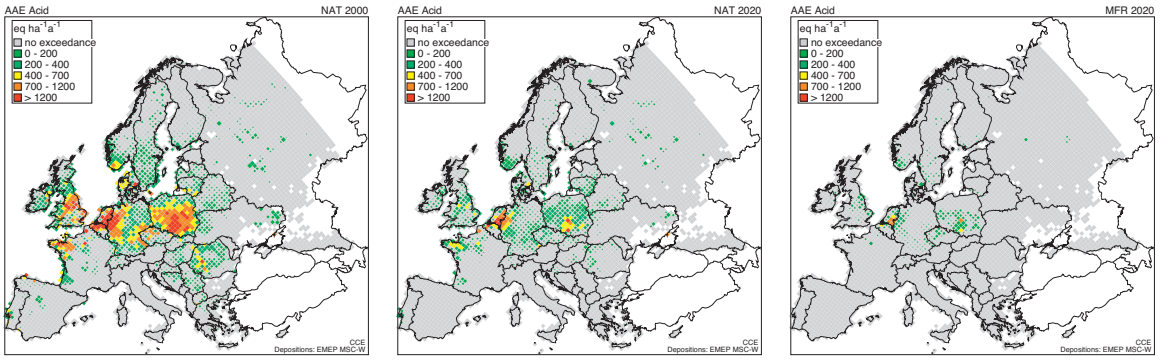

Table 1.3[a] Area at risk of **acidification** in 2000 (col. II) and in 2020 (col. IV) and the reduction of area at risk (col. VI) under the **Baseline** (BL) scenario based on National reports. Also shown is the exceedance (AAE) in 2000 and 2020, implying (col. VII) a reduction under BL of about 78 % over Europe (see Figure 1.2)

	2000 National data		2020 BL National data		Environmental Improvements	
Acidification	Area@risk (%) II	AAE (eq $ha^{-1}a^{-1}$) III	Area@risk (%) IV	AAE (eq $ha^{-1}a^{-1}$) V	Area (%) VI (II-IV)	AAE (%) VII (III-V as %)
AL	0	0	0	0	0	0
AT	1	4	0	0	1	100
BA	12	45	0	0	12	100
BE	29	511	17	123	12	76
BG	0	0	0	0	0	0
BY	18	52	8	10	10	82
CH	9	42	3	12	6	73
CY	0	0	0	0	0	0
CZ	29	288	19	82	10	71
DE	58	409	25	91	34	78
DK	50	385	15	22	34	94
EE	0	0	0	0	0	100
ES	2	16	0	0	2	99
FI	3	5	1	1	2	79
FR	12	55	4	10	9	83
GB	40	257	16	49	24	81
GR	3	14	0	0	3	98
HR	4	25	2	5	3	80
HU	23	116	6	9	18	92
IE	24	113	6	12	18	89
IT	0	0	0	0	0	0
LI	52	178	18	3	34	99
LT	34	213	30	92	4	57
LU	15	166	12	45	3	73
LV	20	42	4	5	15	88
MD	0	0	0	0	0	100
MK	10	21	0	0	10	100
NL	83	2241	76	1178	7	47
NO	16	48	8	12	9	76
PL	77	676	40	175	37	74
PT	7	46	3	7	4	85
RO	47	204	6	5	41	97
RU	1	1	1	1	0	22
SE	16	23	4	2	12	90
SI	7	38	0	0	7	100
SK	17	108	7	14	9	87
UA	6	14	1	2	5	86
YU	15	42	0	0	15	100
EU27	19	108	7	24	12	78
All	10	54	4	12	6	78

[a] By ISO 3166 country codes. Country names can be found in Table 1.1

Table 1.4[a] Area at risk of **acidification** in 2000 (col. II) and in 2020 (col. IV) and the reduction of area at risk (col. VI) under the **Maximum Feasible Reductions** (MFR) Scenario. Also shown is the exceedance (AAE) in 2000 and 2020, implying (col. VII) a reduction under MFR of about 96 % over Europe (see Figure 1.2)

	2000 National data		2020 Maximum Feasible Red.		Environmental Improvements	
Acidification	Area@risk (%)	AAE (eq $ha^{-1}a^{-1}$)	Area@risk (%)	AAE (eq $ha^{-1}a^{-1}$)	Area (% points)	AAE (%)
	II	III	IV	V	II-IV	III-V as %
AL	0	0	0	0	0	0
AT	1	4	0	0	1	100
BA	12	45	0	0	12	100
BE	29	511	6	28	23	94
BG	0	0	0	0	0	0
BY	18	52	0	0	18	100
CH	9	42	1	1	8	97
CY	0	0	0	0	0	0
CZ	29	288	9	19	20	93
DE	58	409	4	8	54	98
DK	50	385	0	0	49	100
EE	0	0	0	0	0	100
ES	2	16	0	0	2	100
FI	3	5	0	0	3	96
FR	12	55	0	0	12	100
GB	40	257	6	7	34	97
GR	3	14	0	0	3	100
HR	4	25	0	0	4	100
HU	23	116	0	0	23	100
IE	24	113	0	0	24	100
IT	0	0	0	0	0	0
LI	52	178	0	0	52	100
LT	34	213	2	1	32	100
LU	15	166	0	0	15	100
LV	20	42	0	0	20	100
MD	0	0	0	0	0	100
MK	10	21	0	0	10	100
NL	83	2241	65	523	18	77
NO	16	48	2	1	14	98
PL	77	676	13	23	64	97
PT	7	46	0	0	7	100
RO	47	204	0	0	47	100
RU	1	1	0	0	1	99
SE	16	23	2	1	15	96
SI	7	38	0	0	7	100
SK	17	108	0	0	17	100
UA	6	14	0	0	6	100
YU	15	42	0	0	15	100
EU27	19	108	2	4	17	96
All	10	54	1	2	9	96

[a] By ISO 3166 country codes. Country names can be found in Table 1.1

1.4 The risk of a significant change of biodiversity in 2000 and 2020

The analysis of the "change of biodiversity" consists of a numerical estimation of the effect of scenario-specific nitrogen deposition in 2000 and 2020 on the species richness of (i) (semi-)natural grasslands (EUNIS class E) and (ii) arctic and (sub-)alpine scrub habitats (EUNIS class F2) and on the Sorensen's similarity index of the understory vegetation of coniferous boreal woodlands (EUNIS class G3 A-C). Thus "change of biodiversity" is used as a common name for any of these indicators.

This analysis is based on dose-response curves (Bobbink 2008, Bobbink and Hettelingh, 2011) that have been applied to these three EUNIS classes in Europe (Hettelingh et al. 2008a), using the European harmonized land cover map (Slootweg et al. 2009).

It is obvious that this procedure is prone to many uncertainties. Firstly because it ignores nitrogen induced changes that may occur to other EUNIS classes for which no dose-response curves are yet available. Secondly, it assumes that available relationships between dose and response do not vary geographically, i.e. they are valid irrespective of where an area is located in Europe. Thirdly, some may consider it a tall order to assume that these dose response curves are representative for a broad regional scale, when these have been established using dose-effect information which is only available for a relatively small number of non-randomly chosen sites.

These uncertainties make it challenging to interpret *absolute magnitudes* of scenario numbers. However, the direction of the change of biodiversity, obtained by *comparison* of one scenario *relative* to another in specific target years is more robust. Not in the least because most, if not all, of the causes of model and data uncertainties do not vary between scenarios.

Keeping these considerations in mind, available dose response relationships have been applied to an important share (53%) of the European natural area, which covers 4.7 million km^2, distributed over EUNIS classes E, F2 and G3 as 26%, 1% and 25%, respectively. This share of the European natural area is denominated the "modelled natural area". However, whether the "modelled natural area" is sufficiently representative of the European natural area cannot be established with the currently available data.

Finally, care was taken to only assess the change of biodiversity if it was computed to be "significant", i.e. when the indicator changed by more than 5% relative to the value of the indicator for the 'control' area used to establish the dose-response curve. Background nitrogen deposition is assumed to be predominant in such areas. The choice of 5% as a threshold percentage for identifying a 'significant' change of biodiversity was arbitrary. It takes stock of widely applied statistical conventions regarding the analysis and representation of phenomena for which confidence levels need to be established.

Results are shown in Table 1.5 where natural areas for each country are quantified for which a change of biodiversity of more than 5% occurs in 2000 and 2020 under the BL and MFR scenarios. By comparison of the area at risk of a significant change of biodiversity in 2000 to BL2020 or MFR2020, it is possible to assess the biodiversity performance of a scenario. From Table 1.5 it can be seen that about 15% of the modelled natural area in the EU27 is at risk of significant change of biodiversity in 2000. This area is reduced to approximately 6% and 1% in 2020 under BL and MFR, implying an 'environmental improvement' of about 9 % and more than 15%, respectively.

In Europe (i.e. the EMEP domain) the modelled natural area at risk of a significant change of biodiversity in Europe in 2000, BL2020 and MFR2020 is about 9%, 4% and 0% respectively (last row). The improvement of the protection against the significant change of biodiversity under BL and MFR compared to 2000 is approximated[2] to be about 6 % (col. V) and about 9 % (col. VI) respectively.

The location of the modelled natural areas where the change of biodiversity exceeds 5% is illustrated for 2000 (Figure 1.3), and for 2020 under the baseline scenario (Figure 1.4) as well as under the Maximum Feasible Reduction (Figure 1.5). The area at risk of a significant change of biodiversity (see maps in the bottom right of Figures 1.3-1.5) turns out to evolve from covering many countries in 2000 to predominantly in the bordering area between Germany and The Netherlands in 2020 under MFR.

[2] Percentage numbers in Table 1.5 have been rounded.

Figure 1.3 The location of modelled natural areas where the change of biodiversity in 2000 is higher than or equal to 5% (red shading) or lower than 5% (grey shading) in terms of species of (semi-) natural grasslands (EUNIS class E; top left), arctic and (sub) alpine scrub habitats (EUNIS class F2; top right), on the Sorensen's similarity index of the understory vegetation of coniferous boreal woodlands (EUNIS class G3 A-C; bottom left)) or any of the three indices (bottom right).

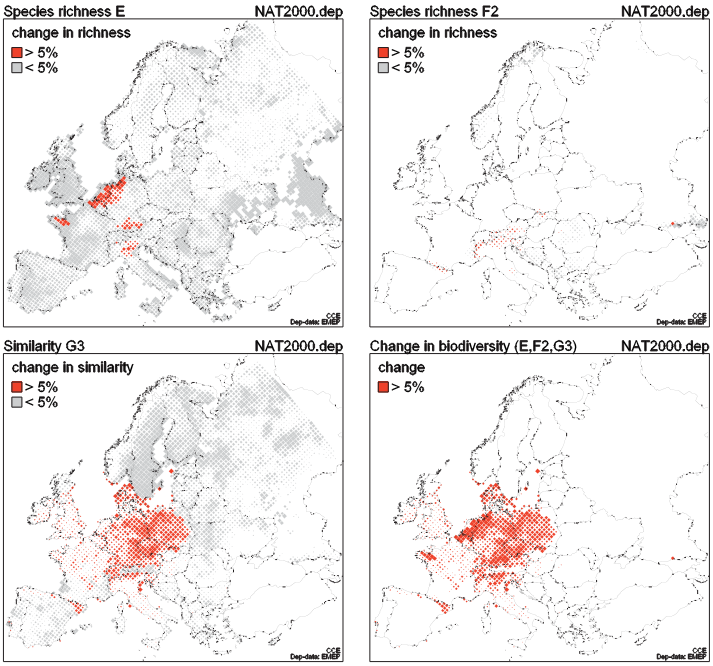

Figure 1.4 The location of modelled natural areas where the change of biodiversity following the Baseline scenario in 2020 is higher than or equal to 5% (red shading) or lower than 5% (grey shading) in terms of species of (semi-) natural grasslands (EUNIS class E; top left), arctic and (sub)alpine scrub habitats (EUNIS class F2; top right), on the Sorensen's similarity index of the understory vegetation of coniferous boreal woodlands (EUNIS class G3 A-C; bottom left)) or any of the three indices (bottom right).

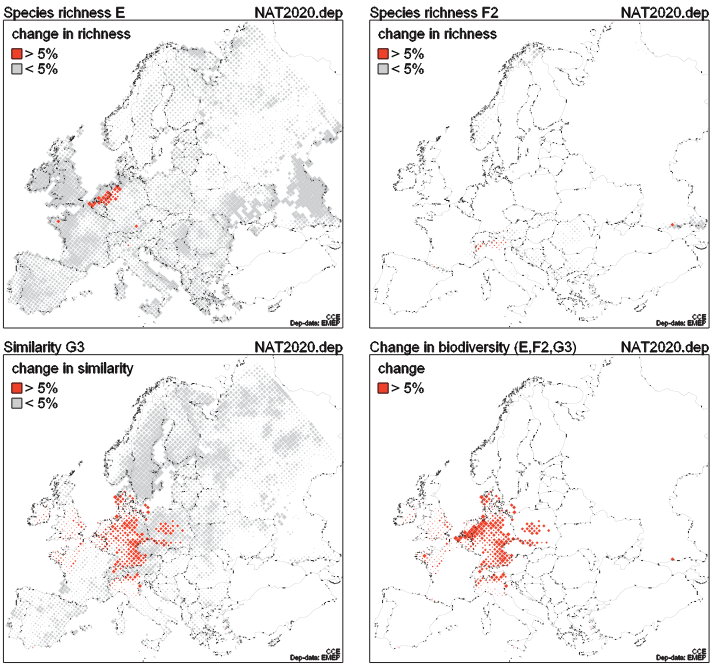

Table 1.5[a] Modelled natural area computed to be at risk of a significant* change of biodiversity in 2000 (col. II), in 2020 under the **Baseline** (col. II) and in 2020 under the **Maximum Feasible Reductions** (MFR) scenario (col. IV).

Species abundance or sp. richness	2000 National data	2020 BL	2020 MFR	Environmental improvements compared to 2000	
	Area@risk of significant* Δ biodiv. (%)	Area@risk of significant* Δ biodiv. (%)	Area@risk of significant* Δ biodiv. (%)	BL (%)	MFR (%)
	II	III	IV	V (II-III)	VI (II-IV)
AL	0	0	0	0	0
AT	32	3	0	29	32
BA	0	0	0	0	0
BE	61	42	6	19	55
BG	0	0	0	0	0
BY	0	0	0	0	0
CH	39	12	0	27	39
CY	0	0	0	0	0
CZ	68	15	0	53	68
DE	68	44	3	25	65
DK	52	37	0	15	52
EE	0	0	0	0	0
ES	5	0	0	5	5
FI	0	0	0	0	0
FR	9	1	0	7	9
GB	5	1	0	3	5
GR	0	0	0	0	0
HR	4	0	0	4	4
HU	2	0	0	2	2
IE	3	2	0	1	3
IT	31	18	0	13	31
LI	14	0	0	14	14
LT	0	0	0	0	0
LU	21	21	0	0	21
LV	0	0	0	0	0
MD	0	0	0	0	0
MK	0	0	0	0	0
NL	86	57	23	29	63
NO	1	0	0	1	1
PL	52	8	0	44	52
PT	1	0	0	1	1
RO	0	0	0	0	0
RU	0	0	0	0	0
SE	1	0	0	1	1
SI	35	0	0	35	35
SK	37	0	0	37	37
UA	0	0	0	0	0
YU	0	0	0	0	0
EU27	15	6	1	9	15
All	9	4	0	6	9

[a] By ISO 3166 country codes. Country names can be found in Table 1.1

* A change of 5% or more of species similarity in EUNIS class G3 or richness in EUNIS classes E and F2 compared to the 'control' of the dose-response curves, i.e. with predominantly background N deposition.

Figure 1.5 The location of modelled natural areas where the change of biodiversity following the Maximum Feasible Reduction (MFR) scenario in 2020 is higher than or equal to 5% (red shading) or lower than 5% (grey shading) in terms of species of (semi-) natural grasslands (EUNIS class E; top left), arctic and (sub)alpine scrub habitats (EUNIS class F2; top right), on the Sorensen's similarity index of the understory vegetation of coniferous boreal woodlands (EUNIS class G3 A-C; bottom left)) or any of the three indices (bottom right).

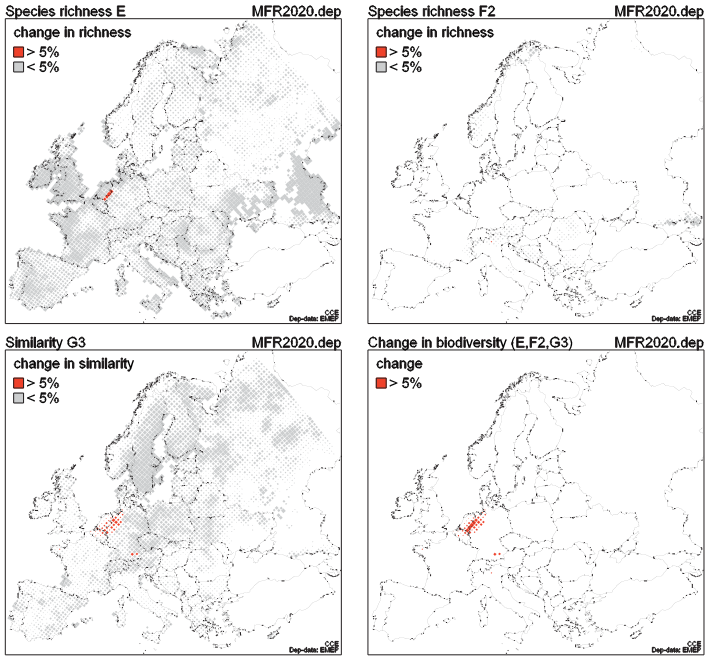

1.5 The risk of delayed effects relative to 2050

Dynamic modelling was applied to analyze the delayed response of soil chemistry to the change of eutrophying depositions in particular under BL and MFR. The result with respect to acidifying depositions is only summarized at the end of the section.

An overview of the development of dynamic modelling and its use in the analysis of effects on soil and water chemistry of air pollution in Europe can also be found in Posch et al. (2003, 2005) and Slootweg et al. (2007) and reports under other International Cooperative Programmes of the LRTAP Convention[3]. New developments – not applied in this chapter yet and also including the relationship with the dynamics of plant species diversity – can be found in Hettelingh et al. (2008b, 2009). The focus of the results described in this chapter revolves around the status of recovery before and after 2050 with respect to the BL in comparison to the MFR scenario.

Recovery of an ecosystem occurs in 2050 provided that the critical load is not exceeded and that the chemical criterion is not - or no longer - violated in 2050 *at the latest*. Processes involved in soil chemistry have it that there is a time delay between non-exceedance of the critical load and non-violation of the chemical criterion. This delay is termed Recovery Delay Time (RDT). Conversely, a delay can also occur between the time of exceedance of the critical load and the time of violation of the chemical criterion; and this is termed Damage Delay Time (DDT). Four combinations can be distinguished between (non-) exceedance and (non-)violation as illustrated in Figure 1.6.

It is obvious that nitrogen depositions under BL, since these tend to be higher than depositions under MFR everywhere in Europe, will lead to differences in RDT and DDT with respect to ecosystem areas in Europe. The results are illustrated in Table 1.6 containing the percentage of the ecosystem area in each country with an RDT and DDT before and after 2050 under both BL and MFR, relative to the area at risk[4] in 2020 under BL. The data behind the analysis are based on submissions of National Focal Centres and the CCE background database for other countries.

[3] See e.g. http://www.unece.org/env/lrtap/WorkingGroups/wge/29meeting_Rev.htm

[4] Critical loads of N were or are still exceeded under BL2020 in 2.2 million km^2 (of 3.7 million km2 total ecosystem area in Europe).

Figure 1.6 Four combinations of critical load (non-)exceedance and criterion (non-)violation

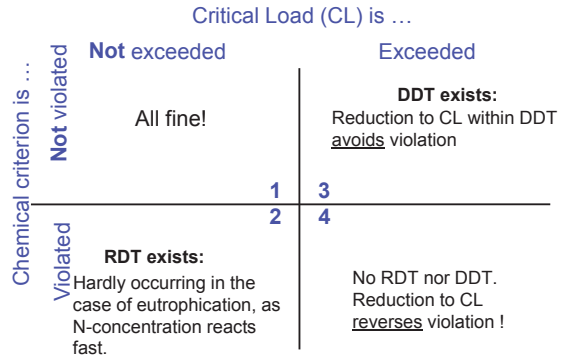

Compared to results described and tabulated earlier in this chapter, it is not straightforward to provide a statistic for "environmental improvement" for all the indicators listed in Table 1.6. The reason is that the reduction of depositions between BL and MFR leads to a move of areas at risk both *within* as well as *between* the quadrants given in Figure 1.6. This is best illustrated by inspecting the results for Europe (Table 1.6, last row). First it is noted that MFR leads to 48% of the areas moving to quadrant 1, i.e. these have become safe in comparison to the situation under BL. The percentage of unrecoverable areas moves from 86% under BL to 39% under MFR. For the remaining 61% of the areas it is seen that MFR includes 2% (RDT < 2050), 1% (RDT > 2050), 10% (DDT >2050) of shifts of areas within and between quadrants and, as already mentioned, 48% safe areas.

For acidification (not tabulated) the percentage of unrecoverable areas under BL, i.e. 47%, moves to 37% whereas 39% becomes safe. The change of area-percentages at risk of acidification between BL and MFR is also interesting for the other indicators, i.e. RDT ≤ 2050 (from 4% to 6%), RDT>2050 (from 3% to 12%), DDT>2050 (from 2 to 6%) and DDT ≤ 2050 (from 47% to 0%).

Table 1.6[a] The natural area in each country and in Europe with an RDT and DDT before or after 2050, under both BL and MFR, expressed as percentage of the area where critical loads for eutrophication are exceeded under BL in 2020.

	RDT≤ 2050		RDT> 2050		DDT>2050		DDT≤ 2050		Unrecoverable		Safe in 2020	
	BL	MFR	BL	MFR	BL	MFR	BL	MFR	BL	MFR	BL	MFR
AL	0	0	0	0	22	16	1	0	77	17	0	67
AT	0	0	0	0	12	33	1	0	87	39	0	27
BA	0	0	0	0	14	31	0	0	86	3	0	65
BE	0	0	0	0	12	9	0	0	88	78	0	13
BG	0	5	0	1	1	5	0	0	99	35	0	55
BY	0	0	0	1	2	9	0	1	98	46	0	43
CH	0	0	0	0	32	34	1	0	67	27	0	38
CY	0	23	0	7	4	0	0	0	96	3	0	67
CZ	0	0	0	0	0	1	0	0	100	99	0	0
DE	0	0	0	0	0	2	0	0	100	94	0	4
DK	0	0	0	0	0	2	0	0	100	96	0	1
EE	0	0	0	0	39	10	0	0	61	2	0	88
ES	0	5	1	6	10	10	0	0	89	36	0	43
FI	0	0	0	0	72	4	0	0	28	0	0	96
FR	0	0	0	0	4	10	0	0	96	59	0	30
GB	0	0	0	0	33	33	2	0	66	39	0	28
GR	0	2	0	1	12	9	0	0	88	25	0	62
HR	0	1	0	0	6	22	0	0	94	20	0	56
HU	0	12	0	11	0	1	0	0	100	51	0	25
IE	0	0	0	0	39	50	2	1	59	21	0	28
IT	0	2	0	1	3	8	0	0	96	41	0	48
LI	0	0	0	0	0	25	0	2	100	72	0	1
LT	0	0	0	0	4	11	0	0	96	62	0	27
LU	0	0	0	0	0	3	0	0	100	97	0	1
LV	0	0	0	0	11	20	0	0	89	15	0	65
MD	4	38	4	3	0	0	0	0	92	54	0	5
MK	0	3	0	3	0	7	0	0	100	43	0	43
NL	0	0	0	0	0	0	0	0	100	100	0	0
NO	0	0	0	0	83	5	0	0	16	0	0	95
PL	0	0	0	0	0	1	0	0	100	97	0	2
PT	0	0	1	0	64	4	1	0	35	1	0	95
RO	1	9	1	1	0	11	0	0	99	36	0	43
RU	0	2	0	2	18	5	0	0	82	20	0	71
SE	0	0	0	0	27	9	0	0	73	4	0	86
SI	0	0	0	0	19	33	1	0	80	8	0	59
SK	0	1	0	0	0	9	0	0	100	78	0	12
UA	0	3	0	1	0	4	0	0	100	51	0	40
YU	0	1	0	0	16	4	0	0	84	30	0	65
Europe	0	2	0	1	14	10	0	0	86	39	0	48

[a] By ISO 3166 country codes. Country names can be found in Table 1.1

1.6 Conclusions and recommendations

Indicators described in this chapter are suited to complete the integrated assessment of scenarios as currently conducted under the Task Force on Integrated Assessment Modelling on the basis of the GAINS model.

From the analyses described in this chapter it is clear that 'environmental improvements' achieved under MFR in comparison to BL are considerable for all the indicators. However, it should be noted that MFR does not lead to non-exceedance of critical loads and requirements for a sustainable soil chemistry (i.e. non-violation of the chemical criterion) for all ecosystem areas in Europe. This implies that technical measures alone are insufficient. The

increasing importance of the relationship between the change of climate and biodiversity under the strategy of the LRTAP Convention may be a good basis for the inclusion of scenarios that take these issues and their interactions and effects into account, including the use of indicators described in this chapter.

The calculation and mapping of critical load exceedances can also be carried out with the GAINS model. However, the analysis of the risk of a significant change of biodiversity and of delayed effects needs to be conducted outside the GAINS model, in what has been termed "expost analysis". A number of International Cooperative Programmes under the LRTAP Convention are participating in this endeavour, each with their own indicators. This chapter illustrates how, within the ICP Modelling and Mapping, a robust picture of the performance of scenarios relative to one another can be obtained.

Near future work aims to increase the compatibility between the analysis of the risk of (i) a significant change of biodiversity and of (ii) delayed effects. For this, models of the dynamics of both soil chemistry and plant species diversity have been distributed among National Focal Centres for their review and reporting at the ICP Modelling and Mapping meeting in 2011 (Bilthoven, 18-21 April). The next challenge includes the regionalized use of the combination of these dynamic models on a European scale.

References

Amann M, Bertok I, Cofala J, Heyes C, Klimont Z, Rafaj P, Schöpp W, Wagner F, 2010. Scope for further environmental improvements in 2020 beyond the baseline projections, Background paper for the 47th Session of the Working Group on Strategies and Review of the Convention on Long-range Transboundary Air Pollution, Geneva, 30 August - 3 September 2010, Centre for Integrated Assessment Modelling (CIAM), International Institute for Applied Systems Analysis (IIASA), CIAM Report 1/2010, http://gains.iiasa.ac.at/index.php/publications/policy-reports/gothenburg-protocol-revision.

Bobbink R, 2008. The derivation of dose-response relationships between N load, N exceedance and plant species richness for EUNIS habitat classes. In: Hettelingh J-P, Posch M, Slootweg J (eds) Critical load, dynamic modelling and impact assessment in Europe, CCE Status Report 2008, PBL, Bilthoven, www.rivm.nl/cce

Bobbink R and Hettelingh J-P (eds), 2011. Review and revision of empirical critical loads and dose response relationships. Proceedings of an international expert workshop, Noordwijkerhout, 23-25 Juni 2010, RIVM-report, Bilthoven, *in press*;

Hettelingh J-P, Posch M, Slootweg J, Bobbink R, Alkemade R, 2008a. Tentative dose-response function applications for integrated assessment. In: Hettelingh J-P, Posch M, Slootweg J (eds) Critical load, dynamic modelling and impact assessment in Europe, CCE Status Report 2008, PBL, Bilthoven, www.rivm.nl/cce

Hettelingh J-P, Posch M, Slootweg J, 2008b. Critical load, dynamic modelling and impact assessment in Europe, CCE Status Report 2008, Netherlands Environmental Assessment Agency Report 500090003, ISBN: 978-90-6960-211-0, 230 pp., www.pbl.nl/cce.

Hettelingh J-P, Posch M, Slootweg J, 2009. Progress in the modelling of critical thresholds, impacts to plant species diversity and ecosystem services in Europe, CCE Status Report 2009, Netherlands Environmental Assessment Agency Report 500090004/2009, ISBN: 978-90-78645-32-0, 130 pp., www.rivm.nl/cce

Posch M, Hettelingh J-P, De Smet PAM, 2001. Characterization of critical load exceedances in Europe. Water, Air and Soil Pollution 130: 1139-1144

Posch M, Hettelingh J-P, Slootweg J (eds), 2003. Manual for dynamic modelling of soil response to atmospheric deposition, RIVM, Bilthoven, www.rivm.nl/cce

Posch M, Slootweg J, Hettelingh J-P (eds), 2005. European critical loads and dynamic modelling, CCE Status Report 2005, MNP, Bilthoven, www.rivm.nl/cce

Slootweg J, Posch M, Hettelingh J-P (eds), 2007. Critical loads of nitrogen and dynamic modelling, CCE Progress Report 2007, MNP, Bilthoven, www.rivm.nl/cce

Slootweg J, Posch M, Warrink A, 2009. Status of the harmonised European land cover map. In: Hettelingh J-P, Posch M, Slootweg J (eds) Critical load, dynamic modelling and impact assessment in Europe, CCE Status Report 2009, PBL, Bilthoven, www.rivm.nl/cce

2
Result of the Call for Data

Jaap Slootweg, Maximilian Posch, Jean-Paul Hettelingh

2.1 Introduction

At its 28th session the Working Group on Effects (WGE) approved the CCE Call for Data to be issued in the autumn of 2009 to help NFCs in (a) focussing on new vegetation-relevant data requirements, in addition to soil-chemical data as in past calls, and (b) familiarizing with a more sophisticated follow-up of the VSD model. The NFCs were requested to select the quality and quantity of sites that meet current capabilities, including collaboration with the local habitat communities.

The shift in attention towards nitrogen (N) and the interaction between N and carbon (C) within the effects community led to improvements and extensions of the process description of the VSD model regarding N- and C-pools and -fluxes. The new version of the model was named VSD+. A description of the model extensions can be found in Appendix B, and a full description in Bonten et al. (2010). New model parameters were introduced for which values need to be set. NFCs have been conducting the application of VSD+ on sites for which measurements were available. Paragraph 2.2 shows the values for the new parameters used by NFCs in their applications.

The focus on vegetation-relevant data in the Call for Data was twofold. Firstly, NFCs were urged to familiarize themselves with the VEG model (Sverdrup et al. 2007). This model predicts the abundance of species based on abiotic conditions. Applying the model is roughly a three-step process: identifying the species of interest, estimate the species parameters for the model, and compare model results with the actual occurrence. Each of the three steps could result in a submission. The NFC submissions of vegetation data are described in paragraph 2.3. Secondly the CCE asked the NFCs to forward contacts for contributing to a database of plant relevés in combination with abiotic measurements. All these persons have been contacted.

Results of the Call for Data have been presented and discussed at the CCE workshop and the M&M Task Force meeting (Paris, 19-23 April 2010). Some parties updated (or submitted for the first time) their data shortly after these meetings. In total 14 countries have responded to (a part of) the call, (see Table 2.1).

Table 2.1 Country submissions for the three parts of the Call for Data

Country	VSD+ Sites	VEG application	relevés with abiotic param.
AT	8	X	X
BE	6		
BG	3		
CH	9	X	X
CZ	2		
DE	22		
FI		X	X
FR	4	X	
GB	1		X
IE	1		
NL	2	X	
NO			X
PL	5	X	
SE		X	X
Number of countries	11	7	6

A complete description of the call can be found in the *Instructions for Submitting*, reprinted in Appendix A of this report. Although this was not asked for in the call, the United Kingdom and Cyprus have submitted updates on their national critical load database.

2.2 New VSD+ parameters

In total 11 countries tested the VSD+ model and tried to apply the model to sites of their choice. These countries, together with the number of sites for which model runs have been made, are listed in Table 2.1.
In this paragraph we look at the new parameters, not present in the VSD model, i.e. we focus on the newly included processes, as described in Appendix B of this report.
In VSD+ the changes in the C and N pools are modelled more directly related to actual processes in the soil. VSD+ splits the C-pool into four compartments, each with an own C:N ratio. The ratios can be set, but users of the model are advised to use the default values (in g/g):

- easily decomposable fresh litter (CN_fe) 17
- recalcitrant fresh litter (CN_fs) 295
- microbial biomass (CN_mb) 9.5
- slowly degradable humic material (CN_hu) 9.5

Inputs of C into the system are from litterfall and root turnover. These input rates depend on growth and for litterfall also on N availability (more on this below). The C transfers between the 4 pools, quantifying mineralization, are depicted in Figure B-1 of Appendix B. A fraction of the pools (k_x) is turned over, partly to other pools (fr_x), where the remainder leaves the system as CO_2. The turnover rates k_x are calculated from maximum turnover rates $k_{x,max}$ by correcting for pH, temperature, wetness and drought. The constants $k_{x,max}$ (x=*fe,fs,mb,hm*), are input parameters to the model, but have default values that the authors of the model advise to use (see Table 2.2). Besides the UK, who modelled a grassland site, none of the NFCs deviated from the defaults.

Table 2.2 Parameters that set the maximum nitrogen flow from and into the pools.

Pool	Maximum fraction leaving the pool ($k_{max,x}$)	fraction turnover to other pool (fr_x)
easily decomposable fresh litter	8.7	0.0002
recalcitrant fresh litter	0.06	0.28
microbial biomass	1	0.95
slowly degradable humic material	0.0013	-

Nitrification and denitrification are modelled much the same way. The maximum rates of both nitrification and denitrification are by default set at 4.0 (at 10 ˚C). These defaults were applied by all NFCs.
The maximum rates of mineralization, nitrification and denitrification are reduced by pH, temperature, wetness and drought, according to equations B-7 and B-17. A tool to estimate the parameters for the reduction functions, called 'MetHyd', has been available on the CCE website since late 2009, under the menu 'Models' (see also Appendix C). Belgium and France used the default value of 1.0 for all reduction factors. The Netherlands and the United Kingdom set values to the reduction factors according to their expert judgment. All other countries applied the MetHyd model to determine values for the

factors (see Table 2.3). Note that for Switzerland rf_min, which equals rf_nit, exceeds 1, resulting in mineralization and nitrification larger than the 'maximum.' (The maximum refers to the maximum rate at a reference temperature). Reduction factors for denitrification are all smaller than 0.16, most are close to zero.

Table 2.3 Reduction factors for mineralization, nitrification and denitrification deviating from the default value.

Site name	rf_denit	rf_min	rf_nit
BGJun	0.0073	0.6395	0.6395
BGStO	0.0073	0.6395	0.6395
BGVit	0.0073	0.6395	0.6395
CH052069	0.0005	1.013	1.013
CH052078	0	1.22	1.22
CH052084	0	1.155	1.155
CH052095	0.007	1.072	1.072
CH052106	0.0145	0.387	0.387
CH052107	0.0001	1.085	1.085
CH052125	0.0001	1.129	1.129
CH052138	0.0018	1.143	1.143
CH052174	0.0545	1.104	1.104
CZLasenice	0.0216	0.6794	0.6794
CZmisecky	0	0.7044	0.7044
DEVSD_1	0.0122	0.3989	0.3989
DEVSD_10	0.0105	0.3143	0.3143
DEVSD_11	0.0108	0.2954	0.2954
DEVSD_12	0.0271	0.9027	0.9027
DEVSD_13	0.006	0.9132	0.9132
DEVSD_14	0.0049	0.8865	0.8865
DEVSD_15	0	0.9896	0.9896
DEVSD_16	0.0325	0.5948	0.5948
DEVSD_17	0	0.7008	0.7008
DEVSD_18	0	0.9995	0.9995
DEVSD_19	0.0452	0.7506	0.7506
DEVSD_2	0	0.443	0.443
DEVSD_20	0.0098	0.24	0.24
DEVSD_21	0.1593	0.7901	0.7901
DEVSD_22	0.0245	0.6176	0.6176
DEVSD_3	0.092	0.2969	0.2969
DEVSD_4	0	0.4094	0.4094
DEVSD_5	0.0129	0.4022	0.4022
DEVSD_6	0	0.4346	0.4346
DEVSD_7	0	0.4847	0.4847
DEVSD_8	0.0127	0.4073	0.4073
DEVSD_9	0	0.4329	0.4329
GBpwllpeiran	0.3	1	0.6
IE	0.0451	0.978	0.978
NL_Hardb	0	0.6	0
NL_Zeist	0	0.2	0.1

The NFCs used different approaches for the growth of the vegetation. Figure 2.1 shows several used growth functions to demonstrate how much they differ. For example, at a 20-year-old site stem growth varies from less than 1 to more than 25 kg m^{-2} yr^{-1}. Most NFCs assumed the growth to increase linear with age, only some applied a logistic function, and none put in a datafile reflecting the actual growth or clear cuts other than at the start of the simulation.

Figure 2.1 Growth functions for a selection of submitted. The grey area delineates the extent of all functions.

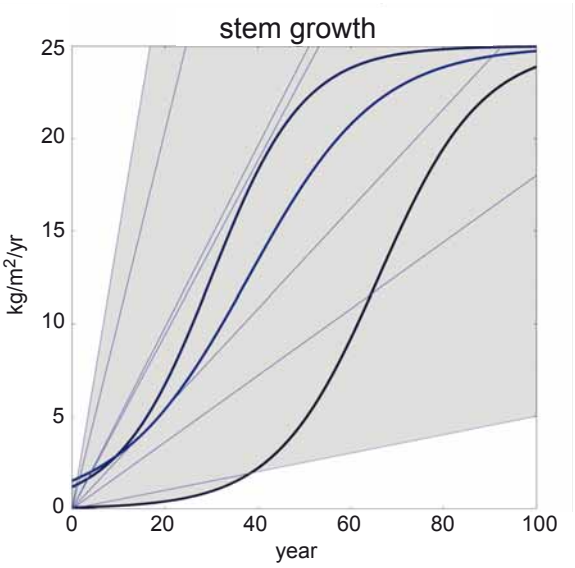

Part of running VSD, and also VSD+, is the calibration. Calibration in VSD usually targets the selectivity constants for Al-BC and for H-BC exchange, and – for the initial year of the run – the base saturation, the C pool, and C:N ratio. Table 2-4 lists the initial C:N ratio and C pool of all sites. If we assume that NFCs with multiple sites that have initial C pools with nicely rounded numbers did not calibrate, we can conclude that Belgium, Switzerland, Czech Republic, Germany, France, the Netherlands and Poland calibrated the C pool, but Austria, Bulgaria, Ireland and the UK just set it . Most sites from Switzerland have very low values for the C pool. The initial year for the simulations of their sites is far back in history, and a small deviation from equilibrium in pre-industrial times forces the model to start with such a low pool. For VSD+ the initial C:N ratio is no longer an input variable, but the N pool is used instead. But the (initial) C:N ratio is still a quantity that can be listed in the model outputs, and from the occurrence of same numbers it is clear that the ratio is considered by some countries, rather than the individual pools.

Table 2.4 Initial C:N ratio and Cpool for all submitted sites.

NFCSiteDir	CNrat_0	Cpool_0
AT1	25	9000
AT27	19	5500
AT28	21	2500
AT33	19	8000
AT40	10	3800
AT44	18	6500
AT50	13	5000
AT60	20	5200
BEChimay	23	1521
BELLNHetre	19	5520
BEupenChene	22	10503
BEupenEpicea	40	22960
BEVirtonHetre	12	963
BEWillerzeEpicea	18	6075
BGJun	18	1500
BGStO	18	1500
BGVit	18	1500
CH052069	385	93
CH052078	23	1145
CH052084	281	2
CH052095	444	4582
CH052106	38	4282
CH052107	95	4
CH052125	363	20
CH052138	301	993
CH052174	22	930
CZLasenice	36	6959
CZmisecky	30	7575
DEVSD_1	24	10568
DEVSD_10	18	7191
DEVSD_11	23	9083
DEVSD_12	10	19701
DEVSD_13	10	19969
DEVSD_14	10	19936
DEVSD_15	10	19971
DEVSD_16	10	17220
DEVSD_17	10	19902
DEVSD_18	10	19882
DEVSD_19	10	19281
DEVSD_2	24	11122
DEVSD_20	10	19793
DEVSD_21	10	19384
DEVSD_22	10	19649
DEVSD_3	23	10568
DEVSD_4	22	11122
DEVSD_5	27	10568
DEVSD_6	25	11122
DEVSD_7	20	11122
DEVSD_8	26	10568
DEVSD_9	20	11122
FRCHS41	50	9926
FREPC08	49	9208
FRPM40c	49	3320
FRSP57	34	4752
GBpwllpeiran	16	4200
IE	18	1500
NL_Hardb	12	2248
NL_Zeist	35	9897
PL_207	11	7174
PL_305	22	7174
PL_323	34	6758
PL_410	37	9536
PL_505	16	8013

For the calibration one needs observations. Table 2.5 lists possible variables that can be used for observations, together with the NFCs that used it. Not all countries submitted results of the calibration, or the variables to be calibrated.

Table 2.5 Observation variables in VSD+ and their use by the NFCs to calibrate

VSD+ observation variable	AT	BG	CH	CZ	DE	FR	NL	PL
AlBcobs			X					
bsatobs	X	X	X	X	X	X	X	X
cAlobs	X		X				X	
cBcobs	X		X				X	
cClobs	X		X				X	
cHobs			X					
cNaobs	X		X				X	
cNH4obs				X			X	
cNO3obs	X		X	X			X	
CNratobs	X	X	X	X		X	X	X
Cpoolobs	X	X	X	X		X	X	X
cSO4obs	X		X	X				
Npoolobs		X	X					
pHobs	X	X	X	X	X		X	X

2.3 Vegetation modelling with VEG

The VEG model (Sverdrup et al. 2007) has been proposed as one of the models that can assess the impact of N deposition (and other geo-chemical parameters) on plant species composition. The initial species for the model were selected on the basis of their functioning within the ecosystem. It has been tested before the Call for data in Sweden and Switzerland. From these applications a list of species with their VEG parameters was compiled and distributed with the Call. The NFCs were asked to:
1) compile a list of species relevant to the ecosystems their country chose to protect,
2) estimate the VEG parameters for these species and
3) test the VEG model for sites for which data was available.
Austria, Finland and the Netherlands responded with a list of relevant species. France, Poland, Sweden and Switzerland submitted lists of species with VEG parameters. Status and/or results of the testing of VEG runs for sites are reported in the national reports of these countries. In Annex 2.A to this chapter an overall list of species implied by one or more countries can be found. The Netherlands sent a larger list, also including animal species like butterflies, birds and reptiles, but only the vascular

plant species are included in the Annex. For Poland a few species are listed twice (hence the '2' in the list) because they submitted a list of species for the 5 sites separately with specific values for some variables.

2.4 Conclusions and recommendations

The given feedback on VSD+ has been an important result of the NFCs testing the model. Most flaws could immediately be corrected or solved. Questions asked also led to improvements of the manual and the making of instruction videos.
VSD+ Studio has successfully been used for sites in 11 countries. Most of the new parameters could be left to their default values or be determined by the MetHyd model, except for the growth functions which were very different over the submissions.
The next steps needed to use VSD+ in the work under the Convention could be to:

- include an interface to the VEG model and/or other vegetation models;
- calculate critical loads;
- scale the model from site-specific to potentially regional use.

With the inventory of national lists of species of interest with respect to vegetation modelling in relation to biodiversity we hope to contribute to an extended European version. From the perspective of policy-relevant studies into biodiversity it can be useful to execute vegetation assessments with a limited list (see Chapter 5 for a discussion on this matter). On the other hand, using a single but complete list might give valuable feedback. If VEG results show species for a site that are not present in reality, or vice versa, there can be a logical explanation, but it could also demonstrate the need for improvements to the model or species parameters. Although Latin names are used by all, some of the names of the species have been altered to match other submissions, most of them just in punctuation.

References

Bonten L, Posch M, Reinds GJ, 2010. The VSD+ Soil Acidification Model – Model Description and User Manual. Alterra and CCE, Wageningen and Bilthoven.

Sverdrup S, Belyazid S, Nihlgård B, Ericson L, 2007. Modelling change in ground vegetation response to acid and nitrogen pollution, climate change and forest management in Sweden 1500–2100 A.D. *Water, Air and Soil Pollution, Focus* 7: 163–179

Annex 2A Species of interest for one or more countries

This Annex consists of two parts. In Table 2A.1 a list is compiled of all species that two or more NFCs have either used or have indicated as being of interest to that country with respect to vegetation modelling in relation to biodiversity. Below the table are the lists of species of interest only to a single country, and therefore not listed in the table.

Table 2A.1 List of species of interest for more than one country. The number indicates the presence of sets of VEG parameters for the species (0: species listed by a country, but no VEG parameters; blank: species not listed by the country). Species names are not checked and listed as provided by NFCs.

Latin name	AT	CH	FI	FR	NL	PL	SE
Abies alba	1	1		0			
Acer campestre	0			0			
Acer platanoides	0			1			
Acer pseudoplatanus	1	1		1	0	1	
Aconitum lycoctonum	1	1	1	1			1
Actaea sp.			0				0
Adenostylus alliaria	0	0		1			
Aegopodium podagraria	0		0			0	0
Agrostis capillaris	1	1	1	1	0		1
Ajuga reptans	0			1	0	0	
Allium ursinum	1	1	1	1			1
Alnus glutinosa	1	1		1	0		
Alnus incana	1	1		1			
Alnus viridis	1	1		0			
Amelanchier ovalis	0			1			
Anemone nemorosa	1	1	1	1		0	1
Antennaria diocia			1				1
Antennaria dioica	1	1		1	0		
Anthoxanthum odoratum				1	0		
Arctostaphylos uva-ursi			0				0
Arnica montana	1	1		1	0		
Athyrium filix-femina	1	1		1	0		
Atrichum undulatum				1	0	1	
Barbilophozia			0				0
Berberis vulgaris	0			1			
Betula pendula	1	1		0	0	2	
Betula pubescens				1	0		
Blechnum spicant	1	1		1			
Brachypodium pinnatum	1	1	1	1			1
Brachypodium sylvaticum	0			1			
Brachythecium + Eurhynchium			1				1
Brachythecium rutabulum				1	0		
Briza media		0			0		
Briza media				1			
Bromus benekenii	1	1	1	1			1
Calamagrostis arundinacea	1	1	1	1		1	1
Calamagrostis epigeios			0				0
Calamagrostis epigejos					0	1	
Calamagrostis purpurea+lanceolata			0				0
Calamagrostis villosa	1	1		1			
Calluna vulgaris	1	1	1	1	0	1	1
Campanula persicifolia	0					0	
Carex caryophyllea		0			0		

Latin name	AT	CH	FI	FR	NL	PL	SE
Carex digitata	0		0	1		1	0
Carex flacca	0			1	0		
Carex globularis			0				0
Carex pendula	1	1		1			
Carex pilulifera	1	1	0	1	0	1	0
Carex sempervirens		0		1			
Carex sylvatica	0		0	1			0
Carpinus betulus	1	1		1		1	
Castanea sativa	1	1		1	0		
Cephalanthera rubra	0			0			
Ceratodon			0				0
Cetraria			0				0
Chaerophyllum hirsutum	0					0	
Cicerbita alpina	0	0	0	1			0
Circaea lutetiana	1	1		1			
circaea lutetiana			0				0
Cirsium helenioides			0				0
Cirsium palustre			0		0		0
Cladina			0				0
Cladonia			0				0
Cladonia chlorophaea					0	1	
Cladonia coniocraea					0	1	
Cladonia fimbriata					0	1	
Cladonia gracilis					0	1	
Cladonia macilenta					0	1	
Climacium dendroides			0		0		0
Convallaria majalis	0		0			0	0
Cornus mas	0			1			
Cornus sanguinea	0			0			
Cornus suecica			0		0		0
Corylus avellana	0		0	1		0	0
Crataegus laevigata	0			0			
Crataegus monogyna	0			1	0		
Crepis paludosa			0				0
Dactylis glomerata				1	0	0	
Dactylorhiza maculata				0	0		
Danthonia decumbens				1	0		
Daphne mezereum	0		0				0
Dentaria pentaphyllos	0	0		1			
Deschampsia caespitosa			1				1
Deschampsia cespitosa	1	1		1			
Deschampsia flexuosa	1	1	1	1	0	1	1
Dicranella heteromalla	1	1		1	0		
Dicranum			0				0

Latin name	AT	CH	FI	FR	NL	PL	SE
Dicranum polysetum					0	0	
Dicranum scoparium				1	0	0	
Dryopteris carthusiana					0	1	
Dryopteris dilatata					0	1	
Dryopteris dilatata coll	1	1	1	1			1
Dryopteris filix-mas	0			1	0	1	
Empetrum nigrum			1		0		1
Epilobium angustifolium	1	1		1			
Epilobium augustifolium			1				1
Epipactis helleborine				0	0		
Equisetum hyemale	1	1		1			
Equisetum sylvaticum	1	1		1			
Erica carnea	0		0				0
Erica tetralix			1	1	0		1
Euonymus europaeus				1	0		
Euphorbia amygdaloides	0			1			
Fagus sylvatica	1	1		1	0	1	
Festuca ovina					0	1	
Festuca ovina sl	1	1		1			
Festuca rubra		0		1	0		
Filipendula ulmaria			0				0
Fragaria vesca	0		0	1	0	0	0
Frangula alnus	0					0	
Fraxinus excelsior	1	1		1			
Galeopsis sp.			0				0
Galeopsis tetrahit					0	0	
Galium aparine	0				0		
Galium boreale	0					1	
Galium odoratum	1	1	1	1			1
Genista pilosa	0				0		
Genista tinctoria	0				0		
Geranium robertianum	1	1		1			
Geranium sylvaticum	1	1	1	1			1
Geum urbanum	0			1	0		
Glechoma hederacea	0				0		
Goodyera repens			0		0	0	0
Hedera helix	1	1		1			
Hepatica nobilis	1	1	1	1			1
Hieracium murorum	0			0		0	
Hieracium pilosella	0			0	0		
Holcus lanatus				1	0		
Holcus mollis				1	0		
Homalothecium lutescens				1	0		
Homogyne alpina	0			0			
hordelymus	1	1		1			
Hultbräken			0				0
Hylocomium mosses	1	1	1	1			1
Hylocomium splendens					0	1	
Hypericum perforatum	0				0		
Hypnum cupressiforme				1		0	
Hypogymnia physodes					0	0	
Ilex aquifolium	1	1		1	0		
Impatiens glandulifera	1	1		1			
Impatiens noli-tangere	1	1		1			
Impatiens parviflora	0		0			1	0

Latin name	AT	CH	FI	FR	NL	PL	SE
Juniperus communis	0			1	0	0	
Lamiastrum galeobdolon			0				0
Larix decidua	1	1		1			
Lathyrus vernus	0		0			0	0
Leontodon hispidus		0		0			
Leucobryum glaucum	1	1		1	0	1	
lichens original			1				1
Ligustrum vulgare	0				0		
Lilium martagon	0					0	
Linnaea borealis			0				0
Listera cordata			0				0
Listera ovata			0				0
Lonicera periclymenum			0	1	0		0
Lonicera xylosteum	0			0			
Lophocolea heterophylla					0	0	
Luzula campestris				1	0		
Luzula luzuloides	1	1		1		1	
Luzula pilosa	0		0	1	0	0	0
Luzula sylvatica	1	1					
Lycopodium annotinum	1	1		1			
Maianthemum bifolium	0				0	0	
Melampyrum pratense	0		0	0	0	0	0
Melandrium rubrum			0				0
Melica nutans	0					0	
Melica uniflora	0			1			
Mercurialis perennis	1	1	1	1			1
Milium effusum	1	1	1	1		0	1
Mnium mosses	1	1		1			
Moehringia trinervia					0	0	
Molinia caerulea	1	1	1	1	0		1
Moneses uniflora			0				0
Mycelis muralis	0		0			0	0
Myrica gale			1	1	0		1
Nardus stricta	1	1	1	1	0		1
Neottia nidus-avis	0			0			
Origanum vulgare	1	1		0			
Ostrya carpinifolia	1	1		1			
Oxalis acetocella			1				1
Oxalis acetosella	1	1		1	0	1	
Paris quadrifolia	0		0				0
Peltigera + Nefr			0				0
Peucedanum oreoselinum	0					0	
Picea abies	1	1		0	0	1	
Pinus cembra	1	1		0			
Pinus sylvestris	1	1		0	0	2	
Plagiomnium affine					0	0	
Plagiomnium undulatum				1	0	0	
Plantago lanceolata				1	0		
Platanthera bifolia	0				0		
Pleurozium			0				0
Pleurozium schreberi				1	0	0	
Poa nemoralis	1	1	1	1			1
Pohlia nutans					0	0	
Polygonatum multiflorum	0				0		
Polygonatum odoratum	0				0	0	

Latin name	AT	CH	FI	FR	NL	PL	SE
Polypodium vulgare				1	0		
Polystichum aculeatum	0			1			
Polytrichum commune					0	1	
Polytrichum formosum	1	1		1	0	1	
Polytrichum juniperinum				1	0		
Polytricum Commune			0				0
Populus tremula	1	1		0	0		
Potentilla erecta	0			0	0	0	
Prenanthes purpurea	0			0			
Prunus laurocerasus	1	1					
Prunus serotina	1	1		1	0	1	
Pseudoscleropodium purum				1	0	0	
Pteridium aquilinum	1	1	1	1	0	1	1
Ptilium crista-castrensis					0	0	
Quercus petraea	0			0	0	1	
Quercus pubescens	1	1		1			
Quercus robur	1	1		0	0	1	
Ranunculus ficaria	0		0				0
Ranunculus lanuginosus	1	1		0			
Rhamnus frangula				1	0		
Rhododendron ferrugineum	1	1		1			
Rhododendron tomentosum			1				1
Rhytidiadelphus loreus			0	1	0		0
Rhytidiadelphus squarrosus				1	0		
Rhytidiadelphus Triquetrus			0	1	0		0
Ribes sp.			0				0
Robina pseudoacacia	1	1					
Rosa arvensis	0			1			
Rosa canina				0	0		
Rubus arcticus			0				0
Rubus fruticosus	1	1	0	1		1	0
Rubus idaeus	1	1	1	1	0	1	1
Rubus plicatus					0	1	
Rubus saxatilis	0					0	
Rumex acetosella					0	0	
Salix aurita				1	0		
Salix caprea	1	1		0			

Latin name	AT	CH	FI	FR	NL	PL	SE
Salix cinerea				1	0		
Salix repens				1	0		
Salix sp.			1	1			1
Sambucus nigra	1	1		1	0		
Sambucus racemosa			0	1	0		0
Sanguisorba minor				0	0		
Scorzonera humilis					0	0	
Scrophularia nodosa			0			0	0
Sesleria coerulea	1	1					
Solidago virgaurea	0			0	0		
Sorbus aria	1	1		1			
Sorbus aucuparia	1	1		0	0	1	
Sphagnum mosses	1	1	1				1
Stellaria holostea	0		0	0			0
Stereocaulon			0				0
Tetraphis pellucida					0	0	
Teucrium chamaedrys	0			0			
Teucrium scorodonia				0	0		
Thuidium tamariscinum				1	0		
Tilia cordata	0			1			
Tilia platyphylla	1	1					
Trachyspermum fortunei	1	1					
Trientalis europaea			1			0	1
Trifolium repens	1	1		1	0		
Ulmus glabra	1	1		0			
Urtica dioica	0		1	1	0	1	1
Urtica doica	1	1					
Vaccinium myrtillus	1	1	1	1	0	1	1
Vaccinium uliginosum			0	1	0		0
Vaccinium vitis-idaea					0	1	
Vaccinium vitis-idea	1	1	1	1			1
Veronica chamaedrys					0	0	
Veronica officinalis					0	0	
Viburnum lantana	0			1			
Viburnum opulus	0			1			
Viola reichenbachiana	0			0		0	
Viola riviniana	0				0		

The following list of species, grouped per country, has been indicated as of interest for that country only.

Austria:

Actaea spicata, Adenostyles glabra, Alliaria petiolata, Anemone ranunculoides, Anthericum ramosum, Arum alpinum, Aruncus dioicus, Asarum europaeum, Asplenium scolopendrium, Asplenium viride, Aster bellidiastrum, Buphthalmum salicifolium, Calamagrostis varia, Campanula cochleariifolia, Campanula rapunculoides, Campanula rotundifolia agg., Campanula scheuchzeri, Campanula trachelium, Cardamine trifolia, Carduus defloratus agg., Carex alba, Carex ferruginea, Carex humilis, Carex pilosa, Carlina acaulis, Cephalanthera damasonium, Cirsium erisithales, Clematis vitalba, Corydalis cava, Cotoneaster tomentosus, Cyclamen purpurascens, Dactylis glomerata agg., Dentaria bulbifera, Dentaria enneaphyllos, Dryopteris carthusiana agg., Epilobium montanum, Epipactis atrorubens, Epipactis helleborine agg., Euonymus europaea, Euonymus verrucosa, Euphorbia cyparissias, Euphorbia dulcis, Festuca heterophylla, Galanthus nivalis, Galeobdolon luteum agg., Galium anisophyllon, Galium lucidum, Galium mollugo agg., Galium rotundifolium, Galium sylvaticum, Gentiana asclepiadea, Gymnocarpium dryopteris, Gymnocarpium robertianum, Helleborus niger, Hieracium lachenalii, Hieracium sabaudum, Hippocrepis emerus, Huperzia selago, Juniperus alpina, Knautia maxima, Lamium maculatum, Laserpitium latifolium, Leontodon incanus, Lonicera alpigena, Lotus corniculatus agg., Lunaria rediviva, Lychnis viscaria, Melampyrum sylvaticum, Melittis

melissophyllum, Moehringia muscosa, Petasites albus, Phegopteris connectilis, Phyteuma orbiculare, Phyteuma spicatum, Pimpinella sp., Pinus mugo, Polygala chamaebuxus, Polygonatum verticillatum, Polypodium vulgare agg., Primula elatior, Prunella grandiflora, Pulmonaria officinalis, Ranunculus montanus agg., Ranunculus nemorosus, Rhamnus saxatilis, Rhododendron hirsutum, Rosa pendulina, Salvia glutinosa, Sanicula europaea, Scabiosa lucida, Sedum maximum, Senecio ovatus, Sorbus chamaemespilus, Stachys sylvatica, Staphylea pinnata, Stellaria nemorum s.str., Symphytum tuberosum, Teucrium montanum, Thymus praecox, Valeriana montana, Valeriana tripteris, Veratrum album, Veronica urticifolia, Vincetoxicum hirundinaria, Viola biflora, Viola collina, Viola odorata

CH:

Anthoxantum alpinum, Gentiana acaulis, Helictotrichon versicolor, Leontodon helveticus, Ligusticum mutellina, Potentilla aurea, Ranunculus villarsii, Trifolium alpinum

FR:

Acer monspessulanum, Acer opalus, Arbutus unedo, Arctostaphyllos uva ursi, Arrhenatherum elatius, Brachypodium retusum, Bromus erectus, Buxus sempervirens, Cirsium acaule, Cistus sp., Cladonia, Coronilla emerus, Coronilla minima, Cotoneaster, Ctenidium molluscum, Daphne laureola, Erica arborea, Erica cinerea, Erica scoparia, Eurynchium striatum, Festuca altissima, Festuca heterophilla, Festuca paniculata, Fissidens taxifolius, Genista sp., Hippocrepis comosa, Hypochoeris radicata, Juniperus oxycedrus, Koeleria sp., Lamiastrum galeobdolum, Lavandula sp., Lotus corniculatus, Maespilus germanicus, Orchidaceae sp., Phyllitis scolopendrium , Pinus halepensis, Pinus nigra subsp. laricio, Pinus nigra subsp. nigra, Pinus pinaster, Pinus uncinata, Pistacia sp., Plagomnium affine, Plantago media, Populus alba, Populus nigra, Prunus avium, Prunus spinosa, Quercus coccifera, Quercus ilex, Quercus pyrenaica, Quercus suber, Rhamnus catharticus, Ribes petraea, Robinia pseudoacacia, Rosmarinus officinalis, Rubia peregrina, Salix acuminata, Salix alba, Salix sp. (non alpine), Sesleria albicans, Sorbus torminalis, Sphagnum de paris, Sphagnum nemorium , Stipa pennata, Tamniobryum alopecurum, Tamus communis, Taxus baccata, Thymus vulgaris, Tilia platyphyllos, Ulex europaeus, Ulex minor, Ulmus laevis, Ulmus minor, Vicia sepium

NL:

Achillea millefolium, Agrimonia eupatoria, Agrostis canina, Agrostis canina ag. (incl. A. vinealis), Agrostis species, Agrostis stolonifera, Agrostis vinealis, Aira caryophyllea, Aira praecox, Allium vineale, Amblystegium serpens, Amelanchier lamarckii, Ammophila arenaria, Anthriscus caucalis, Anthyllis vulneraria, Arabidopsis thaliana, Arabis hirsuta, Arabis hirsuta s. hirsuta, Arenaria serpyllifolia, Asparagus officinalis, Asparagus officinalis s. officinalis, Asparagus officinalis s. prostratus, Aulacomnium androgynum, Aulacomnium palustre, Barbilophozia attenuata, Barbilophozia barbata, Barbilophozia hatcheri, Barbilophozia kunzeana, Bazzania trilobata, Bellis perennis, Betula species, Botrychium lunaria, Brachythecium albicans, Brachythecium velutinum, Bromus hordeaceus, Bromus hordeaceus s. hordeaceus, Bromus hordeaceus s. thominei, Bryoerythrophyllum recurvirostre, Bryum argenteum, Bryum bicolor, Bryum capillare, Bryum species, Calamagrostis canescens, Calammophila baltica, Calliergonella cuspidata, Calypogeia fissa, Calypogeia muelleriana, Campanula rotundifolia, Campylopus flexuosus, Campylopus fragilis, Campylopus introflexus, Campylopus pyriformis, Capsella bursa-pastoris, Cardamine hirsuta, Carex arenaria, Carex ericetorum, Carex hirta, Carex nigra, Carex ovalis, Carex panicea, Carex trinervis, Carlina vulgaris, Centaurea jacea, Centaurium erythraea, Centaurium littorale, Cephalozia bicuspidata, Cephalozia species, Cephaloziella divaricata, Cephaloziella hampeana, Cephaloziella rubella, Cephaloziella species, Cerastium arvense, Cerastium diffusum, Cerastium fontanum, Cerastium fontanum s. vulgare, Cerastium semidecandrum, Ceratocapnos claviculata, Ceratodon purpureus, Cetraria aculeata, Cetraria islandica, Cetraria muricata, Chamerion angustifolium, Cirsium arvense, Cirsium vulgare, Cladina arbuscula, Cladina ciliata, Cladina portentosa, Cladina rangiferina, Cladonia cervicornis, Cladonia chlorophaea/pyx. ag. (incl. C. grayi, pocil.), Cladonia coccifera, Cladonia crispata, Cladonia floerkeana, Cladonia foliacea, Cladonia furcata, Cladonia glauca, Cladonia grayi, Cladonia humilis, Cladonia pocillum, Cladonia pyxidata, Cladonia ramulosa, Cladonia rangiformis, Cladonia species, Cladonia squamosa, Cladonia strepsilis, Cladonia subulata, Cladonia uncialis, Cladonia zopfii, Clinopodium acinos, Cochlearia danica, Corynephorus canescens, Crepis capillaris, Cuscuta epithymum, Cynoglossum officinale, Cytisus scoparius, Daucus carota, Dicranella cerviculata, Dicranoweisia cirrata, Dicranum majus, Dicranum montanum, Dicranum species, Dicranum spurium, Diphasiastrum tristachyum, Diplophyllum albicans, Ditrichum flexicaule, Dryopteris carthusiana + D. dilatata, Echium vulgare, Elymus species, Elytrigia atherica, Elytrigia repens, Encalypta streptocarpa, Equisetum arvense, Erigeron acer, Eriophorum

angustifolium, Erodium cicutarium, Erodium cicutarium s. dunense, Erodium lebelii, Erophila verna, Eryngium campestre, Eupatorium cannabinum, Euphrasia species, Euphrasia stricta, Eurhynchium praelongum, Eurhynchium striatum, Fallopia convolvulus, Festuca arenaria, Festuca arundinacea, Festuca filiformis, Festuca ovina ag. (incl. F. cinerea, F. filiformis), Festuca rubra ag. (incl. F. arenaria), Filago minima, Fissidens adianthoides, Galium mollugo, Galium saxatile, Galium verum, Genista anglica, Gentiana cruciata, Gentiana pneumonanthe, Gentianella campestris, Geranium molle, Gnaphalium sylvaticum, Gymnocolea inflata, Helictotrichon pubescens, Hieracium laevigatum, Hieracium umbellatum, Hieracium vulgatum ag. (incl. H. maculatum), Hippophae rhamnoides, Hydrocotyle vulgaris, Hypericum humifusum, Hypericum pulchrum, Hypnum cupressiforme s.l. species, Hypnum cupressiforme v. lacunosum, Hypnum jutlandicum, Hypnum species, Hypochaeris radicata, Inula conyzae, Jasione montana, Juncus acutiflorus, Juncus conglomeratus, Juncus effusus, Juncus squarrosus, Jungermannia species, Knautia arvensis, Koeleria macrantha, Larix kaempferi, Lathyrus linifolius, Lathyrus pratensis, Leontodon autumnalis, Leontodon saxatilis, Lepidozia reptans, Linaria vulgaris, Linum catharticum, Lophocolea bidentata, Lophozia bicrenata, Lophozia excisa, Lophozia species, Lophozia ventricosa, Lotus corniculatus ag. (incl. L. glaber), Lotus corniculatus v. corniculatus, Luzula multiflora, Luzula multiflora s. congesta, Luzula multiflora s. multiflora, Lycopodium clavatum, Lysimachia vulgaris, Mentha aquatica, Mnium hornum, Myosotis arvensis, Myosotis ramosissima, Myosotis stricta, Odontoschisma sphagni, Ononis repens s. repens, Orchis morio, Ornithopus perpusillus, Orobanche caryophyllacea, Orthodontium lineare, Palmogloea protuberans, Pastinaca sativa, Pedicularis sylvatica, Peltigera neckeri, Peltigera rufescens, Peltigera species, Phleum arenarium, Phleum pratense s. pratense, Phleum pratense s. serotinum, Picris hieracioides, Pimpinella saxifraga, Pinus nigra, Placynthiella uliginosa, Plagiomnium cuspidatum, Plagiothecium denticulatum, Plagiothecium laetum s.l. Schimp. (incl. P. curvifolium), Plagiothecium undulatum, Poa annua, Poa pratensis, Poa trivialis, Polygala serpyllifolia, Polygala vulgaris, Polytrichum longisetum, Polytrichum piliferum, Polytrichum species, Potentilla anglica, Potentilla reptans, Potentilla verna, Prunella vulgaris, Prunus padus, Pseudotaxiphyllum elegans, Pseudotsuga menziesii, Ptilidium ciliare, Pyrola rotundifolia, Quercus rubra, Racomitrium canescens, Ranunculus acris, Ranunculus bulbosus, Ranunculus repens, Rhamnus cathartica, Rhinanthus minor, Rhodobryum roseum, Rhynchostegium megapolitanum, Rhytidium rugosum, Rosa pimpinellifolia, Rosa rubiginosa, Rosa species, Rubus caesius, Rubus fruticosus ag., Rubus species, Rumex acetosa, Russula emetica, Sagina apetala, Sagina nodosa, Sagina procumbens, Salix species, Sanguisorba officinalis, Saxifraga tridactylites, Scapania compacta, Scapania nemorea, Schoenus nigricans, Sedum acre, Senecio jacobaea, Senecio jacobaea s. dunensis, Senecio jacobaea s. jacobaea, Senecio sylvaticus, Senecio vulgaris, Silene nutans, Silene otites, Solanum dulcamara, Sonchus arvensis, Spergula morisonii, Spergularia rubra, Sphagnum fimbriatum, Stellaria graminea, Stellaria media, Stellaria pallida, Succisa pratensis, Syntrichia calcicola, Syntrichia ruralis, Syntrichia ruralis v. arenicola, Taraxacum lacistophyllum, Taraxacum obliquum, Taraxacum rubicundum, Taraxacum sectie Erythrosperma, Taraxacum sectie Ruderalia, Taraxacum species, Taraxacum taeniatum, Taraxacum tortilobum, Teesdalia nudicaulis, Thymus pulegioides, Thymus serpyllum, Tortella flavovirens, Tortula subulata, Trapeliopsis granulosa, Trichophorum cespitosum, Trifolium arvense, Trifolium campestre, Trifolium dubium, Trifolium pratense, Tuberaria guttata, Valeriana officinalis, Veronica arvensis, Veronica serpyllifolia, Vicia cracca, Vicia hirsuta, Vicia lathyroides, Vicia sativa s. nigra, Viola canina, Viola curtisii, Viola hirta, Viola rupestris, Viola tricolour

PL:

Brachytecium rutabulum, Cladonia cenotea, Cladonia digitata, Cladonia ochrochlora, Cladonia rangiferina, Cladonia sp., Clinopodium vulgare, Eurhynchium angustirete, Herzogiella seligeri, Hypocenomyce scalaris, Lecanora conizaeoides, Lepraria incana, Lepraria sp., Micarea prasina, Orthodicranum montanum, Placynthiella dasaea, Placynthiella icmalea, Plagiothecium curvifolium, Plagiothecium laetum, Polytrichastrum formosum, Primula veris, Pseudevernia furfuracea, Sciuro-hypnum reflexum, Silene dioica, Stachys officinalis, Stemonitis sp., Taraxacum officinale, Vicia sylvatica

Part 2
Indicators and Assessment of Change of Plant Species Diversity

3 Results of the Review and Revision of Empirical Critical Loads

Jean-Paul Hettelingh, Roland Bobbink*, Maximilian Posch, Jaap Slootweg
* B-WARE Research Centre, Radboud University Nijmegen, the Netherlands

3.1 Preface

In this chapter the summary of the results of the "Workshop on the review and revision of empirical critical loads and dose response relationships" (Noordwijkerhout, 23-25 June 2010) are reprinted from Bobbink and Hettelingh (2011). To put the results in perspective, the revised empirical critical loads are applied on a European scale and compared to earlier data based on Achermann and Bobbink (2003).
Since the workshop, the results of the workshop (a) have been adopted[5] by the Working Group on Effects of the LRTAP Convention in September 2010, (b) will be applied by National Focal Centres in support of their response, due in March 2011, to the call for data issued by the CCE in November 2010, and (c) have been used for an effect-based analysis by the CCE of draft emission reduction scenarios proposed under the Task Force on Integrated Assessment Analysis at its November 2010 meeting, and will be used for the analysis of scenarios under development in the course of 2011.

[5] http://www.unece.org/env/documents/2010/eb/wge/ece.eb.air.wg.1.2010.14.e.pdf

3.2 Executive summary of the workshop

3.2.1 Introduction

The workshop on the review and revision of empirical critical loads and dose-response relationships was held under the Convention on Long-range Transboundary Air Pollution, in Noordwijkerhout, from 23 to 25 June 2010. The workshop was organised by the Coordination Centre for Effects (CCE) and supported by the Dutch Ministry of Housing Spatial Planning and the Environment, the Swiss Federal Office for the Environment and the German Federal Environment Agency.

The workshop was attended by 51 participants from the Czech Republic, France, Germany, Ireland, the Netherlands, Norway, Portugal, Romania, Spain, Sweden, Switzerland, the United Kingdom and the United States, and by

representatives from the International Cooperative Programme (ICP) on Waters, ICP Vegetation and ICP Modelling and Mapping. The secretariat to the Convention was not represented.

The decision to organise the workshop was adopted at the 27th session of the Working Group on Effects, following recommendations from the 18th CCE workshop (21-23 April 2008) as supported by the 24th session of the Task Force on Modelling and Mapping (24-25 April 2008) held in Berne.

The meeting was opened by Ms M.G. van Empel, Director of the Climate and Air Quality Directorate of the Dutch Ministry of Housing, Spatial Planning and the Environment (VROM).

The Status of the Convention was presented by Ms A.C. Le Gall, chair of the Task Force on Modelling and Mapping, on behalf of the Secretariat to the Convention

3.2.2. Objectives and structure of the workshop

The workshop had the following objectives:

a. Review and revise the empirical critical loads of nitrogen for natural and semi-natural ecosystems, set in 2002, at an expert workshop held in Berne from 11 to 13 November 2002, on the basis of additional scientific information available for the period from late 2002 to 2010, as presented in a new and updated background document.
b. Provide guidance on how to use site-specific, modifying factors to improve the national application of the empirical approach.
c. Review relationships between exceedances of the empirical critical loads and species diversity on a European scale, together with possible regional applications.

The following classes according to the EUropean Nature Information System (EUNIS) were addressed: marine habitats (EUNIS class A), coastal habitats (EUNIS class B), inland surface waters (EUNIS class C), mires, bogs and fens (EUNIS class D), grasslands and lands dominated by forbs, mosses or lichens (EUNIS class E), heathland, scrubland and tundra (EUNIS class F), woodland, forest and other wooded land (EUNIS class G)

An international team of scientists (R. Bobbink, S. Braun, A. Nordin, K. Schütz, J. Strengbom, M. Weijters, H. Tomassen) prepared the background documentation for each EUNIS class. This documentation was reviewed by B. Achermann, M. Ashmore, M. Fenn, J-P. Hettelingh, M. Jenssen, S. Power, J.G.M. Roelofs, G. Schütze, and S. Woodin.

Deliberations on the background documentation, empirical critical loads, modifying factors and further work were structured in three Working Groups[6], the tasks of which were outlined in guidelines designed by R. Bobbink and J-P Hettelingh:

I. Working Group on marine habitats, coastal habitats, inland surface waters and grassland habitats (chair: J. Roelofs; Rapporteur: M. Ashmore)
II. Working Group on mire, bog and fen habitats and heathland, scrub and tundra habitats (chair: S. Woodin; Rapporteur : S. Power)
III. Working Group on forest and woodland habitats (chair: J. Strengbom and M. Jenssen; Rapporteur: M. Fenn)

The working groups exchanged their progress in short plenary sessions. Results, conclusions and recommendations were discussed and summarised in a final plenary session chaired by J-P Hettelingh.

3.2.3 Conclusions

Statistically and biologically significant outcomes of field addition experiments and mesocosm studies were the basis for the assessment of empirical N critical loads. Only studies which have independent N treatments and realistic N loads and durations (below 100 kg N ha^{-1} yr^{-1}; more than 1 yr) were used for the updating and refinement of critical load values. In cases where no appropriate N-addition studies were available, gradient and retrospective studies were given a higher weight.

Studies with higher N additions or shorter experimental periods were only interpreted with respect to the understanding of effects mechanisms, possible N limitation or sensitivity of the system. The methods used in these studies were carefully scrutinised to identify factors related to the experimental design or data analysis, which may constrain their use in assessing critical loads. This includes evaluation of the precision of the estimated values of background deposition at the experimental site.

Empirical critical loads for levels 2 and 3 of the EUNIS classification were agreed on for a range of deposition values for all EUNIS classes, including forest and woodland habitats (EUNIS class G). New results regarding nitrogen effects in surface waters could be included on the basis of activities presented by the ICP Waters. Novel findings for some Mediterranean species could be adopted as well. The reliability of empirical critical loads was qualitatively established, distinguishing between 'reliable', 'quite reliable' and 'expert judgement' symbolised by ##, # and (#), respectively.

[6] Reports of the working groups are included in Bobbink and Hettelingh (2011)

Empirical critical loads for nitrogen resulting from the reviewing and revising procedure were agreed by consensus at the workshop, as summarised in Table 3.1. Table 3.1 also includes the range and reliability of the empirical critical loads established in 2002, for comparison.

Additional qualitative information, in comparison to recommendations provided in 2002, on how to interpret the agreed ranges of critical loads in specific situations for an ecosystem was assigned to a number of modifying factors. However, short of agreement on how to quantify modifying factors for assessments on broad regional scales, consensus was reached to use the minimum value of the ranges of empirical critical loads in every EUNIS class to compare their exceedances under different air pollution abatement scenarios.

To assess effects of exceedances on broad regional scales, it was agreed that specific relationships between the nitrogen load and relevant indicators (see Chapter 10 in Bobbink and Hettelingh, 2011) could be considered, provided that results would only be presented to compare the environmental risk of scenarios in relative terms.

3.2.4. Recommendations

More well-designed experiments with a wide range of N additions at sites with low background deposition are still urgently needed for several (possible) sensitive EUNIS classes or in regions with many unstudied ecosystems, if any more significant progress is to be made in defining and improving empirical critical loads in the coming years.

An increasing number of gradient (survey) studies with respect to atmospheric N deposition have been reported or recently initiated. More rigorous guidelines should be identified for evaluation of these studies, covering the estimation of deposition rates, the quantification of confounding factors and the application of methods for statistical analysis. It is recommended to organise a separate expert workshop on this topic.

Table 3.1 Overview of empirical critical loads of nitrogen deposition (kg N ha^{-1} yr^{-1}) to natural and semi-natural ecosystems (column 1), classified according to EUNIS (column 2), as originally established in Achermann and Bobbink, 2003 (column 3), and as revised in 2010 (column 4).The reliability is qualitatively indicated by ## reliable; # quite reliable and (#) expert judgement (column 5). Column 6 provides a selection of effects that can occur when critical loads are exceeded. Finally, changes with respect to 2003 values are indicated in bold.

Ecosystem type	EUNIS code	2003 kg N ha^{-1} yr^{-1} and reliability	2010 kg N ha^{-1} yr^{-1}	2010 Reliability	Indication of exceedance
Marine habitats (A)					
Mid-upper salt marshes	**A2.53**		**20-30**	(#)	Increase in dominance of graminoids
Pioneer salt marshes and low-mid salt marshes	A2.54 and A2.55	30-40 (#)	**20-30**	(#)	Increase in late-successional species, increase in productivity
Coastal habitats (B)					
Shifting coastal dunes	B1.3	10-20 (#)	10-20	(#)	Biomass increase, increased N leaching
Coastal stable dune grasslands (grey dunes)	B1.4 [a]	10-20 #	**8-15**	#	Increase in tall graminoids, decrease in prostrate plants, increased N leaching, soil acidification, loss of typical lichen species
Coastal dune heaths	B1.5	10-20 (#)	10-20	(#)	Increase in plant production, increased N leaching, accelerated succession
Moist to wet dune slacks	B1.8 [b]	10-25 (#)	**10-20**	(#)	Increased biomass tall graminoids
Inland surface waters (C)[m]					
Soft-water lakes (permanent oligotrophic waters)	C1.1 [c]	5-10 ##	**3-10**	##	Change in the species composition of macrophyte communities, increased algal productivity and a shift in nutrient limitation of phytoplankton from N to P
Dune slack pools (permanent oligotrophic waters)	C1.16	10-20 (#)	10-20	(#)	Increased biomass and rate of succession
Permanent dystrophic lakes, ponds and pools	**C1.4** [d]		**3-10**	(#)	Increased algal productivity and a shift in nutrient limitation of phytoplankton from N to P
Mires, bogs and fens (D)					
Raised and blanket bogs	D1 [e]	5-10 ##	5-10	##	Increase in vascular plants, altered growth and species composition of bryophytes, increased N in peat and peat water
Valley mires, poor fens and transition mires	D2 [f]	10-20 #	**10-15**	#	Increase in sedges and vascular plants, negative effects on bryophytes
Rich fens	D4.1 [g]	15-35 (#)	**15-30**	(#)	Increase in tall graminoids, decrease in bryophytes
Montane rich fens	D4.2 [g]	15-25 (#)	15-25	(#)	Increase in vascular plants, decrease in bryophytes
Grasslands and lands dominated by forbs, mosses or lichens (E)					
Sub-Atlantic semi-dry calcareous grasslands	E1.26	15-25 ##	15-25	##	Increase in tall grasses, decline in diversity, increased mineralisation, N leaching, surface acidification
Mediterranean xeric grasslands	**E1.3**		**15-25**	(#)	Increased production, dominance by graminoids
Non-Mediterranean dry acidic and neutral closed grasslands	E1.7 [b]	10-20 #	**10-15**	##	Increase in graminoids, decline in typical species, decrease in total species richness
Inland dune pioneer grasslands	E1.94 [b]	10-20 (#)	**8-15**	(#)	Decrease in lichens, increase in biomass

Ecosystem type	EUNIS code	2003 kg N ha^{-1} yr^{-1} and reliability	2010 kg N ha^{-1} yr^{-1}	2010 Reliability	Indication of exceedance
Inland dune siliceous grasslands	E1.95 [b]	10-20 (#)	**8-15**	(#)	Decrease in lichens, increase in biomass, increased succession
Low- and medium-altitude hay meadows	E2.2	20-30 (#)	20-30	(#)	Increase in tall grasses, decrease in diversity
Mountain hay meadows	E2.3	10-20 (#)	10-20	(#)	Increase in nitrophilous graminoids, changes in diversity
Moist and wet oligotrophic grasslands					
• *Molinia caerulea* meadows	E3.51	15-25 (#)	15-25	(#)	Increase in tall graminoids, decreased diversity, decrease in bryophytes
• Heath (*Juncus*) meadows and humid (*Nardus stricta*) swards	E3.52	10-20 #	10-20	#	Increase in tall graminoids, decreased diversity, decrease in bryophytes
Moss- and lichen-dominated mountain summits	E4.2	5-10 #	5-10	#	Effects on bryophytes or lichens
Alpine and subalpine acidic grasslands	**E4.3**		**5-10**	#	Changes in species composition; increase in plant production
Alpine and subalpine calcareous grasslands	**E4.4**		**5-10**	#	Changes in species composition; increase in plant production
Heathland, scrub and tundra (F)					
Tundra	F1	5-10 #	3-5	#	Changes in biomass, physiological effects, changes in species composition in bryophyte layer, decrease in lichens
Arctic, alpine and subalpine scrub habitats	F2	5-15 (#)	5-15	#	Decline in lichens, bryophytes and evergreen shrubs
Northern wet heath	F4.11				
• 'U' *Calluna*-dominated wet heath (Upland moorland)	F4.11 [e,h]	10-20 (#)	**10-20**	#	Decreased heather dominance, decline in lichens and mosses, increased N leaching
• 'L' *Erica tetralix*-dominated wet heath (Lowland)	F4.11 [e,h]	10-25 (#)	10-20	(#)	Transition from heather to grass dominance
Dry heaths	F4.2 [e; h]	10-20 ##	10-20	##	Transition from heather to grass dominance, decline in lichens, changes in plant biochemistry, increased sensitivity to abiotic stress
Mediterranean scrub	F5		20-30	(#)	Change in plant species richness and community composition
Woodland, forest and other wooded land (G)					
Fagus woodland	**G1.6**		**10-20**	(#)	Changes in ground vegetation and mycorrhiza, nutrient imbalance, changes in soil fauna
Acidophilous *Quercus*-dominated woodland	**G1.8**		**10-15**	(#)	Decrease in mycorrhiza, loss of epiphytic lichens and bryophytes, changes in ground vegetation

Ecosystem type	EUNIS code	2003 kg N ha^{-1} yr^{-1} and reliability	2010 kg N ha^{-1} yr^{-1}	2010 Reliability	Indication of exceedance
Mesotrophic and eutrophic *Quercus* woodland	**G1.A**		**15-20**	(#)	Changes in ground vegetation
Mediterranean evergreen (*Quercus*) woodland	**G2.1**		**10-20**[n]	(#)	Changes in epiphytic lichens
Abies and *Picea* woodland	**G3.1**		**10-15**	(#)	Decreased biomass of fine roots, nutrient imbalance, decrease in mycorrhiza, changed soil fauna
Pinus sylvestris woodland south of the taiga	**G3.4**		**5-15**	#	Changes in ground vegetation and mycorrhiza, nutrient imbalances, increased N_2O and NO emissions
Pinus nigra woodland	**G3.5**		**15**	(#)	Ammonium accumulation
Mediterranean *Pinus* woodland	**G3.7**		**3-15**	(#)	Reduction in fine-root biomass, shift in lichen community
Spruce taiga woodland	G3.A [i]	10-20 #	**5-10**	##	Changes in ground vegetation, decrease in mycorrhiza, increase in free-living algae
Pine taiga woodland	G3.B [i]	10-20 #	**5-10**	#	Changes in ground vegetation and in mycorrhiza, increase occurrence of free-living algae
Mixed taiga woodland with *Betula*	**G4.2**		**5-8**	(#)	Increased algal cover
Mixed *Abies-Picea Fagus* woodland	**G4.6** [j]		**10-20**	(#)	
Overall					
Broadleaved deciduous woodland	G1 [k,l]	10-20 #	**10-20**	##	Changes in soil processes, nutrient imbalance, altered composition mycorrhiza and ground vegetation
Coniferous woodland	G3 [k,l]	10-20 #	**5-15**	##	Changes in soil processes, nutrient imbalance, altered composition mycorrhiza and ground vegetation

[a] For acidic dunes, use the 8 to 10 kg N ha^{-1} yr^{-1} range, for calcareous dunes use the 10 to 15 kg ha^{-1} yr^{-1} range.
[b] Use the lower end of the range in combination with low base availability, and the higher end in combination with high base availability.
[c] This critical load should only be applied to oligotrophic waters with low alkalinity with no significant agricultural or other human inputs. Use the lower end of the range for boreal and alpine lakes, use the higher end of the range for Atlantic soft waters.
[d] This critical load should only be applied to waters with low alkalinity with no significant agricultural or other direct human inputs. Use the lower end of the range for boreal and alpine dystrophic lakes.
[e] Use the high end of the range for habitats with high levels of precipitation and the low end of the range for those with low precipitation; use the low end of the range for systems with a low water table, and the high end of the range for those with a high water table. Note that water tables can be modified by management.
[f] For EUNIS category D2.1 (valley mires): use the lower end of the range (#).
[g] For high-latitude systems: use the lower end of the range.
[h] Use the high end of the range for areas where sod cutting has been practiced; use the lower end of the range for areas under low intensity management.
[i] In 2003 presented as overall value for boreal forests.
[j] Included in studies that were classified under EUNIS categories G1.6 and G3.1.
[k] In 2003 presented as overall value for temperate forests.
[l] For application at broad geographical scales.
[m] For additional insight see de Wit et al. (2010).
[n] This critical load has been based on one European study in Portugal and evidence from studies in Mediterranean woodlands in California. During the final editing procedure of this report it became clear that the ambient background deposition of N in the Portuguese study had not been taken into account; therefore, the critical load was subsequently adapted to this value.

3.3 Mapping empirical critical loads on European EUNIS classified ecosystems

The European harmonized land cover map (Slootweg et al. 2009) was used to map the revised empirical critical loads and compare the geographical distribution to the results from Achermann and Bobbink (2003). The results are shown in Figure 3.1.

Figure 3.1 illustrates that the use of revised critical loads leads to an increase of sensitive areas, i.e. with values less than 16 kg $ha^{-1}yr^{-1}$. However, this difference is not only due to revised (lower) critical load ranges, but also to the manner by which a value from the critical load range is chosen for each ecosystem (EUNIS class). Following recommendations from the workshop in 2010, *minimum critical loads* from the ranges shown in Table 3.1 have been applied. In the past, so-called *modifying factors* – i.e. as function of weathering and precipitation – were applied (Slootweg et al. 2008; see alos Annex 3A) to map the results from Achermann and Bobbink (2003). A critical load value computed using the latter approach will generally be higher than the minimum of the critical load range for any EUNIS class. Experts at the workshop in Noordwijkerhout recommended to apply modifying factors only when these would include quantified information on management practices. Since the latter information is not available on a regional scale, minimum empirical critical loads are used to compute scenario-specific exceedances; and this is illustrated in Figure 3.2 for the National Baseline scenario in 2020.

From Figure 3.2 it is concluded that the use of revised empirical critical loads is likely to increase both the area at risk and the magnitude of the exceedances in comparison to 2003 results.

Figure 3.1 The area-weighted grid averages of empirical critical loads from Achermann and Bobbink (2003; left) and from Table 3.1 (right)

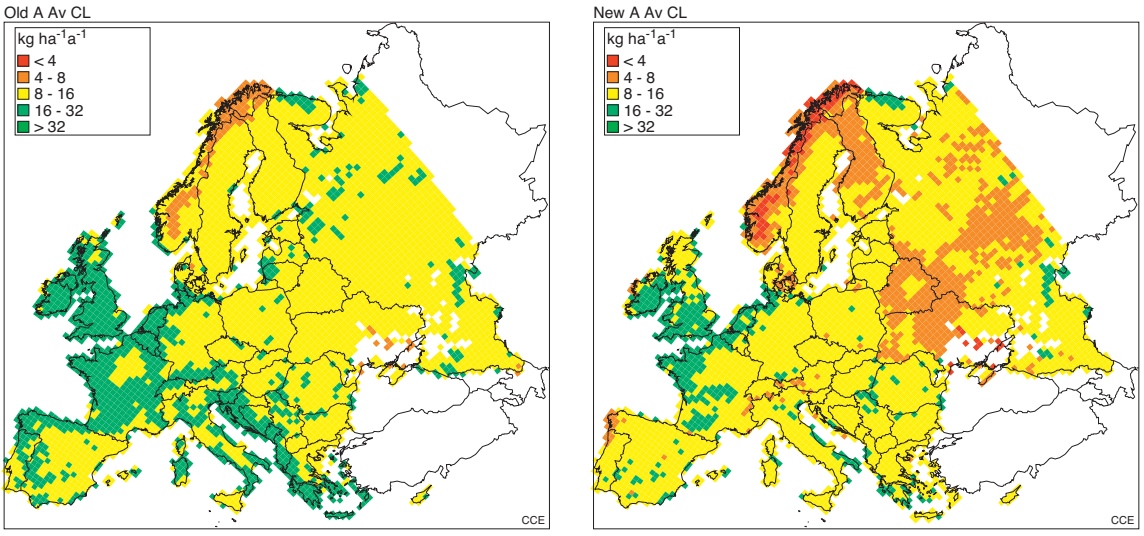

Figure 3.2 The Average Accumulated Exceedance of nitrogen using empirical critical loads from 2003, applying modifying factors (left), and empirical critical loads from 2010 using minima listed in Table 3.1 (right)

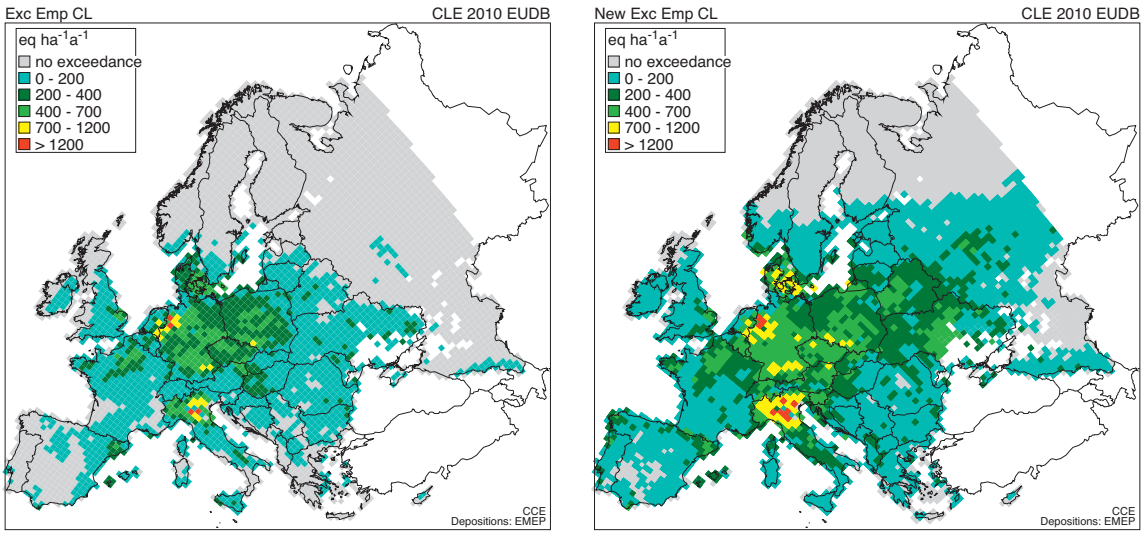

References

Achermann B, Bobbink R, 2003. Empirical critical loads for nitrogen, Proceedings of an expert workshop, Berne, 11-13 November 2002, Environmental documentation nr. 164, Swiss Agency for the Environmenta, Forests and Landscape, Berne, Switzerland.

Bobbink R, Hettelingh J-P (eds), 2011. Review and revision of empirical critical loads and dose response relationships. Proceedings of an international expert workshop, Noordwijkerhout, 23-25 Juni 2010, RIVM-report , Bilthoven, *in press*;

Slootweg J, Posch M, Hettelingh J-P, 2008. Summary of National Data. In: Hettelingh J-P, Posch M, Slootweg J (eds) Critical load, dynamic modelling and impact assessment in Europe, CCE Status Report 2008, PBL, Bilthoven, www.rivm.nl/cce

Slootweg J, Posch M, Warrink A, 2009. Status of the harmonised European land cover map. In: Hettelingh J-P, Posch M, Slootweg J (eds) Progress in the modelling of critical thresholds, impacts to plant species diversity and ecosystem services in Europe, CCE Status Report 2009, PBL, Bilthoven, www.rivm.nl/cce

De Wit, HA, M Lindholm, 2010. Nutrient enrichment effects of atmospheric N deposition on biology in oligotrophic surface waters – a review. ICP Waters report 101/2010. NIVA report 6007 – 2010. Oslo, Norway. ISBN 978-82-577-5742-7

Annex 3A: Empirical critical loads and modifying factors

Empirical critical loads for different EUNIS classes are generally given as an interval, thus necessitating criteria to arrive at a unique value for a given receptor. For several EUNIS classes 'a footnote' provides some guidance on how to select a value from the given range. Much of this guidance can only be obtained from local knowledge, but here we show how some so-called modifying factors could be derived from information extracted from the European Background Database (EU-DB).

Two of the modifying factors are precipitation *P* (lower CL for drier sites; EUNIS classes D1, F4.11, F4.2) and base cation availability Bc_{av} (lower CL for lower Bc availability; EUNIS classes B1.8, E1.7, E1.94, E1.95). Base cation availability is defined as the sum of Bc (=Ca+Mg+K) deposition and Bc weathering at a site. The derivation of these modifying factors depends on the interpretation of 'low' and 'high' for the modifying quantities: what is 'low' in one country can be 'high' in another. To avoid this, a European-wide approach seems appropriate. Figure 1 shows the cumulative distribution functions (CDFs) of *P* for EUNIS classes D1 and F4 as well as of Bc_{av} for EUNIS classes E1.7+E1.9, all derived from the EU-DB.

A modifying factor f_{mod} ($0 \le f_{mod} \le 1$) for a site is obtained from the CDF of the respective variable as indicated in Figure 3A-1, and the unique empirical critical load is then computed as:

$$CL_{emp}(N) = CL_{lo} + f_{mod} \cdot (CL_{up} - CL_{lo})$$

where CL_{lo} and CL_{up} are the lower and upper end of the empirical N critical load interval under consideration. Files with the CDF-data shown here are available in digital form from the CCE.

Figure 3A-1 CDFs of precipitation for EUNIS class D1 (left) and F4 (right) as well as Bc availability for combined EUNIS classes E1.7 and E1.9 (centre). The dashed line on the left shows how to obtain a modifying factor: f_{mod}=0.56 for *P*=600 mm/yr.

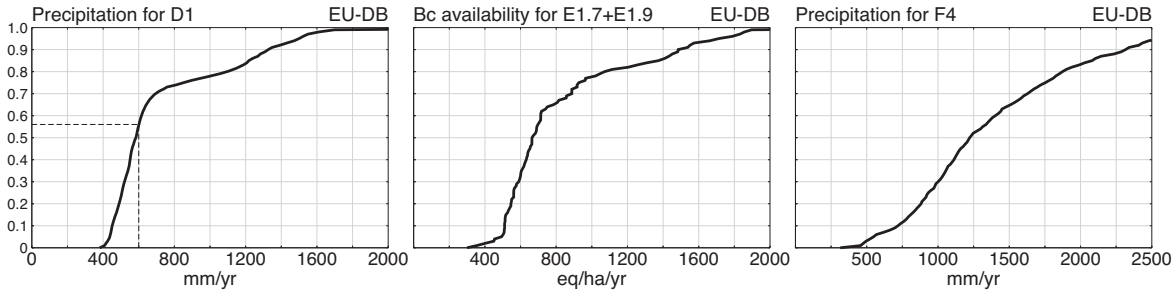

4
The VSD-Veg Model: Progress and Prospects

Maximilian Posch, Salim Belyazid[a], Daniel Kurz[b], Gert Jan Reinds[c]
[a]BCC AB, Sweden, salim@belyazid.com; [b]EKG Geo-Science, Switzerland, geo-science@bluewin.ch;
[c]Alterra, WUR, Wageningen, gertjan.reinds@wur.nl

4.1 Introduction

To facilitate the assessment of nitrogen deposition and other drivers (such as climate) on the biodiversity of plants, the CCE and its collaborators have, with the support of the Swiss Federal Office of the Environment (FOEN) and the Swedish Environmental Protection Agency (SNV), coupled the Veg vegetation composition model to the VSD and VSD+ geo-chemical soil models. Although the development of the linked model system is not yet fully finalised (as is the case with most models J), an interactive stand-alone version of the coupled VSD+Veg model is available from the CCE's website. In the following paragraphs the main issues with regard to the linking of the VSD/VSD+ with the Veg model are discussed.

4.2 The Veg model and its link to geo-chemistry

Veg is a plant community composition model, which has been developed as an add-on to the ForSAFE biogeochemical model (Wallman et al. 2005, Belyazid 2006, Sverdrup et al. 2007, Belyazid et al. 2010), and it has also been described in the 2009 CCE Status Report (Belyazid et al. 2009). Veg simulates the ground cover of a selected set of plant species at a certain site in response to climatic (soil moisture, light and temperature) and geochemical (N and base cation availability, and soil acidity) conditions, using information on plant-specific responses to those drivers. In its standard set-up, Veg is coupled to the multi-layer ForSAFE geochemical model. Since (most of) the drivers of the Veg model are also output from the VSD model (Posch and Reinds 2009), it has been linked to that model and *a fortiori* to the VSD+ model (see Figure 4.1).

Figure 4.1 Schematic view of the input flow to Veg. Left: ForSAFE-Veg model chain. Right: VSD-Veg including the conversion of ForSAFE output to VSD input for making the models (better/systematically) comparable. Abbreviations are: T: average annual temperature (°C); PAR: photosynthetically active radiation (µE $m^{-2}s^{-1}$); P: annual precipitation (m a^{-1}); LGL: annual light intensity at ground level (below tree canopy, µmol photon $m^{-2}s^{-1}$); θ: annual average soil moisture content (m^3 m^{-3}); Q: annual runoff from soil layer (m^3 $m^{-2}a^{-1}$); LF: litterfall of Bc & N ($mmol_c$ $m^{-2}a^{-1}$); GU: gross uptake of Bc and N (meq $m^{-2}a^{-1}$); NM: net mineralization of Bc and N (meq $m^{-2}a^{-1}$); WBC: weathering of base cations (Bc, Na) (keq $ha^{-1}a^{-1}$); BS: base saturation (the subscript L refers to soil layers considered).

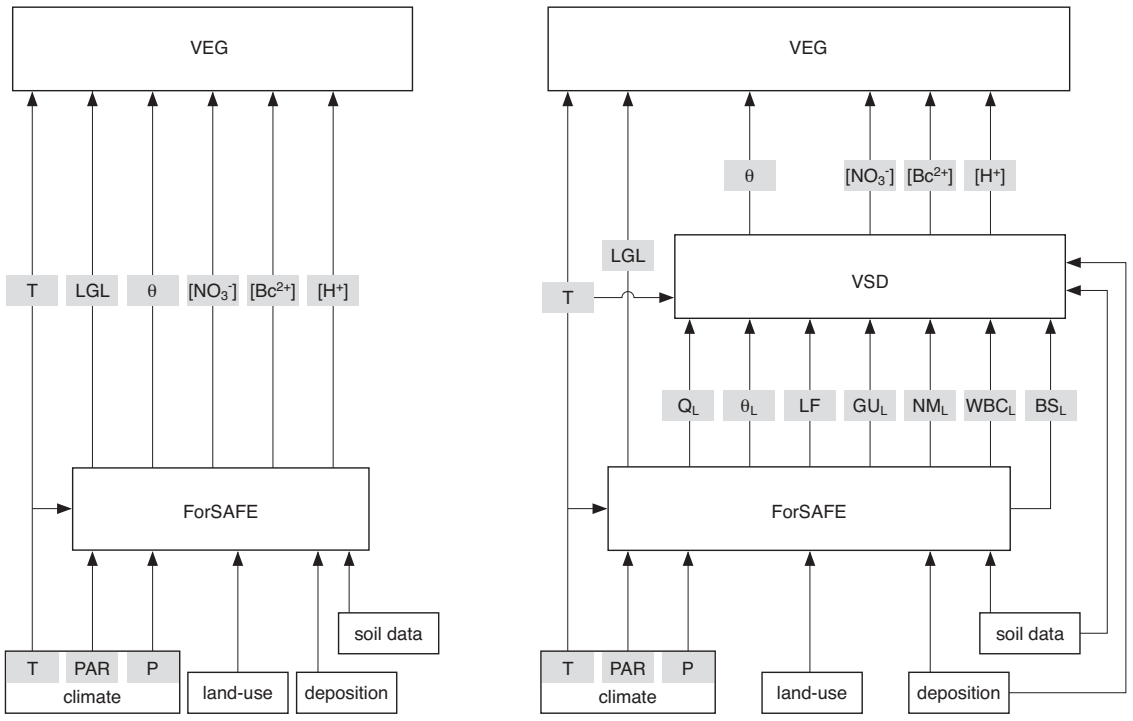

To minimise the influence of the differences in input data on model testing and comparisons, the inputs of the VSD model have been derived from ForSAFE model inputs and outputs by appropriate subroutines that average over the multiple layers of the ForSAFE model and adjust ForSAFE in- and output to VSD input. This is schematically shown in the right pane of Figure 4-1.

Figure 4.2 shows the percentile traces of the Czekanowski similarity indices (which compare the ForSAFE-Veg and VSD-Veg vegetation results) for the ground vegetation of 32 Swiss forest sites. If both models are run with analogous single-layer input (external pre-run averaging over the multiple layers), the similarity of the two vegetation composition predictions was mostly better than 90% (Figure 4.2A). Using the inputs and outputs of a standard multi-layer run of ForSAFE as input for VSD-Veg lead to substantial larger discrepancies in the vegetation output of the two model chains (Figure 4.2B). This is mostly due to the divergence of the chemical drivers, which are in this case derived from the bulk (VSD) and the layered (ForSAFE) soil solution chemistry, respectively. Regarding non-chemical drivers, only soil moisture (q) contributes to the dissimilarity of the ground vegetation composition, as the other drivers were directly taken from the ForSAFE output (Figure 4.2C).

For the stand-alone version of VSD-Veg (and VSD+Veg) the non-chemical drivers have to stand alone as well. Temperature (T) is not a problem, since it is a VSD(+) input. Also soil moisture (θ) is an input to VSD(+); but since Veg needs the normalised moisture content, $(\theta-\theta_w)/(\theta_s-\theta_w)$, where θ_s and θ_w are the moisture content at saturation and wilting point, these two site parameters have to be supplied by the user. Thus, only the light at ground level (LGL), given by photosynthetic active radiation (PAR), has to be computed in addition, and in the following we describe the simple LGL-model implemented in VSD+Veg.

The photosynthetically active radiation (PAR, in µmol/m²/s) at the forest floor, *PAR*, is calculated as:

(4-1) $$PAR = PAR_0 \exp(-k \cdot LAI)$$

where *LAI* the (one-sided!) leaf area index of the forest (tree), *k* and extinction or attenuation coefficient. Aber and

Figure 4.2 Differences in the effects of all drivers (A, B) of Veg on the similarity of the modelled ground vegetation composition if both ForSAFE and VSD are run with single layer (A) and multi-layer (B) input (CzI is the Czekanowski index, see Annex 4A). The bottom graph shows the effects of non-chemical drivers of which only soil moisture contributes to the vegetation output discrepancy.

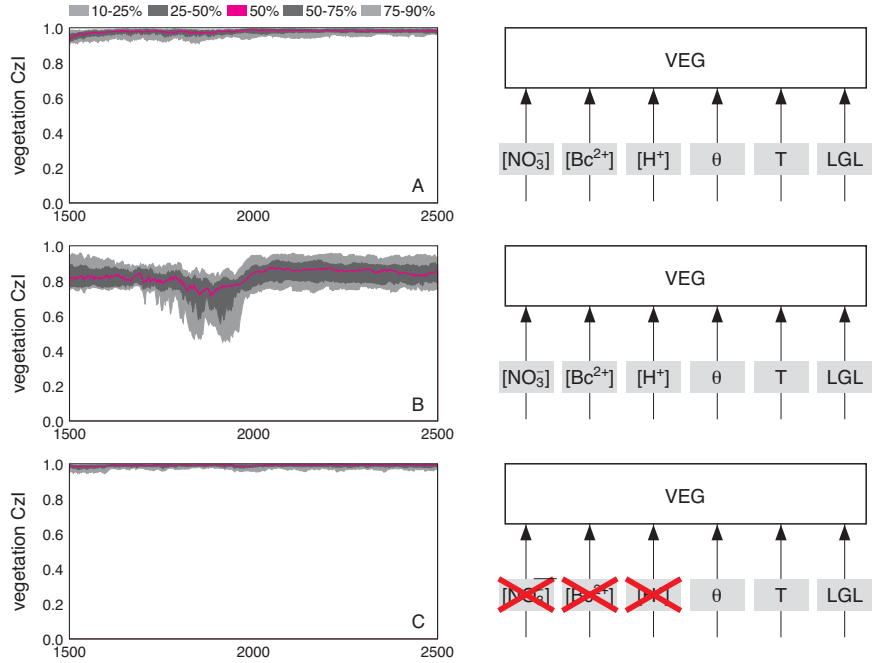

Federer (1992) use k=0.4 for conifers and k=0.5 for deciduous trees, and we use k=0.45, irrespective of tree species. From Fig.4.3a one can see that for *LAI* = 2, 5 and 10 the ground-level PAR is 40%, 10% and 1% of PAR_o, resp. The annual-average daylight PAR at the top of the canopy, PAR_o, is computed from the irradiance (1 W=4.4 µmol/s), which in turn is computed from the location (latitude) and daily values of the cloudiness (see e.g., Monteith and Unsworth 1990); and this computation can be carried out with the program MetHyd (see Appendix C).

An inverse of eq.4-1 is given by:

(4-2) $$LAI = \frac{1}{k}\log\frac{PAR_0}{PAR}$$

and in Figure 1b the *LAI* as function of PAR_o is shown for several values of *PAR*. From Fig.4.3b one can see that if the annual PAR_o is between 500 and 600 (typical for central Europe) and the ground-level PAR should be greater than, say, 10 to allow at least some ground vegetation, then the LAI should not exceed 9, etc.

The LAI, if not measured or simulated, is computed from a forest stand's foliage mass per unit area, m_{fol} (in kg/m²) and the leaf specific mass (also called specific leaf weight, SLW), *LSM* (in kg/m²), of the respective species. In case of a mixture of n tree species, the total LAI is the sum of the individual LAIs:

Figure 4.3 (a) PAR as fraction of PAR_0 as a function of *LAI* (eq.1; k=0.45); (b) LAI as function of top-of-canopy PAR_0 for different values of ground-level PAR (eq.2; k=0.45).

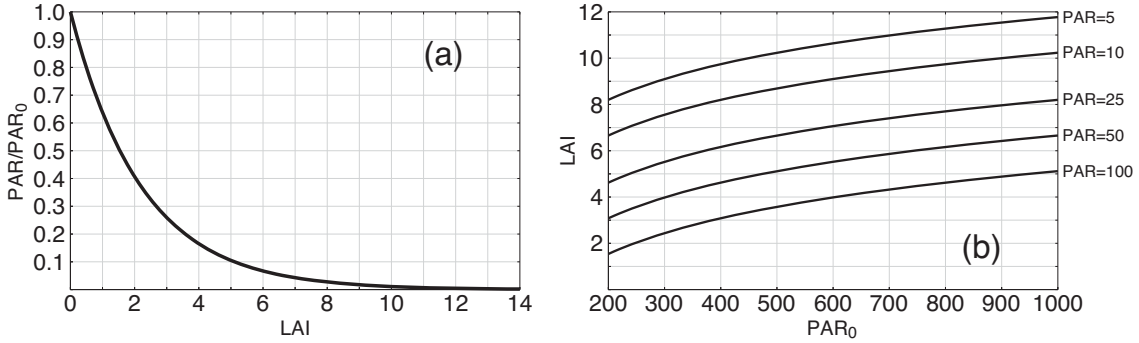

(4-3) $$LAI = \sum_{k=1}^{n} LAI_k = \sum_{k=1}^{n} \frac{m_{fol,k}}{LSM_k}$$

The LSM varies even for the same species, depending on site factors, but in VSD+Veg the default value for spruce is 0.207 kg/m² (an average of the data given in Hager and Sterba, 1984) and for pine the default is 0.500 kg/m² (gleaned from Warren et al., 2003); for broad-leaved species the values are generally below 0.100 kg/m². Note that, instead of the LSM, the inverse is often reported in the literature, called the leaf-specific area, LSA (LSA=1/LSM).

In VSD+Veg the foliage mass is computed from the amount of litterfall, am_{lf} (in kg/m²/a; see Appendix B) multiplied with the average residence time of the foliage on the tree, RTF (in a). For deciduous trees RTF is obviously equal to one, whereas for spruce it's set to 4 years and for pine to 2 years. More testing of the VSD+Veg model is required, and this shall be carried out during 2011.

References

Aber JD, Federer CA, 1992. A generalized, lumped-parameter model of photosynthesis, evapotranspiration and net primary production in temperate and boreal forest ecosystems. *Oecologia* 92: 463–474

Belyazid S, 2006. Dynamic modeling of biogeochemical processes in forest ecosystems. PhD thesis, Lund University, Lund, Sweden

Belyazid S, Kurz D, Sverdrup H, Braun S, Rihm B, 2009. Developing a method for estimating critical loads of nitrogen deposition under a changing climate, based on biological indicators. In: Hettelingh J-P, Posch M, Slootweg J (eds), CCE Status Report 2009, Bilthoven, pp 57–67

Belyazid S, Kurz D, Braun S, Sverdrup H, Rihm B, Hettelingh J-P, 2010. A dynamic modelling approach for estimating critical loads of nitrogen based on plant community changes under a changing climate. *Environmental Pollution* online; doi:10.1016/j.envpol.2010.11.005

Hager H, Sterba H, 1985. Specific leaf area and needle weight of Norway spruce (Picea abies) in stands of different densities. *Can. J. For. Res.* 15: 389–392

Monteith JL, Unsworth M, 1990. *Principles of Environmental Physics.* 2nd edition, Arnold, London, 291 pp

Posch M, Reinds GJ, 2009. A very simple dynamic soil acidification model for scenario analyses and target load calculations. *Environmental Modelling & Software* 24: 329–340

Sverdrup S, Belyazid S, Nihlgård, B, Ericson L, 2007. Modelling change in ground vegetation response to acid and nitrogen pollution, climate change and forest management in Sweden 1500–2100 A.D. *Water, Air and Soil Pollution Focus* 7: 163–179

Wallman P, Svensson MGE, Sverdrup H, Belyazid S, 2005. ForSAFE – an integrated process-oriented forest model for long-term sustainability assessments. *Forest Ecology and Management* 207 (1-2): 19–36

Warren CR, Dreyer E, Adams MA, 2003. *Trees* 17: 359–366

Annex 4A: Indices

In the following x_i and y_i (i=1,...,n) denote two sets of (plant) abundances (x_i, $y_i \geq 0$, but at least one each > 0), either at two different points in time or from two different 'measurements' (model outputs) (at the same time). Occasionally, we will assume that the abundances are normalised to one, i.e. $\Sigma_{i=1,..,n}\, x_i = 1$ (same for the y_i).

1. Similarity indices:

The *similarity* of the two sets x_i and y_i can be characterised with the so-called **Czekanowski (similarity) index** (1913) defined as:

$$CzI = 1 - \frac{\sum_{i=1}^{n} |x_i - y_i|}{\sum_{i=1}^{n} (x_i + y_i)} \qquad \text{(4A-1)}$$

Since $x+y-|x-y| = 2\min\{x,y\}$ for all x and y, this can also be written as:

$$CzI = \frac{2\sum_{i=1}^{n} \min\{x_i, y_i\}}{\sum_{i=1}^{n} (x_i + y_i)} \qquad \text{(4A-2)}$$

This index always lies in the range between 0 and 1, and it is 1 only if $x_i = y_i$ for all i. *CzI* is also known as **Sørensen index** (1948), especially when the x_i and y_i are presence-absence data. 1–*CzI* is also known as **Bray-Curtis dissimilarity index** (1957) or **Hellinger distance** (see, e.g., Wikipedia for further information).

If the abundances are normalised to one, *CzI* becomes:

$$CzI = 1 - \tfrac{1}{2}\sum_{i=1}^{n} |x_i - y_i| = \sum_{i=1}^{n} \min\{x_i, y_i\} \qquad \text{(4A-3)}$$

To compare output of the Veg-model, an index called **'Mondrians'** has been defined to measure the *dissimilarity* of a vegetation assemblage between two points in time (Belyazid et al. 2010). It is defined as the sum of the differences between corresponding abundances, taking care not to count those differences twice. The Mondrian index thus becomes:

$$MoI = \sum_{i=1}^{n} \max\{x_i - y_i, 0\} = \sum_{i=1}^{n} \max\{y_i - x_i, 0\} \qquad \text{(4A-4)}$$

The equality between the two sums is not immediately apparent, and generally does not hold for the individual terms in the sum. However, it can be easily proven, if $\Sigma_{i=1,..,n}\, x_i = \Sigma_{i=1,..,n}\, y_i$, which we assume.

Since $\max\{x-y,0\} = x-\min\{x,y\}$ holds for all x and y, we find by comparing eq.4A-4 with eq.4A-3, assuming that the x_i and y_i, are normalised to one:

$$MoI = 1 - CzI \qquad \text{(4A-5)}$$

Thus it turns out that the Mondrian index is the same as the Bray-Curtis dissimilarity index!

2. Diversity indices:

Diversity indices are defined for a set of abundances x_i, i=1,..,n at a given location and point in time, with the x_i normalized to one. There is a large body of literature that defines and discusses (classes of) diversity indices (e.g., Hill 1973, Tothmeresz 1995, Baczkowski et al. 1997). In VSD+Veg the following three characterisations (indices) of diversity can be computed:

Number of species:
This is simply the number of species with $x_i > \varepsilon$, where $\varepsilon > 0$ is a user-specified limit (e.g., to neglect spurious contributions) with a default value of ε =0.001 (0.1%)

Simpson index (1949):

$$SiI = 1 - \sum_{i=1}^{n} x_i^2 \qquad \text{(4A-6)}$$

This Simpson index obtains its maximum, 1–1/n, if all x_i are equal, i.e. x_i=1/n. Note that *SiI* is often defined without the '1–', but then it's *minimal* for equal x_i (somewhat counter-intuitive).

Shannon index (1948):

$$ShI = -\sum_{i=1}^{n} x_i \ln x_i \qquad \text{(4A-7)}$$

In case of a x_i=0, its contribution to the index is zero (0ln0=0). Also the Shannon index obtains its maximum, ln$n$, if all x_i are equal, i.e. x_i=1/n.

References

Baczkowski AJ, Joanes DN, Shamia GM, 1997. Properties of a generalized diversity index. *Journal of Theoretical Biology* 188: 207–213

Bray JR, Curtis JT, 1957. An ordination of the upland forest communities of Southern Wisconsin. *Ecological Monographs* 27: 325–349

Hill MO, 1973. Diversity and evenness: A unifying notation and its consequences. *Ecology* 54(2): 427–432

Shannon CE, 1948. A mathematical theory of communication. *Bell System Technical Journal* 27: 370–423 & 623–656

Simpson E, 1949. Management of diversity. *Nature* 163: 688

Tothmeresz B, 1995. Comparison of different methods for diversity ordering. *Journal of Vegetation Science* 6: 283–290

5 Plant species Diversity Indicators for Impacts of Nitrogen and Acidity and Methods for their Simulation: an Overview

Han van Dobben*, Jean-Paul Hettelingh, Wieger Wamelink*, Wim de Vries*, Jaap Slootweg, Gert Jan Reinds*
* Alterra, WUR, Wageningen, the Netherlands

Ecological effects of atmospheric deposition were first noticed in the 1960s (Odén 1967) and generated extensive public debate, especially after large-scale forest dieback had been predicted in the 1970s (Ulrich et al. 1979). The debate continues until today, although the focus has shifted from deposition of acidity to deposition of nitrogen compounds, and effects are now defined in terms of biodiversity loss rather than in terms of forest dieback. The present chapter deals with indicators for plant species diversity and their applicability as endpoints in effect models for atmospheric deposition. Indicators will be evaluated with a focus on (a) their utility to reflect diversity as appreciated from various viewpoints regarding ecosystem functions; and (b) their practical feasibility as output of coupled abiotic and biotic models to forecast diversity on the basis of abiotic conditions including atmospheric deposition. In this chapter, section 1 deals with the quantification of biodiversity, and section 2 with the practical application of biodiversity indicators. In section 3 possible effects of deposition on plant species diversity are treated. Section 4 focuses on the use of models to forecast biodiversity indicators on the basis of abiotic scenarios, and section 5 on the coupling of abiotic and biotic models. Here we will concentrate on effects on flora (incl. mosses and lichens), as research on other species groups is virtually lacking, at least as far as predictive methods are concerned.

5.1 Biodiversity indicators

In recent discussions the term biodiversity has an increasingly prominent place. When estimating biodiversity it should be born in mind that the term was originally coined by politicians and not by scientists. Therefore, biodiversity should be regarded as a container concept to summarize the ecological effect of human activity, for which a precise definition should be agreed in each application. Ideally, a biodiversity indicator should (Van Dobben & Wamelink 2009):

(i) agree with conservationists' attitude, i.e. an ecosystem's numerical value should correspond with conservationists' intuitive or generally accepted appreciation of that system;

(ii) be ecologically meaningful and quantifiable on the basis of data that are already available or can be easily collected;
(iii) be scale-independent and comparable over different regions in Europe;
(iv) be politically useful i.e. there should be 'buttons to press' for politicians in order to influence it.

A recent study carried out by the EEA enumerates a huge number of possible biodiversity indicators (EEA 2003), which can be grouped in 26 main groups (EEA 2007). Even these main groups contain a wide range of definitions, based on biotic, abiotic, administrative and societal indicators. Clearly, only definitions related to the presence or absence of species or species combinations are useful in the present context of biological effects. Such definitions could be given the following general form:

$$H = \Sigma_{i=1,n}\ \text{weight}_i \qquad (1)$$

with H, biodiversity indicator; i, species counter; n, total number of species.

The following criteria for weighting might be considered:
1. no weighting, i.e. all species are equally important;
2. weighting to distribution of the abundances over the species. Some of the classical biodiversity measures, e.g. the Simpson and the Shannon-Weaver index use this form of weighting.
3. weighting to the intrinsic 'importance' of each species from a nature conservancy point of view (i.e. considering rareness, decline); the IUCN concept of 'Red Lists', lists of endemics etc. may be the basis of such forms of weighting;
4. weighting to the desirability of certain species to be present in a certain location; the Dutch concept of 'target species' (which is derived from the Red List concept), or the European system of Natura2000 Habitat types and its 'typical species' apply this form of weighting;
5. weighting to functional groups; e.g. primary producers should be present anyway, an ecosystem is only 'complete' if large carnivores are present, or, in a forest, mycorrhiza-forming mushrooms should be present, etc.

Within the context of this chapter, biodiversity will be considered as synonymous for plant species diversity. Criterion (1) makes the biodiversity indicator equal to the number of species. Ecological theories that assume a system to become more stable if it contains more species, provide a rationale for species counting (Margalef 1963). However, according to modern insights such theories are probably not generally true (McCann 2000). Therefore, some form of species weighting should be applied to arrive at a useful indicator. Criterion (2) has been extensively applied in the 'classical' biodiversity indices (see Baczkowski et al. 1997) that summarize two properties of the ecosystem: the 'richness' (i.e. the number of species) and the 'evenness' (i.e. the distribution of the abundances over the species). In the present context these classical measures are considered less useful as their biological meaning is rather unclear despite their mathematical elegance (Hurlbert 1971). An obvious drawback of these measures in the light of requirement (ii) outlined above is that they treat all species equally, i.e. independent of their known properties, and therefore attach equal weight to unwanted, invasive species and to highly desirable Red List species. An additional drawback of simple species counting is that far more species occur on calcareous soils and in hot and dry climates than on acid soils and in cold en wet climates, independent of other environmental conditions. This causes a strong decrease in species richness from South to North over Europe, and makes a comparison over a larger geographical extent difficult (De Vries et al. 2002).

Criterion (3) probably comes nearest to biodiversity as it is intuitively appreciated by ecologists: if the Red List criterion is used, rare and declining species are given a high weight, and the indicator becomes a measure for a location's importance to prevent (local) extinction of species. Such a criterion is extensively described in Van Dobben & Wamelink (2009).

In criterion (4) certain species are considered as prerequisites for a given location to have an ecological value anyway. These species may be given as such, or in the form of a plant community, i.e. a group of species that tend to co-occur, of which a certain proportion should be present. This approach was probably first elaborated for the Netherlands (Bal et al. 1995) but is now implemented in the EU 'Habitat Directive'. Under this Directive, natural areas designated by each Member State are set aside for the occurrence of given species or communities (the 'Habitat species' and 'Habitat types'; see e.g. European Commission 2005). The presence of such targets in their designated locations can be used to evaluate the ecological performance of each site. Many of the biodiversity indicators found in literature (e.g. Lamb et al. 2009) are based on this concept, i.e. comparing the actual species composition of a given site with a 'reference' species composition. This reference may be the species present in an 'intact' or 'pristine' community or under 'natural' conditions. The comparison may be by simply scoring presence or absence of 'reference' species, by comparing abundances or by more sophisticated methods based on multivariate statistics (Flåten et al. 2007). Negative values may be added for 'invasive' or otherwise unwanted species (Rowe et al. 2009). An obvious drawback of such methods is that in Europe nearly all ecosystems are

man-made and it is usually impossible to define a 'pristine' state, but this problem may be overcome by using a 'reference' state that is defined a priori like in the Habitat Directive (Rowe et al. 2009). In that case the 'reference' state (i.e., the species or habitat types assigned to a given area) is usually based on expert opinion of what should be present in that area. Buckland et al. (2005) and Jenssen (2009) emphasize the use of the first observation in a time series as the reference state, however time series are often unavailable or start in a state that is already considered as 'degraded' (Ellis et al. 2011).

Criterion (5) comes closest to the 'ecosystem service' concept, in the sense that certain species groups should be present to fulfil certain functions; such groups could consist of e.g. edible species, species with medical applications, highly productive species in terms of food, timber or fuel; etc. However, note that ecosystem services are not necessarily linked to species; other biotic or abiotic properties of the system can just as well be indicators.

5.2 Evaluation of biodiversity from existing data

The most extensively available plant ecological data are probably vegetation relevés. A relevé is a description of a sample plot (usually 1 - 2500 m^2 in size) in terms of plant species and their abundance. They are being collected both on ad-hoc basis and in monitoring networks, including networks dedicated to the estimation of effects of deposition such as ICP Forest. Some of the monitoring networks collect time series data using permanent sample plots. At present, c. 2 500 000 relevés from all over the world are stored in c. 130 publicly accessible databases (see www.givd.info). Therefore such relevés are an attractive starting point for the assessment of biodiversity at any geographical scale. Evaluations using criteria (1) to (4) outlined above can easily be made on the basis of vegetation relevés. Here we will further concentrate on criteria (3) and (4) because they are expressions of the desirability of certain species to be there, i.e. they attach a certain value to a relevé based on the known properties of each species. Criterion (5) has a wider scope than vegetation alone and is not further considered here.

Besides the species-based approach, vegetation ecology has a long tradition in community-based approaches. In such approaches species combinations are considered rather than individual species, which is justified by the observation that certain species tend to co-occur while others are negatively correlated. An elaborate system exists to describe and classify plant communities (e.g. Braun-Blanquet 1964, Schaminée et al. 1995), defined by the species and their quantities in relevés. Computer programs are available to automatically assign observed combinations of species to communities in a hierarchical taxonomical system (Van Tongeren et al. 2008). Ecological targets are often defined in terms of plant communities, e.g. the definition of the European Habitat types heavily relies on plant communities.

On the basis of the above considerations, three promising approaches emerge for a plant species diversity indicator that meets the above requirements (i) - (iv):
(a) presence of species out of a list of target species for a given location
(b) presence of one or more target communities for a given location
(c) summed (or otherwise combined) intrinsic values of the species present

Of these approaches, (a) and (b) are realisations of criterion (4) above, and (c) is a realisation of criterion (3).

The method that is preferable in a given situation strongly depends on the aim of the application. A drawback of the methods that use predefined targets is that these targets should be known for each location, which is often not the case. Moreover, hard data on which to base these targets (e.g. species in the location's 'original', 'pristine' state) are usually lacking. Also, the method is rather rigid: a situation with great ecological importance can still be classified as 'low value' because the actual situation and the target do not match. On the other hand, methods that use intrinsic values per species require lists of such values, and these may not be present, or may not be applicable to all regions. It should be noted that Red Lists for vascular plant are available for most European countries and are often official government documents, which makes their use attractive. Table 1 gives a summary of the advantages and disadvantages of the various methods.

An example of an assessment based on the presence or absence of species and communities are the periodical reports requested by the EU of the Member States regarding the Conservation Status of sites under the Habitat Directive (European Commission 2005). An example of an assessment based on the total number of species, the number of rare species, and a 'classical' diversity measure (the Simpson index) is found in Van Dobben & De Vries (2010). An example of an assessment based on a Red List-derived indicator is found in Wamelink et al. (2003) and Van Dobben & Wamelink (2009).

5.3 Effects of atmospheric deposition

Effects of atmospheric deposition on the vegetation may be quite subtle and therefore it cannot be taken for granted that such effects always become apparent though changes in biodiversity indicators. Only in extreme cases deposition will lead to local extinction of species or the appearance of new ones. A classical case is the lichen *Lecanora conizaeoides*, that was absent from Europe before c. 1850, strongly increased with SO_2 concentration to reach a peak around c. 1970, and gradually decreased to virtual extinction after that date. Its occurrence appeared to be completely dependant on high SO_2 deposition (Bates et al. 2001). Many nitrophytic vascular species have increased in response to nitrogen deposition, often displacing the species that were originally present. Well-known examples are the grass-encroachment of heathland (Berdowski 1987), the increase of grasses in forest understorey vegetation (Van Dobben et al. 1999) or in dune vegetation (Veer & Kooijman 1997, Remke et al. 2009). The concept of indicator species is based on the idea that certain species respond more clearly or more quickly to deposition than others. Especially in lichens this concept still has a great popularity; e.g. the above-mentioned *Lecanora conizaeoides* is a clear indicator for SO_2, while other species are considered as indicators for nitrogen deposition (Van Herk 1999).

Most studies on the biological effects of deposition are of an observational and transversal nature, and are therefore hampered by the covariance of deposition and other (e.g. climatic) gradients (see e.g. Van Dobben & De Vries 2010). Statistical techniques that treat the community as a whole instead of using a species-by-species approach (i.e. multivariate statistics) are often most successful to reveal such effects (De Vries et al. 2002, Van Dobben & de Vries 2010). But also biological indicator systems may be useful in this respect. Such systems assign a value for a certain environmental variable (e.g. soil pH, water availability, nutrient availability) to each species (Ellenberg 1991, Wamelink et al. 2002, Wamelink et al. 2005). The value of a given species for a given variable represents its optimum with respect to that variable. By taking the (weighted) average over all species in a certain location, an estimate of the value of an environmental variable at that location can be obtained. The most popular indicator system is the one developed by Ellenberg (1991), although many others exist. Ellenberg estimated responses to light, climate (as 'temperature' and 'continentality'), soil pH, water availability and nutrient availability for ca. 2500 species occurring in central Europe. By using an indicator system, effects of e.g. nitrogen deposition may become evident through a statistically significant change in mean nutrient indicator value even if there are no or only a few individual species whose abundance changed significantly (Fischer et al. 2010). An advantage of the use of indicator systems over multivariate statistics is that the indicators yield information on possible causes of the changes instead of just determining the statistical significance of the change. An obvious disadvantage of Ellenberg's (and most other) indicator systems is that they almost entirely rely on expert judgement. As a consequence they have no physical scales (i.e. pH units) but use arbitrary index numbers which are often difficult to relate to physical units (see section 5).

5.4 Model approaches to predict biodiversity indicators

Although it may be difficult to establish a relation between atmospheric deposition and biodiversity indicators in observational studies, such indicators are indispensable in forecasting studies. This is because such studies need a clearly defined and generally acceptable biological endpoint, i.e. one that meets criteria (i) - (iv) outlined in Section 1. Also, forecasting studies are not hampered by the intrinsic variability of ecosystems and the resulting need for many data points to achieve statistical significance. Forecasting studies usually entail a comparison of scenarios, and differences in the predicted biodiversity indicator, however subtle, can be used to make a ranking of such scenarios. Such scenarios can provide the 'buttons to press' referred to in criterion (iv) above.

Methods to predict biodiversity (or any other biological endpoint related to vegetation) make use of a model that predicts relevant soil conditions like pH, nitrogen availability and wetness on the basis of geographically explicit soil, hydrological, climate and deposition data (De Vries et al. 2010). These soil models are usually dynamic models with widely different levels of complexity. In a next step, the biological endpoint is predicted on the basis of a static, regression-based model. Such a model is calibrated by regressing some biological property (e.g., quantity or presence / absence of a certain species) on soil properties (usually: pH, water availability, nutrient availability), and subsequently using the regression model to back predict the biological property. In the calibration step, the abiotic properties can be either directly measured, or themselves derived from vegetation composition e.g. by using the 'Ellenberg' system outlined above. Biological properties predicted by models that are presently in use fall in the three categories (a) - (c) outlined in Section 2: presence of individual species, presence of vegetation types, or intrinsic values of the species present. These approaches will be discussed below, and the linking of biotic and abiotic models will be discussed in section 5.

Individual species

The Dutch model MOVE has the longest history in this approach (Latour et al. 1994), and is treated here as an example. Other models are presently also in use e.g. VEG (Belyazid et al. 2009) or BERN (Schlutow & Huebener 2004) . In its original form the model MOVE predicted the probability of occurrence per species on the basis of three environmental conditions: soil pH, nutrient availability and groundwater level (Latour et al. 1994). Later, salinity, vegetation structure and geographical region were added to these predictors (De Heer et al. 2000). For the Dutch conditions the model is calibrated by multiple logistic regression using a data set of 160 000 vegetation relevés. Most of these relevés do not have information on soil conditions so their abiotic conditions are estimated from the species composition using Ellenberg's indicator system. In turn, Ellenberg's indicator values are linked to soil properties expressed in physical units (e.g. groundwater level in cm below soil surface) on the basis of a far smaller data set of relevés where measurements have been carried out. The output of the combined soil - vegetation model chain is a list of probabilities of occurrence per species under given soil conditions. If there is a given list of target species for a given location, the combined model can be used to predict the amount of realisation of that target. This can be done in two ways:

- the sum of the probabilities of occurrence of species in a given list yields the expected number of species out of this list. This is because both the summed probabilities of occurrence and the average number of species are equal to the number of occurrences divided by the number of locations. The expected number of species as a percentage of the total number of species in the list can be used as a measure for the expected realisation of the target.
- the probabilities of occurrence can be converted into a presence / absence index by setting an arbitrary threshold above which a species is assumed to be present. Again, target realisation can be quantified as the expected percentage of the target species to be present. This method has been extensively applied in the Netherlands (see e.g. Latour et al. 1997).

For both methods it should be realised that the vegetation relevés of the calibration set are squares with surface areas between c. 1 and 2500 m^2, so the back predicted probabilities of occurrence are also on this scale. As the relevés in the training set do not have a uniform size and the probabilities of occurrence depend nonlinearly on the considered surface area, the extrapolation to different areas becomes difficult. This is relevant as targets are usually set for reserves that are at least several ha in size.

Communities

The probability-of-occurrence approach outlined above is not necessarily restricted to the species level. The same procedures can be applied for communities by assigning a community to each relevé in the training set and again carrying out a logistic regression to determine the relation between the presence of each community and soil conditions. The calibrated model can be used to predict the probability of occurrence per community. A fundamental difference with the species approach is that communities are mutually exclusive on the relevé scale while species are not. However, a ranking of communities can be made as to decreasing probabilities of occurrence for a given site, and target realisation can be linked to a certain limit of probability for a given list of target communities to occur. Alternatively, an arbitrary threshold can be set for the probability of occurrence, above which the community is simply assumed to be present. A strength of this approach is that in the EU Habitat directive, targets are defined in terms of Habitat types for each location, and most of the habitat types are directly related to vegetation composition in terms of species or plant communities. The scale problem of the species approach also applies to the community approach but to a lesser extent. An example of an application in the Netherlands can be found in Wamelink et al. (2010).

Intrinsic values

As noted above, a disadvantage of methods that set targets in terms of a priori lists of species or communities is their inflexibility. As a result, sites with a high potential to harbour threatened species may still get a low rating because they do not match a predefined target. Instead, an intrinsic value can be assigned to each species, representing the 'conservancy' or other (e.g. medical or nutritional) value of each of them. The values over all species in a relevé can be combined to a value for that relevé. Negative values can be assigned to undesired species (e.g. invasive ones; Lamb et al. 2009, Rowe et al. 2009). However, as the weights have an arbitrary scale and -dependant on the mathematical procedure used- their effect on the final value is linear or at least monotonic, the method is insensitive to the addition of a fixed number to all species values.

Next, the calibration procedure outlined above can be applied, and an expected value for the indicator can be computed for each combination of soil conditions. This method is described in detail by Van Dobben & Wamelink (2009). Besides its greater flexibility, an advantage of this method is its scale-independence: the model simply yields the expected value for the biodiversity indicator under given soil conditions. However, note that if the intrinsic values per species are location-dependant (which they are in the most promising approaches, i.e. Red Lists are

regionally different), this approach comes closer to the species- or community-oriented one.

5.5 Linking biotic and abiotic models

All three methods outlined above depend on the regression of a certain biotic property of vegetation relevés on their abiotic conditions. To determine the regression coefficients with an acceptable amount of uncertainty a large calibration set is required. However, the number of vegetation relevés with measured abiotic conditions is limited. Therefore, a popular shortcut is not to use measured abiotic conditions, but to estimate these conditions from the relevés themselves by using indicator values (usually Ellenberg's) per species. As outlined above, this yields abiotic conditions expressed in the arbitrary units of the indicator system, while soil models produce their output in physical units e.g. water level in cm relative to soil surface. To link the units of the indicator system to physical units a second calibration set is needed, consisting of relevés that have measured abiotic conditions. It has been shown that the largest contribution to the total uncertainty in the model output is due to the translation of indicator to physical units (Wamelink et al. 2002, van Dobben et al. 2006). Therefore is seems highly desirable to replace the existing, expert-based plant response databases by ones that are based on measured abiotic conditions (Wamelink et al. 2005). Such databases are now well underway although a lot of work still has to be done (see: http://www.botanik.uni-greifswald.de/db_details.html?choosen_db=140&choose=Load). At present, sufficient data are available for pH and possibly also for groundwater level, but for other conditions there is still a strong need for soil chemical measurements carried out in combination with vegetation relevés. Of all soil chemical properties, nutrient availability is the most difficult to tackle as there are many chemical indicators for nutrient availability (such as NO_3, NH_4, total-N, C/N ratio, different fractions of P, K, other base cations) and there seems to be no single indicator that is highly predictive for the vegetation. Table 2 gives an overview of advantages and disadvantages of methods for the coupling of abiotic and biotic models.

The derivation of responses per community based on measured conditions has an extra problem over the species-oriented approach, namely that far less data are available. This is because a vegetation relevé contains many species, but can be assigned to only one (or a few) communities. This means that the number of data points per community is far lower than the number of data points per species. Therefore the number of communities for which the response can be directly derived with an acceptable amount of uncertainty is limited. A shortcut method to arrive at responses of a larger number of communities is to estimate the abiotic conditions of a large set of relevés (that lack abiotic measurements) through the known response of their constituent species (Wamelink et al. 2010).

5.6 Concluding remarks

At present there is a strong need for a single indicator that summarises the 'ecological quality' of a given site. This is both true for its present state, and for its future state under different scenarios. In this chapter the term 'biodiversity' is taken to designate such an indicator. In principle, there appear to be two methods in use to determine a site's ecological quality: by comparing its species composition to a desired 'reference' state, and by adding the intrinsic values of its constituent species, e.g. in terms of extinction risk. Both methods have many variants, and the choice of an indicator strongly depends on the goal in mind. Many of these indicators can be simulated on the basis of abiotic conditions. Abiotic conditions can be projected into the future by coupling them to e.g. emission scenarios, which in turn can be derived from economic scenarios. In this way political decisions can be directly translated into expected changes in biodiversity. The approach of coupling (dynamic) soil models to (static, regression-based) vegetation models is flexible and can accommodate many forms of the indicators outlined above. At present, the largest uncertainty seems to be in the abiotic responses per species, and it is recommended to put considerable scientific effort into the reduction of this uncertainty.

Table 5.1: Summary of advantages and disadvantages plant species diversity indicators

method	reference, target	advantages	disadvantages
species-oriented targets	any given list of species	long history of model application	validation not feasible, or bad performance in validation
		conceptually simple, easy to explain	unsolved scale problems, i.e. calibration and prediction on different scales
		flexible, any list of species can be set as a target	
	list of species present in 'pristine', 'natural' state	ecologically meaningful, i.e. aiming at conservation of ecosystem's original state	usually no data available on 'pristine', 'natural' state
	predefined lists of 'target' species	politically meaningful, i.e. yields metric of target realisation	target may be ecologically rather arbitrary
community-oriented targets	Habitat types	immediately relevant for EU Habitat Directive	targets ecologically rather arbitrary
	other typology	may be relevant as indicator for local target realisation	rigid, inflexible
intrinsic value-oriented targets	list of intrinsic values per species	can be directly related to conservancy targets e.g. protection of Red List species	list of intrinsic value per species must be available
		applicability is location-independent	intrinsic values may be regionally different
		ecologically meaningful, i.e. aiming at conservation of threatened species	no direct relevance for policy-set targets, difficult to explain, many alternative approaches possible

Table 5.2: advantages and disadvantages of methods for coupling of biotic and abiotic models

method	reference, target	advantages	disadvantages
use of indicator values	expert judgement	data available for most species	large uncertainly introduced by translation function
			subjective, dependant on personal opinion
use of direct measurements	field measurements combined with vegetation relevés	no translation function needed	for pH: none
		not dependant on personal opinion	for water level: probably none
			for nutrient availability: no unambiguous chemical indicator available
			for other variables: too few data available

References

Bal, D, Beije, H M, Hoogeveen, Y R, Jansen, S R J, van der Reest, P J. 1995. Handboek Natuurdoeltypen in Nederland. Rapport IKC-N 11, 408 p.

Baczkowski, A.J., Joanes, D.N., Shamia, G.M. 1997. Properties of a generalized diversity index. Journal of Theoretical Biology 188: 207–213

Bates, J.W., Bell, J.N.B., Massara, A.C. 2001.Loss of Lecanora conizaeoides and other fluctuations of epiphytes on oak in S.E. England over 21 years with declining SO_2 concentrations. Atmospheric Environment 35:2557-2568

Belyazid, S., Kurz, D., Sverdrup, H., Braun, S., Rhim, B. 2009. Developing a method for estimating critical loads of nitrogen deposition under a changing climate, based on biological indicators. In: J-P. Hettelingh, M. Posch, J. Slootweg (eds.): Progress in the modelling of critical thresholds, impacts to plant species diversity and ecosystem services in Europe: CCE Status Report 2009, Coordination Centre for Effects, Bilthoven, p. 57-67

Berdowski, J J M. 1987. The catastrophic death of Calluna vulgaris in Dutch heathland. Diss Utrecht, 132 p.

Braun-Blanquet, J. 1964. Pflanzensoziologie. Grundzüge der Vegetationskunde. 3. Aufl. Springer Verlag, Wien / New York.

Buckland, S.T., Magurran, A.E., Green, R.E., Fewster, R.M. 2005. Monitoring change in biodiversity through composite indices. Philosophical Transaction of the Royal Society B 360:243-254

De Heer, M., Alkemade, R., Bakkenes, M., van Esbroek, M., van Hinsberg, A., de Zwart, D. 2000. MOVE: nationaal Model voor de Vegetatie, versie 3: de kans op voorkomen van ca. 900 plantensoorten als functie van 7 omgevingsvariabelen. RIVM rapport 408657 002. Bilthoven, 63 p.

De Vries, W., Reinds, G.J., Van Dobben, H., De Zwart, D., Aamlid, D., Neville, P., Posch, M., Auee, J., Voogd, J.C.H., Vel, E.M. 2002. Intensive monitoring of forest ecosystems in Europe. 2002 Technical Rapport. EC, UN/ECE, Brussels, Geneva (available through http://www.icp-forests.org/pdf/TRLII2002.pdf).

De Vries, W., Wamelink, G.W.W., Van Dobben, H., Kros, J., Reinds, G.J., Mol-Dijkstra, J.P., Smart, S.M., Evans, C.D., Rowe, E.C., Belyazid, S., Sverdrup, H.U., Van Hinsberg, A., Posch, M., Hettelingh, J-P., Spranger, T., Bobbink, R. 2010. Use of dynamic soil–vegetation models to assess impacts of nitrogen deposition on plant species composition: an overview. Ecological Applications, 20: 60–79

EEA, 2003. An inventory of biodiversity indicators in Europe. Office for Official Publications of the European Communities, Luxembourg

EEA, 2007. Halting the loss of biodiversity by 2010: proposal for a first set of indicators to monitor progress in Europe. EEA Technical Report 11/2007. Office for Official Publications of the European Communities, Luxembourg

Ellenberg, H. 1991. Zeigerwerte der Gefäszpflanzen (ohne Rubus). Scripta Geobotanica 18, 9-166.

Ellis, C.J., Yahr, R., Coppins, B.J. 2011. Exposing conservation's selective memory – loss of epiphyte biodiversity across the threshold of industrialisation. Proceedings of the Royal Society B, in press.

European Commission. 2005. Note to the Habitats Committee. Subject: Assessment, monitoring and reporting of conservation status – Preparing the 2001-2007 report under Article 17 of the Habitats Directive. (DocHab-04-03/03 rev. 3). European Commission, Brussel.

Fischer R, Lorenz M, Granke O, Mues V, Iost S, Van Dobben H, Reinds GJ, De Vries W. 2010. Forest Condition in Europe, 2010 Technical Report of ICP Forests. Work Report of the Institute for World Forestry 2010/1, Hamburg, 175pp.

Flåten, G.R., Botnen, H., Grung, B., Kvalheim, O.M., 2007. Quantifying disturbances in benthic communities - comparison of the community disturbance index (CDI) to other multivariate methods. Ecological Indicators 7:254-276.

Hurlbert, S.H. 1971. The noncencept of species diversity: a critique and alternative parameters. Ecology 52:577-586.

Jenssen, M. 2009. Assessment of the effects of top-soil changes on plant species diversity in forests, due to nitrogen deposition. In: J-P. Hettelingh, M. Posch, J. Slootweg (eds.): Progress in the modelling of critical thresholds, impacts to plant species diversity and ecosystem services in Europe: CCE Status Report 2009, Coordination Centre for Effects, Bilthoven, p. 83-99

Lamb, E.G., Bayne, E., Holloway, G., Schieck, J., Boutin, S., Herbers, J., Haughland, D.L. 2009. Indices for monitoring biodiversity change: Are some more effective than others? Ecological Indicators 9:432–444

Latour JB, Staritsky IG, Alkemade JRM, Wiertz J. 1997. De natuurplanner; Decision Support Systeem natuur en milieu. Versie 1.1. RIVM Rapport 711901019. Bilthoven, 69 p.

Latour, J B, Reiling, R, Slooff, W. 1994. Ecological standards for eutrophication and desiccation: perspectives for a risk assessment. Water, Air, and Soil Pollution 78:265-279.

Margalef, R. 1963. On certain unifying principles in ecology. Americal Naturalist 97:357-374

McCann, K.S., 2000. The diversity - stability debate. Nature 405: 228–233

Odén, S. 1967. Nederbördens försurning. Dagens Nyheter, October 24.

Remke, E., Brouwer, E., Kooijman, A., Blindow, I., Esselink, H., Roelofs, J.G.M. 2009. Even low to medium nitrogen deposition impacts vegetation of dry, coastal dunes around the Baltic Sea. Environmental Pollution 157, 792–800.

Rowe, E.C., Emmett, B.A., Smart, S.M. 2009. A single metric for defining biodiversity damage using Habitats Directive criteria. In: J-P. Hettelingh, M. Posch, J. Slootweg (eds.): Progress in the modelling of critical thresholds, impacts to plant species diversity and ecosystem services in Europe: CCE Status Report 2009, Coordination Centre for Effects, Bilthoven, p. 101-107.

Schaminée, J H J, Stortelder, A H F, Westhoff, V. 1995. De vegetatie van Nederland I. inleiding tot de plantensociologie: grondslagen, methoden en toepassingen. Opulus Press, 296 p. Uppsala.

Schlutow, A., Huebener, P. 2004.The BERN Model: Bioindication for Ecosystem Regeneration towards Natural conditions. Environmental research of the Federal Ministry of the Environment, Nature Conservation and Nuclear Safety, Research Report 200 85 221. Berlin, 56 p.

Tongeren, O., Gremmen, N., Hennekens, S. 2008. Assignment of releves to pre-defined classes by supervised clustering of plant communities using a new composite index. Journal of Vegetation Science 19:525-536

Ulrich, B, Mayer, R, Khanna, P K. 1979. Deposition von Luftveruntreinigungen und ihre Auswirkung in Waldokosystemen in Solling. Sauerländer, Frankfurt a/M, 291 p.

Van Dobben, H F, Ter Braak, C J F, Dirkse, G M. 1999. Undergrowth as a biomonitor for deposition of nitrogen and acidity in pine forest. Forest Ecology & Management 114:83-95.

Van Dobben, H., de Vries, W. 2010. Relation between forest vegetation, atmospheric deposition and site conditions at regional and European scales. Environmental Pollution 158:921-933

Van Dobben, H., Wamelink, W. 2009. A Red-List-based biodiversity indicator and its application in model studies in the Netherlands. In: J-P. Hettelingh, M. Posch, J. Slootweg (eds.): Progress in the modelling of critical thresholds, impacts to plant species diversity and ecosystem services in Europe: CCE Status Report 2009, Coordination Centre for Effects, Bilthoven, p.77-81.

Van Dobben, H.F., Van Hinsberg, A., Schouwenberg, E.P.A.G., Jansen, M., Mol-Dijkstra, J.P., Wieggers, H.J.J., Kros, J., De Vries, W., 2006. Simulation of critical loads for nitrogen for terrestrial plant communities in The Netherlands. Ecosystems 9:32-45.

Van Herk, C.M. 1999. Mapping of ammonia pollution with epiphytic lichens in the Netherlands. Lichenologist 31: 9-20.

Veer, M.A.C., Kooijman, A.M. 1997. Effects of grass-encroachment on vegetation and soil in Dutch dry dune grasslands. Plant and Soil 192:119-128

Wamelink, G.W.W, Goedhart, P.W., Dobben, H.F van & Berendse, F. 2005. Plant species as predictors of soil pH: replacing expert judgement by measurements. Journal of vegetation science 16:461-470.

Wamelink, G.W.W., Joosten, V., van Dobben, H.F. Berendse, F. 2002. Validity of Ellenberg indicator values judged from physico-chemical field measurements. Journal of Vegetation Science 13:269-278

Wamelink, G.W.W., Ter Braak, C.J.F., Van Dobben, H.F. 2003. Changes in large-scale patterns of plant biodiversity predicted from environmental economic scenarios. Landscape Ecology 18: 513–527

Wamelink, G.W.W., van Adrichem, M.H.C., van Dobben, H.F. 2010. Milieutekorten in Gelderse habitatgebieden; nulmeting op basis van vegetatieopnamen. Alterra Report 1892, Wageningen, 92 p.

Part 3
Heavy Metals

Executive Summary

Revision of the Heavy Metals Protocol: Calculation of Emissions, Costs, Depositions and Exceedances of Four Scenarios.

Wil J.M. Prins[a] and Jaap Slootweg
*Ministry of Infrastructure and the Environment

The long-range transport of air pollution is an important factor affecting ecosystems and the human population. The United Nations Economic Commission for Europe (UNECE) Convention on Long-range Transboundary Air Pollution (LRTAP) is aimed at reducing and preventing air pollution. The LRTAP Convention has a number of legally binding protocols, covering specific categories of air pollutants. The Protocol on Heavy Metals (HM) was signed in 1998 and came into force in 2003. The objective of the HM Protocol is to introduce measures for the reduction of cadmium (Cd), lead (Pb) and mercury (Hg) emissions into the atmosphere, with a view to preventing adverse effects on human health and the environment. It describes the measures and the best available techniques for controlling emissions, and indicates programs, strategies and policies for achieving the heavy metals limit values specified in the protocol.

Currently the process for the revision of the Heavy Metals Protocol is underway. A draft text for the revised protocol and its annexes has been submitted by Switzerland (ECE/EB.AIR/WG.5/2010/6). This draft has partly been prepared based on the work of the Task Force on Heavy Metals.

To support the negotiations on the proposed amendments on the Heavy Metals Protocol a research project has been commissioned by the Netherlands producing four scenarios for which emissions, costs of emission reductions, depositions and exceedances of critical loads have been calculated. The four scenarios for cadmium, lead and mercury are:

1. 2010 current legislation and current ratifications of the HM Protocol (CLE)
2. 2020 full implementation of the HM Protocol (FIHM)
3. 2020 full implementation of the amended HM Protocol Option 1 for dust plus Hg measures (Option 1)
4. 2020 full implementation of the amended HM Protocol Option 2 for dust plus Hg measures (Option 2)

The "options" under scenario 3 and 4 refer to the specific emission limit values (ELV's) for particulate matter (PM) that are proposed in the draft revised protocol. Option 1 is the most ambitious, while Option 2 is somewhat less stringent. The study covers all countries taking part in the LRTAP Convention within the European domain.
The research project was a cooperative effort of several research institutions. First, TNO (Netherlands Organisation for Applied Scientific Research) made a projection of the emissions and emission reductions under the four scenarios. TNO also estimated the additional costs of the measures involved. This is described in Chapter 6. The next step was to calculate the depositions of the scenarios, based on the emission data. This has been executed by the Meteorological Synthesizing Centre-East (MSC East) and is described in Chapter 7. Finally, these depositions were used by the Coordination Centre for Effects (CCE) to determine to what extent critical loads for ecosystems and human health would be exceeded, as described in Chapter 8. The deposition causes elevated concentrations in the soil solution. Chapter 9 describes a preliminary analysis of the eco-toxicological effects of these elevated concentrations.

Conclusions and recommendations

The full implementation of the HM Protocol (FIMH) leads to substantial emission reductions in 2020 for cadmium and lead in Convention countries not part of EU27, except CHE and NOR. . Compared to the situation in 2010 under current legislation (2010 CLE) overall emission reductions of 97 and 1931 tons for Cd and Pb per year respectively, are projected for the European UN-ECE countries. Option 2 reduces a further 46 and 866 tonnes per year of Cd and Pb and seems a realistic choice if the ambition is to revise the HM protocol on par with the IPPC BAT Directive. Under Option 1, 76 and 1.598 tonnes per year of Cd and Pb are reduced on top of FIMH.

The situation for mercury is somewhat different. Hg emissions are expected to increase with 25 tons under the 2020 FIHM scenario compared to 2010 CLE. Under Options 1 and 2 modest emission reductions of 42 and 35 tonnes per year are projected, again in comparison to CLE 2010. Hg emissions are mostly gaseous, and therefore the reductions under Option 1 and Option 2, both including the same additional Hg measures, are very similar. High flow rates of emissions of coal fired power plants lead to substantial emissions of gaseous Hg, in spite of ELV < 0.03 mg Nm^{-3} (selective removal of gaseous Hg from PP flue gasses are not addressed in IPPC BAT).

The costs of revision of the HM protocol for UNECE Europe are estimated to be 1.3 and 11.6 billion € for Option 2 and Option 1, respectively. The reduction of emissions is not only beneficial regarding heavy metal pollution, the measures taken in Option 2 and Option 1 may also bring about considerable reductions of PM2.5 emissions in Europe. For the additional Hg emission reduction measures another 2.6 billion € should be added for both options.

The depositions of heavy metals are reduced, but not to the same extent as the reductions in emissions, due to the process of re-suspension. While the emission reductions are reflected in the lowering of critical load exceedances everywhere, still large parts of Europe's nature remain at risk.
Uncertainty analysis requires further assessment of the state of implementation of the current protocol and of the origins of re-suspended deposition.

6
Heavy Metal Emissions and Reduction Costs

Antoon Visschedijk, Hugo Denier van der Gon, Jeroen Kuenen, Hans van der Brugh
TNO Built Environment and Geosciences, Apeldoorn, The Netherlands

6.1 Introduction

In order to support negotiations on the revision of the Heavy Metals Protocol the emissions of cadmium (Cd), lead (Pb) and mercury (Hg) have been established for current legislation (CLE) in 2010. These emissions are compiled from officially reported country emission data, TNO projected emissions data from a similar TNO study in 2005 and the independent ESPREME heavy metal inventory. The compilation of the complete set is described in section 6.2. The methodology to estimate costs and emission reductions due to a possible revision of the HM protocol in 2020 for three scenarios can be found in section 6.3. The resulting emissions and its allocation over Europe are described in section 6.4 and the costs in section 6.5. This chapter is an abstract of the full report "Emissions, emission reductions and costs of options for a revision of the Heavy Metal Protocol for the priority heavy metals cadmium, mercury and lead" (Visschedijk et al. 2010).

6.2 Base year 2010 emission data for cadmium, lead and mercury

To assess the impact of a revision of the HM Protocol a new base year emission data set was needed. The new base year of choice was 2010. However, no reported emissions for 2010 are yet available. Therefore either projected 2010 data have to be used or officially reported data for a recent year as close as possible to 2010 can be taken as a best representation of the 2010 situation. Projected 2010 HM emission data were available from Denier van der Gon et al. (2005). But in line with this previous study which assessed the effectiveness of the Heavy Metal protocol (Denier van der Gon et al., 2005) officially reported data were preferred as they are supported by the national representatives and have more status in policy formation. To compile the 2010 baseline emissions, officially reported emissions have been compared to projected TNO 2010 emission estimates from Denier van der Gon et al. (2005).

Reported heavy metal emissions for the period 2003–2007 have been downloaded from the website of the Centre on Emission Inventories and Projections (CEIP) on 19 February 2010. Some countries do not report HM, while others show large (unexplainable) variations between years. In a previous study to the effectiveness of the UNECE Heavy Metals Protocol, TNO estimated emissions of heavy metals for the year 2000 (Denier van der Gon et al. 2005). This year 2000 inventory was, where possible, based on official reported emissions by countries. TNO default estimates have been used to complete the emission dataset where reported emissions were lacking or reported data deviated more than a factor 3 from TNO default estimates. Using the year 2000 emission inventory as a starting point, projected emissions for 2010 were developed which included assumptions on developments in activity data, based on baseline scenarios developed in the framework of the Clean Air For Europe (CAFÉ) program (Amann et al. 2005). Emission projections were made for two scenarios: 1) current legislation and current ratification and, 2) full implementation of the HM protocol. The assumptions underlying the TNO 2010 projected emission data are described in detail by Denier van der Gon et al. (2005).

Modification of road transport emissions

Compared to the 2010 data as described by Denier van der Gon et al. (2005), one important correction was made. Since the previous study TNO was able to measure heavy metal contents in road transport fuels (Denier van der Gon et al. 2009). These emission factors were used to recalculate the emissions from road transport for countries where no official reported data for road transport were available. This especially influenced the calculated lead emissions. The methodology and revision of emission estimates are described in detail in Denier van der Gon and Appelman (2009).

When comparing the two datasets two conclusions were apparent:

- Out of the total of 45 countries, 15 do not report emissions of heavy metals. These countries include a number of NIS countries[1], however also some EU Member States are not reporting HM emissions (Luxembourg, Greece).
- For the 30 countries that do report, differences are variable. Most pronounced differences are seen for the larger countries, such as Germany, Ukraine and Poland, but also for smaller countries differences can be very large.

[1] NIS countries (Newly Independent States) refers to countries that were part of the former Soviet Union

In case no officially reported data were available, the TNO-projected emissions were used. When both officially reported data and TNO projections were available these datasets were compared. If the two estimates were within a factor two from each other, the reported emissions were used. If the two estimates differed by more than a factor two, the estimate was chosen which is closest to the independent ESPREME heavy metal inventory (http://espreme.ier.uni-stuttgart.de/) which started in 2004. In the case of Germany the TNO emission estimate for 2010 was adjusted because of a high discrepancy with the officially reported data.

6.3 Methodology to estimate cost and emission reductions in 2020 due to a possible revision of the 1998 HM Protocol

For an accurate emission projection it is important to consider the expected developments of source activity rates. Future activity rates are derived from scenarios. The scenario data are used to estimate, e.g., future usage of various fuel types and industrial production. Several types of scenario data were used for projecting activity rates from the base year to the target year (2020) for the relevant source types:

- Energy use and fuel type shares (combustion by stationary sources and transport)
- Physical industrial production (industrial process emissions)
- Population growth and GDP development (waste generation and product use)

To project the year 2010 emissions to the year 2020 following different mitigation scenarios, assumptions have to be made about the change in activities over time. Denier van der Gon et al. (2005) used the baseline scenarios developed in the framework of the Clean Air for Europe (CAFE) program (Amann et al. 2005). These include two energy pathways: a Baseline scenario (BL) without climate policies and the Climate policy energy pathway (CP). Denier van der Gon et al. (2005) investigated the sensitivity of the HM projections for the choice of energy pathway. In general, the climate policies are found to have a small but positive effect on the emissions of HM, mostly due to a reduced use of coal. Comparison of emissions for the CP scenario and the BL scenario illustrated that the projections are not very sensitive to the exact definition of the energy pathway; for HM emissions the reduction measures and technologies implemented are much more important.
For the current study the activity projections as available from IIASA were revisited and the most recent appropriate

activity scenario (Primes 2009) was downloaded from http://gains.iiasa.ac.at/. This scenario was developed by IIASA for the revision of the Gothenburg Protocol and the revision of the NEC Directive (Amann et al. 2008) and used to project relevant HM emitting activities from 2010 to 2020.
Using the above outlined projection data the 2010 baseline emissions were projected to 2020 resulting in the 2020 current legislation emission scenario (2020_CLE). We have assumed that all currently agreed legislation, such as the IPPC Directive, has been implemented according to schedule, which is before 2010. For all countries that ratified the HM protocol, the 2020_CLE emission scenario assumes full implementation of the HM protocol. The 2020_CLE itself was not the objective of the present study but is necessary to properly construct the desired emission scenarios for the full implementation of the HM Protocol and any additional measures.
The second emission scenario constructed was full implementation of the HM protocol (FIHM) in all UNECE Europe countries in 2020. By definition this scenario only results in changes in emissions for countries that have not ratified the HM protocol in 2009 or before. Changes as a result of full implementation do furthermore not occur in countries where more stringent legislation is already in place (such as the IPPC Directive in the EU27). The HM Protocol has not changed since the previous study by Denier van der Gon et al. (2005) and their relative emission reductions per substance and per measure as a result of full implementation are still valid. The relative emission reductions per type of measure for these countries going from current legislation to full implementation of the HM protocol were hence taken from Denier van der Gon et al. (2005). The absolute emission changes differ from the values in Denier van der Gon et al. (2005), because a new base line was used.

Emission limit values (ELVs) for Option 1 and Option 2 of a revised HM protocol

The third and fourth emission scenario for the present study were emission reductions in 2020 following possible revision of the HM protocol due to the implementation of measures outlined in the "Draft possible amendments to the 1998 HM Protocol" (UNECE 2009). This UNECE internal document describes various proposed changes to the current HM Protocol. Regarding the specific emission limit values (ELVs) for major stationary sources in Annex V.II of the 1998 protocol, three options for new more stringent ELVs are proposed. Option 1 is the most ambitious, Option 3 the least stringent and Option 2 is in between Option 1 and 3. For the present study only emission reductions resulting from a revision following Option 1 and Option 2 have to be quantified.

Since emissions of Cd and Pb (and a minor part of Hg) are particle-bound, the ELVs of Option 1, 2 and 3 are expressed as maximum allowable particulate matter (PM) concentration in waste gas (UNECE 2009). PM-based ELVs are preferable over substance-based ELVs because PM monitoring is easier than monitoring HM concentrations in flue gases. Although UNECE (2010) also proposes component mass-based ELVs parallel to the PM-based ELVs, it was decided, after consultation of the commissioner of the project (VROM, personal communication), that only the PM-based Option 1 and Option 2 will be taken into account, except for Hg. Hg emissions are largely in gaseous form and therefore the additional Hg mass-based ELV for selected Hg sources was considered. Proposed Cd or Pb mass-based limit values, as well as Option 3 as described in UNECE (2010) were not taken into account.

The draft amendments to the Protocol make a distinction between existing installations and new installations for several activities. The ELVs for new installations are more stringent. Towards 2020 new installations will to a certain extent replace existing ones in Europe. However, due to the high capital intensiveness of the activities under consideration it is expected that only few new installations will be built in this 10 year timeframe, and production is likely to be increased (if increased at all) by modernisation of existing plants only. Furthermore, although some penetration of new plants and closure of existing plants in power generation and waste incineration is expected, no list of installations to be replaced exists. Hence it is not known what contribution the possibly replaced installations make to the total 2010 or 2020 CLE emissions. To simplify our analysis we therefore only take the ELVs for existing installations into account, and for the moment ignore those proposed for new plants. Especially for large combustion plants this may cause some overestimation of emissions.

Selected mercury emission control measures

Besides ELVs for dust, component mass-based ELVs are considered for addition to a revised HM Protocol . As mentioned earlier, it has been decided to only regard the proposed mercury ELVs for major sources of Hg. Based on Denier van der Gon et al. (2005) the production of cement and coal-fired power plants were identified as the two main sources of Hg, accounting for almost 70% of the remaining Hg emission after full implementation of the HM Protocol.

To revise the current HM Protocol several measures related to the use of Hg-containing products are considered as well. Hg-containing products can cause air emission of Hg when they are disposed of in waste incinerators. According to Denier van der Gon et al. (2005)

waste incineration makes a contribution to the total Hg emission of less than 1% after full implementation of the current HM Protocol. The proposed revision of the ELV for Hg would furthermore roughly cut this emission in half, based on the difference in ELVs for Hg. Because of the fact that Hg from waste incineration is specifically controlled to remain under the ELV we see no significant direct influence of the proposed measures related to product use on the total air emission of Hg (which does not mean that these measures would have no positive effect). In this study these Hg measures will not be taken into account.

The use of reference documents on Best Available Techniques (BREF)

Option 1 and Option 2 to revise the current HM Protocol consist of different ELVs for PM, complemented with additional mercury emission control measures to achieve the Hg ELVs. The revision is aimed at bringing the HM Protocol in line with other European air emission legislation, such as the IPPC BAT Directive. The European IPPC Bureau produces reference documents on Best Available Techniques, called BREFs (see http://eippcb.jrc.es/reference/). BREFs are the main reference documents used by competent authorities in Member States when issuing operating permits for the installations that represent a significant pollution potential in Europe. The ELVs under Option 1 and Option 2 proposed by the Task Force on Heavy Metals are primarily based on the Task Force's own research and the IPPC BREF documents. The BREF documents often specify a Best Available Technology Associated Emission Level (BAT AEL), which entails the expected lower and upper boundary of the emission when BAT is implemented. Option 1 and Option 2 are defined as follows (personal communication M. Hiete 2010):

- "Option 1 is a demanding but technically feasible option with the objective of achieving a high level of reduction. The ELV is based on a value between the lower and upper BAT AEL (where it is available)
- Option 2 while technically demanding, pays greater attention to the costs of the measures for achieving reduction. The ELV is a value based on the upper BAT AEL (where it is available)"

In order to associate ELVs to these definitions, the Task Force defined techniques that can be considered as BAT (largely where available but not exclusively based on the BREF) and then determined an AEL. As there are often several BATs (each with its specific AEL range), the AELs for different techniques considered as BAT also result in a range. For example, in some cases both fabric filters and ESPs (electrostatic precipitators) have been identified as BAT. Then an ESP might be enough to achieve the Option 2 ELV and a fabric filter needed for the Option 1 ELV. In less complex cases, Option 1 basically represents the lower boundary and Option 2 the upper boundary of the AEL. It is important to realize that the exact choice of reduction measures is not clearly defined and there is considerable room for interpretations.

For the current study it is essential to know if and when Option 1 and/or 2 will be automatically met by implementation of autonomous measures such as the IPPC Directive. If this is the case Option 1 and/or 2 will be met by current legislation and no additional emission reduction and costs are foreseen. This will be discussed per source category in more detail. According to our findings implementation of the IPPC Directive does not always mean that Option 1 or even 2 will be met, in spite of both options being theoretically achievable by the best performing technique.

Estimation of emission reduction due to Option 1 and Option 2

Starting point for the estimation of the effect of amending the current HM Protocol according to Option 1 and Option 2 are the projected HM emissions in 2020 after full implementation of current Protocol (also for countries that have not ratified) plus all agreed and planned emission reduction measures under current legislation (e.g. IPPC Directive and other UNECE Protocols for countries that have ratified them). This is referred to as the 2020 FIHM scenario. HM emission reduction as a result of tighter ELVs is estimated based on the difference in particle concentration before and after implementation of the limit values. We assume that the old ELVs and the new ELVs are a good indication of the actual PM emissions; Parties are not likely to reduce emissions further than what is required by legislation. However, in some cases this approach may cause a mismatch between presumed concentrations and the actual performance of real world measures.

The method to estimate the emission reductions and costs of Option 1 and Option 2 builds on the work by Visschedijk et al. (2006) who evaluated a range of options to revise the current HM Protocol. In many cases the control options proposed by Visschedijk et al. (2006) resemble those required for Option 1 or Option 2, and the measures required are comparable. Emission reduction of particle-bound HM is not always linearly dependent on PM concentration due to the so-called enrichment effect. There is enrichment of heavy metals in smaller sized particles whereas particle removal tends to favour larger particles. Visschedijk et al. (2006) compensated for this effect by estimating both the degree of HM enrichment and particle size dependent removal efficiencies. This was predominantly of influence when going from high (e.g. >100 mg/Nm^3) to low (e.g. 20 mg/Nm^3) concentrations (with the particle size distribution changing from a mixture

of larger and smaller particles to almost entirely fine particles). With the residual PM concentrations after full implementation of the HM protocol and EU CLE (below 20 mg/Nm^3), we assume that the PM already exclusively consists of fine particles and that further HM emission reduction (e.g. from 20 to 10 or 5 mg/Nm^3) is proportional to the further decrease in PM concentration. Moreover, the techniques required by Option 1 and Option 2 (such as fabric filters) have an equal (or sometimes even better) removal efficiency for smaller compared to larger particles. In these cases enrichment is not relevant anymore. In summary, in general we used the reduction factors derived from Visschedijk et al. (2006) to go from high (>20 mg/Nm^3) to low (<20 mg/Nm^3) PM concentrations (taking enrichment and selective removal of fine PM into account) and estimated further emission reduction (down to e.g. 5–10 mg/Nm^3) by assuming particle-bound HM emission to be proportional to PM concentration.

Estimation of costs of Option 1 and Option 2

Specific measures and control technologies that result in achieving the specific ELV have been identified for each individual sector to estimate the costs of implementation of Option 1 and Option 2. The selected control technologies have been successfully implemented in the past for the type of installation under consideration and their performance has proved to be adequate to meet the ELVs of Option 1 or Option 2. The selection of measures is for a considerable part based on the work by Visschedijk et al. (2006) who collected and presented cost data for a series of measures to revise the current Protocol. Visschedijk et al. (2006) specified ELVs after implementation of the measures that are in many cases close to Option 1 or 2. This information has been supplemented by additional literature information when necessary.
We aimed to identify a control technology for each case that is the most cost-efficient way to meet the ELVs under Option 1 or Option 2. This however proved only to be possible to a certain degree. The estimated costs by measure are a first order indication because:

- The Task Force on Heavy Metals aimed to pay greater attention to costs with Option 2 compared to Option 1. However, at this stage there is no quantitative data available.
- In order to meet an ELV for PM of less than 20 mg/Nm^3, in certain cases a fabric filter will be the only technique able to achieve this. In these cases it will often not make a difference whether the ELV is 20, 15, 10 or 5 mg/Nm^3 as the same technique will have to be implemented. There will be differences in investment and operational costs for achieving these different ELVs but as long as the techniques are similar such differences are difficult to quantify without going into much more installation-specific detail which is out of scope of the present study.
- Often a measure that is guaranteed to meet a certain ELV is likely to reach lower emission levels in practice. This is especially the case when an installation operates only a little bit above Option 1 or 2. For example, if an installation operates at 30 mg/Nm^3 and needs to be brought down to 20 mg/Nm^3 with an additional fabric filter, actual emission after implementation will probably be close to 5 mg/Nm^3 or even below that value. There is often no technique identifiable that will only achieve a decrease of ~30 to 20 mg/Nm^3. It is important to note that this leads to a mismatch between the ELVs in the legislation and the actual achieved concentrations.
- It is impossible to predict down to a few mg/Nm^3 how a specific control technology will generally perform for a specific sector or source. Vice versa, a measure that represents the minimal effort to meet an ELV is often hard to identify. This is especially true for the concentration ranges between 5-30 mg/Nm^3.

These complications may prohibit the identification of individual measures down to a level where we can differentiate between Option 1 and Option 2. This will have consequences for the assessment of cost-effectiveness of Option 1 or Option 2. In addition, the limitations of costs data as discussed by Visschedijk et al. (2006) apply here as well. To summarize, the cost estimation provide an indication of the costs of different measures but it should be acknowledged that there is considerable uncertainty, especially when distinguishing at the individual sector level between the two revision packages.

6.4 HM emissions in 2010 and projected emissions for 2020 following different scenarios

Cadmium

Under current legislation the emission of Cd will grow with 7% to 356 tonnes per year in 2020. Full implementation of the HM protocol reduces total emissions by 120 tons per year, compared to the 2020 CLE scenario, due to measures in the non-EU27 countries that have not ratified the HM protocol as of 2009. The Option 1 scenario is more stringent than Option 2; compared to the FIHM scenario emissions are reduced by 76 and 46 tons/yr, respectively. Total Cd emissions by country are presented in Table 6.1. Emissions per sector and the reductions for the scenarios are plotted in Figure 6.1.

Table 6.1 National Cd emissions (kg) in UNECE Europe in 2010 and 2020 for the different scenarios

Country (ISO3)	2010 CLE	2020 CLE	2020 FIHM	2020 Option 1	2020 Option 2
ALB	196	197	184	159	165
ARM	156	156	151	150	151
AUT	1219	1244	1244	1120	1244
AZE	2767	2767	2758	832	1348
BEL	1597	1918	1918	1738	1918
BGR	3511	3628	3628	2537	3628
BIH	1572	1468	647	429	488
BLR	2583	2590	1718	1069	1291
CHE	2892	2579	2579	2480	2579
CYP	1205	528	528	275	528
CZE	1134	1129	1129	931	1129
DEU	10293	10981	10981	9740	10981
DNK	747	941	941	845	941
ESP	17787	19415	19415	17298	19415
EST	687	494	494	279	494
FIN	1106	1099	1099	969	1099
FRA	9056	8646	8646	6570	8646
GBR	3368	3537	3537	3202	3537
GEO	265	265	255	155	182
GRC	2378	2521	2521	1943	2521
HRV	790	777	745	378	466
HUN	1484	2219	2219	1460	2219
IRL	626	618	618	482	618
ISL	85	98	98	76	82
ITA	8648	9167	9167	8643	9167
KAZ	22386	22386	13573	5493	6979
KGZ	433	433	346	328	333
LTU	408	459	459	252	459
LUX	55	64	64	64	64
LVA	592	587	587	363	587
MDA	327	325	325	275	289
MKD	9623	9286	4475	744	1227
MLT	617	617	617	617	617
NLD	1942	2059	2059	1772	2059
NOR	587	609	609	596	609
POL	39648	36160	36160	32971	36160
PRT	2350	2119	2119	1537	2119
ROM	2466	2530	2530	2293	2530
RUS	123849	143314	62448	26490	35305
SVK	3321	3623	3623	3178	3623
SVN	1320	1522	1522	1389	1522
SWE	607	494	494	431	494
TUR	17915	20764	10048	5668	6964
UKR	19093	19800	12744	9635	10900
YUG	8426	9408	3103	1314	1749
Grand Total	332,117	355,544	235,127	159,169	189,426

Figure 6.1 Cd emissions per sector, and the reductions under the four scenarios.

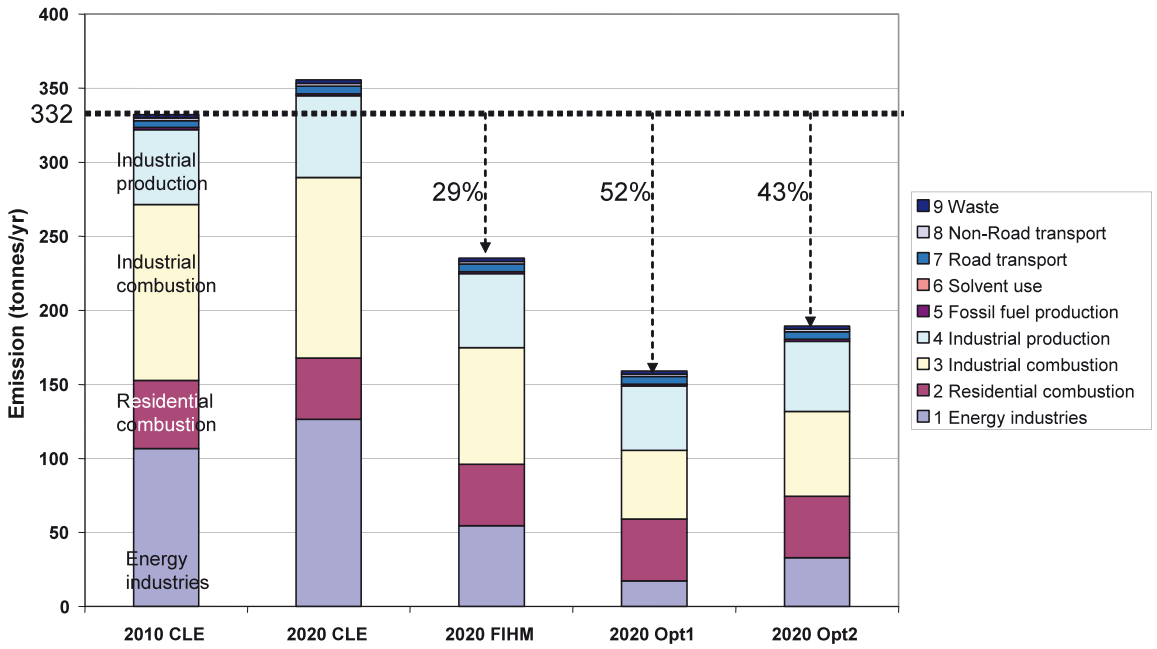

Lead

Under current legislation the emissions of Pb will increase by 5% to 6230 tons per year in 2020. Full implementation of the HM protocol reduces total emissions by 2253 tons per year, compared to the 2020 CLE scenario, due to measures in the non-EU27 countries that have not ratified the HM protocol as of 2009. The Option 1 scenario is more stringent than Option 2; compared to the FIHM scenario emissions are reduced by 1598 and 866 tons/yr, respectively. Total Pb emissions by country for the different scenarios are presented in Table 6-2.

Under the current legislation, Pb emissions are dominated by the energy production sector as well as industrial combustion and production. These sectors are addressed in the FIHM scenario and even more so in the Option 1 and Option 2 scenarios. The result is that eventually Pb emissions from the energy industries (power plants) are significantly reduced and Pb emissions are dominated by industry sectors (combustion and production). For Pb the source sector SNAP 3 “Industrial combustion” covers all process emissions from the non-ferrous metals and non-metallic minerals production sector while SNAP 4 “Industrial production” includes almost the entire iron and steel industry. Both sectors are important for Pb emission, as can be seen in Figure 6.2.

Table 6.2 National Pb emissions (kg) in UNECE Europe in 2010 and 2020 for the different scenarios

Country (ISO3)	2010 CLE	2020 CLE	2020 FIHM	2020 Option 1	2020 Option 2
ALB	1340	1343	939	871	887
ARM	618	618	498	461	464
AUT	15336	16220	16220	13061	16220
AZE	7823	7823	7588	4229	5122
BEL	60549	71210	71210	55960	71210
BGR	65851	68345	68345	40590	68345
BIH	91102	27326	7457	2979	4180
BLR	58992	58993	41680	14404	18097
CHE	19877	19842	19842	19014	19842
CYP	977	952	952	842	952
CZE	44065	42689	42689	28256	42689
DEU	289850	311065	311065	247197	311065
DNK	6166	5894	5894	4213	5894
ESP	278059	322493	322493	257592	322493
EST	11193	9658	9658	5985	9658
FIN	21210	21835	21835	16777	21835
FRA	109027	111886	111886	85770	111886
GBR	71134	72017	72017	55125	72017
GEO	14755	14755	14455	14249	14304
GRC	12117	13130	13130	11478	13130
HRV	9184	10793	10481	4747	5316
HUN	34561	39393	39393	26962	39393
IRL	14779	12080	12080	11519	12080
ISL	197	205	204	142	158
ITA	273719	289441	289441	228764	289441
KAZ	650982	650982	369683	176102	219523
KGZ	8445	8445	4372	3478	3712
LTU	6797	6898	6898	5355	6898
LUX	5174	6099	6099	6090	6099
LVA	1170	1729	1729	1321	1729
MDA	1112	914	914	868	879
MKD	59949	40900	23667	4123	6568
MLT	848	848	848	848	848
NLD	39352	40543	40543	33242	40543
NOR	7041	7355	7355	6802	7355
POL	276459	262308	262308	213229	262308
PRT	22080	21060	21060	15365	21060
ROM	77378	83692	83692	67272	83692
RUS	2015655	2450767	998831	353183	530920
SVK	27269	27555	27555	19441	27555
SVN	14382	15372	15372	14904	15372
SWE	16016	15245	15245	13217	15245
TUR	187079	203004	128082	73533	88239
UKR	785004	804164	436643	214994	288958
YUG	193796	32527	14845	5029	7381
Grand Total	5,908,469	6,230,414	3,977,194	2,379,582	3,111,562

Figure 6.2 Pb emissions per sector, and the reductions under the four scenarios.

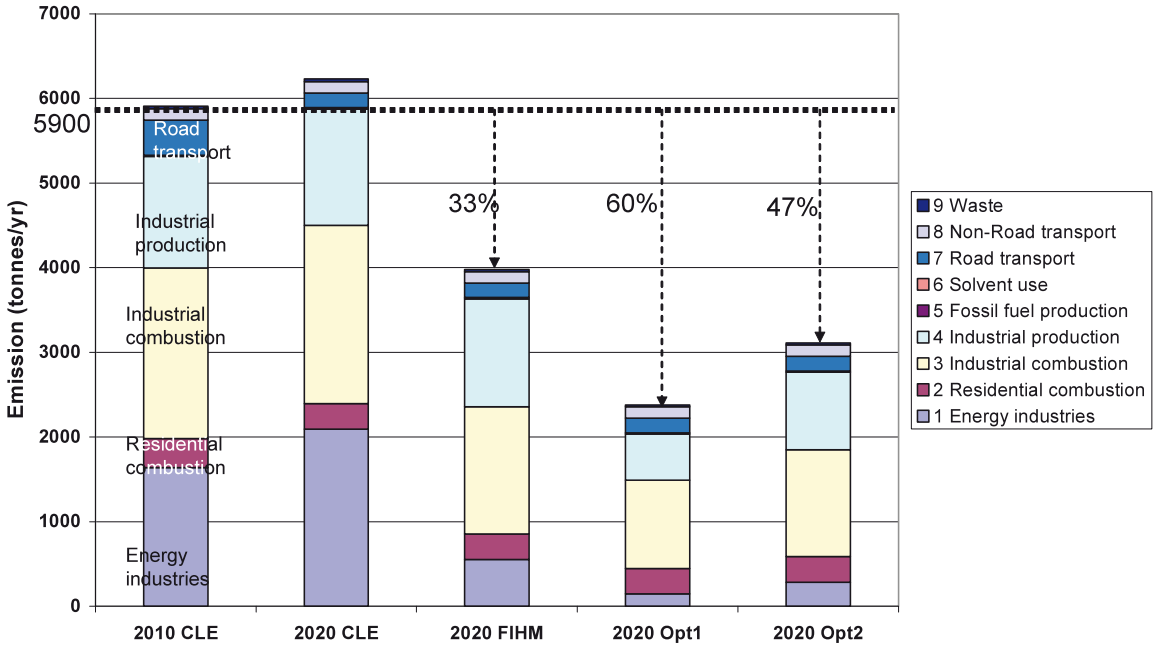

Mercury

Under current legislation the emission of Hg will increase with 15% to 292 tons per year in 2020. Full implementation of the HM protocol reduces the total emissions by 12 tons per year, compared to the 2020 CLE scenario, due to measures in the non-EU27 countries that have not ratified the HM protocol as of 2009. For Hg there is little difference between the Option 1 and Option 2 scenarios as they assume implementation of the same measures; compared to the FIHM emissions are reduced by 67 and 61 tons/yr, respectively. The small additional reduction under the Option 1 scenario is caused by dust control measures in the energy transformation sector (power plants). Total Hg emissions by country for the different scenarios are presented in TableTable 6-3 National Hg emission (kg) in UNECE Europe in 2010 and 2020 for the different scenarioshe contributions to the total emissions per sector and the reductions are shown in Figure 6.3.

Under the current legislation, Hg emissions are dominated by the energy production sector and industrial combustion. This remains the case following the FIHM scenario, but under the Option 1 and Option 2 scenarios the Hg emissions from industrial combustion are abated. The result is that Hg emissions are dominated by the energy production sector (~ 60%), and industrial combustion contributes another ~23%. Reductions in industrial combustion (SNAP 3) are the result of Hg control measures in the cement industry. The major remaining emissions are in SNAP 1 and due to coal-fired power plants for which there are no specific additional Hg control measures planned.

Table 6.3 National Hg emission (kg) in UNECE Europe in 2010 and 2020 for the different scenarios

Country (ISO3)	2010 CLE	2020 CLE	2020 FIHM	2020 Option1	2020 Option 2
ALB	195	194	189	152	153
ARM	197	197	192	148	148
AUT	1054	1130	1130	761	772
AZE	1174	1174	1168	1009	1041
BEL	2737	3324	3323	2171	2195
BGR	1612	1722	1722	1104	1124
BIH	1841	1670	1559	1376	1429
BLR	741	741	695	301	305
CHE	1050	945	945	541	543
CYP	672	701	701	318	322
CZE	3922	3970	3970	2874	2932
DEU	9780	10144	10144	6999	7152
DNK	1119	1053	1053	863	876
ESP	10804	12338	12289	7456	7608
EST	656	628	628	597	615
FIN	812	846	846	604	618
FRA	6904	6063	6063	4843	4928
GBR	7190	6837	6808	5153	5225
GEO	305	305	297	223	225
GRC	7784	8657	8641	4266	4343
HRV	624	692	665	405	415
HUN	2829	3086	3086	1755	1772
IRL	858	969	959	507	512
ISL	106	109	96	61	63
ITA	10712	11246	11221	7194	7260
KAZ	19516	19516	18575	17180	17676
KGZ	732	732	705	596	604
LTU	431	445	445	299	306
LUX	290	315	315	112	113
LVA	30	36	36	35	36
MDA	137	126	126	108	112
MKD	1793	1597	1528	1256	1275
MLT	626	626	626	626	626
NLD	655	676	676	560	572
NOR	759	792	792	623	626
POL	15880	16089	16089	12931	13227
PRT	2758	2645	2645	1779	1812
ROM	4130	4099	4099	3513	3572
RUS	92713	117565	110165	95340	98828
SVK	2722	3301	3301	1683	1695
SVN	571	683	683	438	447
SWE	640	533	533	417	422
TUR	22337	30278	28249	13682	13943
UKR	7558	7741	6874	6228	6429
YUG	5343	5899	5495	4642	4823
Grand Total	255,299	292,438	280,347	213,728	219,720

Figure 6.3 Hg emissions per sector, and the reductions under the four scenarios.

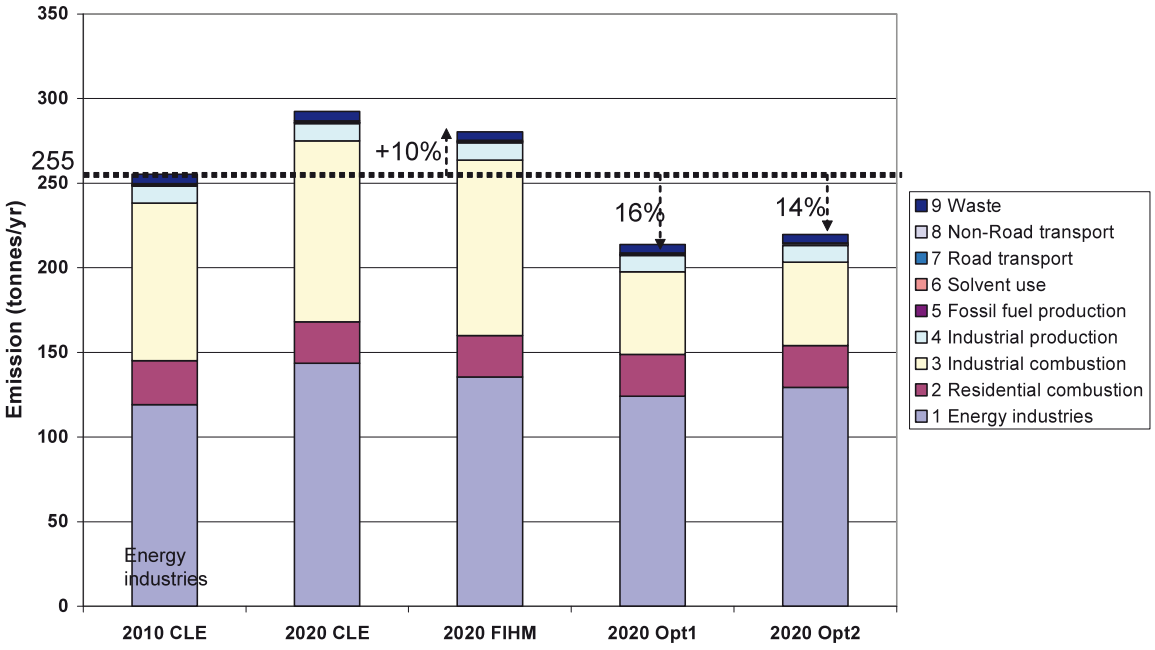

Spatial distribution of the emission data

The emission data were spatially distributed using the TNO tools developed under the UBA project PAREST (Denier van der Gon et al. 2010a) and EU FP6 project EUCAARI (Denier van der Gon et al. 2010b). For each source category a split was made between emissions from point sources and area sources. Examples of point sources are power plants, refineries and major industries, such as iron and steel plants. Examples of area sources are road transport and residential combustion. For the point sources a new highly detailed database was compiled whereas for the area sources new geographical distribution maps were compiled for use as proxies (e.g. population density is used to distribute emissions from residential combustion). For a detailed description of the gridding tools we refer to Denier van der Gon et al. (2010a). On request of EMEP MSC-East, the emissions were gridded on a 25×25 km² EMEP grid.

6.5 Estimated costs of a possible revision of the HM protocol

Revision of the HM protocol following Option 2 is less ambitious than Option1 and as a consequence less expensive. Total estimated costs for implementation of option 2 in UNECE Europe are 1.3 billion €. These costs will have to be met by the non-EU27+ (=EU27+NOR+CHE) countries. This is somewhat misleading because the costs will also be born by EU27+ countries, but as a consequence of the IPPC and other EU directives. Hence it is considered current legislation and no "additional" costs are incurred by EU27+ to meet Option 2. Option 1 is more ambitious and substantially more expensive. Total costs in UNECE-Europe are estimated at 11.6 billion €. The majority of these costs (66%) will have to be met by the EU27+ countries. Clearly the more stringent Option 1 ELVs are not covered by current legislation and therefore, cause additional costs for all countries in UNECE Europe.
Total costs for implementing the additional Hg measures was estimated at 2.6 billion €; again about 2/3 of these costs are located in the EU27+ countries and about 1/3 in other UNECE-Europe. Table 6.4 lists the costs per country and Figure 6.4 shows the cost by sector for Option 1, Option 2 excluding the separately plotted package of additional Hg measures.

It is remarkable that the additional Hg measures only bring about substantial costs in the cement production industry despite the fact that it is not the largest source of Hg in UNECE Europe. Coal-fired power plants on average meet the proposed ELV of the additional Hg measures but due to the large flow rates of flue gasses, they still emit substantial amounts of Hg. This observation also indicates that, exactly because of the high flow rates and relatively low concentrations, costs of additional reduction measures that would address the release from coal-fired power plants will be high, as was also estimated by Visschedijk et al. (2006).

Table 6.4 Estimated costs of implementation (in million €) of a revision of the UNECE HM protocol following Option 1 or Option 2 and additional Hg measures.

Region	Country ISO3	Option 1	Option 2	Hg measures
EU27+NOR+CHE				
	AUT	107	0	28
	BEL	159	0	61
	BGR	180	0	19
	CHE	10	0	31
	CYP	1.9	0	16
	CZE	402	0	35
	DEU	2345	0	197
	DNK	99	0	14
	ESP	562	0	333
	EST	69	0	5.4
	FIN	139	0	10
	FRA	323	0	148
	GBR	745	0	78
	GRC	232	0	119
	HUN	59	0	23
	IRL	49	0	19
	ITA	408	0	304
	LTU	2.7	0	4.8
	LUX	0.4	0	4.9
	LVA	3.1	0	1.5
	NLD	165	0	14
	NOR	14	0	12
	POL	1138	0	120
	PRT	73	0	46
	ROM	190	0	53
	SVK	81	0	27
	SVN	48	0	9.1
	SWE	72	0	15
EU27+NOR+CHE subtotal		7676	0	1748
Other UNECE-Europe				
	ALB	0.4	0.4	0.0
	ARM	0.6	0.5	1.4
	AZE	7.6	7.5	1.7
	BIH	68	6	0.0
	BLR	17	10	12
	GEO	0.8	0.5	2.2
	HRV	25	4.6	25
	ISL	0.1	0.0	0.0
	KAZ	597	227	7.6
	KGZ	7.5	0.8	2.9
	MDA	27	6.6	1.4
	MKD	30	4.9	0.0
	RUS	1367	487	209
	TUR	921	385	514
	UKR	600	154	34
	YUG	237	25	0.0
Other UNECE-Europe subtotal		3906	1319	812
Total UNECE Europe		11,583	1,319	2,560

Figure 6.4 Cost by sector for Option 1, Option 2 and, separately, the costs of the package of additional Hg measures.

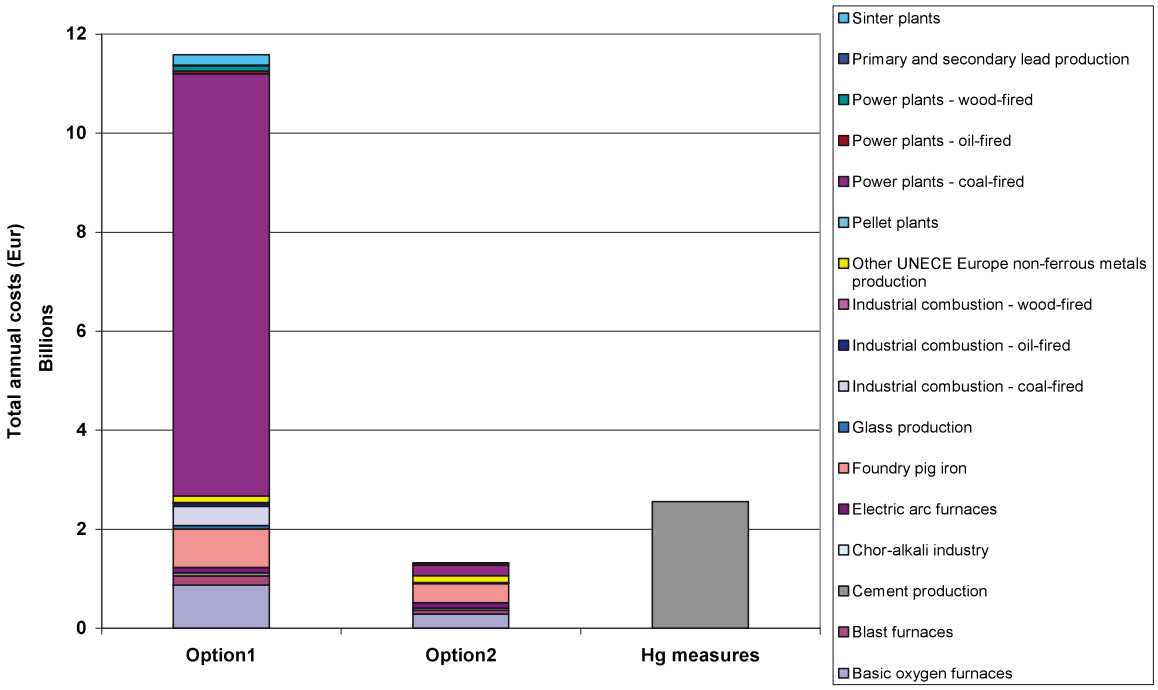

6.6 Discussion and Conclusions

Full implementation of the HM protocol (FIHM) in 2020 brings about a substantial reduction in non-EU27 counties, except for countries that have comparable environmental legislation such as Norway and Switzerland. Emission reductions following the FIHM_2020 scenario compared to 2020 CLE amount to 120, 12 and 2253 tons of Cd, Hg, and Pb, respectively. Likewise, the implementation of a revision of the HM protocol following Option 2 brings about further emission reductions (and costs) in the non-EU European countries but not in the EU27+NOR+CHE because the current legislation like the EC IPPC Directive asks for similar measures. Obviously, implementing the IPPC directive brings about substantial costs, but costs considered under current legislation (CLE) are not considered in this study. Emission reductions under the Option 2 scenario compared to the FIHM_2020 scenario amount to 46 and 866 tonnes of Cd and Pb, respectively. Revising the HM protocol following Option 1 brings about a reduction of 76 tons of Cd and 1598 tons of Pb, compared to the FIHM_2020 scenario. The emission reductions due to a revision of the HM protocol for Cd and Pb following Option 2 are located in the UNECE –Europe countries that do not belong to the EU27+NOR+CHE.

This study showed that while Option 1 may be based on IPPC BAT AELs, additional measures on top of IPPC BAT are often necessary to meet Option 1. A complication for proper interpretation is that a BAT AEL is not the same as an ELV nor should it be interpreted as such. If the ambition is to revise the HM protocol in such a way that it is on par with the IPPC BAT Directive, Option 2 appears a realistic choice, but clearly substantial further reduction is achieved following Option 1.

The reduction of Hg is roughly the same under Option 1 and Option 2, because the same additional measures to combat gaseous releases of Hg are proposed. Implementation of additional Hg measures result in 67 and 61 tonnes Hg reduction following Option 1 and Option 2, respectively. The slight difference is due to additional particle bound Hg reductions following Option 1. Since the additional abatement of gaseous Hg emissions is not foreseen in EU CLE and the Hg emission reductions for both options are comparable, the spatial distributions of emission reductions for both options are similar and substantially different from Pb and Cd. Only slightly more Hg reductions occur under Option 1 as a result of some dust reduction measures. Hg emissions are largely gaseous and are only slightly affected by conventional PM control measures. Hg removal requires a different type of measure, more similar to end-of-pipe measures aimed at removal of gaseous PCDD/F emission. Coal-fired power plants and cement production are the most important Hg sources in the sectors addressed by a revision of the HM protocol.

Amending the HM Protocol according to Option 1 and Option 2 may bring about significant additional reductions

of PM2.5 emissions in Europe. This is especially the case for the non-EU countries, because the sectors addressed by a revision of the HM Protocol are major sources of PM in these countries. Moreover, no autonomous measures comparable to the EC directives (e.g., LCP, IPPC) are foreseen in these countries. However, the data sets to estimate the emission reductions were not fully compatible, and additional investigations of the co-benefits of a revision of the HM Protocol for PM reduction are highly recommended.

References

Amann M, Bertok I, Cofala J, Gyarfas F, Heyes C, Klimont Z, Schöpp W, Winiwarter W, 2005. Baseline Scenarios for the Clean Air for Europe (CAFE) Programme. Final Report, IIASA February 2005

Amann M, Bertok I, Cofala J, Heyes C, Klimont Z, Rafaj P, Schöpp W, Wagner F, 2008. NEC Scenario Analysis Report Nr. 6, National Emission Ceilings for 2020 based on the 2008 Climate & Energy Package International Institute for Applied Systems Analysis (IIASA), Laxenburg, Final version July 2008

Denier van der Gon HAC, Appelman WAJ, 2009. Lead emissions from road transport in Europe. A revision of current estimates using various estimation methodologies. *Science of the Total Environment* 407: 5367–5372

Denier van der Gon H, Verheul M, Appelman W, Klaver G, Bosch P, 2009. Metal contents of diesel and petrol fuel sold on the European Market, poster presented at CONCAWE, Workshop on Environment & Health, Evaluating European Air Quality Research and Translating Priorities into Actions, 19 & 20 January 2009, Hotel Bedford, Brussels (Belgium)

Denier van der Gon HAC, Van het Bolscher M, Visschedijk AJH, Zandveld PYJ, 2005. Study to the effectiveness of the UNECE Heavy Metals Protocol and costs of possible additional measures; Phase I: Estimation of emission reduction resulting from the implementation of the HM Protocol, TNO Report B&O-A R 2005/193.

Denier van der Gon HAC, Visschedijk AJH, Van der Brugh H, Dröge R, 2010a. A high resolution European emission data base for the year 2005, A contribution to UBA-Projekt PAREST (Particle Reduction Strategies), TNO report (in prep.)

Denier van der Gon HAC, Visschedijk AJH, Dröge R, Johansson C, Klimont Z, 2010b. A high resolution emission inventory of particulate elemental carbon and organic carbon for Europe in 2005 (submitted)

ESPREME project - Integrated Assessment of Heavy Metal Releases in Europe, http://espreme.ier.uni-stuttgart.de/

Pulles T, Appelman W, 2008. Air pollution from electricity-generating large combustion plants. EEA Technical Report No.4/2008

UNECE, 2009. Draft possible amendments to the 1998 HM Protocol, 18-12-2009

UNECE, 1998. The 1998 Aarhus Protocol on Heavy Metals; http://www.unece.org/env/lrtap/hm_h1.htm

Visschedijk AJH, Denier van der Gon HAC, Van het Bolscher M, Zandveld PYJ, 2006. Study to the effectiveness of the UNECE Heavy Metals (HM) Protocol and cost of additional measures. Phase II: Estimated emission reduction and cost of options for a possible revision of the HM Protocol, TNO-Report 2006-A-R0087/B

WEPP, 2008. World Electric Power Plants Database. http://www.platts.com/

7 Calculations of Depositions of Lead, Cadmium and Mercury for different Options for the Revision of Heavy Metals Protocol

Ilia Ilyin, Oleg Travnikov
Meteorological Synthesizing Centre East, Moscow, Russia

7.1 Introduction

In this chapter the depositions that result from the emissions described in Chapter 6 are presented and discussed.

7.2 Brief model description

Calculations of atmospheric transport and deposition of heavy metals lead (Pb), cadmium (Cd) and mercury (Hg) over the EMEP domain were carried out using the EMEP heavy metal (HM) model MSCE-HM. It is a three-dimensional off-line eulerian model with terrain-following vertical coordinate. Vertically the model domain is split into 15 layers from the surface to about 15 km. The thickness of the lowest layer is around 70 m. The horizontal spatial resolution of the model is 50 × 50 km. The model includes the main processes governing atmospheric transport and deposition of heavy metals, such as dispersion, wet and dry ecosystem-dependent deposition, wind re-suspension of particles containing heavy metals, and atmospheric chemistry of mercury. A more detailed description of the model is available in Travnikov and Ilyin (2005). The reliability of MSCE-HM model was analysed in the framework of the model review procedure, curried out under EMEP [http://www.unece.org/env/lrtap/emep/emep30_docs.htm].

This model was used to calculate the deposition of lead, cadmium and mercury for several emission scenarios developed by TNO. The following scenarios were considered:

CLE 2010	:	2010 current legislation and current ratification of the HM Protocol
FIHM	:	2020 full ratification of the HM Protocol
Option 1	:	2020 full ratification of the amended HM Protocol Option 1 for dust plus Hg measures
Option 2	:	2020 full ratification of the amended HM Protocol Option 2 for dust plus Hg measures

Previous work on the modelling of heavy metal pollution levels on the basis of emission scenarios for 2010 and 2020 can be found in Hettelingh and Sliggers (2006). Both the

model and the input data have been modified since then. First of all, emission scenario data have been updated. The main difference in modelling is that re-suspension scheme for heavy metals has been significantly improved (Gusev et al. 2006, Ilyin et al. 2007), although the uncertainties associated with wind re-suspension are still high. Besides, the EMEP modelling domain was extended eastward in 2008 in order to cover also the territory of the Central Asian countries (Kazakhstan, Kyrgyzstan, Turkmenistan, Uzbekistan and Tajikistan). Finally, MSC-E started using the ECMWF (European Centre for Medium-range Weather Forecasts) analysis instead of the NCEP/DOE re-analysis data for the generation of meteorological parameters.

7.3 Input data for modelling

Input data to the model include meteorological information, emission data and geophysical information (land cover distribution, soil properties etc.). Since the idea of scenario calculations is to trace changes in pollution levels in response to changes in emission data, it is reasonable to keep all input data except the emissions the same for all scenarios. That is why the same meteorological data (for the year 2008) and land-cover were used in calculations.

The concentration of heavy metals in top soils is one of the key parameters for computing wind re-suspension. This concentration consists of a natural and of a historical component, accumulated over a long (decades-centuries) period of anthropogenic pollution. Emissions of heavy metals in Europe generally decline since about 2000. Therefore, in the long run, also soil concentrations will decrease. It was assumed that changes in soil concentrations between 2010 and 2020 were minor. However, when modelling over longer periods, the long-term changes of soil concentrations should be considered, e.g., by using dynamic modelling including deposition, leaching, wind erosion, etc. Since wind re-suspension of heavy metals is assumed to depend on meteorological parameters, soil concentrations and land cover distribution, it has been kept constant in the calculations for all scenarios. Air concentrations at the EMEP boundaries can also change between 2010 and 2020. However, there are no reliable data on long-term projections of heavy metals emissions in the regions surrounding the EMEP domain. That is why the same boundary concentrations were used in the modelling of all four scenarios.

The emission data compiled by TNO cover the territory of Europe. For the Central Asian region, the eastern part of Russia, northern Africa and other remaining parts of Asia, emission data prepared by MSC-E were used. The purpose of this was to avoid possible underestimation of pollution levels. A detailed description of the emission data is available in the EMEP Status Report (Ilyin et al. 2009). Emission totals for Kyrgyzstan are based on the TNO emission inventory (Denier van der Gon et al. 2005). Lead emission totals in the eastern part of Russia, in Turkmenistan, Tajikistan and Uzbekistan, in remaining parts of Asia and northern Africa are based on the global lead emission inventory for 1990 (Pacyna et al. 1995; http://www.ortech.ca/cgeic/index.html) and scaled to present time. Emissions of mercury for these regions were derived from the global mercury inventory for 2005 (AMAP/UNEP 2008). No changes in mercury emission were assumed between 2005 and 2020. Global emission inventories for cadmium are currently not available. That is why Cd emission data for the Asian part of the EMEP domain and for northern Africa were obtained on the basis of the global mercury inventory (AMAP/UNEP 2008). Cadmium emissions were assumed to be proportional to Hg emissions with a coefficient depending on the region: $E_{Cd} = \alpha \cdot E_{Hg}$. For the eastern part of Russia the proportionality coefficient (α) was taken the same as for the European part (1.14). The coefficient for Kyrgyzstan (0.56) was applied for the other Central Asian countries (Kazakhstan, Uzbekistan, Turkmenistan, and Tajikistan). For the other Asian countries and Africa the coefficient was taken equal to that for Turkey (0.91). All coefficients were estimated on the basis of the TNO inventory (Denier van der Gon et al. 2005). The spatial distribution of all emissions for the Asian part of the EMEP domain and northern Africa was obtained by interpolating global gridded emissions with 1°×1° spatial resolution into the model grid.

7.4 Modelling results

Comparison of country-averaged deposition simulated on the base of different emission scenarios demonstrated that the most significant changes in heavy metal pollution levels are projected for countries located in the south-eastern and the eastern parts of Europe (Fig. 7-1). In countries of the central, western and the northern parts of Europe the differences in deposition are relatively small. For example, the difference in country-averaged deposition of Pb, Cd and Hg, based on the four emission scenarios, is within ±20% in Austria, Germany, France, etc. (Figure 7.1). However, in the FYR of Macedonia, Russia and the Ukraine the differences can be 1.5–2-fold. The reason for this lies in the make-up of the emission scenarios. Most of countries in the central, western and the northern parts of Europe have already ratified the HM Protocol and their emissions have already declined following the requirements of the Protocol. Therefore, the long-term changes in the emissions in these countries are relatively low. Hence, also changes in deposition in these countries are expected to be insignificant. A number of countries of south-eastern and eastern Europe (Bosnia and

Figure 7.1 Country-averaged deposition fluxes of lead (a), cadmium (b) and mercury (c) to countries of Europe and Central Asia calculated on the base of different TNO emission scenarios.

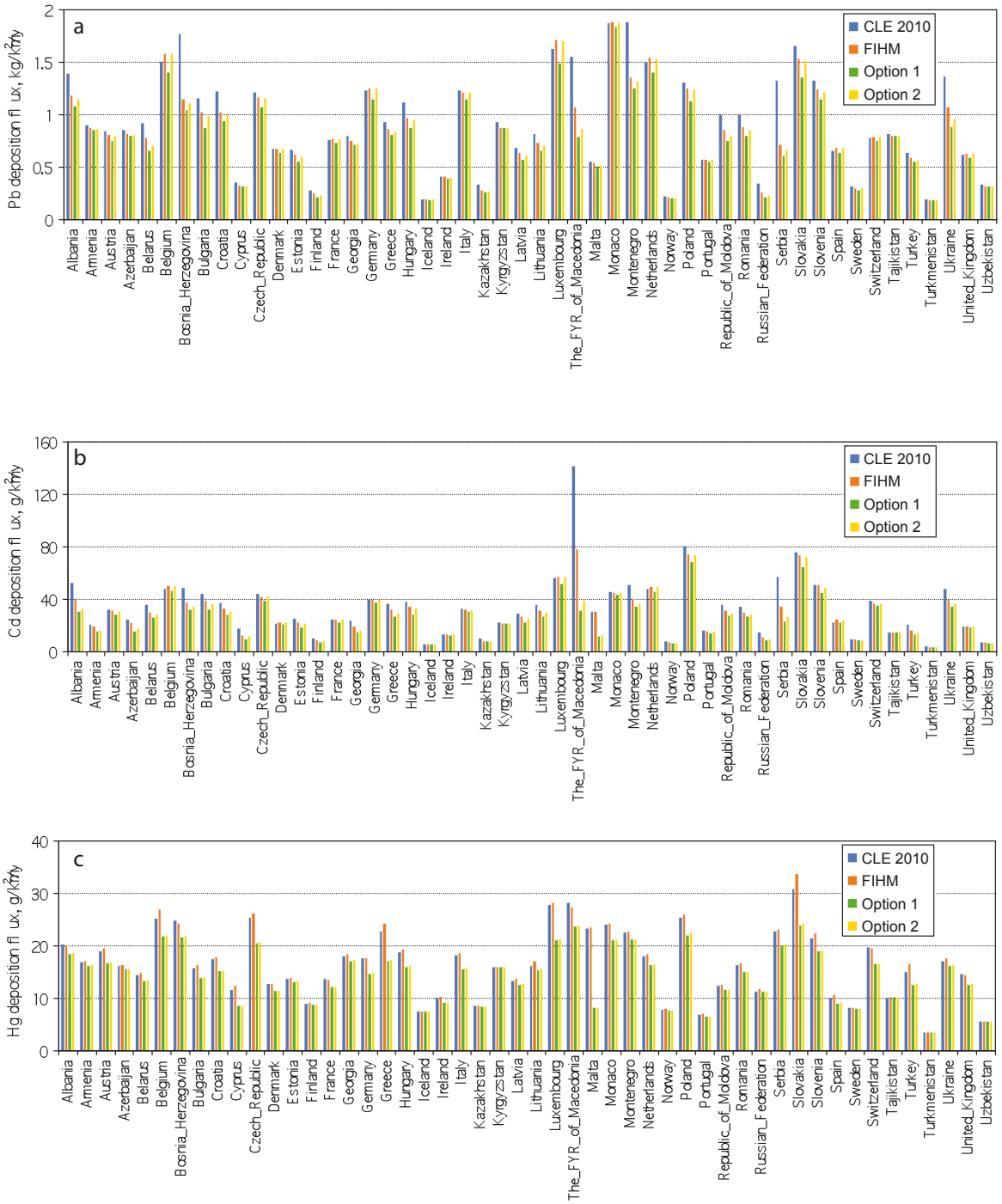

Herzegovina, Montenegro, Kazakhstan, Russia, Ukraine, etc.) have not yet joined the Protocol. Since the emission scenarios for 2020 assume full implementation of the Protocol in all EMEP countries, significant changes in emissions, and consequently, in calculated pollution levels of heavy metals are expected.

The spatial distribution of depositions calculated for the emission scenarios look quite similar in countries where differences in total emissions are relatively small, and vice versa. Figure 7.2 shows maps of Pb, Cd and Hg deposition based on CLE 2010 and Option 1 scenario. The biggest changes can be seen in the central part of Russia, the eastern part of Ukraine, in the south-eastern part of Europe (e.g., Romania, Bulgaria, Serbia, Croatia). In the western, central and northern parts of Europe the changes in deposition fields are minor.

Figure 7.2 Spatial distributions of total deposition of lead (a), cadmium (b) and mercury (c) based on CLE 2010 (left) and Option 1 scenario in 2020 (right).

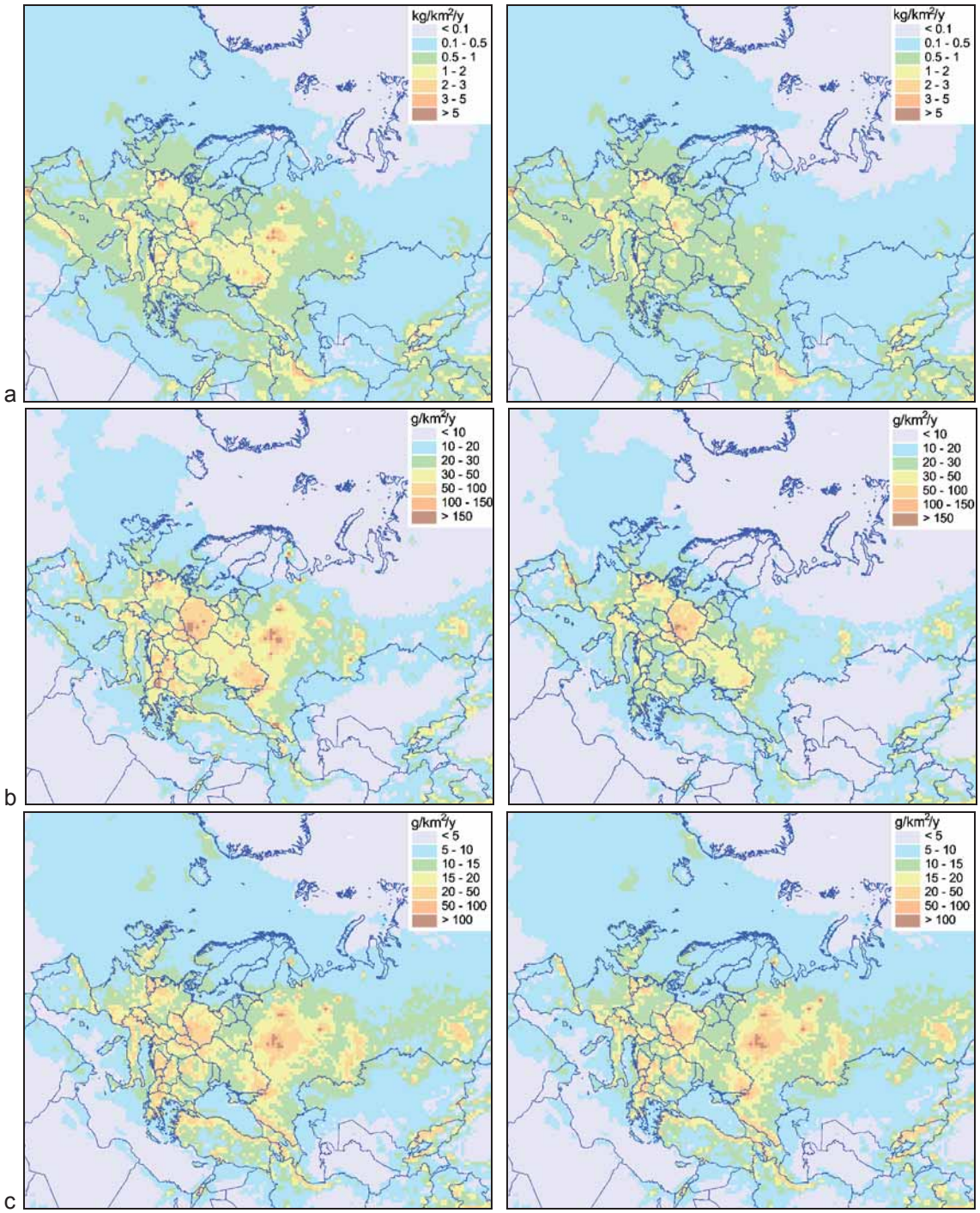

7.5 Analysis of heavy metal deposition changes

The differences of heavy metal deposition in individual countries due to the decline in emissions between 2010 and 2020 can be analyzed on the example of lead. Changes between country-averaged anthropogenic emissions for CLE 2010 and Option 1 are compared with the changes in deposition fluxes simulated for these scenarios (Figure 7.3). Positive values of the change mean a reduction of deposition or emissions between 2010 and 2020. In some countries (Bosnia Herzegovina, FYR of Macedonia, Ukraine etc.) the reduction in anthropogenic emissions (expressed in absolute terms) is greater than the reduction in deposition. However, in a number of countries (e.g., Croatia, Hungary, Latvia, Lithuania etc.) it is the opposite: the decrease in emissions is smaller that the decrease of depositions to the country. The reason for this is the influence of atmospheric circulation which causes dispersion and transboundary atmospheric transport of the emitted mass. For example, country-averaged emissions of Pb in Hungary declined by 0.08 kg/km^2/yr between 2010 and 2020 for the Option 1 scenario. However, in the main contributors of transboundary HM deposition to Hungary (Poland Slovakia, Serbia, Bulgaria) the decline in emissions was larger. That is why the decrease of deposition in Hungary (0.25 kg/km^2/yr) was even stronger than the reduction of national emissions. The situation for the FYR of Macedonia is opposite: in spite of strong reduction of the emissions the deposition declined to a smaller extent. The reductions in anthropogenic emissions in neighbouring countries are smaller, and thus the reduction of transboundary transport from them is also smaller. In addition to this, only part of mass emitted by national sources is deposited within the country, and the rest is transported outside the country. Total decrease of the anthropogenic emissions in all European and Central Asia countries is quite similar to the decline of deposition: 3300 vs. 2700 tons. The value of deposition reduction is somewhat smaller than that of the emission because of transport outside the modelling domain. Hence, the model adequately responds to the emission changes.

When the changes in emissions and depositions in countries are expressed in relative terms, the reductions of anthropogenic emissions are typically (but not always) larger than the decline in depositions (Figure 7.4). There are three sources for deposition: anthropogenic emissions, wind re-suspension of historically accumulated metals in soils and transport from non-EMEP sources. Therefore, the change in emission only partly affects the deposition. The total anthropogenic emission reduction for Europe and Central Asia is 52%, and for the deposition over this region 24%. However, the decline of total atmospheric input (anthropogenic, re-suspension, sources in Asia and Africa) of Pb between CLE 2010 and 2020 (Option 1) made up 25%, which is consistent with the reduction of deposition. The magnitude of re-suspension and non-EMEP sources used in the modelling of depositions has not changed for all the scenarios, and that is why the relative changes in deposition are smaller than the changes in anthropogenic emissions.

Re-suspension depends on a number of environmental factors, such as meteorological conditions, soil properties and concentrations of heavy metals in soils. Concentrations in soils consist of natural and historically accumulated anthropogenic components. Since the anthropogenic emissions in Europe tend to decline, the concentrations in soils should also gradually decrease, which favours the decrease of re-suspension. Thus, the further development of the re-suspension scheme should include the temporal dynamics of soil concentrations.

Figure 7.3 Absolute decrease of country-averaged emission and deposition fluxes of Pb in countries of Europe and Central Asia between 2010 and 2020 (Option 1). Left: countries with the highest changes of emissions. Right: other countries. Positive values mean the reduction of deposition or emission between 2010 and 2020.

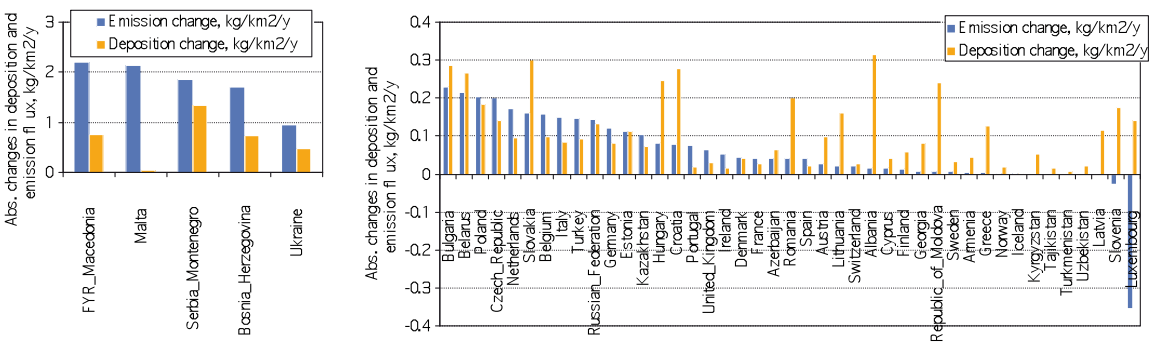

Figure 7.4 Relative decrease of country-averaged emission and deposition fluxes of Pb in countries of Europe and Central Asia between 2010 and 2020 (Option 1). Positive values mean the reduction of deposition or emission between 2010 and 2020.

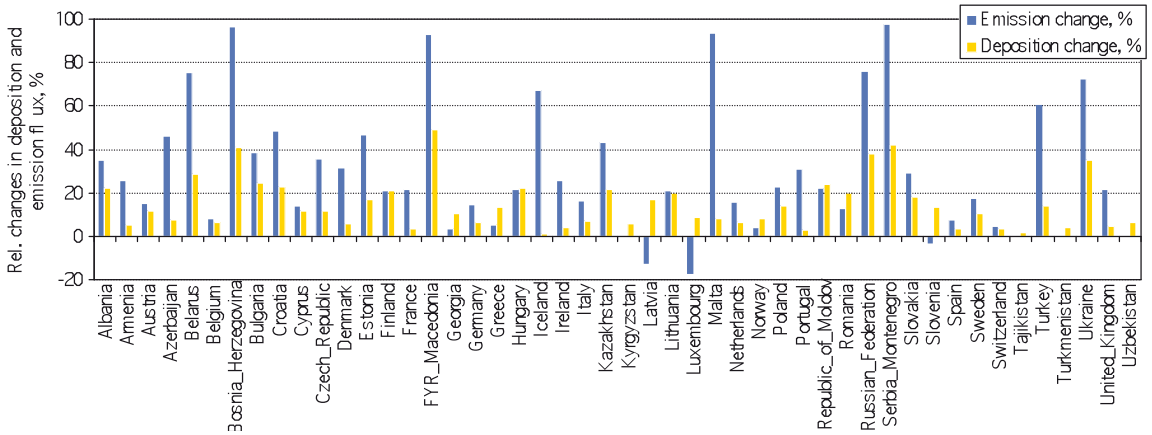

The contribution of wind re-suspension to Pb deposition in countries ranges from 20% (Tajikistan) to 75% (Iceland) for scenario 1 (Figure 7.5). Approximately in half of the countries its contribution exceeds 50%, and for Europe and Central Asia as whole it makes up 39%. It is important to note that the estimates of wind re-suspension of heavy metals are subject to large uncertainties. Nevertheless, the use of this parameter significantly improves the agreement between the modelled and measured concentrations and depositions. The model parameterization of re-suspension is constrained on measured concentrations and deposition. The measured values, in turn, include an anthropogenic component, which also contains uncertainty. Therefore, relatively high values of re-suspension may compensate a possible underestimation of anthropogenic emissions. The contribution of non-EMEP sources is less than 20% in most of the countries, and amounts to 17% for Europe and Central Asia as whole. However, in some countries located close to the sources in Asia (e.g., Armenia, Tajikistan, Turkmenistan) or Africa (Cyprus), this contribution can reach or even exceed 50%. However, the emissions prescribed for the African and Asian region are subject to high uncertainty, and thus the estimates of contribution of these sources to deposition are also highly uncertain.

On the basis of our analysis it is possible to conclude that the reduction of total deposition of Pb to countries in Europe and Central Asia as whole between CLE 2010 and various scenarios for 2020 range within 15–24 % depending on the considered scenario. These changes are resulted from the reduction of anthropogenic emission in this region within 33–52%. The corresponding reduction for total atmospheric input is 16–25%. For Cd the reduction of deposition ranges from 15 to 27% for Europe and Central Asia as a whole. For Hg the deposition changes vary between a growth of 3.6% to a reduction of 4.6%. Relatively low changes of Hg deposition are explained by the significant influence of intercontinental transport. The changes for individual countries are highly variable because of the influence of transboundary transport.

Figure 7.5 Country-averaged deposition fluxes of Pb from the European and Central Asian anthropogenic sources (CLE 2010), wind re-suspension and non-EMEP sources in 2010.

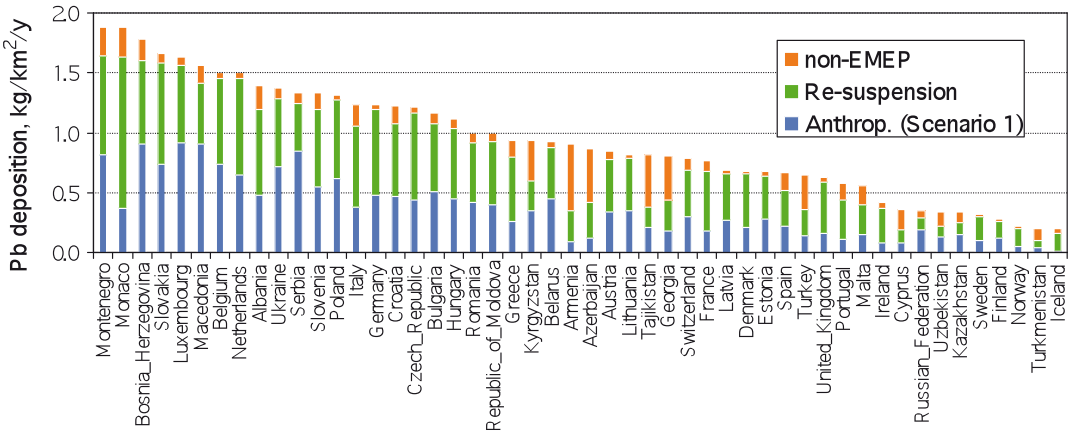

References

AMAP/UNEP, 2008. Technical Background Report to the Global Atmospheric Mercury Assessment. Arctic Monitoring and Assessment Programme / UNEP Chemicals Branch (http://www.chem.unep.ch/mercury/Atmospheric_Emissions/Technical_background_report.pdf)

CITEPA, 2010. Inventaire des emissions de polluants atmospheriques en France au titre de la convention sur la pollution atmospherique transfrontaliere a longue distance et de la directive Europeenne relative aux plafonds d'emissions nationaux (NEC). CEE–NU/NFR & NEC Mars 2010, 221 pp

Denier van der Gon HAC, Van het Bolscher M, Visschedijk AJH, Zandveld PYJ, 05. Study to the effectiveness of the UNECE Heavy Metals Protocol and costs of possible additional measures. Phase I: Estimation of emission reduction resulting from the implementation of the HM Protocol. TNO-report B&O-A R 2005/193

Gusev A, Ilyin I, Mantseva E, Rozovskaya O, Shatalov V, Travnikov O, 2006. Progress in further development of MSCE-HM and MSCE-POP models (implementation of the model review recommendations). EMEP/MSC-E Technical Report 4/2006, 114 pp

Hettelingh J-P, Sliggers J (eds), 2006. Heavy metal emissions, depositions, critical loads and exceedances in Europe. Joint report of TNO, MSC-E, Alterra, VROM and Netherlands Environmental Assessment Agency, 93 pp

Ilyin I, Rozovskaya O, Sokovyh V, Travnikov O, 2007. Atmospheric modelling of heavy metal pollution in Europe: Further development and evaluation of the MSCE-HM model. EMEP/MSC-E Technical Report 4/2007, 52 pp

Ilyin I, Rozovskaya O, Sokovyh V, Travnikov O, Aas W, 2009. Heavy Metals: Transboundary Pollution of the Environment. EMEP Status Report 2/2009, 55 pp

Murrells TP, Passant NR, Thistlethwaite G, Wagner A, Li Y, Bush T, Norris J, Whiting R, Walker C, Stewart RA, Tsagatakis I, Conolly C, Brophy NCJ, Okamura S, 2010. UK Informative Inventory Report (1970 to 2008). UK Emissions Inventory Team, AEA Group, 50 pp

Nielsen O-K, Winther M, Mikkelsen MH, Hoffmann L, Nielsen M, Gyldenkaerne S, Fauser P, Plejdrup MS, Albrektsen R, Hjelgaard K, 2010. Annual Danish Informative Inventory Report to UNECE. Emission inventories from the base year of the protocols to year 2008. NERI Technical Report no.774, 34 pp

Pacyna JM, Scholtz MT, Li Y-F (Arthur), 1995. Global budget of trace metal sources. *Environ. Rev.* 3(2): 145–159

SEPA, 2010. Informative Inventory Report 2010. Sweden. Annexes. Swedish Environmental Protection Agency, 74 pp

SYKE, 2010. Air Pollutant Emissions in Finland 1980-2008. Informative Inventory Report. Finnish Environment Institute. Consumption and Production Centre, Environmental Performance Division Air Emissions Team, 55 pp

Travnikov O, Ilyin I, 2005. Regional Model MSCE-HM of Heavy Metal Transboundary Air Pollution in Europe. EMEP/MSC-E Technical Report 6/2005, 59 pp

8 Critical Loads of Heavy Metals and their Exceedances

Jaap Slootweg, Jean-Paul Hettelingh, Maximilian Posch

8.1 Critical Loads for cadmium (Cd), lead (Pb) and mercury (Hg)

In the context of the revision of the Heavy Metal protocol deposition for 4 scenarios have been calculated, see Chapter 7. To assess the effects these depositions are compared to the critical loads of the European ecosystems.

Critical loads of heavy metals have been modelled and mapped with respect to the following effect-end points:

1 = human health effect (drinking water) via terrestrial ecosystem;
2 = human health effect (food quality) via terrestrial ecosystems;
3 = Eco-toxicological effect on terrestrial ecosystems;
4 = Eco-toxicological effect on aquatic ecosystems;
5 = human health effect (food quality) via aquatic ecosystems.

Effects 1 to 4 are based on critical concentrations of the metal in the soil solution. Using a mass balance for the root layer, this concentration is related to the deposition. Fertilisation of agricultural areas also causes Cd and Pb to enter soil systems, but this is not taken into account in this assessment. For each ecosystem the minimum of the critical loads for all effects is taken. Effect 5 is directly related to the concentration in rainwater. More on the calculations of critical loads can be found in the Mapping Manual (UBA 2004).

Following a request from the Woking Group on Effects, a call for data regarding critical loads of heavy metals was issued in 2004, and 18 National Focal Centres of the CCE submitted data (Slootweg 2005). Table 8.1 lists the NFCs that submitted critical load data to the CCE and the effects they addressed. Countries in bold have updated their data in 2006, other submissions are responses to the call in 2004. Critical loads for other countries were calculated with the CCE background database for heavy metals (Slootweg 2005).

Table 8.1 Overview of the country response on the call for critical loads of cadmium, lead and mercury and the 5 effects.

Country	Country code	Effect number[1]									
		Cd				Pb			Hg		
		1	2	3	4	1	3	4	1	3	5
Austria	AUT	x	x	x		x	x		x	x	
Belarus	BLR			x			x				
Belgium	BEL	x		x	x	x	x	x	x	x	x
Bulgaria	**BGR**	x				x					
Cyprus	**CYP**	**x**	**x**	**x**		**x**	**x**		**x**		
Czech Republic	CZE	x				x			x		
Finland	FIN										x
France	FRA			x			x				
Germany	DEU	x	x	x		x	x		x	x	
Italy	**ITA**			**x**			**x**				
Netherlands	**NLD**	x	x	x		x	x			x	
Poland	POL			x			x			x	
Russia	RUS	x		x		x	x				
Slovakia	SVK			x			x			x	
Sweden	SWE		x	x			x			x	x
Switzerland	CHE	x		x		x	x			x	
Ukraine	**UKR**	**x**				**x**					
United Kingdom	GBR			x			x				
Total	18	10	5	14	1	10	14	1	5	7	3

Figure 8.1 The 5th percentile of the critical loads for Cd(top row), Pb(bottom row) for heath effects, 1 and 2 (left), eco-toxicological effect, 3 and 4 (centre) and all effects combined (right).

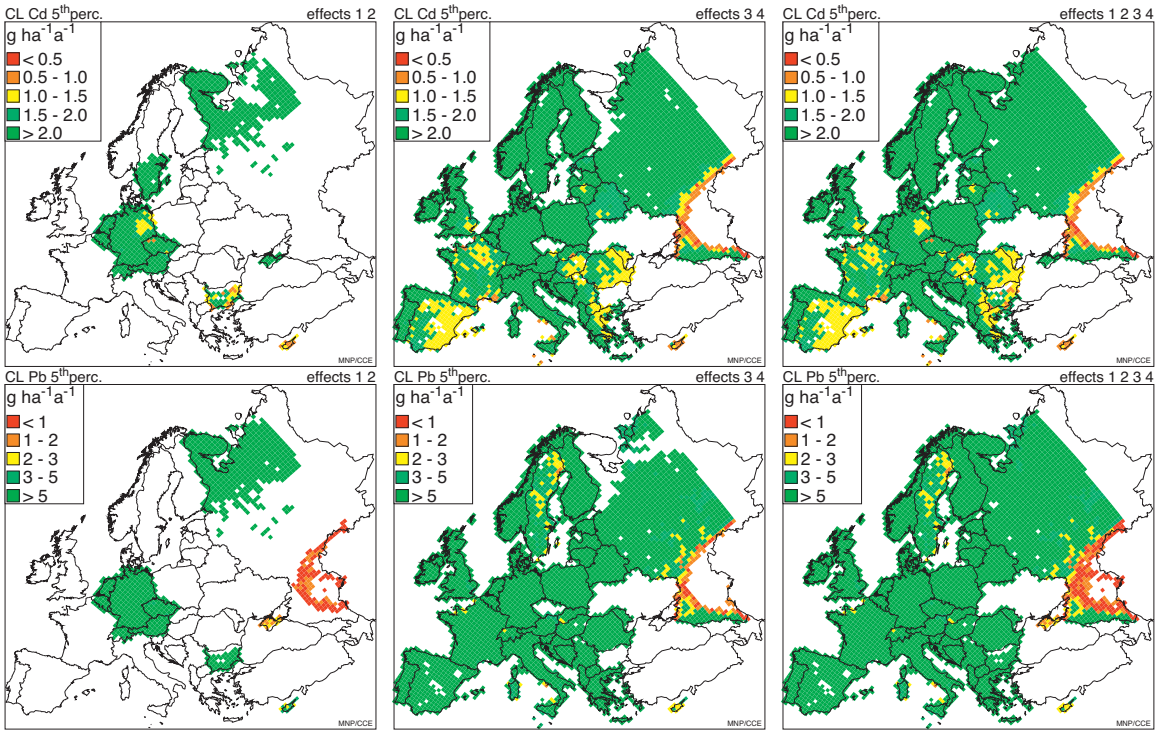

Figure 8.2 The 5th percentile of the critical loads for Hg for heath effects (1 and 2; top-left), eco-toxicological effects (3 and 4; top-right) and the four effects combined (bottom-left), completed with the critical concentration in rainwater (effect 5; bottom-right).

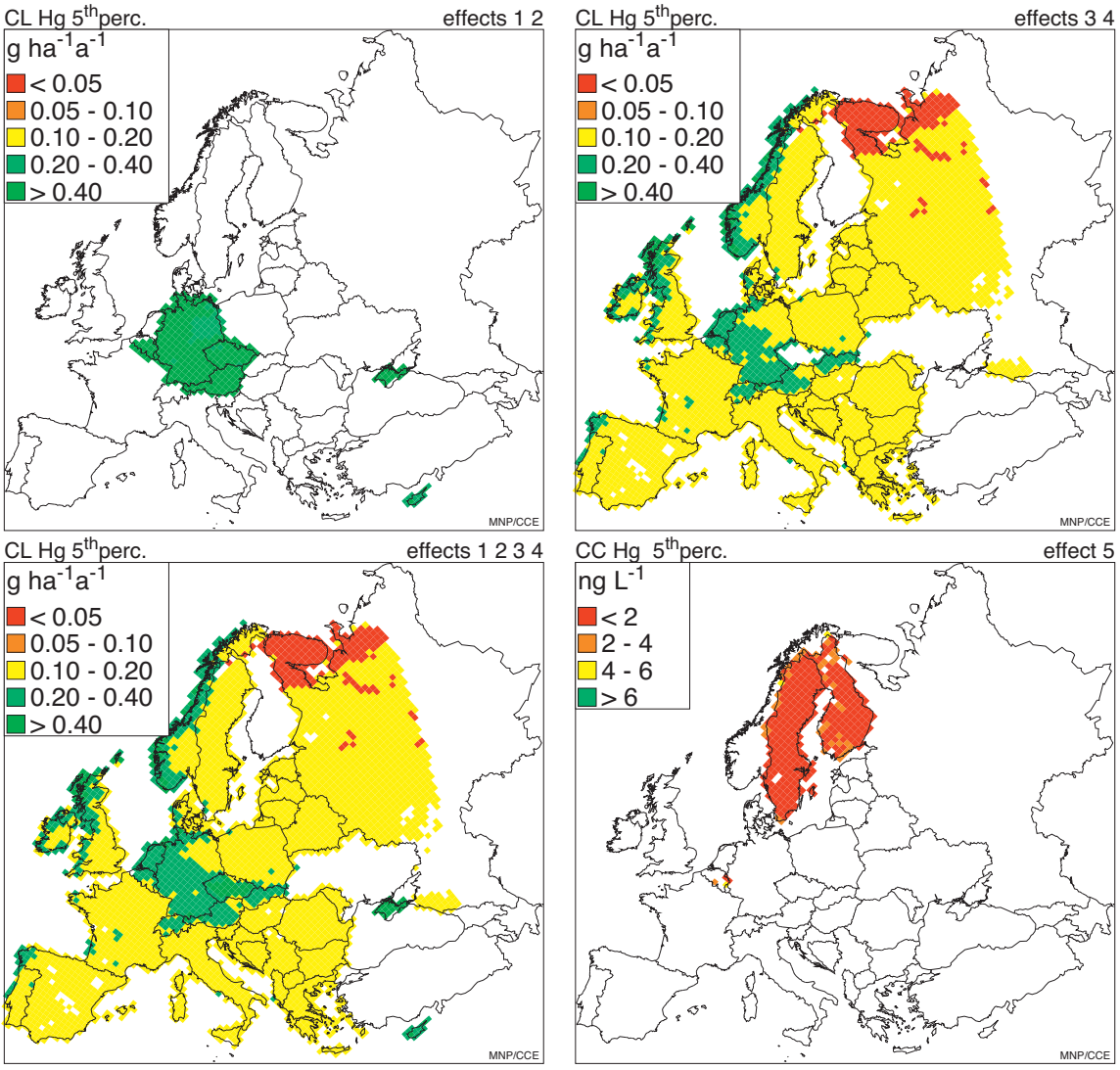

Critical loads of Pb and Cd for human health (effects 1 and 2), for eco-toxicological effects (3 and 4) and for all effects combined are shown in Figure 8.1. The most sensitive areas are in the south of Russia.

For Hg also the critical concentration in rainwater (effect 5) is mapped. For this effect only three countries submitted critical loads, but with many sensitive areas in the north of Russia for Hg; and Fig. 8-2 show the critical loads.

8.2 Average Accumulated Exceedance

Average Accumulated Exceedances (AAE) were computed to identify and map areas (grid cells) where atmospheric metal depositions are higher than critical loads. An AAE is the ecosystem area-weighted sum of the individual exceedances (deposition minus critical load, with zero for non-exceedance) of all ecosystems in a grid cell, defined as:

$$AAE = (A_1Ex_1 + \ldots + A_nEx_n)/(A_1 + \ldots + A_n)$$

where A_i is the area of the i-th ecosystem in a grid cell and Ex_i its exceedance (i=1,...,n) (see also Posch et al., 2001).

For the current legislation and the three scenarios the exceeded area of ecosystems and the AAE has been calculated. Tables 8.2, 8.3 and 8.4 show lists the results of the exceedances of Cd, Pb and Hg respectively for all European countries. Blank cells in the table indicate zero values; the value '0.0' indicates a value rounded down to zero.

The share of exceeded area of ecosystems in the European countries for Cd are all below 1 %, with the exception of Bulgaria, which has lower critical loads than other countries in that region, and Macedonia. For Pb the area and size of the exceedances are much higher, only few countries are not exceeded. Hg has the largest exceedances, more that half of the countries have over 90% of their ecosystem area exceeded. Also for effect 5, for which only three countries have submitted data, the critical concentration of Hg is exceeded nearly everywhere (see Table 8.5). The reductions in exceedances in this case are minimal for Option 1 and 2, although they include specific Hg measures.

Table 8.2 Exceedance for Cd (g ha^{-1} a^{-1}) for the three scenarios, with the present (CLE 2010) as a reference.

Country	EcoArea	CLE 2010		FI 2020		Opt. 2 2020		Opt. 1 2020	
	(km^2)	Ex.%	AAE	Ex.%	AAE	Ex.%	AAE	Ex.%	AAE
AL	10082			0.0		0.0		0.0	
AT	131809								
BA	30726								
BE	10465								
BG	48330	15.0	0.020	9.3	0.012	4.8	0.009	1.8	0.004
BY	121128	0.3	0.001	0.0		0.0		0.0	
CH	11611								
CY	20231	0.7	0.001	0.0		0.0		0.0	
CZ	25136								
DE	724217	0.0		0.0		0.0		0.0	
DK	5280								
EE	29398								
ES	99616	0.6	0.006	0.7	0.009	0.7	0.009	0.5	0.008
FI	255890								
FR	170638	0.1		0.1		0.1		0.0	
GB	50075	0.0		0.0		0.0		0.0	
GR	30989	0.7	0.005	0.2	0.003	0.2	0.003	0.2	0.003
HR	23666								
HU	10560	0.0		0.1		0.1			
IE	4193								
IT	278146								
LT	18099								
LU	705								
LV	35898								
MD	2227								
MK	12068	16.6	0.625	8.4	0.122	0.3	0.001		
NL	61894								
NO	126685								
PL	88383	0.2		0.0		0.0			
PT	14572								
RO	89580								
RU	1818725	1.0	0.009	0.5	0.002	0.4	0.001	0.3	
SE	173482								
SI	13538								
SK	19253	0.5	0.001	0.5	0.001	0.4	0.001	0.2	0.001
UA	18002								
YU	43858	1.0	0.012						
EU27	2410379	0.4	0.001	0.2	0.001	0.2	0.001	0.1	
All	4629156	0.6	0.006	0.4	0.002	0.2	0.001	0.1	

Table 8.3 Exceedance for Pb (g ha^{-1} a^{-1}) for the three scenarios, with the present (CLE 2010) as a reference.

Country	EcoArea (km^2)	CLE 2010		FI 2020		Opt. 2 2020		Opt. 1 2020	
		Ex.%	AAE	Ex.%	AAE	Ex.%	AAE	Ex.%	AAE
AL	10082	15	0.79	7	0.02	3	0.06	1	0.01
AT	122741	6	0.23	6	0.17	5	0.18	5	0.14
BA	30726	53	3.47	12	0.26	11	0.32	9	0.16
BE	10465	32	2.30	35	3.00	35	3.01	24	1.60
BG	48330	70	3.39	48	2.04	39	2.28	27	1.08
BY	121128	9	0.44	3	0.02	1	0.07	0	0.01
CH	11611	3	0.20	3	0.20	3	0.21	3	0.19
CY	16295	25	0.70	22	0.51	21	0.56	20	0.46
CZ	25136	33	3.71	32	3.38	32	3.43	29	2.64
DE	580006	8	1.00	8	1.06	8	1.07	7	0.84
DK	5280	0	0.00	0	0.00	0	0.00	0	
EE	29398	1							0.00
ES	99616	16	2.32	17	2.68	17	2.68	16	1.81
FI	255890								0.00
FR	170638	30	1.80	30	1.84	30	1.84	28	1.63
GB	50075	12	1.27	12	1.29	12	1.29	12	1.17
GR	30989	20	0.61	11	0.30	8	0.35	5	0.26
HR	23666	19	0.77	7	0.15	7	0.18	4	0.09
HU	10560	32	1.28	21	0.82	20	0.88	13	0.39
IE	4193								0.00
IT	278146	17	0.55	17	0.53	16	0.54	14	0.40
LT	18099	1	0.01	0	0.00	0	0.00	0	0.00
LU	705	3	0.24	4	0.31	4	0.31	2	0.15
LV	35898								0.00
MD	2227	27	0.48	7	0.02	6	0.08	0	0.00
MK	12068	45	5.42	18	0.06	6	1.17	1	0.00
NL	44627	15	0.54	15	0.60	15	0.60	14	0.40
NO	126685								
PL	88383	8	1.15	6	1.05	6	1.06	5	0.72
PT	14572	1	0.11	1	0.10	1	0.10	1	0.09
RO	89580	2	0.10	1	0.10	1	0.10	1	0.09
RU	1844700	31	3.13	21	0.92	16	1.45	14	0.72
SE	151432	5	0.10	4	0.08	4	0.09	3	0.07
SI	13538	10	0.17	7	0.08	6	0.10	1	0.04
SK	19253	27	3.37	25	2.92	25	2.98	23	2.30
UA	18002	100	5.77	100	4.00	100	4.51	100	3.71
YU	43858	29	1.44	4	0.13	4	0.15	3	0.09
EU27	2213848	12	0.86	11	0.85	11	0.86	9	0.65
All	4458601	20	1.82	15	0.82	13	1.05	11	0.64

Table 8.4 Exceedance for Hg (g ha^{-1} a^{-1}) for the three scenarios, with the present (CLE 2010) as a reference.

Country	EcoArea (km^2)	CLE 2010		FI 2020		Opt. 2 2020		Opt. 1 2020	
		Ex.%	AAE	Ex.%	AAE	Ex.%	AAE	Ex.%	AAE
AL	10082	99	0.162	99	0.159	99	0.136	99	0.133
AT	93971	9	0.007	10	0.008	6	0.005	6	0.004
BA	30726	100	0.218	100	0.209	100	0.178	100	0.175
BE	10457	48	0.069	49	0.079	36	0.046	36	0.045
BG	42512	100	0.151	100	0.158	100	0.126	100	0.124
BY	86812	100	0.120	100	0.126	100	0.105	100	0.103
CH	11611	30	0.018	28	0.017	15	0.007	15	0.007
CY	8148	4	0.008	4	0.010	1	0.001	1	0.001
CZ	25136	2	0.005	3	0.007	1	0.003	1	0.003
DE	389869	13	0.014	13	0.014	9	0.009	9	0.008
DK	5280	99	0.109	99	0.106	98	0.081	98	0.079
EE	29398	83	0.071	83	0.073	83	0.066	83	0.064
ES	99616	89	0.095	90	0.108	86	0.078	86	0.077
FI	0	0	0.000	0	0.000	0	0.000	0	0.000
FR	123923	84	0.072	84	0.070	78	0.053	78	0.052
GB	68621	34	0.045	34	0.043	29	0.030	29	0.030
GR	30989	100	0.272	100	0.292	100	0.194	100	0.191
HR	23666	100	0.143	100	0.147	97	0.111	97	0.109
HU	10560	100	0.232	100	0.246	100	0.168	100	0.165
IE	4193	38	0.022	38	0.025	28	0.010	28	0.010
IT	94729	99	0.167	99	0.171	98	0.126	98	0.126
LT	18099	99	0.118	99	0.132	98	0.110	97	0.107
LU	705	100	0.176	100	0.180	100	0.105	100	0.103
LV	35898	92	0.066	93	0.072	91	0.060	91	0.059
MD	2227	100	0.111	100	0.115	100	0.100	100	0.099
MK	12068	100	0.321	100	0.305	100	0.256	100	0.253
NL	2842	93	0.117	93	0.130	85	0.095	85	0.091
NO	126685	13	0.002	14	0.002	12	0.002	11	0.002
PL	88383	100	0.260	100	0.267	99	0.210	99	0.205
PT	14572	23	0.004	24	0.005	21	0.003	21	0.003
RO	89580	100	0.147	100	0.150	100	0.126	100	0.124
RU	950933	100	0.163	100	0.192	100	0.175	100	0.170
SE	151179	28	0.005	30	0.005	24	0.004	24	0.003
SI	13538	98	0.127	98	0.138	95	0.101	95	0.099
SK	19253	73	0.145	78	0.186	53	0.062	51	0.060
UA	18002								0.000
YU	43858	100	0.194	100	0.198	100	0.164	100	0.160
EU27	1471452	54	0.075	55	0.079	51	0.058	51	0.057
All	2788122	71	0.108	71	0.120	69	0.101	69	0.098

Table 8.5 Exceedance of the critical concentration of Hg (ng L–1) for the three scenarios, with the present (CLE 2010) as a reference.

Country	EcoArea (km^2)	CLE 2010		FI 2020		Opt. 2 2020		Opt. 1 2020	
		Ex.%	AAE	Ex.%	AAE	Ex.%	AAE	Ex.%	AAE
BE	9	100	9.258	100	9.749	100	7.68	100	7.605
FI	16856	99.99	5.96	99.99	6.1	99.99	5.845	99.99	5.807
SE	292007	96.86	4.453	96.92	4.489	96.85	4.301	96.85	4.283

The exceedances are also calculated for each EMEP grid. Maps of the Average Accumulated Exceedance (AAE) of Cd, Pb and Hg for current legislation (CLE) in 2010 and for the scenarios with full implementation and the additional Options 1 and 2 (in 2020) are shown in Figures 8.4, 8.5 and 8.6. The exceedances of Pb and Hg are widespread over Europe, but for Cd only a few grids are exceeded, mostly in Russia. Exceedances are reduced by the measures in all scenarios, with largest effects in Option 1, but remain present in most of the grids exceeded at present.

Figure 8.4 Exceedance (AAE) of critical loads of Cd for the three scenarios, with the present (CLE 2010) as a reference. The left column shows the exceedance for health effects (1 and 2), the centre column for eco-toxicological effects (3 and 4), and the right column for all effects combined.

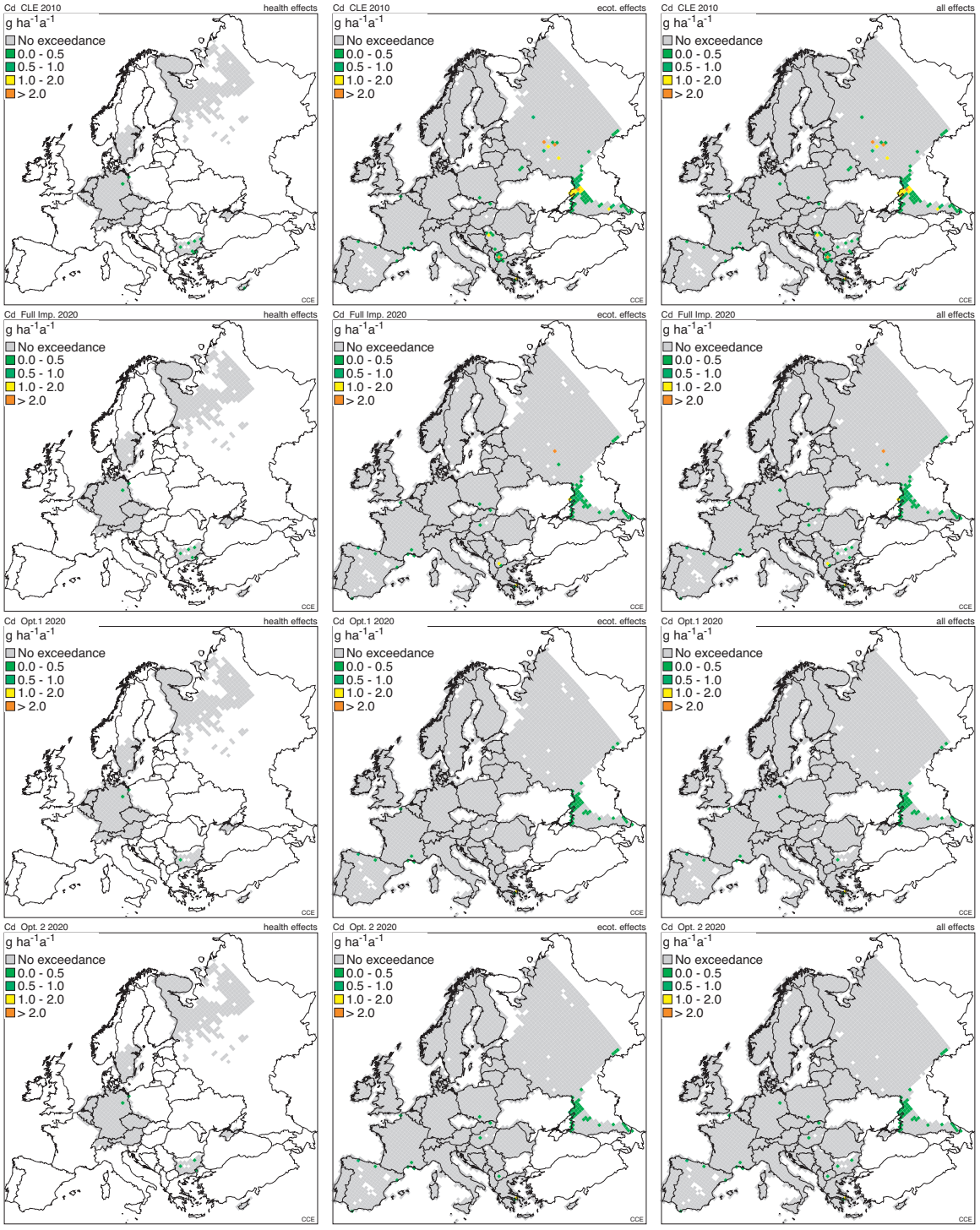

Figure 8.5 Exceedance (AAE) of critical loads of Pb for the three scenarios, with the present (CLE 2010) as a reference. The left column shows the exceedance for health effects (1 and 2), the centre column for eco-toxicological effects (3 and 4), and the right column for all effects combined.

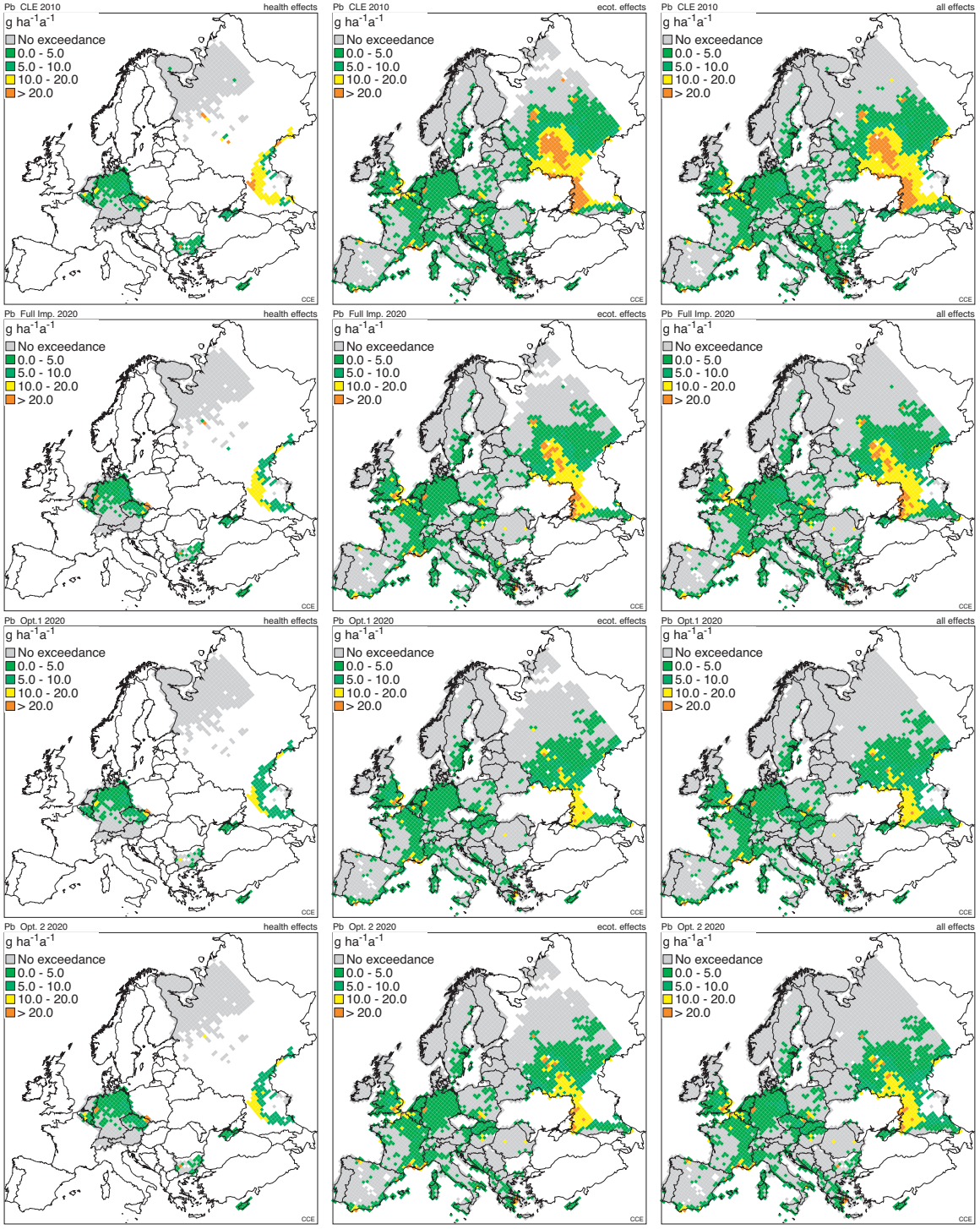

Figure 8.6 Exceedance of Hg for the three scenarios, with the present (CLE 2010) as a reference. The left column shows the exceedance for health effects (1 and 2), the centre column for eco-toxicological effects (3 and 4), the right column for unhealthy concentration in fish (effect 5).

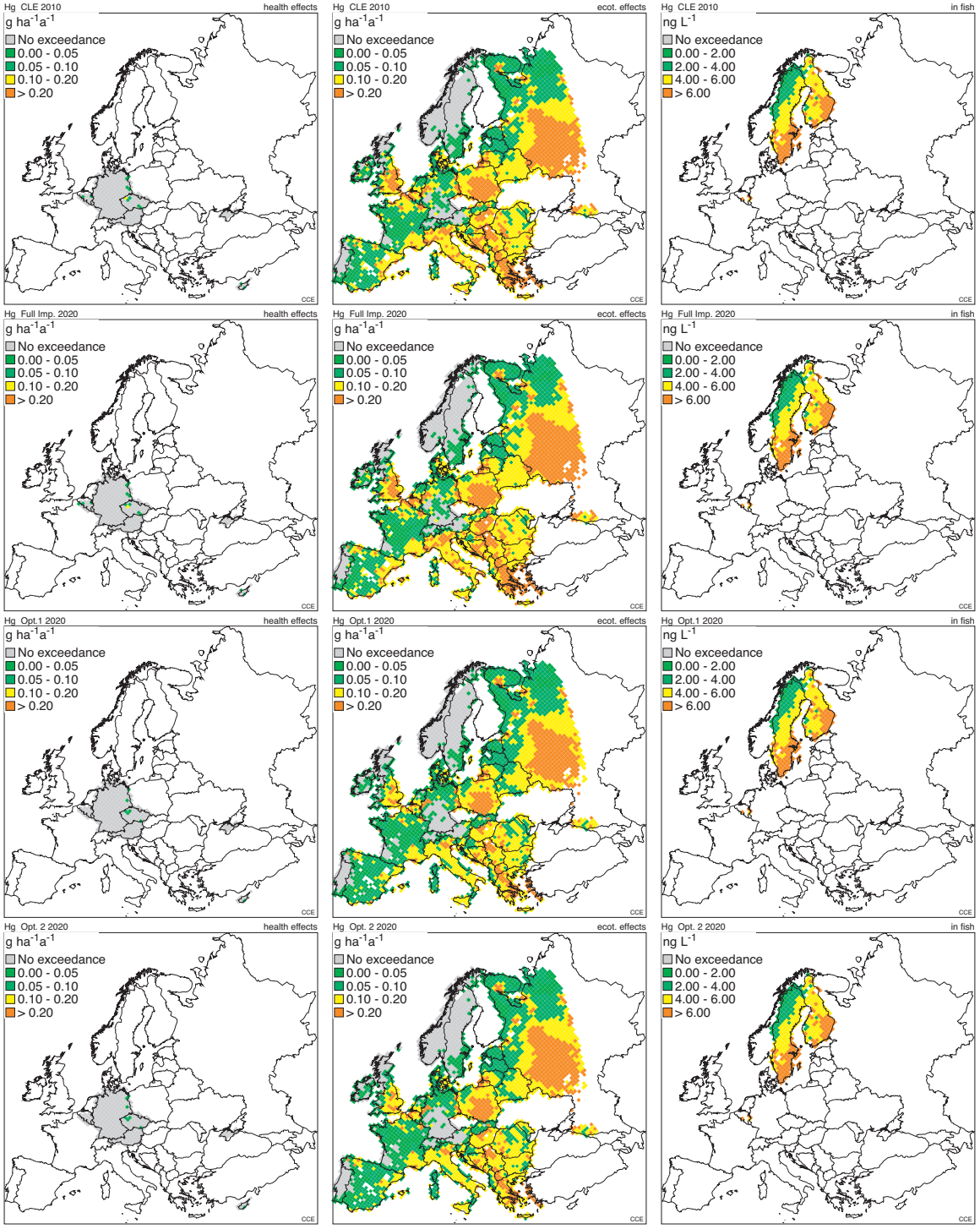

8.3 Critical loads of Cd and Pb, re-suspension and exceedances

Chapter 7 of this report states that re-suspension is an important part of deposition. Re-suspension is that part of the deposition that originates from other sources than emission sources directly, i.e. is (re-)emitted from soils, in the form of particulate matter (wind erosion). However, in the calculation of critical loads this outflux of re-suspension is not taken into account. Within an effects-based approach three solutions are conceivable.

A. Since critical loads do not take re-suspension into account, it should be deducted from the depositions before calculating an exceedance.
B. Add the re-emission (at critical level) to the critical load.
C. Another way to assess scenarios all-together is to model concentrations of heavy metals in the soil and the soil solution dynamically. This would result in violations rather than exceedances of the critical load, i.e. areas where the concentration in a particular year exceeds the critical limit.

For all options more knowledge on re-suspension is needed to assess the need for measures. Two sources of the metal in the soil can be distinguished, from the parent material (as a mineral), and anthropogenic from either historic depositions or otherwise, for example by fertilizer input. In the context of this study, measures aimed at reducing re-suspension from agricultural sources have not been considered.

References

Posch et al., 2001. Characterization of Critical Load exceedance in Europe, WASP 130: 1139-1144

Slootweg J, Hettelingh J-P, Posch M, Dutchak S, Ilyin I, 2005. Critical loads of cadmium, lead and mercury in Europe, Collaborative report by ICP-M&M/CCE and EMEP/MSCE, MN-ReportP 259101015/2005, www.rivm.nl/cce

UBA 2004. Manual on methodologies and criteria for modelling and mapping critical loads & levels and air pollution effects, risks and trends. UNECE Convention on Long-range Transboundary Air Pollution, Federal Environmental Agency (Umweltbundesamt), Berlin

9 Loss of Species due to Cadmium and Lead Depositions in Europe

Dick de Zwart, Jaap Slootweg, Dik van de Meent, Maximilian Posch

9.1 Introduction

One of the endpoints for the critical loads of cadmium (Cd) and lead (Pb) is the eco-toxicological effect of metal ions in soil solution on soil micro-organisms, plants and invertebrates. Depositions will (eventually) result in a concentration in soil solution in equilibrium with each other, depending on the ecosystem properties like leaching, uptake and soil properties (pH, organic matter and clay contents) as described in section 9.2. The European background database (EU-DB), as used by the CCE to compute critical loads provides these properties and is used to map the concentrations for ecosystems in Europe, given the depositions at current legislation (CLE). The concentration can be high enough to intoxicate part of the species present in the ecosystem. The dose-response relationship between concentration and fraction of species lost is described in section 9.3. With the concentration-response relationship the fraction loss of species can be computed for the ecosystems in EU-DB at CLE, and section 9.4 shows the results. The results are not completely in line with the exceedances of the critical loads as mapped in Chapter 8. To explain the discrepancies, the response functions are compared to the critical concentrations as used in the critical load computations in section 9.5.

9.2 Steady-state total metal ion concentration in soil solution computed from metal input and runoff

At steady state, $[M]_{tot}$ can be computed from the net input of metal M, M_{in} (Posch and De Vries 2009):

$$[M]_{tot} = \frac{M_{in}}{Q} = \frac{M_{inp} - M_u}{Q} \quad (9\text{-}1)$$

where Q (in m/a) is the water flux leaving the soil layer (assumed equal to the precipitation excess), M_{inp} (in mg/m²/a) is the input flux of metal M, i.e. the sum of fertilisers, manure and deposition, and M_u (in mg/m²/a) is the net growth uptake (biomass removal) of metal M from the soil layer considered.

9.3 Loss of species estimated by species sensitivity distributions

Analyzing the results of the world's resources on laboratory derived toxicity observations revealed that species

differ in their sensitivity towards a single chemical. This may be due to differences in life history, physiology, morphology and behaviour. Without attempting to explain the cause of variability in species sensitivity, this recognition led to attempts to describe the variation with statistical distribution functions, thereby putting the concept of species sensitivity distribution (SSD) into existence (Posthuma et al. 2002, Van Straalen and Denneman 1989). The basic assumption of the SSD concept is that the sensitivities of a set of species can be described by some kind of statistical distribution. The available eco-toxicological data are seen as a sample from this distribution and are used to estimate the moment parameters of the SSD. The moments of the statistical distribution are used to calculate a concentration that is expected to be safe for most species of interest, which can be used to set an environmental quality criterion. A more recent application is the use of SSDs in risk assessments of contaminated ecosystems. For setting quality standards SSDs are commonly constructed in a more conservative manner by using chronic no observed effect data (NOEC). For environmental risk assessment related to the loss of biodiversity, the SSD curves are generally based on acute mortality data (LC50).

Figure 9.1 Exemplary cumulative distribution function of species sensitivity log-normally fitted (curve) to observed chronic toxicity values (NOEC; dots). The arrows indicate the inference of risk as a Potentially Affected Fraction of species (PAF-value) and the inference of an environmental quality criterion as a hazard concentration for 5% of the exposed species (HC_5).

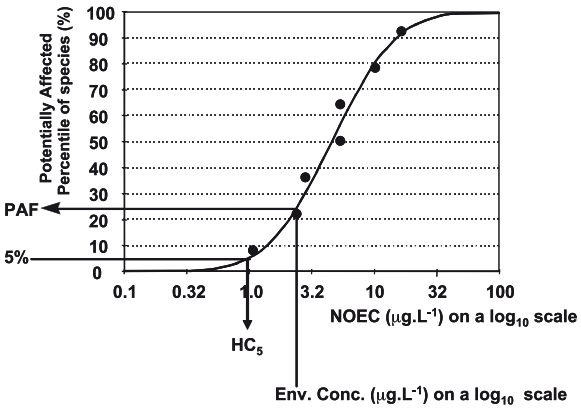

Toxicity data for soil dwelling organisms and terrestrial plants are comparatively scarce.
For the present study we therefore used publicly available data on acute median lethal or effective concentrations (LC50 or EC50) based on aquatic toxic tests to derive SSDs. These SSDs reflect the concentration-response relationship between total dissolved porewater concentration and the loss of species. In the literature there is no indication that the sensitivity of organisms living in soil is intrinsically different from the sensitivity of organisms living in surface waters, provided that the evaluation is based on the truly bio-available fraction of the toxicants.

For both cadmium (Cd) and lead (Pb) an SSD is obtained from the literature derived toxicity data by fitting a normal model to the log toxicity data. For the log-normal procedure, the SSDs are fully characterized by the median (Mu) of the distribution which is equal to the average (Sigma) of the log-transformed toxicity data and by the slope of the distribution that equals the standard deviation of log-transformed toxicity data. The moments (Mu and Sigma) of the acute SSD curves for Cd and Pb are given in Table 9.1.

The SSDs reflecting the concentration-response relationship between total dissolved porewater concentration ([M]) and the loss of species are given in Figure 9.2.

Figure 9.2 SSD curves for cadmium and lead as used in the present risk assessment..

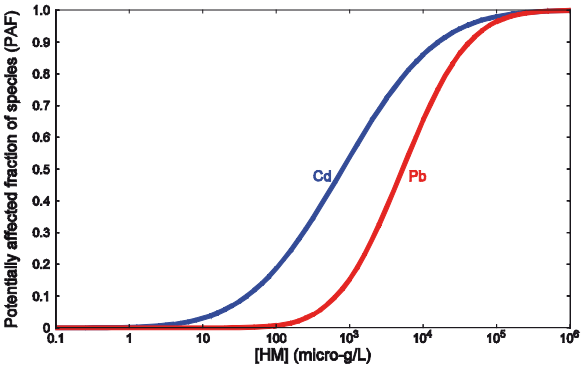

Table 9.1 The moments for the acute SSD's for cadmium and lead.

CAS	English name	chemical code	#Species	MuAcute (µg/L)	SigmaAcute (µg/L)	TMoA
7439-92-1	lead dissolved	Pb dis	19	3.72	0.707	Pb
7440-43-9	cadmium dissolved	Cd dis	68	2.90	1.016	Cd

9.4 Loss of species in Europe

For the European critical load background database (Reinds, 2008) and given the depositions at current legislation (CLE) the metal concentration has been calculated according to the formula in Section 9.2. The loss of species, according to the response function for the concentration in soil solution for each of the 1.6 million ecosystems has been mapped for Cd and Pb and the 99th percentile in every EMEP grid cell are shown in Figure 9-3. The 99th percentile is shown, because the vast majority of the ecosystems are not affected.

The loss of species has also been calculated for the combined effect of Cd and Pb (Figure 9.4). Because most ecosystems are unaffected, but the combined effect of the sensitive ecosystems is much higher than the individual metals, it seems likely that the same ecosystems are sensitive to both metals.

As stated earlier in this chapter, the loss of species is depicted in the maps for the 99th percentile, which means that 99 % of the ecosystem area within a grid has a lower (or equal) value than the values in the maps. Figure 9.5 shows the cumulative distribution of the combined effect of both metals to the loss of species. It shows that effects are close to zero in the vast majority of the ecosystems.

Figure 9.4 The 99th percentile of loss of species at steady state with CLE depositions for the combined effect of Cd and Pb.

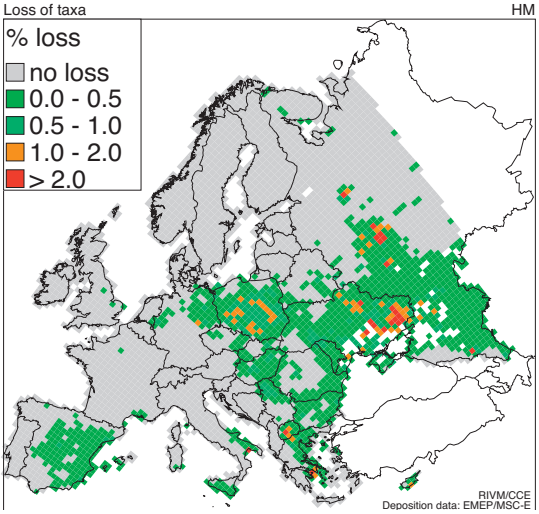

Figure 9.3 The 99th percentile of loss of species at steady state with CLE depositions for cadmium (left) and lead (right).

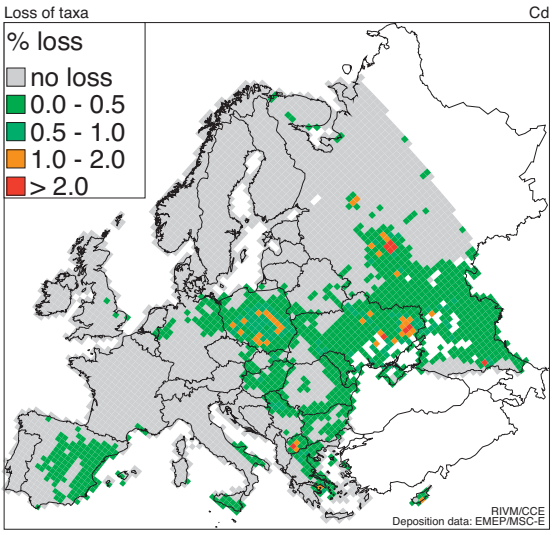

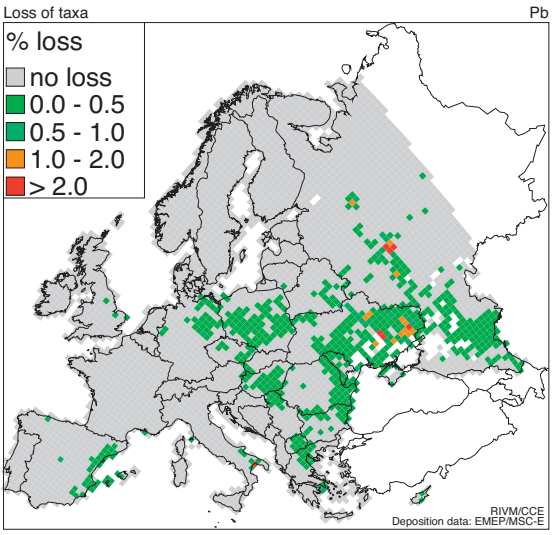

Figure 9.5 Cumulative distribution of the potentially affected fraction of species at the long-term constant CLE deposition rate onto EUNIS land cover classes.

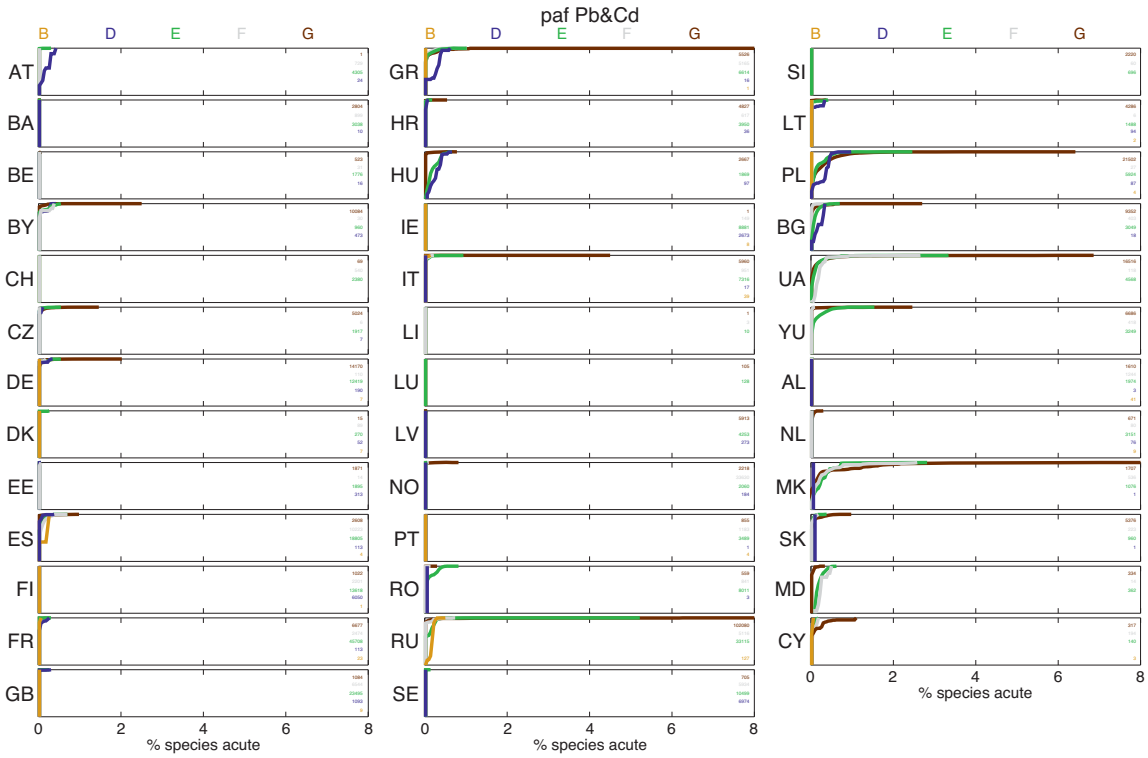

Why are much less than 5% of the ecosystems affected in grids in which critical loads are exceeded for each of the individual metals? (Compare with the top centre maps of Figures 8.4 and 8.5). The major difference is that the SSD reflects the acute lethal effects, and that the critical load approach is based on (De Vries et al, 2007) critical concentrations derived from NOEC values That protect 95% of the species from damage. Other differences are related to the fact that the limits for the Mapping Manual (UBA 2004) are

- not based on a postulated statistical distribution, like the log-normal distribution in the SSD, but by a bootstrapping method;
- include a toxicity-dependence on pH;
- related to the free concentration rather than the total concentration;
- corrected for described deviations for toxicity in ecosystems from laboratory experiments.

References

De Vries W, Lofts S, Tipping E, Meili M, Groenenberg JE, Schütze G, 2007. Impact of soil properties on critical concentrations of cadmium, lead, copper, zinc, and mercury in soil and soil solution in view of ecotoxicological effects. *Rev Environ Contam Toxicol* 191: 47–89

Posch M, De Vries W, 2009. Dynamic modelling of metals – time scales and target loads. *Environmental Modelling & Software* 24: 86–95

Posthuma L, Suter GW, II, Traas TP (eds), 2002. Species Sensitivity Distributions in Ecotoxicology. Boca Raton, FL, USA: Lewis Publishers, 587 pp

Reinds GJ, Posch M, De Vries W, Slootweg J, Hettelingh J-P, 2008. Critical loads of sulphur and nitrogen for terrestrial ecosystems in Europe and Northern Asia using different soil chemical criteria. *Water, Air and Soil Pollution* 193: 269–287

UBA 2004. Manual on methodologies and criteria for modelling and mapping critical loads & levels and air pollution effects, risks and trends. UNECE Convention on Long-range Transboundary Air Pollution, Federal Environmental Agency (Umweltbundesamt), Berlin

Van Straalen NM, Denneman CAJ, 1989. Ecotoxicological evaluation of soil quality criteria. *Ecotoxicology and Environmental Safety* 18: 241–251

Part 4
NFC Reports

This part consists of the reports on national data on dynamic modelling calculations submitted to the Coordination Centre for Effects by the National Focal Centres (NFCs) following the CCE call for data of 2009. The reports have not been editted.

Austria

National Focal Centre

Erik Obersteiner
Department of Datamanagement & Reporting
erik.obersteiner@umweltbundesamt.at

Thomas Dirnböck
Department of Ecosystem Research and Monitoring
thomas.dirnboeck@umweltbundesamt.at

Umweltbundesamt GmbH (Federal Environment Agency, Austria)
Spittelauer Lände 5
1090 Vienna
fax: +43-1-31 304-3700
http://www.umweltbundesamt.at

Status

In response to the 2009 Call for input data to test dynamic modelling of vegetation changes in selected sites in a country, the dynamic model VSD+ was calibrated for several permanent soil-vegetation plots of the ICP Integrated Monitoring site Zöbelboden. This site has been chosen because it represents very important forests in Austria with regard to biodiversity and ecosystem services (e.g. major drinking water resources). Also deposition of N is high in the northern part of the European Alps, where the study site is located. Bedrock materials are carbonates so that soils have a very high base saturation. The focus is thus on eutrophication effects of N and not on acidification. The knowledge of effects of N in such forests is very scarce, though comparable forest sites can be found all over the Alps. Several on-site studies showed that chronic N deposition has already affected soils, forest ground vegetation, epiphytic lichens and mosses (Zechmeister et al. 2007, Umweltbundesamt 2007, Hülber et al. 2008, Dirnböck et al. 2009, Dirnböck & Mirtl 2009, Diwold et al. 2010). These results represent valuable evaluations of the VSD+ and VEG outcomes.
The second part of the call can only be fulfilled partly. We provide two lists of plant species but no parameterization due to a lack of time and data. First, we provide the dominant species of the ICP IM site Zöbelboden which can, if parameterized, be used with the VEG module in order to assess long-term changes of the ground vegetation and its biodiversity. Second, we compiled, according to objective criteria, a list of plant species which are dominant in the forests of the Austrian part of the European Alps. In future, with these species, an Alps-wide assessment of acidification and eutrophication following air pollution would be feasible.

Data sources

Dynamic modeling with VSD+

Dynamic models were calibrated for the ICP Integrated Monitoring site Zöbelboden. The site is characterized by a very high variability of soil properties. In order to get a grip on this variability separate models were calibrated for 7 sites (called permanent plots thereafter) within the 90 ha catchment area. There, and on 50-60 further plots, long-term soil physical and chemical data as well as vegetation data is available. Soil water information and deposition was taken from two intensive plots, which are typical for the two gross site types of the area and was allocated to the respective permanent plots. Long-term meteorological data is available on site (clearing area) (Table AT.1, Figure At.1).

Site description

The Austrian ICP Integrated Monitoring site has a size of 90 ha and is situated in the northern part of the national park "Northern Limestone Alps" (N 47°50'30", E 14°26'30") (www.umweltbundesamt.at/im). The altitude ranges from 550 m to 956 m a.s.l.. The main rock type is Norian dolomite (Hauptdolomit), which is partly overlayed by limestone (Plattenkalk). Due to the dominating dolomite, the watershed is not as heavily karstified as limestone karst systems, but shows typical karst features such as conduits and sink holes. The long-term average annual temperature is 7.2° C. The coldest monthly temperature at 900 m a.s.l. is -1°C (January), the highest is 15.5°C (August). Annual rainfall ranges from 1500 to 1800 mm. Monthly precipitation ranges from 75 mm (February) to 182 mm (July). Snowfall occurs between October and May with an average duration of snow cover of about 4 months.
The watershed can be divided into two distinct sites: A very steep (30–70°) slope from 550–850 m a.s.l. and an almost flat plateau (850-956 m.a.s.l.) on the top of the mountain. The plateau is dominated by Norway spruce (*Picea abies*) following plantation after a clear cut around the year 1910, whereas a mixed mountain forest with beech (*Fagus sylvatica*) as the dominant species, Norway spruce (*Picea abies*), maple (*Acer pseudoplatanus*), and ash (*Fraxinus excelsior*) covers the slope. At the plateau and the slope, one intensive plot has been selected for in-depth measurements of hydrochemical processes. Intensive plot I (IP I) is located on the plateau where Chromic Cambisols and Hydromorphic Stagnosols are found. Intensive plot II (IP II) is located on the slope and is dominated by Lithic and Rendzic Leptosols (FAO/ISRIC/ISSS, 2006). Mull and moder humus forms that indicate quick turnover of the forest floor predominates both plots. Mor humus can be found. The soils of IP II are generally richer in N and exhibit

Figure AT.1 Overview of the ICP IM site Zöbelboden with the location of the main meteorological measurements, the two intensive plots, and the permanent plots (=soil sampling points). Contour lines are shown every 50 m a.s.l.

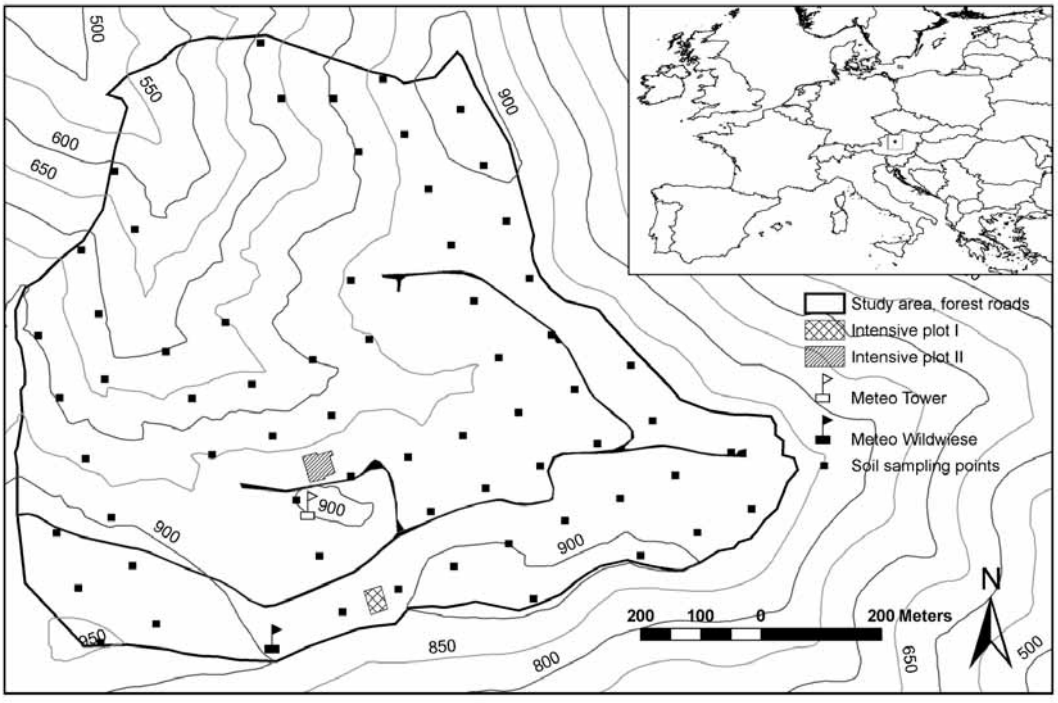

lower mineralization rates than the soils of IP I. See Table AT.1 for the description of soil characteristics.
Permanent plots exist along a 100 x 100 m grid across the watershed totalling to 64 (Figure AT-1). For VSD+ dynamic models a representative part of these plots were chosen because they capture the full variability of the site. Soil and tree layer information is derived from surveys in the years 1992 and 2004. Vegetation was recorded in the years 1993, 2004 and 2008 (and will be recorded in this year, 2010). From the start of the project in 1992 onwards forest management has been restricted to single tree harvesting in case of bark beetle infestation (the IP I has been exposed to bark beetle infestation in the year 2004, impaired deposition samplers were excluded, no lysimeter was affected).

Data sources

Table AT.2 describes all parameters and methods which were used for VSD+. The following parameters were calibrated with VSD studio: lgKAlBC, lgKHBC, lgKAlox, CNrat_o, Ca_we and Mg_we. For all parameters not listed the default values of the last VSD+ version were taken. Two or three permanent plots covering the C/N ratio within each soil type (Stagnosols, Cambisols, Leptosols) were selected, totalling to 7 plots. It is assumed that these plots are representative for the study area.
We used three deposition scenarios for NO_x and NH_3: 1) same as last measuring year (2008), 2) half of the deposition compared with the year 2008 by the year 2050, 3) double deposition compared with the year 2008 by the target year 2050.
All models were run from 1980 to 2100. The 1980 deposition was taken from the respective EMEP grid cell and multiplied by a receptor specific factor (mean of the ratio of bulk deposition/throughfall deposition from 1996 to 2008). Initial base saturation was assumed to be in steady state (bstat_o set to -1).

Table AT.1 Forest and soil characteristics of intensive plot 1 (IP I) and intensive plot 2 (IP II) at the ICP IM site Zöbelboden. Soil chemistry is taken from 16 locations (each 4 soil pits) on a 4 x 4 m grid adjacent to the intensive plots in the year 2004. Mean values and standard deviations in parenthesis. [a] Net mineralization (Nnet min) and gross consumption (Ngross cons) of ^{15}N labelled NH_4^+ applying pool dilution experiments with 37 (IP I) and 39 (IP II) samples acquired on a 5x5 m grid in August in the year 2007 adjacent to the intensive plots.

			IP I	IP II
Actual forest type			Spruce dominated forest	Mixed beech, spruce, maple and ash forest
Potential natural vegetation			*Cardamino trifoliae-Fagetum* sensu Willner 2002	*Adenostylo glabrae-Fagetum* sensu Willner 2002
Soil types			Chromic Cambisols and Hydromorphic Stagnosols	Lithic and Rendzic Leptosols
aspect [°]			0-5	25-35
average soil depths [cm]			51	12
pH_{CaCl2}	organic layer		5.3 (0.6)	5.7 (0.4)
	0-10 cm		6.3 (0.6)	6.7 (0.3)
	10-20 cm		6.6 (0.3)	6.9 (0.1)
C_{org} [%]	organic layer		36 (9.2)	44 (6.1)
	0-10 cm		10.1 (3.5)	20.3 (6.6)
	10-20 cm		5.1 (1.6)	12.7 (1.7)
N_{ges} [%]	organic layer		1.3 (0.2)	1.5 (0.2)
	0-10 cm		0.6 (0.2)	1.2 (0.2)
	10-20 cm		0.4 (0.1)	0.8 (0.2)
[a]$N_{net\ min}$ [mg.kg^{-1}.d^{-1}]		0-5 cm	-3.2 (5.2); max 5.8; min -26.0	-1.7 (2.1); max 1.8; min -10.9
[a]$N_{gross\ cons}$ [mg.kg^{-1}.d^{-1}]		0-5 cm	15.1 (11.0); min -1.9; max 59.5	5.3 (4.4) ; min -1.2; max 23.0

Table AT.2 Methods for the derivation of parameter values for VSD+ input. File names or long-term data..

Keyword	Unit	Value/Filename	Method
SiteInfo	–	ZOE[plot number]	
period	yr yr	1980 to 2100	
thick	m	input*.dat	summation of the depths of the mineral soil horizons of which a soil sample and therefore the bulk density has been calculated
bulkdens	g/cm	input*.dat	the bulk density of a soil sample is the ratio of the oven dried weight (105°) of the fine soil (<2mm) to the volume of the respective sample - the mean bulk density of the profile was calculated by formula 6.22 in Mapping Manual 2004
Theta	m^3/m^3	input*.dat	mean values taken from continuous volumetric water content measurements at two intensive plots (differentiated into soil types)
pCO2fac	–	18	[log10pco2 = -2.38 + 0.031 * Temp (°C)]; atmospheric CO2 pressure = 0.00039 atm; (equation recommended by CCE)
CEC	meq/kg	input*.dat	as the CEC has not be analysed in the subsoil in 2004, the data of the first soil inventory in 1992 has been used - to scale the measured CEC to a value at pH = 6,5, formula 6.29 in Mapping Manual 2004 has been used - the CEC at pH = 6,5 was calculated by formaula 6.28 in Mapping Manual 2004 - the mean CEC of the profile was calculated with the formula 6.23 in Mapping Manual 2004
Excmod	–	1	Gaines-Thomas
lgKAlBC		input*.dat	calibrated with VSD+
lgKHBC		input*.dat	calibrated with VSD+
lgKAlox	((mol/l)1-a)	input*.dat	9.8602 – 1.6755 * log(organic matter [%]) (SAEFL 2005); mineral horizons 0-5 and 5-10 were averaged
Cpool 0	g/m^2	input*.dat	best guess using observed values
CNrat 0	g/g	input*.dat	calibrated with VSD+
RCOOmod	–	1	mono-protic
RCOOpars	–	4.5	according to Mapping Manual
cRCOO	mol/m^3	0.32	according to Mapping Manual: m=0.029; the DOC concentration taken as the mean value of continuous measurements at two intensive plots: 11 mg/l
TempC	°C	input*.dat	mean values taken from continuous measurements at two intensive plots (differentiated into soil types)
percol	m/yr	wabil*.dat	values between 1993 and 2006 taken from a Brook90 calibration for two intensive plots (differentiated in conifer and decideous forest; for mixed forests the mean has been used)
Ca_we	eq/m3/yr	input*.dat	calibrated with VSD+
Mg_we	eq/m3/yr	input*.dat	
SO2 dep	eq/m2/yr	dep*.dat	throughfall deposition from continuous measurements at two intensive plots (differentiated into conifer and deciduous forest; mixed forest taken as the mean value); 1980 values were taken from the EMEP grid and multiplied by a receptor specific constant
NOx dep	eq/m2/yr		
NH3 dep	eq/m2/yr		
Ca_dep	eq/m2/yr		
Mg_dep	eq/m2/yr		
K dep	eq/m2/yr		
Na_dep	eq/m2/yr		
Cl dep	eq/m2/yr		

Table AT.2 continued

Keyword	Unit	Value/Filename	Method
age_veg	yr	input*.dat	age in the year 1980
growthfunc		input*.dat	2 parameter model: annual growth rate was taken from inventories in the years 1993 and 2005; annual litterfall was measured continuously at two intensive plots
veg_type		input*.dat	spruce forest=1; beech forest=4; mixed forest =4
Observations:			
Cpoolobs	g/m^2	bodchem*.obs	available for the years 1992 and 2004; topsoil is defined as organic layer, mineral soil horizon (0-5cm) and mineral soil horizon (5-10cm) - Cpool is calculated by formula: Cpool = depth of soil horizon (cm) * bulk density of soil horizon (g/cm3) * Corg (%) * 100
CNratobs	g/g	bodchem*.obs	available for the years 1992 and 2004; topsoil is defined as organic layer, mineral soil horizon (0-5cm) and mineral soil horizon (5-10cm) - C:N ratio in topsoil was calculated by formula C:N-ratio = Cpool/Npool - the Npool was calculated in the same way as the Cpool
bsatobs		bodchem*.obs	available for the years 1992 and 2004; as the BS has not be calculated in the subsoil in 2004, the data of the first soil inventory in 1992 has been used - the mean BS of the profile was calculated with the formula 6.24 in Mapping Manual 2004
pHobs			
cSO4obs	eq/m^3		
cNO3obs	eq/m^3		available between the years 1998 to 2008; continuous soil water data (plate lysimeter) of the two intensive plots were allocated to plots according to their soil type
cBcobs	eq/m^3	bowaObs*.obs	
cNaobs	eq/m^3		
cClobs	eq/m^3		
cAlobs	eq/m^3		

Results and discussion

The focus is on eutrophication due to nitrogen deposition because acidification is not a big issue for the carbonate soils of the IM site Zöbelboden. However, the model results of parameters relevant for acidification (e.g. pH of the soil solution) did well match with observed values. Figure AT.2, AT.3 and AT.4 show the model results of 7 permanent plots for the three different soil types of the ICP IM site Zöbelboden - Leptosols, Cambisols and Stagnosols - which capture the main variability within the site and probably also within major parts of the Northern Limestone Alps.

Observed C/N ratios of Leptosols are between 14 and 20 in the year 2004. Regardless of the deposition scenario C/N ratio is constantly and quite similarly decreasing to around 12 by 2100. C pool is converging to around 6000 g/m^2. Reasonable N leaching starts between 2020 and 2030 in the baseline scenario and reaches 0.05 eq/m^2/yr whereas in the double deposition scenario leaching starts 10 years earlier and reaches almost 0.15 eq/m^2/yr. A critical C/N ratio for reasonable N leaching seems to be approx. <13. Overall, the permanent plots with Leptosols behave very similar (Figure AT.2).

C/N ratios of Cambisols are very different, ranging between 12 and 22 in the year 2004. C pools range between 4000 and 8000 g/m^2 during the entire modeling period and N pools between 300 and 550 g/m^2. Two permanent plots show low changes of the C/N ratio in the baseline scenario and N leaching depends strongly on absolute C/N status. For one of these plots, a relatively high C/N ratio is maintained due to a much higher growth rate than the other permanent plot. One plot shows strong decrease of the C/N ratio and reaches the same magnitude by 2030 as the low C/N plot. The permanent plot with the low starting value of C/N shows reasonable N leaching parallel to N deposition; only a half deposition scenario shows decreasing leaching. The plot with the high growth rate seems to be relatively insensitive to N deposition and only with the double deposition scenario reasonable N leaching is predicted. Interestingly, this is a spruce stand whereas the others are mixed spruce-beech stands. Other results showed the contrary, namely that N retention is higher in beech stands of the IM site. A critical C/N ratio for reasonable N leaching seems to be approx. <14 (Figure AT.3).

C/N ratios of Stagnosols are in the range of 15 to 20 in the

year 2004. C pools range between 2500 and 7000 g/m² during the entire modeling period and N pools between 100 and 300 g/m². The two permanent plots differ strongly regarding the growth rate of the forest stands. With low growth rate and the resulting decrease of the C/N ratio reasonable N leaching occurs as soon as deposition is >0.1 eq/m²/yr or in the long run. On the other hand, leaching only occurs during the double deposition scenario (Figure AT.4).

That sensitivity of sites to N leaching in the study area increases from Leptosols to Stagnosols corroborating earlier results. However, comparison of the model results with measured and modelled N leaching shows that the calibrated models for the 7 permanent plots predict much lower N leaching than was observed. Long-term observations between the years 1993 and 2007 show that 7.5 to 20 kg/ha/yr inorganic N (0.05 - 0.14 eq/m²/yr) leaches with the soil water to the ground water. With VSD+ such values are only predicted to occur in the long term and under higher deposition of N than today. In addition, all models show a strong deviation from observed NO_3 concentrations found in lysimeter samples between the year 1996 and 2008. There are four possible explanations we may think of:

1) N processes exhibit very strong seasonal variation so that annual means might not be very representative.

2) Preferential flow through macropores is common in the soils found at the IM site Zöbelboden. The concentration in the lysimeter samples which are designed for capturing all seepage, but could potentially be biased towards matrix flow, might not be representative or at least not comparable to what the model does. Since hydrological processes are very important for the long-term trends of C and N in soils, these could be incorporated into VSD+ with more detail.

3) By using throughfall deposition alone other important deposition pathways - or part of it - are ignored, namely dry and occult (fog and cloud) deposition. It is known for the IM site Zöbelboden (measurements of fog samples an application of fog and dry deposition models) that total deposition might be double the throughfall deposition, particularly in stands with a high proportion of conifers such as spruce. These deposition pathways should be incorporated in future.

4) In further modelling efforts an age dependent growth function should be parameterized because of the prime importance of growth for long-term N immobilisation. Presently we used only a constant function with the growth rate taken from the difference of only two time points (1992 and 2004). It is probable that week predictions result from this rough approximation.

Figure AT.2 Time trends of deposition and C and N components of two permanent plots (different colours in the C/N and N leaching plot) of the ICP IM site Zöbelboden with Leptosols. Deposition scenarios: baseline=100% (full line); 50% (dashed line); 200% (dotted line).

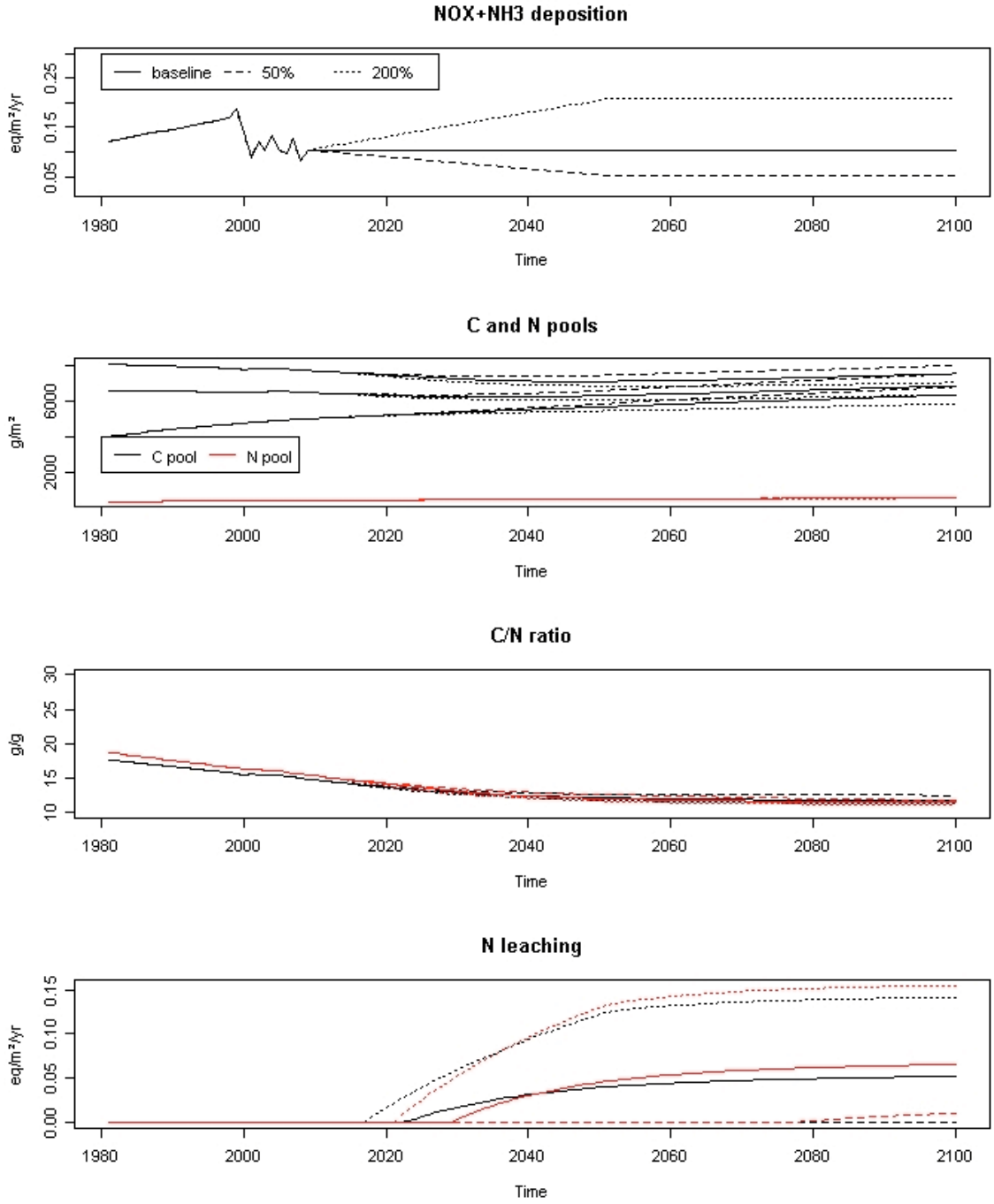

Figure AT.3 Time trends of deposition and C and N components of two permanent plots (different colors in the C/N and N leaching plot) of the ICP IM site Zöbelboden with Cambisols. Deposition scenarios: baseline=100% (full line); 50% (dashed line); 200% (dotted line).

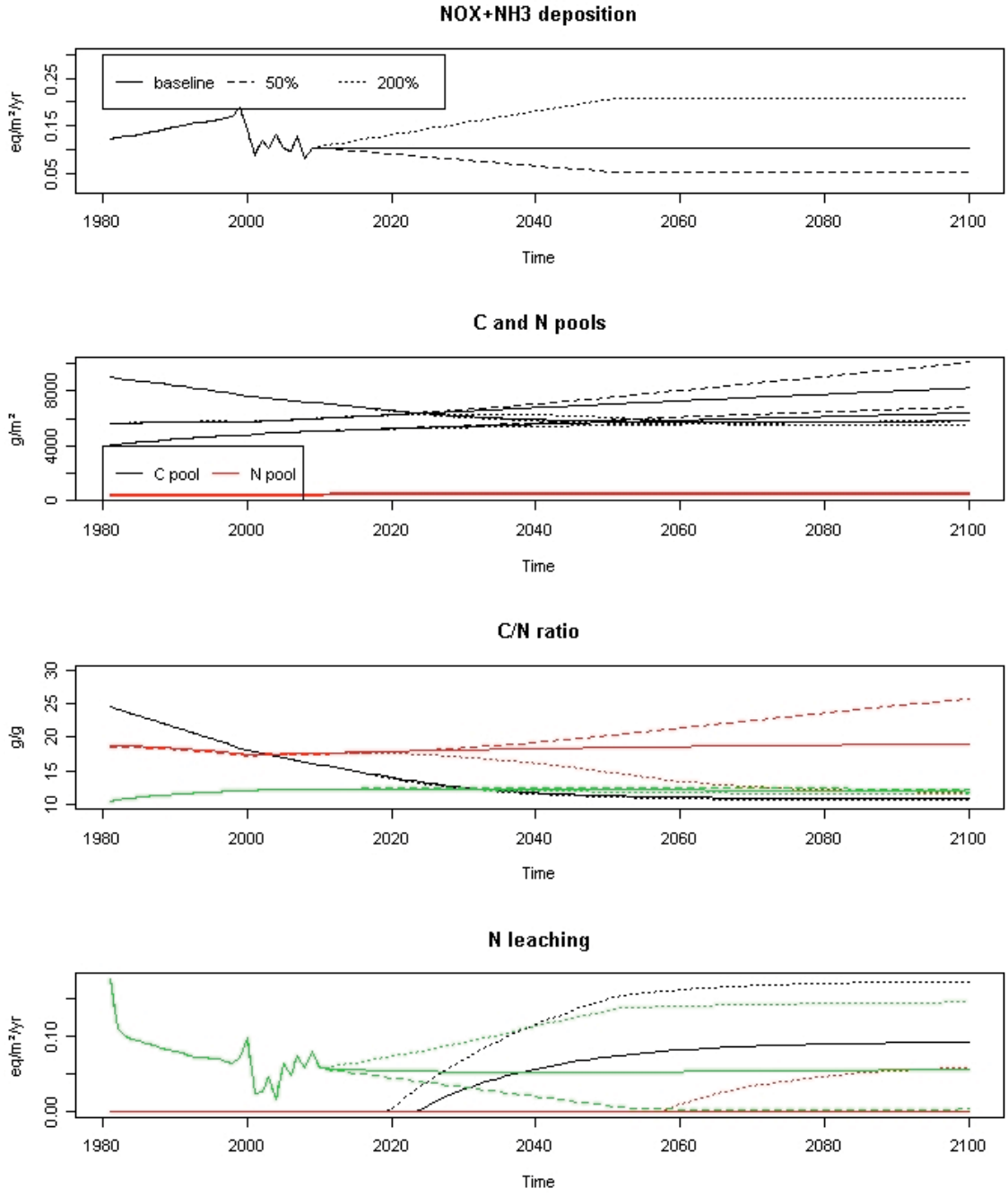

Figure AT.4 Time trends of deposition and C and N components of two permanent plots (different colours in the C/N and N leaching plot) of the ICP IM site Zöbelboden with Stagnosols. Deposition scenarios: baseline=100% (full line); 50% (dashed line); 200% (dotted line).

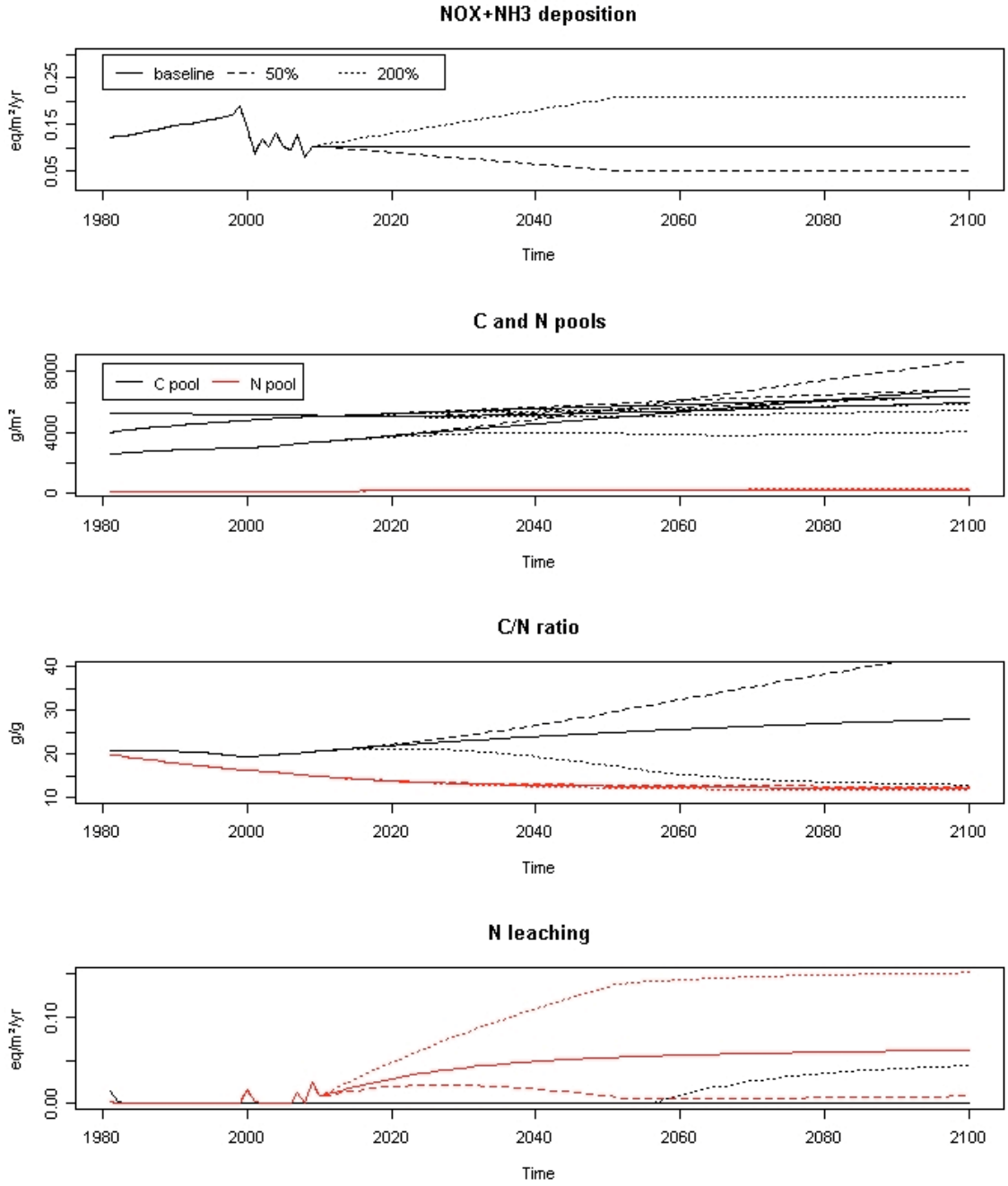

Conclusions

In general, the dynamic model VSD+ did well in calculating long-term trends of the major soil properties of the ICP IM site Zöbelboden in Austria as affected by deposition of eutrophying and acidifying substances. However, with the used parameterization, there are reasonable deviations from observed values particularly with regard to the N cycle. Above, we discuss potential future improvements of the model and the parameterization.

The variation of outcomes is a result of the high variation of soil properties and tree species composition in the study area. This variability is, however, typical for the many parts of the European Alps. Thus, single-plot studies should be interpreted with caution when regional or national assessments are targeted.

Future activities with dynamic models should act on several sites across Austria, preferably within the European Alps because only little knowledge is available from there. Potential sites would be ICP forest level II plots and some scattered long-term studies on alpine pastures and other grasslands (see listed contacts in "Relcontact" below).

Model bugs

Once a calibration results to "less than 20%..." the program fails during the next calibration and it has to be restarted. (Red. This reported bug has been solved in later versions)

Vegetation data

Two lists of species were added to the existing VegPars: 1) the plant species occurring in the plots of the ICP IM site Zöbelboden which were modelled with VSD+ (see above) and which are part of 2) ; 2) Austrian forest plant species occurring in the main plant communities of the Alps.

1) **ICP IM Zöbeboden species**: In total, 33 species already exist in the template database, which means that or these species parameterization is available. A part of the additional species (115) might have been included in the collection described in VegParameterManual.pdf. Therefore and because such a parameterization is much more advisable for all Austrian forest species with additional plot data (see below) parameters are not delivered now. Data on species cover per plot (from the years 1993, 2005, 2008 (and 2010)) are available upon request (T. Dirnböck, E-mail see above).
2) **Austrian forest plant species**: Forest plant communities occurring in the European Alps are the focus of the contribution of Austria, because other plant communities are covered elsewhere as well. We tried to reduce the number of species in order to focus on "important" ones and to hold the list as short as possible. However, one should be aware, that rare species, often important for biodiversity, hence are excluded. Forest species were taken from Willner & Grabherr (2007) by including all alliances apart from riverine or wetland forests (Alnetea glutinosae, Alnenion glutinoso-incanae, Vaccinio uliginosi-Pinetea), those not relevant in the Alps (Quercion pubescenti-petraeae, Ulmenion), and very rare ones (Fraxino ornio-Ostryon, Ononido-Pinion, Pinus nigra forests). Moreover, only species which occurred in more than 20% of the relevés of the respective syntaxon were selected. In total 46 of these species are already included in the CCE list. For the further 176 species (may be some of those are included in the lists mentioned in the VegParameterManual.pdf) parameterization is not yet done but work could, depending on financial resources and data availability, continue by including data from the Austrian ICP Forest program.

Relevés with measured soil parameters

Available relevés with measured soil parameters exist in forests and managed grassland. Three relevant contacts are given in "Relcontact": 1) the data holder of the ICP IM site for which VSD+ was calibrated (see above); 2) the data holder of the Austrian ICP forest level I and II plots; 3) a reasonable dataset on grasslands is available in the Austrian Research Centre for Agriculture in Raumberg-Gumpenstein.

Data structure

VSD+ files:

All files are compiled in ZOEvsd.zip; three deposition scenarios have the following suffix: "_50Proz" for the half deposition and "_200Proz" for the double deposition scenario, the baseline scenario has no suffix.

calibrate.dat – distribution of parameters for Bayesian calibration

input[plot number][deposition suffix].dat – main input file for each plot

dep[plot number][deposition suffix].dat – deposition file (1979 values are set to unusually high values because of "too little N available" - problems)

wabil[plot number].dat – percolation file

bodchem[plot number].obs – observations for Cpoolobs, CNratobs and bsatobs

bowaObs[plot number].obs – observations for pHobs, cSO4obs, cNO3obs, cBcobs, cNaobs, cClobs, cAlobs.

Vegetation database:

VegPars_orig – original table

VegPars_AT_extended – original species and Austrian forest species (duplicates were removed); nomenclature follows Adler et al. (1994)

SpeciesNamesTranslate – table which can be used to translate different species nomenclature (CCE list, AT list and AT IM list)
Relcontact – contact for relevés with measured soil parameters

References

Adler W, Oswald K, Fischer R, 1994. Exkursionsflora von Österreich. Verlag Eugen Ulmer, Stuttgart and Vienna

Dirnböck T, Jost G, Mirtl M, 2009. Langfristige Dynamik des Stickstoffaustrages ins Bodenwasser kalkalpiner Wälder. 13. Gumpensteiner Lysimetertagung: Lysimeter – Perspektiven in Forschung und Anwendung, 21- 22. April 2009, Lehr- und Forschungszentrum für Landwirtschaft Raumberg-Gumpenstein, Arbeitsgruppe Lysimeter, pp 55-58

Dirnböck T, Mirtl M, 2009. Integrated monitoring of the effects of airborne nitrogen and sulfur in the Austrian Limestone Alps. Is species diversity a reliable indicator? – Mountain Research and Development 29: 153–160; doi:10.1659/mrd.1072

Diwold K, Dullinger S, Dirnböck T, 2010. Effect of nitrogen availability on forest understorey cover and its consequences for tree regeneration in the Austrian limestone Alps. Plant Ecology, online; doi:10.1007/s11258-009-9715-z

Hülber K, Dirnböck T, Kleinbauer I, Willner W, Dullinger S, Karrer G, Mirtl M, 2008. Long-term impacts of nitrogen and sulphur deposition on forest floor vegetation in the Northern limestone Alps, Austria. Applied Vegetation Science 11: 395–404

UBA, 2004. Manual on methodologies and criteria for modelling and mapping critical loads and levels and air pollution effects, risks and trends. Umweltbundesamt Texte 52/04, Berlin www.icpmapping.org

Umweltbundesamt, 2007. Effects of nitrogen and sulphur deposition on forests and forest biodiversity. Austrian Integrated Monitoring Zöbelboden. Report 0077, Umweltbundesamt GmbH, Vienna, Austria

Willner W, Grabherr G (eds), 2007. Die Wälder und Gebüsche Österreichs. Ein Bestimmungswerk mit Tabellen. Spektrum Akademischer Verlag, Heidelberg

Zechmeister HG, Dirnböck T, Hülber K, Mirtl M, 2007. Assessing airborne pollution effects on bryophytes - Lessons learned through long-term integrated monitoring in Austria. Environmental Pollution 147: 696–705

Belgium (Wallonia)

National Focal Centre/Contacts

A. Fourmeaux
Ministry of Walloon Region, DGRNE
Avenue Prince de Liège 15
B-5100 Namur
tel : +32 -81-325784
fax : +32-81-325784
email: A.Fourmeaux@mrw.wallonie.be

Coordinators/Contacts

V. Vanderheyden, J-F. Kreit
SITEREM S.A.
Cour de la Taillette, 4
B-1348 Louvain-la-Neuve
email: info@siterem.be

Interdisciplinary Team/Contacts

S. Eloy
Scientific Institute for Public Services (ISSEP)
Rue du Chera, 200
B-4000 Liège
email: s.eloy@issep.be

National contribution

This year, the CCE suggested that National Focal Centres apply the VSD+ model to selected sites in their country. VSD is the simplest extension of the steady-state Simple Mass Balance (SMB) model into dynamic soil model by including cations exchange and time-dependent N immobilisation. .

Study sites in Wallonia

In 1999, 10 forest sites were studied in details (Brahy and Delvaux 2000). The parameters of soil and soil solutions were analysed by horizons until 50 cm depth.

Measurements and Calculation methods - Wallonia

For each sites, the different horizons were intensively characterised as illustrated for one site in table BE.1.
To introduce a specific value for the various parameters of VSD model (CEC, Bast, logKAlBc...), weighted averages are calculated for a 50 cm depth layer (recommended layer thickness to calculated critical loads for forest ecosystems). For soil solution parameters, average values of monthly lysimetric measurements were calculated.

Table BE.1 Soil parameters for Louvain-la-Neuve site.

Horizons	Profondeur /cm	pH H_2O	pH KCl	Cond. élect. /µS	C. org. /%	N /%	C/N
Ah	0-10	4.57	3.42	45	7.46	0.388	19.24
E	10-40	4.54	3.88	37	0.61	<0.05	-
Bt	40-50	4.36	3.86	44	0.00	<0.05	-

Horizons	Granulométrie /%			Eléments échangeables au Ba /$cmol_c\ Kg^{-1}$							[a]CEC éff.	[b]V
	50-2000 µ	2-50 µ	< 2 µ	Na^+	K^+	Ca^{2+}	Mg^{2+}	Fe^{3+}	Mn^{2+}	Al^{3+}	H^+	/$cmolc\ Kg^{-1}$	/%
Ah	16.63	71.66	11.71	0.05	0.34	1.25	0.39	0.54	0.11	4.79	1.65	9.13	22.33
E	15.37	70.75	13.88	0.04	0.08	0.28	0.05	0.20	0.08	2.70	0.24	3.67	12.10
Bt	12.72	67.33	19.95	0.03	0.10	0.15	0.05	0.00	0.05	3.88	0.28	4.53	7.08

Horizons	Analyse totale /%									
	Na_2O	K_2O	CaO	MgO	Fe_2O_3	MnO	Al_2O_3	SiO_2	TiO_2	Perte au feu
Ah	0.88	2.02	0.27	0.27	3.00	0.03	6.26	71.61	0.59	15.07
E	1.02	2.11	0.29	0.26	2.78	0.07	6.84	82.96	0.70	2.97
Bt	1.01	2.46	0.48	0.25	4.17	0.06	9.16	79.07	0.73	2.58

Horizons	Réserve en bases /$cmol_c\ Kg^{-1}$					[d]Fe_d	[e]$_mANC_s$	Refus	Masse terre fine/volume
	Na	K	Ca	Mg	[c]TRB	/mg g^{-1}	/$cmol_c\ Kg^{-1}$	/%	/ g cm^{-3}
Ah	28.52	42.92	9.54	13.17	94.14	11.27	514.6	0.00	0.74
E	33.00	44.84	9.34	14.34	101.52	8.64	562.0	0.00	1.24
Bt	32.68	52.22	9.03	23.63	117.57	10.01	759.6	0.00	1.59

[a]CECéff. = CEC éffective = $H^+ + Ca^{2+} + Mg^{2+} + Na^+ + K^+ + Mn^{2+} + Fe^{2+} + Al^{3+}$ échangeables au Ba.

[b]V = Taux de saturation en bases = $(Ca^{2+} + Mg^{2+} + Na^+ + K^+)_{éch.} * 100/ECEC$

[c]TRB = Réserve totale en bases = $(Ca^{2+} + Mg^{2+} + Na^+ + K^+)_{tot.}$

[d]Fe_d = Fe extrait au DCB = Fe "libre", non silicaté.

[e]$_mANC_s$ = Capacité à neutraliser l'acidité du sol = TRB + 6(Al_2O_{3tot}) + 6 (Fe_2O_{3tot}-Fe_2O_{3d}), TRB exprimé en $cmol_c\ Kg^{-1}$ et () en concentration molaire.

Some calculation methods are explained in more details hereafter.

The equilibrium K = $[Al^{3+}]/[H^+]^3$ criterion: The Al^{3+} concentration was estimated by or 1) experimental speciation of soil solutions enabling to rapidly measuring reacting aluminium, Alqr (Clarke *et al.* 1992) ; 2) calculation of Al^{3+} concentration from Alqr using the SPECIES speciation software. The K values established for 10 representative Walloon forest soils were more relevant than the gibbsite equilibrium constant recommended in the manual (UBA 1996).

Weathering rate: In *Wallonia* the base cations weathering rates (BC_{we}) were estimated for 10 different representative soil types through leaching experiments. Increasing inputs of acid were added to soil columns and the cumulated outputs of lixiviated base cations (Ca, Mg, K, Na) were measured. Polynomial functions were used to describe the input-output relationship (Figure BE.1). The BC_{we} in Table BE.3 is the weathering measured for an acid input (NOx+NH4+SOx] fixed at 900 eq $ha^{-1}yr^{-1}$.

Ni parameter: The Tables BE.2 summarises the values given to N_i parameter. These values come from the report "Improvement of steady-state and dynamic modelling of critical loads and target loads for nitrogen, Alterra, MNP-CCE 2005.

Table BE.2 Values of Ni parameter.

Parameter	Value
N_i	5.6 kg N $ha^{-1}yr^{-1}$ coniferous forest
	7.7 kg N $ha^{-1}yr^{-1}$ deciduous forest
	6.65 kg N $ha^{-1}y^{--1}$ mixed forest

The flux of drainage water leaching, Q_{le}, from the soil layer (entire rooting depth) was estimated from EPICgrid model (Faculté Universitaire des Sciences Agronomiques de Gembloux). The results of the EPICgrid model are illustrated in Fig BE-2.

Figure BE.1 base cations weathering in relation with input of acidity.

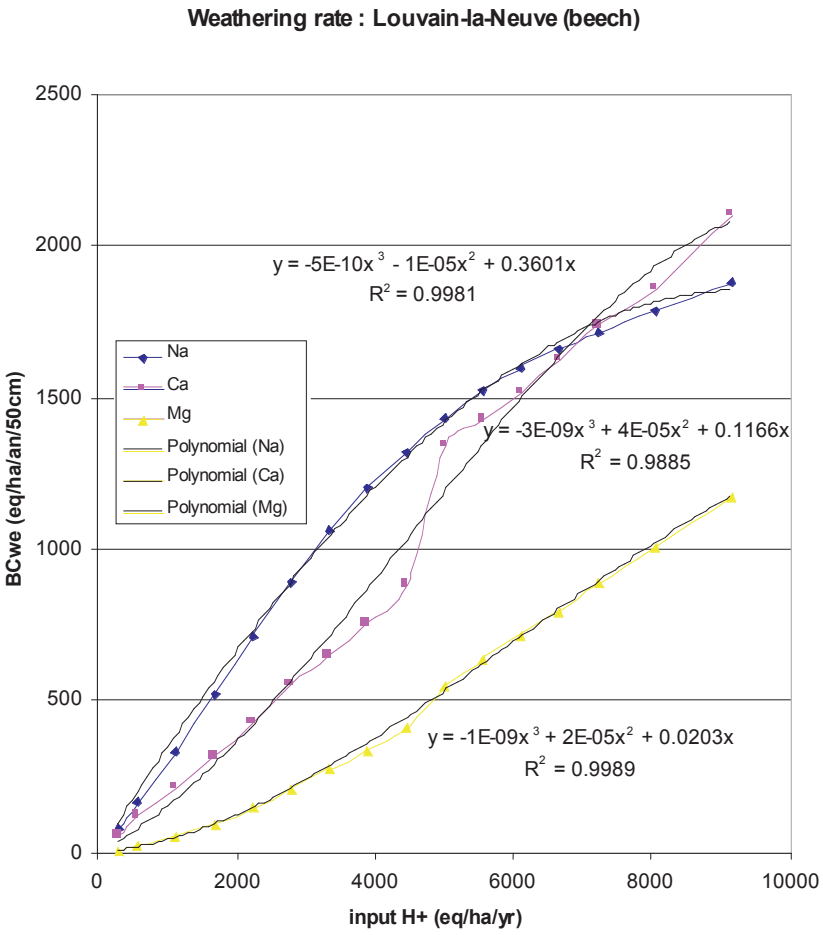

Figure BE.2 Flux of drainage at 50 cm depth in Wallonia for the 2001–2005 period.

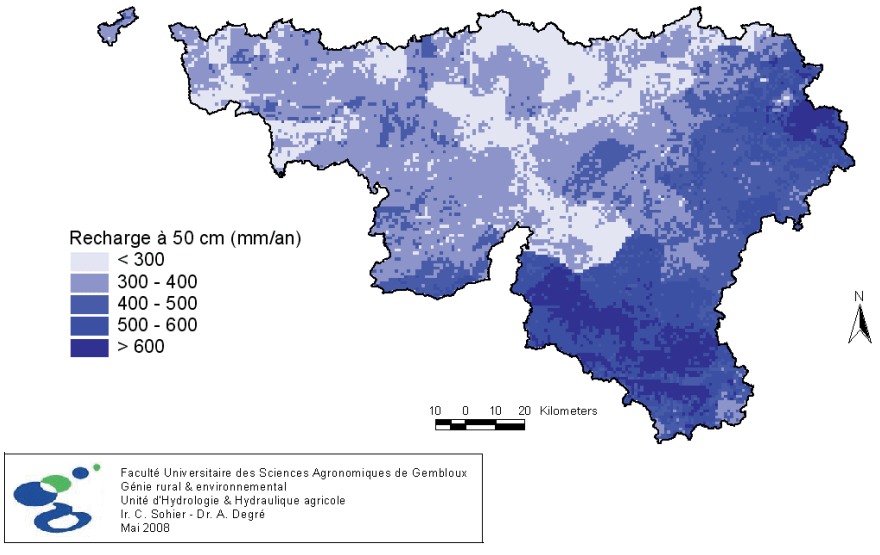

Net growth uptake of base cations and nitrogen

In Wallonia, the net nutrient uptake (equal to the removal in harvested biomass) was calculated using the average growth rates measured in 25 Walloon ecological territories and the chemical composition of coniferous and deciduous trees. The chemical composition of the trees (Picea abies, fagus sylvatica, Quercus robus, Carpinus betulus) appears to be linked to the soil type (acidic or calcareous) (Duvigneaud et al. 1969, Bosman et al. 2001, Unité des Eaux et Forêts 2001).

The net growth uptake of nitrogen ranges between 266 and 822 eq $ha^{-1}yr^{-1}$, while base cations uptake values vary between 545 and 1224 eq $ha^{-1}yr^{-1}$ depending on trees species and location in Belgium.

Base cations deposition

In Wallonia, actual throughfall data collected in 8 sites, between 1997 and 2002, were used to estimate BCdep parameters.

N and S deposition

The deposition data in forests come from the VSD model (2008 version). The N and S depositions are given by grid 50x50 km (Table BE.3).

For this call of data, the simulation for 6 sites (Chimay, Eupen Oak, Eupen Picea, Louvain-la-Neuve, Ruette and Willerzie have been realised.

Comparison between measured values and output of VSD+ model – Wallonia

The table BE.04 gives the comparison between the measured parameters in soil or in soil solutions (lysimetric data) and the few estimated values by VSD+ model. We observe, in all sites, large differences in pH values for soil or soil solution, and in [SO4+], [NH4+] and [NO3-] concentrations in soil solutions. The C/N ratio is well predicted for Louvain-la-Neuve and Eupen sites but large discrepancies

Table BE.3 Summary of the main parameters for use with VSD+ model.

Parameters	Unit	Bande	Chimay	Eupen	Eupen	Hotton	Louvain-la-Neuve	M-D-Virton	Transinne	Ruette	Willerzie
vegetation type		oak-birch-picea	oak	oak	Picea abies	oak	beech	oak-beech	beech	beech	Picea abies
Grid EMEP	i50-j50	60-42	59-40	61-43	61-43	60-42	59-42	61-41	60-41	61-41	60-41
soil type	-	GbGq	Gdbf	Gixr	Ghxr	GBBK	(x)Aba	Zaa	Gbbfi	Ebdy	Gbbr1
thick	m	0.5	0.5	0.5	0.5	0.5	0.5	0.5	0.5	0.5	0.5
CEC	meq/kg	59	55	87	76	135	46	20	41	218	57
Bsat	-	0.067	0.092	0.055	0.04	0.992	0.125	0.072	0.069	0.859	0.065
bulkdens	g/cm3	0.714	1.191	0.732	1.225	1.086	1.21	1.098	0.631	1.043	0.785
Cpool (Ah)	g/m2	368	1521	10503	22960	4282	5520	2240	3845	963	6075
C/N ratio (Ah)	g/g	22.94	22.72	21.6	39.54	11.89	19.24	19.6		12.39	17.89
pH soil solution	-	5.16	5.61	4.81	3.5	8.19	4.37	5.4	4.61	6.12	4.67
DOC	ppm	28.094	10.3	28.7	25.6	8.47	26.9	10.13	21.235	1.93	10.495
logKAlBc	-	0.707	0.861	0.713	0.685	-0.988	0.232	0.602	0.232	-0.349	1.027
logKHBc	-	3.549	4.517	0.682	1.819	3.529	2.508	3.449	2.508	1.125	2.078
LogKAlox	(l/mole)2	7.67	8.14	8.91	6.92	8.96	8.34	8.89	9.07	9.25	8.93
Corg	éq/m3	0.103	0.0378	0.1052	0.0939	0.0311	0.0986	0.0371	0.0779	0.0071	0.0385
Kwe	éq/m3/an	0.0299	0.0095	0.0255	0.0121	0.0019	0.0027	0.0029	0.0027	0.0022	0.0023
Nawe	éq/m3/an	0.0506	0.0764	0.0863	0.0790	0.0525	0.0668	0.0290	0.0479	0.0519	0.0536
Cawe	éq/m3/an	0.0322	0.1376	0.1244	0.0510	0.7785	0.0429	0.0471	0.0425	0.6419	0.0520
Mgwe	éq/m3/an	0.0094	0.0651	0.1752	0.0283	0.0404	0.0152	0.0145	0.0189	0.0102	0.0113
Bcwe	éq/m3/an	0.1220	0.2886	0.4114	0.1704	0.8732	0.1276	0.0934	0.1120	0.7062	0.1192
yearly growth	m3/ha/year	5.323	2.575	3.77	15.197	3.77	7.789	5.323	5.532	6.187	17.594
litterfall											
leaf, wood, peels	kg/m2/year	0.43	0.54	0.53	0.28	0.44	0.46	0.57	0.49	0.6	0.37

Table BE.04 Measured parameters on sites and estimated parameters by the VSD+ model.

	Year 1999	pH soil	C/N ratio	EBc	[H+]	[Ca+Mg+K]	[SO4+]	[NH4+]	[NO3-]
					Concentration in soil solutions [eq/m3]				
Louvain-la-Neuve	measured	[4.4-4.6]	19.24	[0.06-0.2]	9.37E-03	1.80E-01	1.69E-01	1.90E-02	4.80E-01
	VSD+	5.36	19.47	0.621	4.37E-03	1.87E-01	5.42E-01	7.30E-12	5.80E-08
Eupen Oak	measured	[4.0-4.4]	21.6	[0.03-0.06]	8.10E-03	1.90E-01	1.59E-01	9.40E-02	8.40E-02
	VSD+	6.53	28.34	0.92	2.90E-04	5.34E-01	2.01E-01	4.28E-41	5.12E-09
Eupen Picea	measured	[3.4-4.3]	39.5	[0.032-0.059]	3.00E-01	2.20E-01	1.69E-01	1.06E-01	8.64E-01
	VSD+	5.28	36	0.531	5.10E-03	7.50E-02	2.98E-01	1.10E-13	1.18E-09
Chimay	mesured	[4.1-4.5]	22.72	-	3.66E-03	5.80E-01	4.79E-01	3.00E-03	6.50E-02
	VSD+	6.78	40.32	0.767	1.64E-04	7.92E-01	3.36E-01	7.50E-24	2.70E-08
Ruette	measured	[5.2-5.7]	12.39	[0.65-0.95]	2.20E-03	4.00E-01	1.51E-01	2.00E-02	1.89E-01
	VSD+	7.26	48.89	1	5.37E-05	2.09E+00	1.91E-01	5.35E-38	8.11E-12
Willerzie	measured	[3.9-4.6]	17.89	[0.054]-0.062	9.40E-03	1.80E-01	1.62E-01	1.90E-02	4.85E-01
	VSD+	5.93	40.7	0.388	1.10E-03	1.12E-01	4.75E-01	6.30E-19	8.89E-09

are observed for others sites. The concentrations of base cations are well estimated, probably owing to the existing relationship between the inputs in acidity and weathering rate.

To improve the reliability of the predicted parameters of VSD+ model, the relationships between inputs in acidity and [SO4+], [NH4+] [NO3-] concentrations in soil solutions could be inserted into the model. In addition, replacement of the inputs of total acidity by the net acidity ones which take into account the base cations depositions data, could give rise to supplementary relevance.

References

Bosman B, Remacle J, Carnol M, 2001. Element removal in harvested tree biomass: scenarios for critical loads in Wallonia, south Belgium. Water, Air and Soil Pollution, in press

Brahy V, Delvaux B, 2000. Estimation des quantités d'ammonium et de bases cationiques mobilisées à partir de dix sols forestiers wallons, suite à des apports croissants d'acide. Vérification de la pertinence de l'utilisation du modèle gibbsitique pour prédire l'activité en Al3+ critique. Université catholique de Louvain. Published for Ministère de la Région wallonne, DGRNE, Belgique

De Vries W, Reinds GJ, Posch M, Kämäri J, 1994. Simulation of soil response to acidic deposition scenarios in Europe. Water, Air and Soil Pollution 78: 215–246

De Vries W, 1994. Soil response to acid deposition at a different regional scale: field and laboratory data, critical loads and model predictions. PhD dissertation, Univ. Wageningen, The Netherlands, 487 pp

De Vries W, 1990. Methodologies for the assessment and mapping of critical acid loads and of the impact of abatement strategies on forest soils in the Netherlands and in Europe. Winand Staring Centre Report, Wageningen, The Netherlands, 91 pp

Dupriez, Sneyers, 1979. Les nouvelles cartes pluvio-métriques de la Belgique. Rapport a/103. Institut Météorologique de Belgique, Uccle, Bruxelles

Duvigneaud P, Kestemont, Ambroes P, 1969. Productivité primaire des forêts tempérées d'essences feuillues caducifoliées en Europe occidentale. Unescco, 1971. Productivité des écosystèmes forestiers, Actes du Colloque de Bruxelles (écologie et conservation), pp.259–270

Eloy S, 2000. Modeling, Mapping, and Managing critical loads for forest ecosystems using a geographic information system: approach of Wallonia, Belgium, to study of long-range transboundary air pollution effects on ecosystems in Europe. Environmental Toxicology and Chemistry 19, 4(2): 1161–1166

Fevrier (1996) Charges critiques d'acidité pour les eaux de surface dans le massif des Ardennes. DEA Physique et chimie de la Terre, ULP STRASBOURG, 38 pp.

Maréchal R., Tavernier R. (1970). Association des sols, pédologie 1/500 000. Atlas de Belgique, Bruxelles, Belgium.

UBA (1996) Manual on Methodologies and Criteria for Mapping Critical Levels/Loads and geographical areas where they are exceeded. UN/ECE Convention on Long-range Transboundary Air Pollution. Federal Environmental Agency (Umweltbundesamt), Texte 71/96, Berlin

Unité des Eaux et Forêts (mai 2001), Exportation de minéraliomasse par l'exploitation forestière. Université Catholique de Louvain, Belgique.

Siterem (2001) Estimation des charges critiques et des excès en polluants acidifiants pour les ecosystèmes forestiers et aquatiques wallons.
Editor : Siterem s.a, Autors : Vanderheyden V. and Kreit J-F, Co-Autors : Bosman B., Brahy V., Carnol M., Delvaux B., Demuth C., Eloy S., Everbecq E., Halleux I., Jonard M., Marneffe Y., Masset F., Remacle J., Thome J.P. Published for Ministère de la Région wallonne, DGRNE, Belgique.

Siterem (2006) Analyse spatio-temporelle du dépassement des charges critiques en polluants acidifiants en région wallonne. Analyse selon le type d'écosystème et mise en relation avec les quantités émises de substances acidifiantes.
Editor : Siterem s.a, Autors : Vanderheyden V with collaboration of ISSEP and CELINE. Published for Ministère de la Région wallonne, DGRNE, Belgique.

Weissen F., Hambuckers A., Van Praag H.J., & Remacle,J. (1990). A decennial control of N-cycle in the Belgian Ardenne forest ecosystems. Plant and Soil 128: p.59-66

Bulgaria

National Focal Centre
Borislava Borisova
Executive Environmental Agency
Tzar Boris III Str., 136
BG - 1618 Sofia
tel: +359 2 940 64 18
+359 2 955 90 11
fax: +359 2 966 90 15
e-mail: borissova@nfp-bg.eionet.eu.int

In response to the call data of November 2009 a new dataset of critical loads and dynamic modelling we present the following information and data.

Data Sources

National maps (soils):

Soil type information on the FAO soil map of Bulgaria;
Geological map of Bulgaria 1 : 500 000
Vegetation map of Bulgaria 1 : 500 000
Mean annual temperature map 1: 500 000
Mean annual precipitation map 1: 500 000
The monitoring of the soil is in 10 years - Jundola, Vitinya and Staro Oryahovo..

Ecosystem: Two forest ecosystem types have been investigated according to EUNIS classification: **G1** (Fagus sylvatica and Querqus fraineto, Querqus cerris); **G3** (Picea abies, Abies alba).

Runoff: of water under root zone has been measured in grid cells of 10 x 10 km^2 for the entire country (Kehayov, 1986).

Depositions: Sulfur and Nitrogen deposition time series provided only by Bullgarian Air Immissins Data. Since 2005, not carried out such measurements in Jundola, Vitinya and Staro Oryahovo.

Receptors: Coniferous and deciduous forests in 3 EMEP 50/50 km network stations:

Station Name	LON_ degrees	LAT_ degrees	I50	J50
Jundola	23.8900	41.9200	131	62
Vitinya	23.9200	42.9200	129	63
Staro Oryahovo	27.8200	43.0600	132	69

Figure BG.1 Map of investigated areas by the EMEP 50/50 km GRID

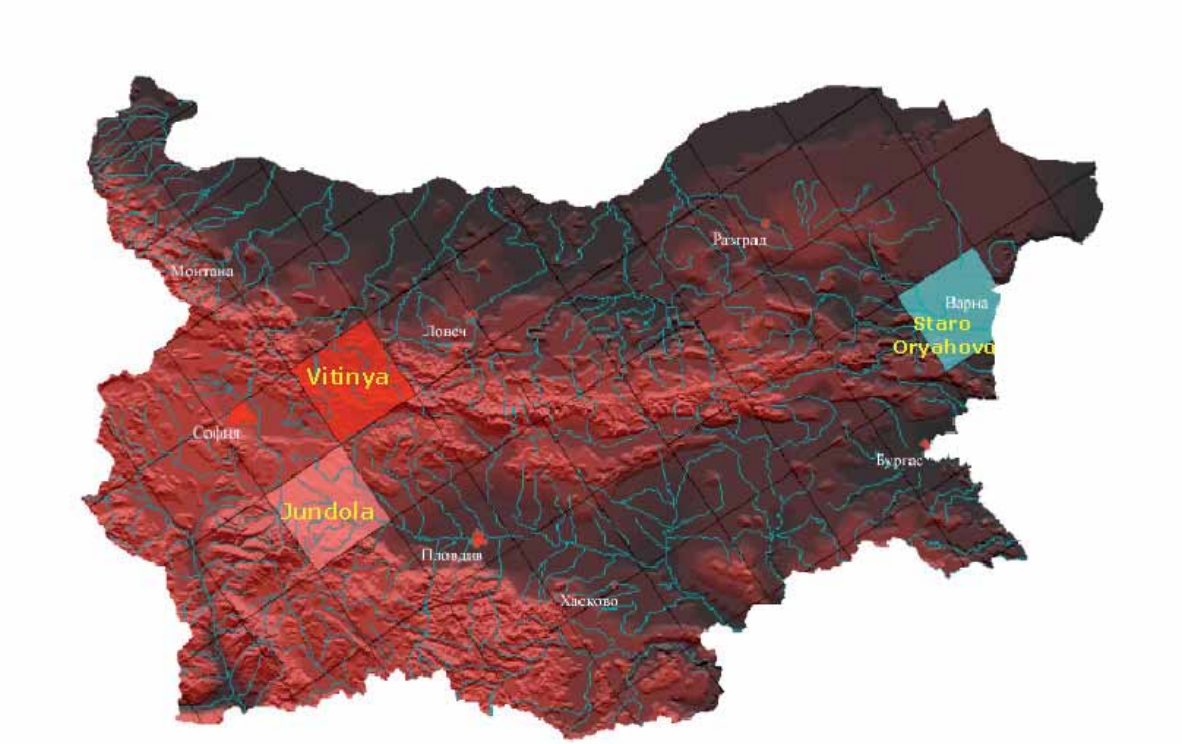

Calculation data and Methods

- In the absence of more specific data on the production of basic cations through mineral weathering for most of study regions, weathering rates have been calculated according to the dominant parent material obtained from the lithology map of Bulgaria and the texture class taken from the FAO soil map for Europe, according to the clay contents of the Bulgarian forest soils (UBA 1996).
- Gibbsite equilibrium constant Kgibb for the Al - H relationship (m^6 / eq^2) has been estimated in accordance with the soil organic matter in % and type of soils using the manual (UBA, 1996).

A detailed description and the data and methods used for derivation is given in Table BG.1

Table BG.1 Input parameters for the VSD+ model. DATA DESCRIPTION, METHODS and SOURCES

Keyword	Description	Explanation and Unit
SiteInfo	Area of the ecosystem within the EMEP grid cell (-)	Calculated from Bulgarian forest inventory data
period	Starting and ending time of simulation	1960 to 2010
thick	Thickness of the soil compartment	0.5 m
bulkdens	Average bulk density of the soil	Manual for Dyn.modelling 5.1.3. Eq. 5.1 (g/cm$^{3)}$
Theta	Water content of the soil	from Bulgarian forest Inventory data (m/m)
pCO2fac	CO_2 pressure in soil solution (multiple of pCO2[atm] in air)	BG Inventory Report 2004 (-)
CEC	Cation exchange capacity	BG Inventory Report 2004 (meq/kg)
Bsat_0	initial base saturation	BG soil inventory - in 10 years, next 2010
Excmod	Cation exchange model option (1=Gaines-Thomas)	1
lgKAlBC	log10 of selectivity constant for Al-Bc exchange	Calibrated by VSDp; starting value 0.16
lgKHBC	log10 of selectivity constant for H-Bc exchange	Calibrated by VSDp; starting value 3.0
expAl	exponent (>0) in [Al]=KAlox·[H]^a	used: 3 (gibbsite eq.)
lgKAlox	log10 of gibbsite equilibrium constant	used: 7.9 (gibbsite eq.)((mol/l)$^{1-a)}$
Cpool_0	Initial amount of C in topsoil (per unit area)	BG Inventory Report 2004 (g/m$^{2)}$
CNrat_0	Initial C:N ratio in topsoil	BG Inventory Report 2004 (g/g)
RCOOmod	Organic acid model: 0=Oliver, 1=mono-protic	M
RCOOpars	1 or 3 parameters for organic dissociation model	M
cRCOO	total concentration of organic acids (m*DOC) (V/F)	M=0.004 (mol/m$^{3)}$
TempC	Average soil temperature	M = 8 °C
percol	Percolation (precipitation surplus)	M=0.3 (m/yr)
Ca_we	weathering rate of Ca	M eq/m^3/yr
Mg_we	weathering rate of Mg	M eq/m^3/yr
K_we	weathering rate of K	M eq/m^3/yr
Na_we	weathering rate of Na	M eq/m^3/yr
SO2_dep	deposition of SO2	Air immisions data_ BG (2008, 2009) - (Reidmann&Hertz, 1991) (eq/m^2/yr)
NOx_dep	deposition of NO_x	Air immisions data_ BG (2008, 2009) (Reidmann&Hertz, 1991) (eq/m^2/yr)
NH3_dep	deposition of NH_3	M eq/m^2/yr
Ca_dep	deposition of Ca	Air immisions data BG (eq/m^2/yr)
Mg_dep	deposition of Mg	Air immisions data BG (eq/m^2/yr)
K_dep	deposition of K	Air immisions data BG (eq/m^2/yr)
Na_dep	deposition of Na	Air immisions data BG (eq/m^2/yr)
Cl_dep	deposition of Cl	Air immisions data BG (eq/m^2/yr)
cCa_min	minimum [Ca] in soil solution	eq/m^3
cMg_min	minimum [Mg] in soil solution	M (eq/m^3)
cK_min	minimum [K] in soil solution	M (eq/m^3)
kmin_fe	mineralisation rate of easily degradable fresh litter	M (yr^{-1})
kmin_fs	mineralisation rate of recalcitrant fresh litter	M (yr^{-1})
kmin_mb	mineralisation rate of microbial soil organic matter	M (yr^{-1})
kmin_hu	mineralisation rate of humified soil organic matter	M (yr^{-1})
frhu_fe	fraction easily degradable fresh litter transferred to microbial soil organic matter	M
frhu_fs	fraction recalcitrant fresh litter transferred to microbial biomass	M
frhu_mb	fraction microbial transferred to humified soil organic matter	M

Keyword	Description	Explanation and Unit
CN_fe	C:N ratio of easily degradable fresh litter	M (g/g)
CN_fs	C:N ratio of recalcitrant fresh litter	M (g/g)
CN_mb	C:N ratio of microbial soil organic matter	M (g/g)
CN_hu	C:N ratio of humified soil organic matter	M (g/g)
CN_rt	C:N ratio of root turnover	M (g/g)
Nstmin	minimum N content of stems	M (g/kg)
Nstmax	maximum N content of stems	M (g/kg)
Ninmin	N input below which no effect on N content of stems	M (eq/m^2/yr)
Ninmax	N input above which no effect on N content of stems	M (eq/m^2/yr)
knit	maximum nitrification rate at Tref	M (yr^{-1})
kdenit	maximum denitrification rate at Tref	M (yr^{-1})
Nfix	N fixation	M (eq/m^2/yr)
ctCast	Ca content of stems	M (g/kg)
ctMgst	Mg content of stems	M (g/kg)
ctKst	K content of stems	M (g/kg)
rf_min	reduction of mineralisation because of moisture and temperature	M
rf_nit	reduction of nitrification because of moisture and temperature	M
rf_denit	reduction of denitrification because of moisture and temperature	M
age_veg	age of the vegetation at the start of the simulation period	from Bulgarian forest inventory data (yr)
growthfunc	Growth function for the vegetation (2, 3 or 4 parameters)	M
veg_type	Vegetation type	M
Nlfmax	maximum N content of litterfall	M (g/kg)
Nlfmin	maximum N content of litterfall	M (g/kg)
ncf	ratio between root turnover and litterfall	M
expNlfdep	Exponent for relation between N in litterfall and N deposition	M

*M – data from VSDp (Gaines-Thomas)

Results and comments

The VSD model simulates soil solution chemistry and soil nitrogen pools for natural and semi-natural ecosystems. The model consists of a set of mass balance equations that describe the soil input-output relationships of ions, and a set of equations that describe the rate-limited and equilibrium soil processes.
The VSD model has been used for dynamic modeling procedure. The most important additional soil data, concerning soil parameters, have been the carbon content in the soil, carbon/nitrogen ratio, soil bulk density, clay and sand content, as well as the soil pH.

Jundola

SiteInfo VSD+ "Jundola"

Latitude	41° 55' 34"
Longitude	23° 53' 40"
Species	Picea abies
	Abies alba
Age	170

Fig. BG-2 Results of the dynamic modeling- VSDp for Jundola site for the period 1960 – 2010

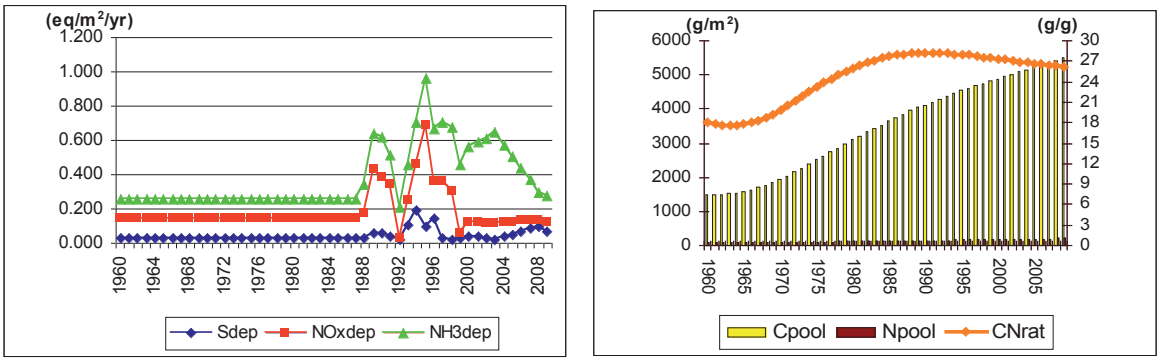

Vitinya

SiteInfo VSD+ "Vitinya"

Latitude	42° 55' 39"
Longitude	23° 55' 48"
Species	Fagus sylvatica
Age	140

Figure BG.3 Results of the dynamic modeling - VSDp for Vitinya site for the period 1960 - 2010

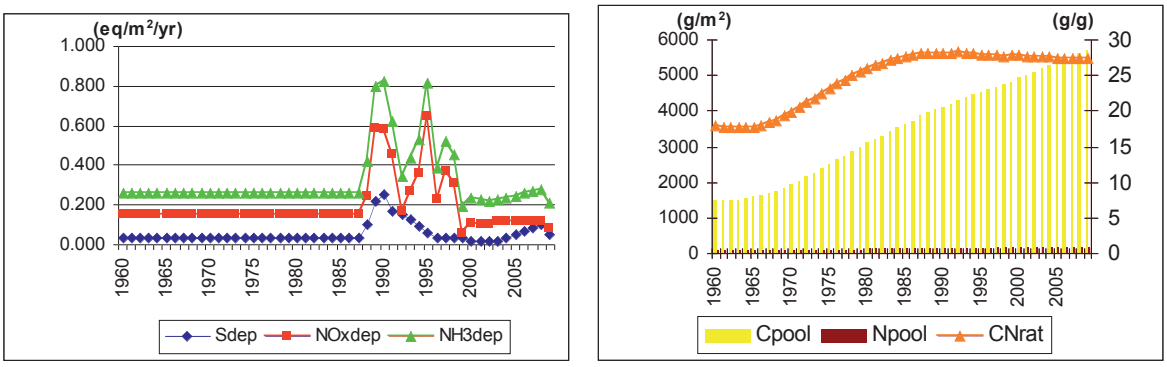

Staro Oryahovo

SiteInfo VSD+ "Staro Oryahovo"

Latitude	43° 03' 52"
Longitude	27° 03' 52"
Species	Querqus frainetto
	Querqus cerris
Age	156

Figure BG.4 Results of the dynamic modeling –VSDp for Staro Oryahovo site for the period 1998 – 2010

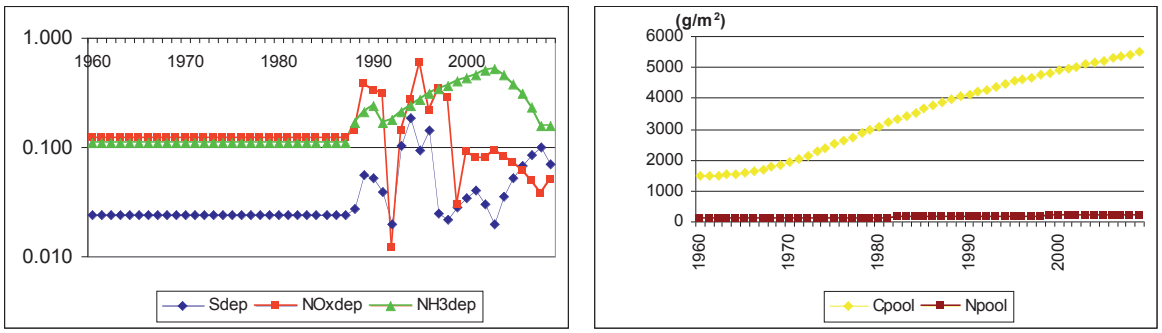

Czech Republic

Czech National Focal Centre

Irena Skořepová (irena.skorepova@geology.cz
Jaroslav Skořepa
Daniela Fottová (daniela.fottova@geology.cz)
Jakub Hruška (jakub.hruska@geology.cz)

Review of recent work

In comparison to the steep reduction of atmospheric depositions of sulphur and nitrogen during the final decade of the last century the last decade has been distinguished by the moderate decreasing sulphur and nitrogen. The decrease in the total atmospheric depositions of sulphur and nitrogen can be documented by the trend of throughfall and bulk depositions observed in the network of the small catchments GEOMON operated by the Czech Geological Survey from 1994. Figures CZ.1 and CZ.2 show these trends. With the relative decrease of sulphur and nitrogen depositions the healthy state of forests in the Czech Republic have shown continuing damage demonstrated by the defoliation of conifers and broadleaves. Defoliation slowly increasing from the class I (10-25% of defoliation) to the class II (25-60%). Present defoliation of stands older than 59 years reaches 30% in average. Young stands (less than 59 years) both broadleaves and conifers are generally of lower defoliation (MZeČR 2009).

The positive change in the air quality in the last two decades has improved the dynamics of defoliation development of wood species. In spite of this fact the defoliation has still increased in the last years. This trend shows the delay between doses of pollutants from the atmosphere and the response of forests tree species. In addition nitrogen deposition has not much changed or even increased in some areas. As a consequence, critical loads for nutrient nitrogen have been important for comparison of the impact of nitrogen atmospheric deposition on natural and semi-natural ecosystems. The critical loads of nitrogen based on the mass balance method were computed (Skořepová et al. 2007) and empirical critical loads of nitrogen were compiled (Skořepová et al. 2009). The land cover map provided by the CCE was applied for mapping of empirical critical loads of nitrogen. The following types of natural and semi-natural habitats given in Table CZ.1 have been used in the mapping of empirical critical loads (Figure CZ.3) and their exceedances (Figure CZ.4).

Table CZ.1 Natural and semi-natural habitats used in the mapping of empirical critical loads

EUNIS description	Code in the SEI map	EUNIS class	
Closed and open non-Mediterranean dry acid and neutral grasslands	5179	E 1.7	+E. 1.9
Mesic grasslands without Mountain hay meadows	5209	E 2	- E 2.3
Mountain hay meadows	5230	E 2.3	
Seasonally wet and wet grasslands	5300	E 3	
Alpine and subalpine grasslands	5400	E 4	
Woodland fringes and clearings and tall forb stands	5500	E 5	
Broadleaved deciduous woodland	7100	G 1	
Coniferous woodland	7300	G 3	
Mixed deciduous and coniferous woodland	7400	G 4	

The availability of nitrogen is the one of the most abiotic factors which determines the species composition in many natural and semi-natural ecosystems. Nitrogen is limiting factor in many natural ecosystems. But the atmospheric nitrogen is not the only source of nitrogen in ecosystems. For example, decomposition of soil organic matter offers further source of nutrient nitrogen. The excess of nitrogen causes many negative events in ecosystems followed up by changes in natural ecosystem composition or by the complete lost of vegetation species. To understand the mechanisms of the adverse impact of nitrogen in temporal and spatial scales dynamic modelling with VSD+ has been applied.

Figure CZ.1 Decrease in the total sulphur deposition in the small catchments network GEOMON in the period 1994–2008; as the average of annual amounts of throughfall sulphur depositions in the coniferous forests from 14 catchments

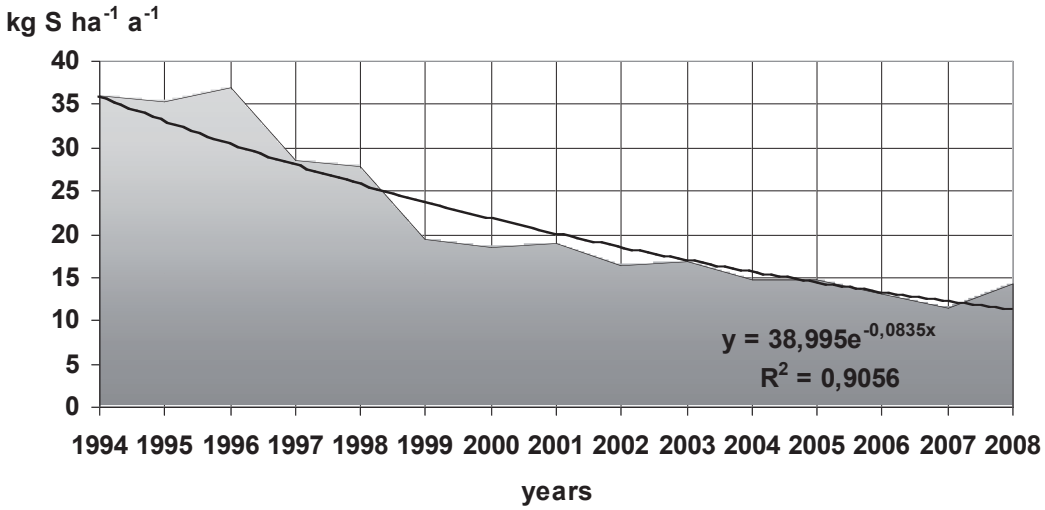

Figure CZ.2 Decrease in the total nitrogen deposition in the small catchments network GEOMON in the period 1994–2008; as the average of annual amounts of throughfall oxidized nitrogen and bulk reduced nitrogen depositions in the coniferous forests from 14 catchments

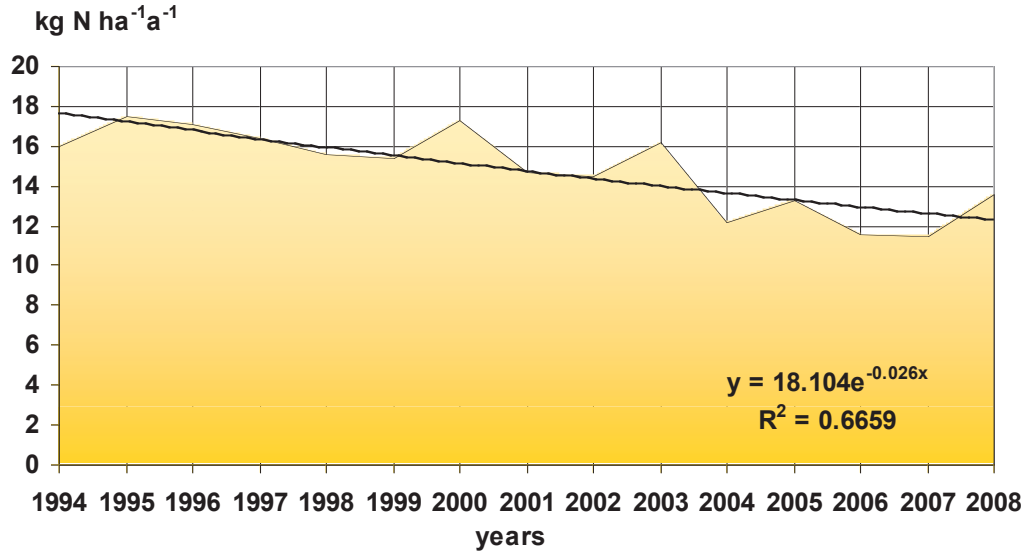

Figure CZ.3 Empirical critical loads of nitrogen for some natural and semi-natural ecosystems in the Czech Republic

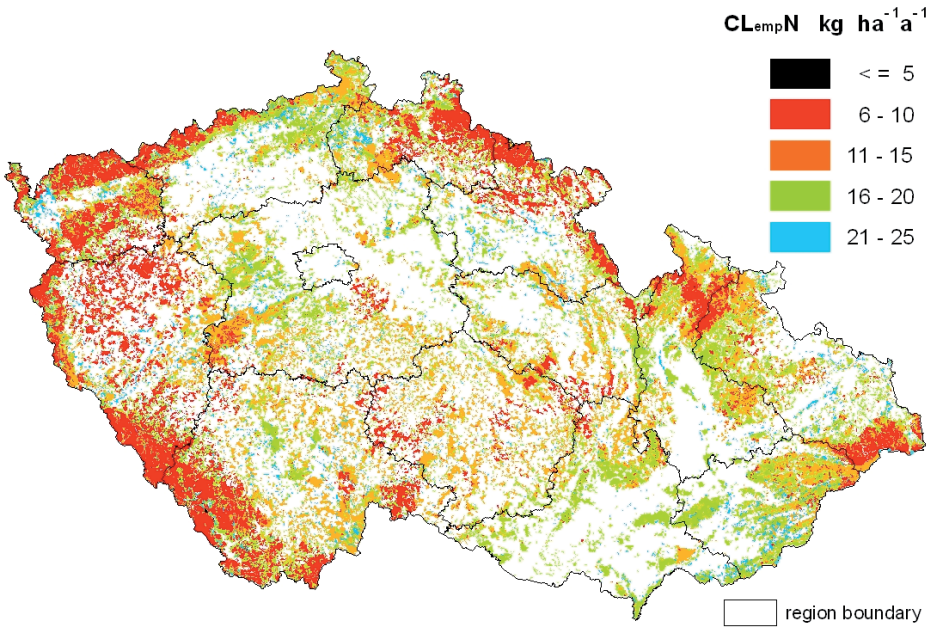

Figure CZ.4 Exceedances of empirical critical loads for nitrogen (at the beginning of this century)

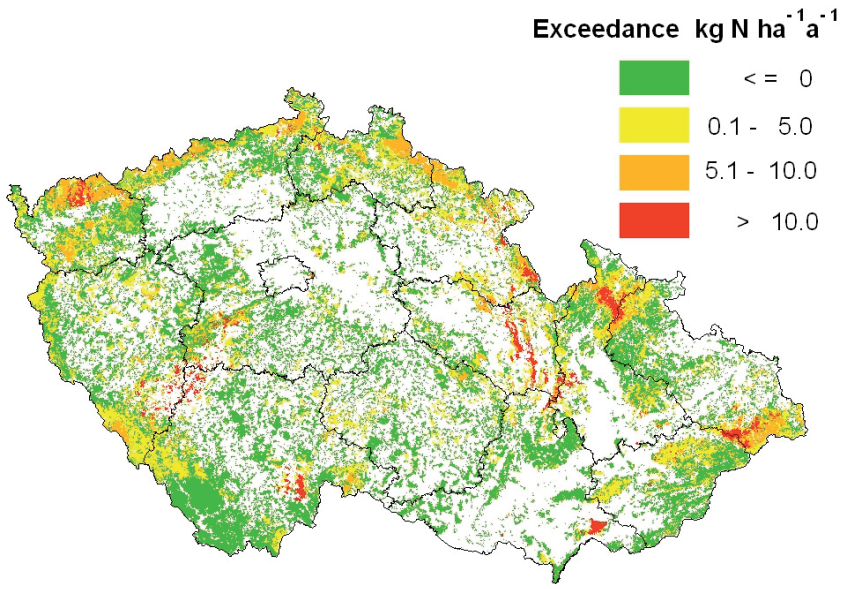

Work with VSD+ and MetHyd models

The VSD+ model enables to connect soil processes to demands of vegetation species for nutrients. Therefore information on vegetation composition of natural and semi-natural ecosystems is needed. Mapping the natural habitats in the territory of the Czech Republic has been carried out by the AOPK ČR (Agency for Nature and Landscape Protection) in the framework of the Natura2000 and the first comprehensive classification has been published at the beginning of this decade (Chytrý et al. 2001). The classification of forest habitats and their species composition in the Czech Republic have been used to complete the soil database prepared for the calculation of critical loads in the last years. The ranges of some soil properties connected to the occurrence of the main forest tree species are shown in the following tables (CZ.2, CZ.3) for example.

Three localities of forest stands have been used for modelling. These forest sites belong to the monitoring sites of the level II of the ICP F in the Czech Republic (Boháčová et al. 2007, Boháčová et al. 2009). Monitoring sites are operated by the VÚLHM (Forestry and Game Management Research Institute) in Strnady – Zbraslav. They are Mísečky (site 2), Lásenice (site 3) and Medlovice (site 4).

Site 2 (Mísečky) is located in the National Park Krkonoše mts. It is based on biotite slates and covered by Haplic Podzols. Forest stand is created by slope spruce-beech forest with ferns and the main species *Fagus sylvatica* and other species *Picea abies*. Acidophilous mountain spruce-beech forest *ass. Calamagrostio villosae-Fagetum* with admixture of fir and sycamore maple is the forest type. Ground vegetation forms relatively rich layer with typical species of the mountain beech and spruce forests dominated by vaccinium myrtillus.

Site 3 (Lásenice) is situated in the Czech Moravian hills. Dune sands among stones of the two mica granit form geological background of the locality. Haplic podzols create a soil cover. *Picea abies* belongs to the main species and *Fagus sylvatica*. *Abies alba* and *Quercus petraea* to others. *Galium odoratum* dominates in the ground vegetation cover in the herb-rich beech stand of natural character of *Fagion ass.* occurred at this site.

Site 4 (Medlovice) is located in the mountain range of Chřiby in the Central Moravian Carpathian. Claystones and sandstones of glauconic rocks are built up the background and Endoeutri-Stagnic Cambisols create soils of the site. From the tree species *Fagus sylvatica* (main), *Larix decidua* and *Pinus sylvestris* occur in this locality. Fresh beech-oak forest with *Luzula luzuloides* and *Galium odoratum* in the herb layer is the forest type of the site.

Soil texture data for these three sites were derived from the soil properties of the closed localities with measured data (forest soil database – used for critical load calculations in the past). Chemical analyses of site soils were produced in 2005. At first average hydrology data and reduction functions of nitrification and denitrification for localities were calculated with use of the MetHyd model.

Table CZ.2 Statistics (minimum, maximum, average and standard deviation) of the soil base saturation for the main forest tree species in the Czech Republic

types	min_bsat	max_bsat	avg_bsat	std_bsat	N
Acer platanoides	0.01	0.70	0.25	0.20	22
Acer pseudoplatanus	0.01	0.82	0.23	0.22	35
Alnus glutinosa	0.01	0.85	0.31	0.24	29
Alnus incana	0.82	0.82	0.82	0.00	1
Betula pubescens	0.05	0.27	0.13	0.08	10
Carpinus betulus	0.05	1.00	0.40	0.28	110
Fagus sylvatica	0.01	0.95	0.33	0.89	1435
Fraxinus angustifolia	0.01	0.85	0.49	0.33	34
Picea abies	0.01	0.82	0.38	1.45	136
Pinus rotundata	0.11	0.28	0.18	0.09	3
Pinus sylvestris	0.01	0.78	0.18	0.19	85
Quercus petraea	0.01	1.00	0.28	0.25	211
Quercus robur	0.01	1.00	0.25	0.24	260

Table CZ.3 Statistics (minimum, maximum, average and standard deviation) of soil pH values for the main forest tree species in the Czech Republic

types	min_pH	max_pH	avg_pH	std_pH	N
Acer platanoides	3.58	6.04	4.44	0.58	22
Acer pseudoplatanus	3.57	6.63	4.39	0.64	35
Alnus glutinosa	3.79	7.85	4.67	1.03	29
Alnus incana	6.63	6.63	6.63	0.00	1
Betula pubescens	3.53	4.27	3.82	0.24	10
Carpinus betulus	3.76	7.85	4.94	1.05	110
Fagus sylvatica	3.02	7.85	4.30	0.62	1435
Fraxinus angustifolia	3.70	5.93	5.00	0.82	34
Picea abies	3.02	6.63	4.05	0.74	136
Pinus rotundata	3.74	4.24	3.91	0.29	3
Pinus sylvestris	3.53	5.79	4.10	0.47	85
Quercus petraea	3.58	7.73	4.52	0.82	211
Quercus robur	3.58	7.73	4.43	0.91	260

Meteorology files with inputs of average month temperature, precipitation amounts (monitored in the monitoring sites) and sunshine percentage (derived from the Meteorological Atlas, Tolasz et al. 2007) were used in the calculation. Output data from MetHyd were merged into the VSD+ model input. Some data from observations were included to the input file as well (e.g. some of soil solution data, soil parameters). EMEP deposition data were used in this elaboration (data sent to us for the call for data in 2008). The input data considered the main tree species only (and with partial values according to the species occurrence). Growth parameters were obtained from literature sources (Černý et al. 1996, Slodičák et al. 2005).

Future work in modelling should prefer the data obtained from measurements in the experimental sites in the larger extent. In many cases the monitoring sites of level II are equipped for continuous measurements (soil wetness, temperature, precipitation etc.). The attention should be focused to the temporal point of view.

References

Boháčová L, Lomský B, Šrámek V, 2009. Monitoring zdravotního stavu lesa v České republice (Forest Condition Monitoring in the Czech Republic). Ročenka programu ICP Forest/Forets Focus 2006–2007. ISBN 978-7417-003-4, VÚLHM, Zbraslav – Strnady, 134 pp

Boháčová L, Uhlířová H, Šrámek V (eds), 2007. Monitoring zdravotního stavu lesa v České republice (Forest Condition Monitoring in the Czech Republic). Ročenka programu Forets Focus/ICP Forest 2005. ISBN 978-80-86461-75-5, VÚLHM, Zbraslav – Strnady, 155 pp

Černý M, Pařez J, Malík Z, 1996. Růstové tabulky hlavních dřevin ČR. Ústav pro výzkum lesních ekosystémů, s.r.o., Jílové u Prahy, 245 pp

Chytrý M, Kučera T, Kočí M (eds), 2001. Katalog biotopů České republiky. Interpretační příručka k evropským programům Natura 2000 a Smaragd. ISBN 80-86064-55-7, Agentura ochrany přírody a krajiny ČR, Praha, 1. vydání, 307 pp

Skořepová I, Fottová D, Skořepa J, 2009. Příspěvek k odhadu účinků atmosférické depozice dusíku a síry. In Holoubek Ivan: Ovzduší 2009, s. 249-253. Masarykova universita. Brno, ISBN 978-80-210-4829-4

Skořepová I, Skořepa J, Beneš S, Fottová D, Hruška J, 2007. Czech Republic – the national database of nutrient nitrogen critical loads. In: J Slootweg et al. (eds): Critical Loads of Nitrogen and Dynamic Modelling. CCE Progress Report 2007, MNP Report 500090001, Bilthoven, pp.129–132

Slodičák M, Novák J, Henžlík V, Zeman M, Petr T, 2005. Expertní a poradenská činnost při zjišťování biomasy v lesních ekosystémech (6635). Výroční zpráva za rok 2005. VÚLHM – Výzkumná stanice, Opočno, 20 pp

Tolasz R et al., 2007. Atlas podnebí Česka (Climate Atlas of Czechia). ISBN 978-80-86690-26-1, Český hydrometeorologický ústav, Praha, Universita Palackého, Olomouc, 1. vydání, 255 pp

MZeČR, 2009. Zpráva o stavu lesa a lesního hospodářství České republiky v roce 2008. ISBN 978-80-7084-861-6, Ministerstvo zemědělství ČR, Praha, 1. vydání, 132 pp

France

National Focal Centre

Dr. Anne Probst
Dr. Estelle Bortoluzzi
M. Arnaud Mansat

ÉcoLab (UMR 5245 CNRS/UPS/INPT)
Campus ENSAT-INP
Av. de l'Agrobiopole
Auzeville-Tolosane BP 32607
F-31 326 Castanet-Tolosan cedex
Email: anne.probst@ensat.fr
estelle.bortoluzzi@ensat.fr
amansat2@ensat.fr

Collaborating institutions

Dr. Laurence Galsomiès
ADEME
Centre de Paris - Vanves
Dép. Surveillance de la Qualité de l'Air
27, rue Louis Vicat
F-75 737 Paris cedex 15

M. Manuel Nicolas
Office National des Forêts
Direction Technique
Dép. Recherche et Développement
RÉNÉCOFOR
Boulevard de Constance
F-77 300 Fontainebleau

Dr. Jean-Claude Gégout
UMR AgroParisTech – ENGREF – INRA
« Ressources Forêt-Bois » (LERFoB)
Equipe Ecologie Forestière
14, rue Girardet - CS 14216 –
54042 NANCY Cedex

Dr Thierry Gauquelin
Equipe Diversité Fonctionnelle des Communautés Végétales
IMEP UMR CNRS-IRD 6116
Université de Provence
3, place Victor Hugo
13331 Marseille Cedex 03

Dr Didier Alard – Dr Emmanuel Corcket
UMR INRA 1202 BIOdiversité, GÈnes et COmmunautés
Equipe Ecologie des Communautés
Université Bordeaux 1
Bâtiment B8 - RdC
Avenue des Facultés
F-33405 Talence

Dr Jean-Paul Party
Sol-Conseil
251 rte La Wantzenau - Robertsau
F-67 000 Strasbourg

Dr. Jean-Luc Dupouey
Equipe Phyto-écologie forestière
UMR Ecologie et Ecophysiologie Forestières
INRA-Centre de Nancy
Biogéochimie des Écosystèmes Forestiers
F-54 280 Champenoux

Dr Anne-Christine Le Gall
Direction des Risques Chroniques
Unité MECO
INERIS BP N°2
F-60 550 Verneuil-en-Halatte

Mr Marc Rico
Ministère de l'Écologie, de l'Énergie, du Développement Durable et de l'Aménagement du Territoire
Direction de la Pollution et de la Prévention des Risques
20, avenue de Ségur
F-75 007 Paris

Developments for a future Soil-vegetation model chain for nitrogen critical loads

The objectives of the 2010 call for data were to familiarize with a more sophisticated follow up of the VSD+ model and to focus on new vegetation-relevant data requirements.
The French national Focal Centre (NFC) is participating in the trial of the new VSD+ model with its improved and connected nitrogen and carbon cycles, on a few number of well documented sites with an observed gradient in C/N ratio, in N deposition and with different kinds of vegetation.
(1) The first step was to collect the data for few forested sites, followed by tests with VSD+, calibrations of the model and preliminary result analysis.
(2) The NFC extended the list of species for French ecosystem conditions that should be predicted by a vegetation module in a soil-vegetation model chain to investigate the relationship between nitrogen deposition and biodiversity. This database was build up by French phytoecological experts and in collaboration with Swedish modellers.
Moreover, the French NFC is working on the first tests of the ForSAFE model for French forest ecosystems within the framework of a French-Swedish research project. A database is in progress and tests will be undertaken on some sites for calibration to prepare ForSAFE-Veg simulations.
(3)This step of the call for data required a possible contribution to the European database of relevés with measured soil parameters. In France, a database linking soil parameters and vegetation called Ecoplant, already exists (Gégout et al., 2005). It will be presented at the 20th CCE Workshop. The NFC participates to its extension on the Mediterranean zone, by the way of a research program supported by the French environmental Agency (ADEME).

1-Dynamic modelling using VSD+

1.1 Calculation method

The data of four intensively documented forested sites from RENECOFOR (the network of heath forest survey from the National Forest Office and belonging to the ICP-Forest) were investigated using the VSD+ model. The VSD+ model requires data for a lot of parameters (see Table FR.1). Contrary to the Simple Mass Balance (SMB), VSD+ is especially done for using on a regional/national scale (Bonten et al. 2009b) and includes carbon and nitrogen modelled cycles.

Figure FR.1 Location of selected sites

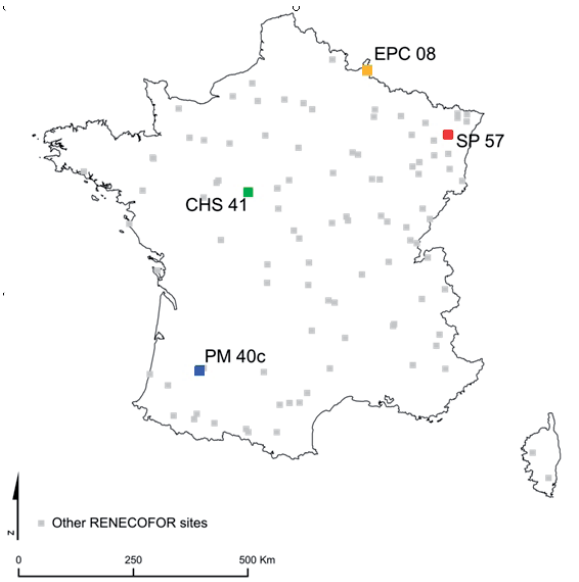

Table FR.1 Sources of parameters used for running the dynamic model VSD+

Variable	Explanation	Unit	Data sources or settings
SO_2_dep, NOx_dep, NH_3_dep	Total deposition of sulphur and acid and nutrient nitrogen	eq $m^{-2}yr^{-1}$	EMEP deposition (CFD2008)
Cadep, Mgdep, Kdep, Nadep	Total deposition of base cations	eq $m^{-2}yr^{-1}$	RENECOFOR measured data
Cawe, Mgwe, Kwe, Nawe	Weathering rate of base cations	eq $m^{-3}yr^{-1}$	PROFILE simulations (Party, 1999)
All soil parameters			From RENECOFOR data (Brêthes *et al.* 1997, Badeau and Ulrich 2008) and from Gandois (2009)
All vegetation parameters			From RENECOFOR data (Ponce et al. 1998) and Inventaire Forestier National (1998) and Mapping Manual section (Posch 2004)

Table FR.2 Input values of soil parameters (from Brêthes et al. 1997, Fillion et al. 1999, Gandois 2009)

Variable	Designation	Units	Min	Max	Median
bulkdens	Bulk density	$g.cm^{-3}$	1.047	1.542	1.136
Theta	Water content of soils	$m.m^{-1}$	0.065	0.175	0.100
pCO2fac	CO_2 pressure in soil solution	[atm]	8	9.8	8.3
lgKAlBC	Log10 of selectivity constant for Al-BCexchange		-3.247**	0.526**	-1.351**
lgKHBC	Log10 of selectivity constant for H-BC exchange		1.401**	2.700**	2.00**
Percol	Percolation (precipitation surplus)	$m.yr^{-1}$	0.250	1.077	0.496
cRCOO	Total concentration of organic acids	$mol.m^{-3}$	0.0022	0.0245	0.0179
CEC	Cation Exchange Capacity	$meq.kg^{-1}$	31.9	76.9	41.15
Bsat_0	Initial Base saturation	-	-1*	-1*	-1*
Cpool_0	Initial amount of carbon in the topsoil	$g.m^{-2}$	3320**	9926**	6979**
CNrat_0	Initial C/N ratio in the topsoil		15.94**	49.9**	49.1**
CNrat_obs	C/N ratio measured on site		17	26	18.5

*Calculated by the model.
**Obtained with the Bayesian calibration, from known values for CEC, Cpool, Bsat and C/Nratio measured in 1995 in RENECOFOR (Badeau and Ulrich 2008), some of the given values have no real soil function validity.

1.2 Data sources

Data are mainly extracted from the French RENECOFOR network database. The total concentration of organic acids in soil solution was calculated as follows:
Corg (meq/l)= 0.00525 DOC (ppm) + 0.0235 pH – 0.127 (Fillion et al. 1999)
or extracted from the French critical load database.
Growth function was calculated using yearly vegetation growth ($kg.m^{-2}.yr^{-1}$) and yearly litterfall (derived from yearly mean) (Croisé et al. 1999). For other parameters, refer to details given in tables FR-2 and 3.
EMEP deposition values have been used from 1880 to 2100, since the calibration process needs past deposition data to calibrate initial values on deposition history, based on a charge balance considered as equilibrated at this time. Ca, Mg, Na and K atmospheric depositions are those measured in the RENECOFOR network (assuming they were constant over time).
Indeed EMEP deposition has been compared to corresponding measured depositions (bulk deposition) for each RENECOFOR sites for the period 1993 to 2008. Significant differences can be observed (Fig. 2, SP57 site given as an example), with EMEP overestimating NOx deposition. This may lead to significant differences in VSD simulation results, but indeed impossible to evaluate. Moreover, as suggested by VSD+ modellers to go through a VSD+ limitation, initial N deposition value (1880) has been multiplied by 100 in order to run the model without restriction message displaying "*Too little N available*". Only one site (SP57) was able to run without this added initial N input. Hence, x100 initial N input was performed for all the sites to allow a suitable comparison. Even if this initial input change does not seem to affect long term prediction (see result comments), one must keep in mind that it may have some importance in model pattern simulation.

Table FR.3 Input data for the selected sites

Sites	Unit	CHS41	EPC08	PM40c	SP57
Concerned period		1880-2100			
*Thick***	m	0,4	0,2	0,4	0,2
*Bulkdens***	$g.cm^{-3}$	1,543	1,055	1,219	1,047
Theta (m/m)	m/m	0,175	0,131	0,070	0,065
*CEC (meq/kg)***	$meq.kg^{-1}$	45,8	76,9	36,5	31.9
bsat_0		-1	-1	-1	-1
*Bsatobs***		0.323	0,042	0,474	0,175
Cpool_0	$g.m^{-2}$	9926	9208	3320	4751
*Cpoolobs***	$g.m^{-2}$	5732	4937	4544	2240
CNrat_0	g/g	49.97	49.42	48.78	15.94
*CNratobs***	g/g	19	17	26	18
cRCOO	$mol.m^{-3}$	0,0245	0,0022	0,0244	0,0116
percol	$m.yr^{-1}$	0,250	1,077	0,357	0,636
Ca_we	$eq.m^{-3}.yr^{-1}$	0,00774	0,00304	0,00016	0,00026
Mg_we	$eq.m^{-3}.yr^{-1}$	0,0018	0,0004	0	0,0018
K_we	$eq.m^{-3}.yr^{-1}$	0,00146	0,00042	0,00014	0,0013
Na_we	$eq.m^{-3}.yr^{-1}$	0,00988	0,00766	0,00012	0,00048
age_veg	yr	95	35	15	54
growthfunc	$kg.m^{-2}.yr^{-1}$	0,1922 0,09	0,6619 0,07	0,4905 0,12	0,4990 0,18
veg_type		Oak	Spruce	Pine	Pine
Dominant species		Quercus petraea (L.)	Picea abies (L.)	Pinus pinaster (Ait.)	Abies alba (Mill.)

** Measured values in 1995

Figure FR.2 Comparison between modelled (EMEP, dash line) and measured deposition (continuous line) on SP57 RENECOFOR site (Croisé et al. 2002) for Ammonium (A), Nitrate (N) (eq $ha^{-1}yr^{-1}$).

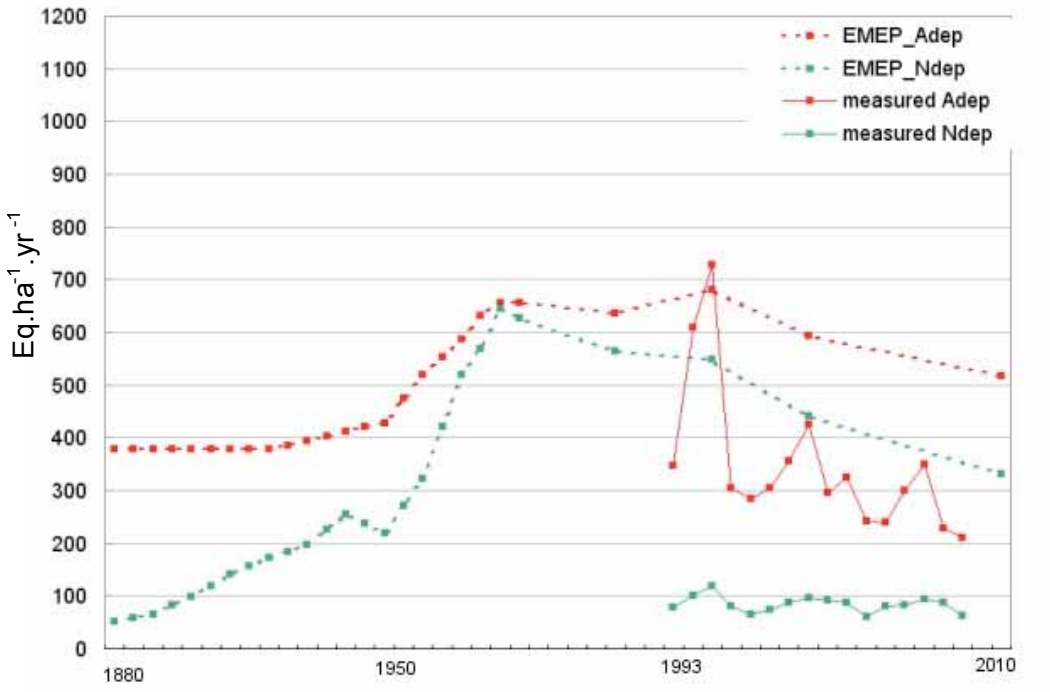

2. Results: outputs of VDS+ for 4 forested French sites

Figure FR.3 VSD + output simulations (continuous lines) for the 4 forested RENECOFOR sites. When available, the measured data (1995) are noticed (squares). For SP57, the simulation without multiplying by 100 the initial N input is presented as a comparison (dash line).

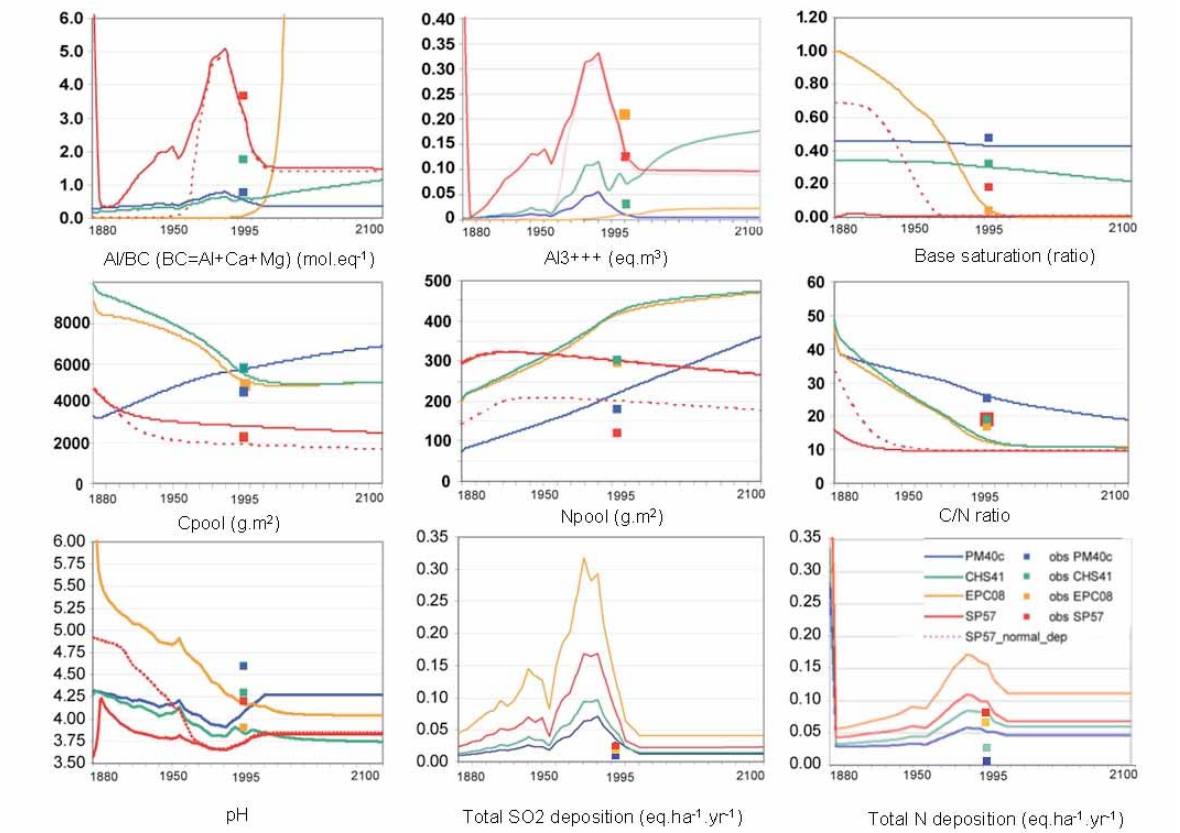

The selected four sites have really different environmental conditions. Indeed, this brings a good chance to observe different reactions of the model to test VSD+ sensitivity. But the heterogeneity of the sites makes difficult the interpretation of the site responses to the atmospheric input scenarios. The Figure FR.3 shows the simulations for the main soil parameters.

The gradation of S and N deposition between the sites plays a significant role on VSD+ simulation patterns and thus on site response to acidification. This role seems more important than the type of vegetation or soil as already shown by Moncoulon et al. (2007). With the lowest deposition level, PM40c shows the smallest perturbations. On the opposite, EPC08 with the highest deposition level is the most affected site. The fall of pH is the highest without recovery and a complete depletion of soil, in spite of the highest initial base saturation and the most important buffering capacity measured in 1995. With a higher S and N deposition and in spite of a soil litter easily decomposable, CHS41 with *Quercus petraea*, is more affected without any recovery than PM40C with a weakly decomposable litter of *Pinus pinaster.*

As shown in Figure FR.3 the Cpool trend seems to be well predicted with a good agreement between observed and modelled values. For PM40c site, the Cpool is increasing and this prediction corresponds to the pattern described in Bonten et al. (2009a), whereas it is decreasing for the three other sites. Moreover, as stated by De Vries (2009), this shows that Cpool site response to N deposition is not universal and does not always lead to an increase of carbon pool in soil as a consequence of increasing forest growth. This also leads to an interrogation about the impact of vegetation age and growth function on simulated Cpool. A test on the yearly harvest parameter did not show any changes in the outputs, and after 200 years of simulation, the age of vegetation does not reflect the reality of forest exploitation anymore.

The simulated N pool is overestimated for all sites, slightly less for PM40c. As shown by comparing the two simulations for the SP57 site, the initial Npool is dependent of the

'artificial' addition of N. Without this addition, the Npool is divided by 2 for SP57. The simulation trend does not change in both cases but the initial difference is nearly kept all along the simulation. Moreover, a high N initial deposition lowered the initial trends of base saturation, pH value, Al/BC ratio and C/N but the two simulations met by 1950. Besides, this comparison was only possible for SP57 site, whose soil response to S and N increasing deposition did not follow exactly the same trends as the other soils.
The decreasing trend of C/N ratios corresponds to the expected response for VSD+ (Bonten et al., 2009a), but due to a higher simulated Npool, the C/N ratios are underestimated except for PM40c.
The base saturation ratio was well predicted for 3 sites even for the very much depleted soil EPC08. For SP57, the model predicted a completely depleted soil since 1960, whereas the observed value in 1995 gained 0.2. With higher initial N deposition, the site was initially completely base cation depleted, leading to a high Al/BC ratio.
About the pH trends, beyond an overestimation for EPC08 and an underestimation for the other sites, PM40c and SP57 seemed to reach a restored level whereas EPC08 and CHS41 were not able to recover a higher pH as a consequence of N and S deposition decrease even by 2100.
These trends of acidification and of exceeded critical loads were already predicted by Moncoulon et al. (2007) for both SP57 and PM40c.
Finally, forest history may have a great influence on soil initial stage and this would be check in modelling exercises.

3-Extension of the list of species for the vegetation model with Veg-parameters – data sources

The extension of the species list for France was set up during a dedicated workshop with vegetation experts in October 2009. Relevant species were chosen to represent the various French forest ecosystems on the basis on expert knowledge. The objective was to have a good representation of common and/or characteristic species of the main French ecosystems. For each plant added to the plant list already documented for Sweden and Switzerland, the Veg-parameters have been completed compiling several sources of data. For some parameters, the link between existing databases and the Veg-parameters needed a scale calibration.
- The delay time done in years, based on average generation time and lifespan was drawn from the French Flora (Rameau et al. 1989, 1994, 2008) and expert opinions.
- The promoting nitrogen classes were based on C/N values extracted from the Ecoplant database (Gégout et al., 2005) and adapted to the Veg classes. For the missing species of Ecoplant, the information was found in the French Flora (Rameau et al. 1989) and using the Ellenberg parameter N (Julve 1998).
- The retarding nitrogen, the water and the light response classes were deduced from the French flora (Rameau et al. 1989).
- The lowest pH value was from Ecoplant database and from the French Flora when missing (Rameau et al. 1994).
- The temperature minimum: the lowest annual average temperature when the plant can start taking ground, was extracted from the Ecoplant database and from the French Flora when missing (Rameau et al. 1994).
- The effective shading height was deduced from the French Flora (Rameau et al. 1989). For trees and shrubs, the height was considered only for seedling with a standard height of 0.1.
- The browsing based on the food palatable classification was extracted from literature, pastoral floras (Dorée 1995, Morelleta and Guibert 1999, Bruneton 2001; Gusmeroli et al. 2007, Boulanger et al. 2009) and expert advices.

4-Outlooks

The French NFC has begun to test various biogeochemical soil models and vegetation models to evaluate their sensibility and applicability according to the scale of application and available input data considering the large variety of French forest ecosystems. The aim is to assess the biodiversity response and biogeochemical soil responses to nitrogen deposition, in the way of CCE objectives, at different scales in order to apply the most relevant soil-vegetation chain model at the national scale.

5-Acknowledgments

The French NFC thanks Harald Swerdrup and Salim Belyazid for their implication in our common project to adapt Forsafe-Veg, the CCE for fruitful exchanges and the French experts mentioned in the collaborating institutions for the setup of the Veg-table.

References

Badeau V, Ulrich E, 2008. Renecofor - Etude critique de faisabilité sur : la comparabilité des données météorologiques Renecofor avec celles de Météo France, l'estimation de la réserve utile en eau du sol et le calcul des volumes d'eau drainée en vue du calcul de bilans minéraux sur les placettes du sous-réseau Cataenat. Office National des Forêts, direction technique et commercial bois, 274 pp

Bonten LTC, Mol J, Reinds G, 2009a. Dynamic modelling of effects of deposition on carbon sequestration and nitrogen availability: VSD plus C and N dynamics (VSD+). In: N.E.A. Agency (ed), Progress in the modelling of critical thresholds, impacts to plant species diversity and ecosystem services in Europe, pp. 69–73

Bonten LTC, Posch M, Reinds GJ, 2009b. The VSD+ Soil Acidification Model. Model Description and User Manual. Version 0.11

Boulanger V, Baltzinger C, Saïd S, Ballon P, 2009. Ranking temperate woody species along a gradient of browsing by deer. Forest Ecology and Management 258: 1397–1406

Bruneton J, 2001. Plantes toxiques, Végétaux dangereux pour l'Homme et les animaux, Paris, 564 pp

Croisé L, Cluzeau C, Ulrich E, Lanier M, Gomez A, 1999. RENECOFOR - Interprétation des analyses foliaires réalisées dans les 102 peuplements du réseau de 1993 à 1997 et premières évaluations interdisciplinaires ONF, Département Recherche et Développement, 413 pp

Croisé L, Duplat P, Jaquet OUE, 2002. RENECOFOR - Deux approches indépendantes pour l'estimation des dépôts atmosphériques totaux hors couvert forestier sur le territoire français en vue d'établir des cartes d'excès de charge critique d'acidité. ONF, Département Recherche et Développement, 102 pp

De Vries W, 2009. Assessment of the relative importance of nitrogen deposition and climate change
on the sequestration of carbon by forests in Europe: an overview. Forest Ecology and Management 258: vii-x

Dorée A, 1995. Flore pastorale de montagne Tome 1 : les graminées, Saint Martin d'Hères, 207 pp

Fillion N, Probst A, Probst, J-L, 1999. Dissolved organic matter contribution to rain water, throughfall and soil solution chemistry: Humic substances. Analysis 27: 409–413

Gandois L, 2009. Dynamique et bilan des Eléments Traces Métalliques (ETM) dans des écosystèmes forestiers français. Modélisation, Spéciation et Charges Critiques, Toulouse III - Paul Sabatier, Toulouse

Gégout J-C, Coudun C, Bailly G, Jabiol B, 2005. EcoPlant: A forest site database linking floristic data with soil and climate variables. Journal of Vegetation Science 16: 257–260

Gusmeroli F, Della Marianna G, Puccio C, Corti M, Maggioni L, 2007. Indici Foraggeri di Specie Legnose ed Erbacee Alpine per il Bestiame Caprino. Quaderno SOZOOALP 4: 73–81

Julve P, 1998. Baseflor. Index botanique, écologique et chorologique de la flore de France. Version: "10/03/2010". perso.wanadoo.fr/philippe.julve/catminat.htm

Moncoulon D, Probst A, Martinson L, 2007. Modeling acidification recovery on threatened ecosystems: application to the evaluation of the Gothenburg protocol in France. Water, Air and Soil Pollution: Focus 76: 307–316

Morelleta N, Guibert B, 1999. Spatial heterogeneity of winter forest resources used by deer. Forest Ecology and Management 123: 11–20

Ponce R, Ulrich E, Garnier F, 1998. Essai de synthèse sur l'histoire des 102 peuplements du réseau RENECOFOR. Office National des Forêts, Département des Recherches Techniques, 235 pp

Posch M, 2004. Manual on methodologies and criteria for modelling and mapping critical loads and levels and air pollution effects, risks and trends - section 5.3. In: T Spranger, U Lorenz, H-D Gregor (eds), Umweltbundesamt, Berlin, pp. v10–v28

Rameau J-C, Mansion D, Dumé G, 1989. Flore forestière Française - Tome 1: Plaines et Collines IDF, 1785 pp

Rameau J-C, Mansion D, Dumé G, 1994. Flore forestière Française. IDF, 1785 pp

Rameau J-C, Mansion D, Dumé G., 2008. Flore forestière Française - Tome 3: Région Méditerranéenne IDF, 2426 pp

Germany

National Focal Centre

OEKO-DATA
Hans-Dieter Nagel
Hegermuehlenstr. 58
D – 15344 Strausberg
tel.: +49 3341 3901920
fax: +49 3341 3901926
email: hans.dieter.nagel@oekodata.com

Collaborating Institution

Institute of Navigation, Universität Stuttgart
Thomas Gauger
Breitscheidstr. 2
D – 70174 Stuttgart
tel.: +49 711 68584177
fax: +49 711 68582599
email: thomas.gauger@nav.uni-stuttgart.de

Application of the VSD+ Model to Selected Sites in Germany

Description of Selected Sites in Germany

The German NFC participates in the test run of the new VSD+ model with its improved and connected nitrogen and carbon cycles. The VSD+ model was applied to 22 selected sites in Germany. To ensure wide regional distribution 11 sites of the ICP Forests Level II program were included into the test run, which already have been studied with the UBA project MOBILE 2010. Another 11 sites represent a well investigated NATURA 2000 study area in the North-East German Plain close to the city of Greifswald.

The 22 chosen sites match 10 different soil classes and 6 different vegetation types (see Table DE.1). They are also located in quite different landscapes and climate regions (see Figure DE.1).

Figure DE.1 Selected sites for testing the VSD+ model in Germany.

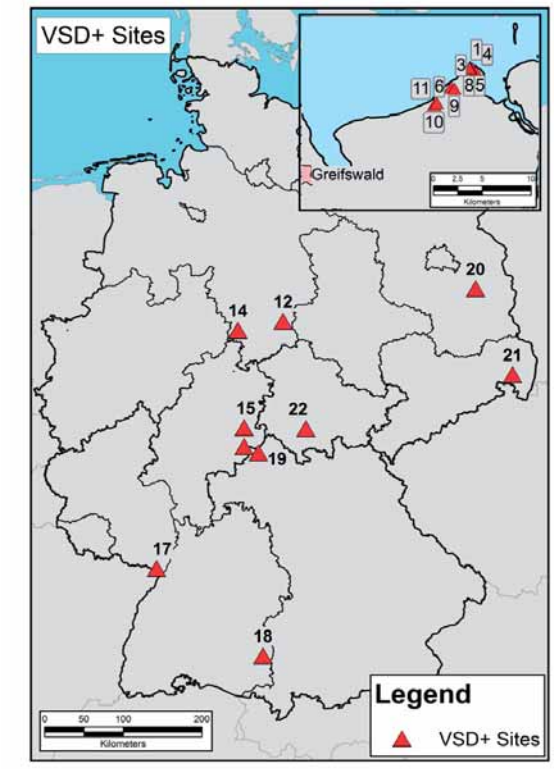

The German sites for the VSD+ model application represent not only different ecosystems but also different environmental and soil chemical conditions (see Tab. DE-2). Also shown from Tab. DE-2 is that the German sites are located in regions of different air pollution. The pollution with Nitrogen ranges from 17 kg N $ha^{-1}yr^{-1}$ (e.g. Site 1) up to 45 kg N $ha^{-1}yr^{-1}$ (e.g. Site 10). The deposition of sulphur varies between 2000 eq $ha^{-1}yr^{-1}$ (Site 9) and 5400 eq $ha^{-1}yr^{-1}$ (Site 12). In the same manner varies the deposition of the base cations as well.
Since the Level-II plots had measurements for pH values, they were chosen for the VSD+ internal Bayesian calibration. But only the parameters C pool and C:N ratio were calibrated.

Input parameters

The data set for the deposition was derived by data of the MAPESI project (UBA 2010, FKZ 3707 64 200). Even if the project offers several time steps only the values for 2005 were chosen. These values were used to create modelled Nitrogen deposition time series, were the original given times series of the VSD+ model was the reference. The same was done for the sulphur deposition.
The parameter "growth function" was set to include 3 parameters: yearly vegetation growth, yearly litterfall and yearly harvest (all in kg $m^{-2}yr^{-1}$). The values for these 3

Table DE.1 Vegetation types of selected sites for testing the VSD+ model in Germany

Model code (veg-type)	Vegetation type	German test sites (Site ID)
1	spruce	12, 14, 18, 21, 22
2	pine	3, 20
3	broadleaf softwood	4
4	broadleaf hardwood	10, 11, 13, 15, 16, 17, 19
5	evergreen broadleaf	none
6	shrubs	none
7	grassland	1, 2, 8, 9
8	heather	5, 6, 7

Table DE-2: Environmental conditions of selected sites for testing the VSD+ model in Germany

starting [1] ***C : N ratio***		
low	median	high
7,9,10,12,13,14,15,16,17,18,19,20,21	1, 2, 3, 4, 11	5, 6, 8
expected C : N ratio (year 2100)		
low	median	high
18	0	4
nitrogen deposition		
low	median	high
1, 2, 5, 6, 7, 8, 9, 17, 20	15, 16, 18, 19, 21, 22	3, 4, 10, 11, 12, 13, 14

[1] "starting" means observed values for the NATURA 2000 plots (1-11) and calibrated values for Level-II plots (12-22)

parameters were estimated for each vegetation type. The yearly harvest parameter was set to zero since we do not expect harvesting at sites.
The estimation of the weathering rates of the base cations was not trivial and should be discussed. Since the original input data (and all these data of previous calls) was given in eq $ha^{-1}yr^{-1}$ and now the unit for VSD+ was asked as eq $m^{-3}yr^{-1}$ a transformation of the units was necessary. This transformation was done by using the German soil classification BÜK1000 (BGR 2008) and their expectation for the soil depths. The combination of the known depth of the matching soil type and the weathering rates (in eq $ha^{-1}yr^{-1}$) produces weathering rates of base cations in the asked unit (eq $m^{-3}yr^{-1}$).
The thickness of the soil, the water content of the soil and the percolation was derived from the "MetHyd" tool proposed by the CCE.

Discussion of the Results of the VSD+ Model

Unlike the first attempts of using the VSD+ model the C:N ratio shows different results for each plot. The plots were the C:N ratio and C pool were calibrated show the same C:N development. The curve always starts at 10 and ends up around 10 and 11. Plots with no calibration have different start C:N ratios (18-26) and end up higher (47-52) or lower (9-15). The curves for the C pool also vary quite a lot. The starting points for the non-calibrated plots are between 7190 and 11122 g/m^2 while the C pool for the Level-II plots are always calibrated to almost 20000 g/m^2. The development of the C pool is highly related to the type of vegetation. The heather sites have a decreasing C pool, the vegetation types 1, 2, 3 and 4 have a constant or slightly increasing C pool and the grassland has a really fast growing C pool. The results for the modelled pH value differ from site to site. For some sites (e.g. Site 5) the modelled values meet quite well the expected pH value.

The "expected" pH value was derived in two different ways. For the Level-II plots the measured pH values (average of the rooted soil layers) were used. The average pH-value given by the German soil classification system (BÜK1000) was used as reference value for the other plots. In some sites the modelled pH value is higher than the expected reference pH value (e.g. Site 22), for some Sites pH value fits quite well (Site 5). But for all Sites is true that usually the starting pH value is higher than the modelled value in the year 2100 (see Figure DE.2).

The development of the parameter base saturation (EBc) shows also different results. Here an expected reference value given by the BÜK 1000 (BGR 2008) was used to "validate" the VSD+ results. For some plots modelled base saturation decreases from the year 1960 more or less rapidly and in some cases it has a steady state. This is true for sites with different vegetation types, different pollution levels and different soil properties.

Figure DE-2: pH value modelled with the VSD+ model and reference values for Site 22 (left) and Site 5 (right).

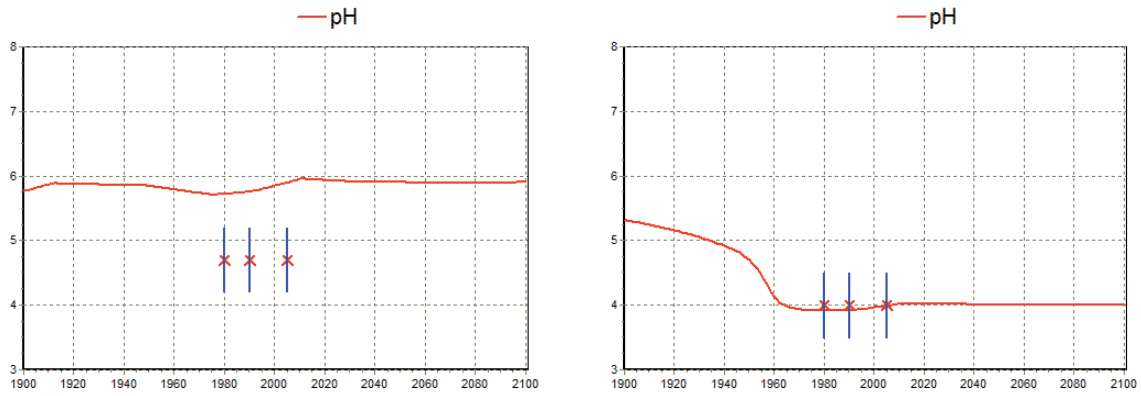

Figure DE.3 Base saturation modelled with the VSD+ model and reference value Site 13(left) and Site 3(right).

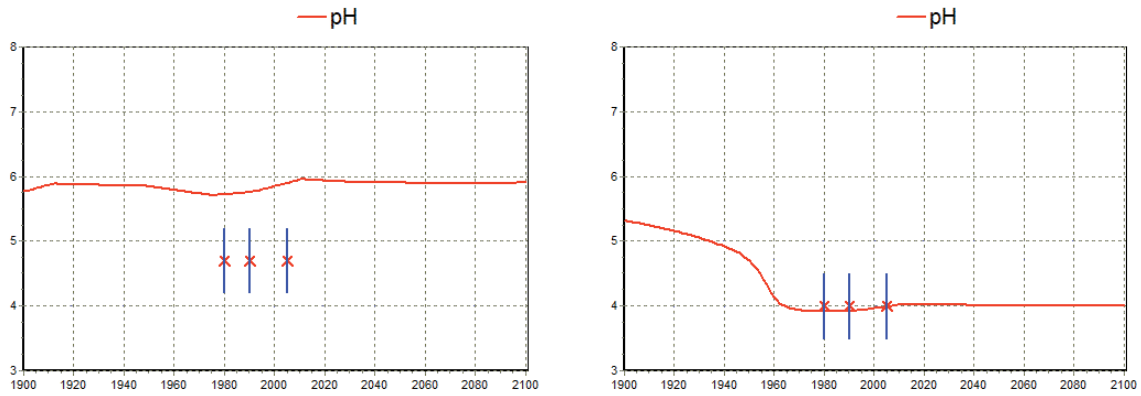

Conclusions

The VSD+ model is a quite useful and well documented tool for dynamic modelling of several soil-related parameters depending on the modelled ecosystem. The needed input parameters are numerous and not easy to receive. Some parameters offer a default value; this is very useful to start with the modelling. The calibration of different input parameters seems to be very useful, but in some cases the resulting values are far away from reasonable or measured values. So this calibration needs to be better understood and maybe needs further documentation. The so called "MetHyd" tool that comes with the VSD+ model is easy to use, but needs to be checked. The program cannot handle dots as limiter for floating numbers and commas can't be saved in the datafile. The background meteorological data should be described better. It seems that this database ends at a Longitude above 13.500.

This brief study showed that the VSD+ model can be used for different sites in Germany. The next step would be a deep analysis of the results and a validation of the model output. Also a check of the input parameters and the default values needs to be done.

References

Bonten L, Posch M, Reinds GJ, 2010. The VSD+ Soil Acidification Model, Model Description and User Manual (version 0.13), Coordination Centre for Effects, Bilthoven, March 2010 (see: www.rivm.nl/cce)

BGR, 2008. Nutzungsdifferenzierte Bodenübersichtskarte der Bundesrepublik Deutschland 1:1.000.000 (BÜK 1000N, Version 2.3)

CCE, 2009. Instructions for the 2009 CCE Call for data, Coordination Centre for Effects, Bilthoven, November 2009 (see: www.rivm.nl/cce)

MAPESI, 2010. Modelling of Air Pollutants and EcoSystem Impact (MAPESI), UBA FKZ 3707 64 200, see: www.mapesi.de

MOBILE, 2010. Modelling and mapping of spatial differentiated impacts of nitrogen input to ecosystems within the framework of the UNECE Convention of Long-range Transboundary Air Pollution, UBA-FB 001341 Part I – IV, UBA-Texte 07/, 08/, 09/, 10/2010

UBA, 2004. Manual on methodologies and criteria for modelling and mapping critical loads and levels and air pollution effects, risks and trends. Umweltbundesamt Texte 52/04, Berlin (updated version of 2008, see: www.icpmapping.org)

Ireland

National Focal Centre

David Dodd
Environmental Protection Agency
McCumiskey House, Richview
Clonskeagh Road, Dublin 14
tel: + 353 1 268 0142
fax: + 353 1 268 0199
email: d.dodd@epa.ie

Collaborating institutions

Julian Aherne
Environmental and Resource Studies
Trent University, 1600 West Bank Drive
Peterborough, Ontario, K9J 7B8, Canada
tel: +1 705 748 1011 ×7887
fax: +1 705 748 1569
email: julian.aherne@ucd.ie

Dynamic modelling of vegetation change

The objective of the 2009 call was to direct NFCs to (a) focus on new vegetation-relevant data requirements, and to (b) evaluate the new VSD+ model. Specifically, NFCs were asked to provide (1) results from trial applications of the VSD+ model at a selected site (or sites), (2) species parameters for the soil-vegetation model chain, and (3) plant relevés with measured soil parameters. The Irish NFC responded to (1) and (3).

The VSD+ model was applied to the Roundwood ICP Level II forest monitoring plot (Farrell et al. 2001). Model inputs were obtained from site observations (soil depth, bulk density, cation exchange capacity and rainfall volume and chemistry), nearby meteorological stations (temperature and sunshine hours [Casement Aerodrome]), previous studies (i.e., weathering rates [Farrell et al. 2001]) or default parameters (i.e., mineralization, etc). Soil chemistry was simulated from 1955 (planting year) to 2010. The long-term deposition sequence was taken from Schöpp et al. (2003) and scaled to site observations. Model specific meteorological inputs were estimated using the MetHyd model and monthly long-term climate data. The application of VSD+ will be expanded to all ICP (Level I and II) forest monitoring plots with soil observations (n = 30–40). Work is currently underway to refine model inputs for nitrogen parameters, and future applications will calibrate initial carbon (and nitrogen) pools and exchange coefficients against current observations (not carried out in the current trial).

In consultation with national agencies, plant relevés from grasslands and measured soil parameters have been obtained for ~3000 sites sampled during the 1970s. In addition, 1000 soil samples have been acquired from plant

relevés sampled during 2010. Additional soil analyses will be carried out to support the development of plant species and soil chemical relationships for 2010 sample sites. In addition, changes in plant species and soil chemistry between 1970 and 2010 will be evaluated.

References

Farrell EP, Aherne J, Boyle GM, Nunan N, 2001. Long-term monitoring of atmospheric deposition and the implications of ionic inputs for the sustainability of a coniferous forest ecosystem. Water, Air and Soil Pollution 130: 1055–1060

Schöpp W, Posch M, Mylona S, Johansson M, 2003. Trends in acid deposition (1880–2030) for sensitive freshwater regions in Europe. Hydrolgy and Earth System Sciences 7: 436–446

Poland

National Focal Centre

Tomasz Pecka, Wojciech A. Mill, Adrian Schlama
Institute of Environmental Protection
Section of Integrated Modelling
Grunwaldzka Str. 7B/2
PL-41-106 Siemianowice Śl.
tel/fax: +48 32 2281482
tomasz.pecka@ios.edu.pl
mill@silesia.top.pl

Collaborating institutions

State Inspectorate of Environmental Protection,
Department of Monitoring
Institute of Meteorology and Water Management the
Wrocław Branch
Parkowa Str. 30PL-51-616
Wrocław
tel: +48 71 3281446

Forest Research Institute the operator of the II-level Forest Monitoring System funded by the Chief Inspectorate of Environment Protection
Braci Leśnej Str. 3
Sękocin Stary
05-090 Raszyn

Introduction

In response to the CCE call for data of November 2009 dynamic modelling results and vegetation parameters are submitted. The VSD+ version 3.1.7 model was used for calculations of soil response to S and N depositions. Vegetation parameters for plant species were derived following the CCE instructions.

General site information

Five sites were chosen to run the VSD+ model and to specify vegetation parameters. The sites were selected from the II-level forest monitoring plots in a combination of high, medium and low C/N ratio and high/low depositions.

Table PL.1 General site information

Plot No	LAT (deg/min/sec)	LON (deg/min/sec)	altitude (m)	FAO soil type	dominant tree species	forest age in 2009	C/N	N dep
207	53°58'35"	23°07'50"	140	Ferralic Arenosol	pine	75	low	low
305	53°18'50"	16°50'00"	105	Haplic Arenosol	pine	61	medium	medium
323	51°57'50"	17°12'20"	102	Haplic Arenosol	pine	69	high	high
410	53°11'00"	21°05'00"	125	Haplic Arenosol	pine	73	high	low
505	50°53'50"	17°38'40"	140	Gleyic Arenosol	pine	75	low	high

Dynamic modelling

Key soil chemical parameters were taken or calculated form II- level forest monitoring plots data.

Table PL.2 VSD+ input data

Keyword	Description	Data input
SiteInfo	text describing the site (max 128 chars)	VSD+_PL_[PlotNo]
period	starting and ending time of simulation (integers)	1880 2010
thick	thickness of the soil compartment	0.45
bulkdens	bulk density of the soil	II-level monitoring plots (Wawrzoniak et al. 2005)
Theta	water content of the soil	II-level monitoring plots (Wawrzoniak et al. 2005)
pCO2fac	CO_2 pressure in soil solution (multiple of pCO_2[atm] in air) (V/F)	estimated
CEC	cation exchange capacity	II-level monitoring plots (Wawrzoniak et al. 2005)
Bsat_0	initial base saturation	II-level monitoring plots (Wawrzoniak et al. 2005)
Excmod	cation exchange model option (1=Gaines-Thomas; 2=Gapon)	2
lgKAlBC	log10 of selectivity constant for Al-Bc exchange	0
lgKHBC	log10 of selectivity constant for H-Bc exchange	2
expAl	exponent (>0) in $[Al]=K_{Alox}\cdot[H]^a$	3
lgKAlox	log10 of gibbsite equilibrium constant	8
Cpool_0	initial amount of C in topsoil (per unit area)	II-level monitoring plots (Wawrzoniak et al. 2005)
CNrat_0	initial C:N ratio in topsoil	II-level monitoring plots (Wawrzoniak et al. 2005)
RCOOmod	organic acid model: 0=Oliver, 1=mono-protic	0
RCOOpars	1 or 3 parameters for organic dissociation model	a=0.96, b=0.9 and c=0.039
cRCOO	total concentration of organic acids (m*DOC) (V/F)	0
TempC	average soil temperature (V/F)	8
percol	percolation (precipitation surplus) (V/F)	site specific calc. (New et al. 2004)
Ca_we	weathering rate of Ca (V/F)	Eq. 5.39 (UBA 2004)
Mg_we	weathering rate of Mg (V/F)	0.001
K_we	weathering rate of K (V/F)	0.001
Na_we	weathering rate of Na (V/F)	0.001
SO2_dep	deposition of SO_2 (V/F)	EMEP / CCE
NOx_dep	deposition of NO_x (V/F)	EMEP / CCE
NH3_dep	deposition of NH_3 (V/F)	EMEP / CCE
Ca_dep	deposition of Ca (V/F)	const. (long-term ave)
Mg_dep	deposition of Mg (V/F)	const. (long-term ave)
K_dep	deposition of K (V/F)	const. (long-term ave)
Na_dep	deposition of Na (V/F)	const. (long-term ave)
Cl_dep	deposition of Cl (V/F)	const. (long-term ave)

Table PL.2 VSD+ input data (Continued)

Keyword	Description	Data input
cCa_min	minimum [Ca] in soil solution	0.0001
cMg_min	minimum [Mg] in soil solution	0.0001
cK_min	minimum [K] in soil solution	0.0001
kmin_fe	mineralization rate of easily degradable fresh litter	8.7
kmin_fs	mineralization rate of recalcitrant fresh litter	0.06
kmin_mb	mineralization rate of microbial soil organic matter	1.0
kmin_hu	mineralization rate of humified soil organic matter	0.0013
frhu_fe	fraction easily degradable fresh litter transferred to microbial soil organic matter	0.0002
frhu_fs	fraction recalcitrant fresh litter transferred to microbial biomass	0.28
frhu_mb	fraction microbial transferred to humified soil organic matter	0.95
CN_fe	C:N ratio of easily degradable fresh litter	17
CN_fs	C:N ratio of recalcitrant fresh litter	295
CN_mb	C:N ratio of microbial soil organic matter	9.5
CN_hu	C:N ratio of humified soil organic matter	9.5
CN_rt	C:N ratio of root turnover	40
Nstmin	minimum N content of stems	1
Nstmax	maximum N content of stems	2
Ninmin	N input below which no effect on N content of stems	0.07
Ninmax	N input above which no effect on N content of stems	0.42
knit	maximum nitrification rate	4
kdenit	maximum denitrification rate	4
Nfix	N fixation	0
ctCast	Ca content of stems	Table 5.8 (UBA, 2004)
ctMgst	Mg content of stems	Table 5.8 (UBA, 2004)
ctKst	K content of stems	Table 5.8 (UBA, 2004)
rf_min	reduction of mineralization because of moisture and temperature	1
rf_nit	reduction of nitrification because of moisture and temperature	1
rf_denit	reduction of denitrification because of moisture and temperature	0.1
age_veg	age of the vegetation at the start of the simulation period	II-level monitoring plots (Wawrzoniak et al. 2005)
growthfunc	growth function for the vegetation (2, 3 or 4 parameters) (V/F, if 2 or 3)	4 parameters estimated (Borowski 1974; Wawrzoniak et al. 2005)
veg_type	vegetation type (integer)	pine
Nlfmin	minimum N content of litterfall	10.7
Nlfmax	maximum N content of litterfall	15.1
expNlfdep	exponent for relation between N in litterfall and N deposition	10.8
ncf	ratio between root turnover and litterfall	0.6

Vegetation parameters database

The plant species inventory data were available for each plot. Latin names of the species were added into table '*VegPars*' for each plot respectively. The plant response functions were set by adoption of data existed in table and recommended papers (Sverdrup et al. 2007, De Vries et al. 2007). To set up response functions for species not listed in the '*VegPars*' table with original parameters, similarity of species were analyzed (when appropriate) to get the final parameters.

Table PL.3 General vegetation information

Plot No	Plant inventory year	Plant association (Braun-Balnquet)	Number of species in each forest layer			
			trees	bushes and shrubs	herbs and forbs	lichens and mosses*
207	2008	Pinus-Oxalis / Corylo-Picetum	3	4	44	9 (11)
305	2008	Querco roboris - Pinetum	1	7	17	10 (18)
323	2008	Querco roboris - Pinetum	3	5	19	10 (18)
410	2008	Leucobryo-Pinetum typicum	2	2	13	8 (21)
505	2008	Calamagrostio-Quercetum petraea	2	5	20	4 (13)

* – soil species (incl. deadwood and bark located species)

Full list of plant species with their response functions – where it was possible to establish – contains the table '*VegPars*' for each plot in the template database (mdb).

Contribution to the European vegetation database

Currently the Polish NFC is gathering information on habitat experts who may assist in improving the site specific biotic and abiotic information in databases for critical loads and dynamic modelling. The information about persons who can participate in this research area will be provided as soon as possible.

References

Borowski M, 1974. Przyrost drzew i drzewostanów [*The increment of trees and forests*], PWRL, Warszawa

De Vries W, Kros H, Reinds GJ, Wamelink W, Mol J, Van Dobben H, Bobbink R, Emmett B, Smart S, Evans C, Schlutow A, Kraft P, Belyazid S, Sverdrup H, Van Hinsberg A, Posch M, Hettelingh J-P, 2007. Developments in deriving critical limits and modeling critical loads of nitrogen for terrestrial ecosystems in Europe. Report 1382, Alterra WUR, Wageningen, The Netherlands, 206 pp

New M, Lister D, Hulme M, Makin I, 2002. A high-resolution data set of surface climate over global land areas. Climate Research 21: 1–25

Sverdrup H, Belyazid S, Nihlgård B, Ericson L, 2007. Modelling change in ground vegetation response to acid and nitrogen pollution, climate change and forest management at in Sweden 1500–2100 A.D. Water, Air and Soil Pollution: Focus 7: 163–179; doi: 10.1007/s11267-006-9067-9

UBA, 2004. Manual on Methodologies and Criteria for Modelling and Mapping Critical Loads and Levels and Air Pollution Effects, Risks and Trends. Umweltbundesamt, Berlin

Wawrzoniak J, Małachowska J, Wójcik J, Liwińska A, 2005. Stan uszkodzenia lasów w Polsce w 2004 r. na podstawie badań monitoringowych *[Forest Monitoring in Poland, Report 2004]*, Biblioteka Monitoringu Środowiska, PIOŚ, Warszawa

Switzerland

National Focal Center/Contact:

Federal Office for the Environment (FOEN)
Air Pollution Control and NIR Division
Beat Achermann
CH - 3003 Bern
tel: 41-31-322.99.78
fax: 41-31-324.01.37
beat.achermann@bafu.admin.ch

Collaborating Institutions:

METEOTEST
Beat Rihm
Fabrikstrasse 14
CH - 3012 Bern
tel: 41-31-307.26.26
fax: 41-31-307.26.10
office@meteotest.ch

EKG Geo-Science
Daniel Kurz
Maulbeerstrasse 14
CH - 3011 Bern
tel: 41-31-302.68.67
fax: 41-31-302.68.25
geo-science@bluewin.ch

Overview

In response to the 2009 CCE call for data, Switzerland participated in the trial of the new VSD+ model by applying it to nine selected forest sites. Inputs, results and experiences made in the test runs are presented in the following sections by Daniel Kurz.

Site description

VSD+ was applied to a series of forest sites monitored by the Institute for Applied Plant Biology (IAP, Schönenbuch). The sites are also part of the national dataset used to derive critical sulphur and nitrogen loads. Some generic information of the sites is listed in Table CH.1 and CH.2 and their location is plotted in Figure CH.1.

Table CH.1 Generic data for the sites selected:

Site name	Code	Owner	CH_X (km)	CH_Y (km)	Height (m) a. s. l.	EMEP_I50	EMEP_J50
Brislach	31_Fichte	IAP	608.606	254.171	413	67	39
Muttenz	10_Buche	IAP	614.724	262.841	355	67	39
Olsberg	32_Buche	IAP	623.889	264.338	381	67	39
Busswil	78_Fichte	IAP	629.341	226.767	596	68	38
Wengernalp	92_Fichte	IAP	637.670	158.306	1837	69	37
Zofingen	63_Buche/ Fichte	IAP	639.596	237.846	533	68	39
Muri	61_Fichte	IAP	669.425	235.600	486	68	39
Rafz	74_Fichte	IAP	683.135	275.325	537	68	40
Winterthur	41_Fichte	IAP	698.200	262.920	519	68	40

Table CH.2 Tree species composition at the sites selected:

Site name	Site ID	vegetation	1	2	3	4	5	6	7	8	9	10	11	12
Brislach	CH052069	spruce	74	3	0	0	0	5	5	1	0	10	0	2
Muttenz	CH052078	beech	0	0	0	0	0	0	99	0	0	0	0	1
Olsberg	CH052084	beech	2	5	0	0	0	0	86	0	0	5	0	1
Busswil	CH052095	spruce	52	35	2	3	0	7	0	0	0	0	0	0
Wengernalp	CH052106	spruce	100	0	0	0	0	0	0	0	0	0	0	0
Zofingen	CH052107	beech	19	2	0	0	0	0	75	0	0	2	0	0
Muri	CH052125	spruce	100	0	0	0	0	0	0	0	0	0	0	0
Rafz	CH052138	spruce	88	0	4	0	0	0	7	0	0	0	0	0
Winterthur	CH052174	spruce	96	2	0	0	0	0	0	0	3	0	0	0

1: spruce, 2: fir, 3: pine, 4: larch, 5: stonepine, 6: other coniferous, 7: beech, 8: maple, 9: ash, 10: oak, 11: chestnut, 12: other deciduous, unit: mass %.

Figure CH.1 Geographic location of the sites used for testing purposes.

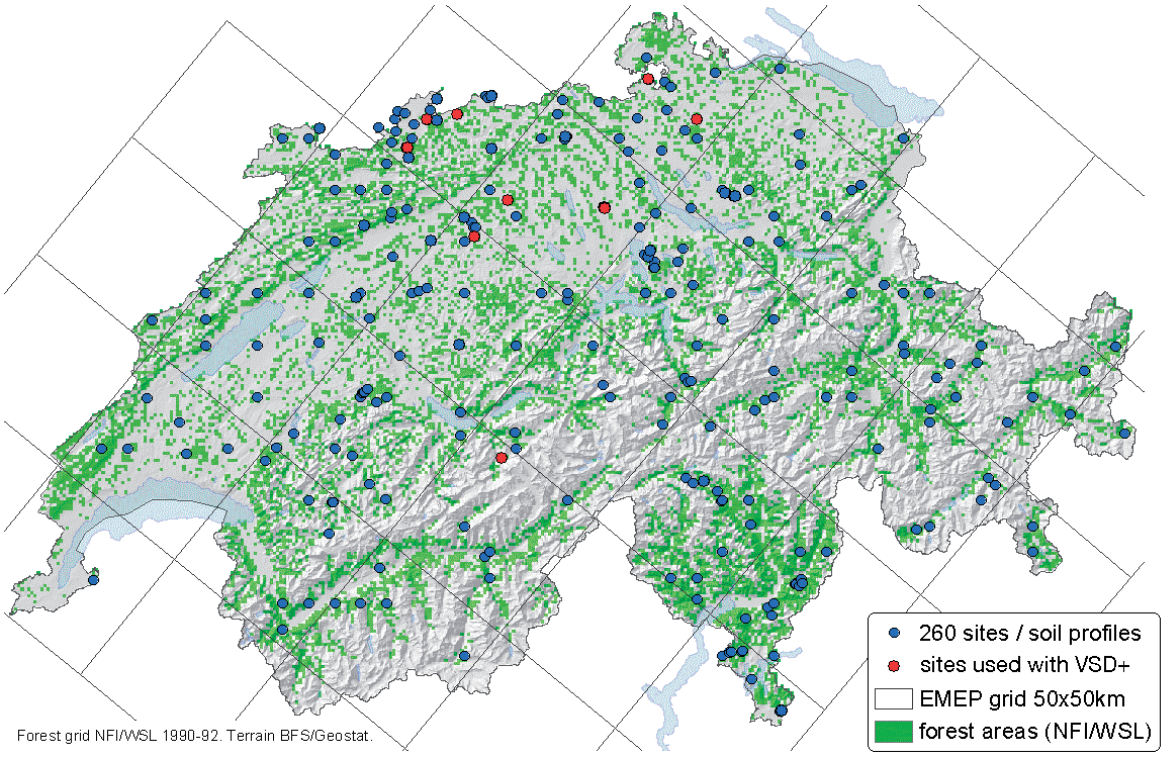

Input derivation

Since the sites considered have been used for SAFE and ForSAFE model exercises, input for the VSD+ can be derived from the multi-layer model runs. Soil input does virtually not differ among the multi-layer model variants, and it is therefore irrelevant from which run it is taken. The multi-layer structure, however, makes it necessary to average certain quantities regarding their use with VSD+. We have limited the soil compartment to the rooting zone, which consists in the multi-layer notation of 1 to n layers.

Table CH.3 Variables extracted from multi-layer models' site files:

Variable name	SAFE/ForSAFE variable(s)	VSD variable	Units[1]	Eqn[2]
layer thickness	$z_1, .., z_n$	*thick*	m	$= \sum_{l=1}^{n} z_{bulk,l}$
bulk density	$\rho_1, .., \rho_n$	*bulkdens*	kg m^{-3} → g cm^{-3}	$= 10^{-3} \frac{1}{z} \sum_{l=1}^{n} z_l \rho_l$
volumetric water content[3]	$\theta_1, .., \theta_n$	*Theta*	m^3 m^{-3}	$= \frac{1}{z} \sum_{l=1}^{n} z_l \Theta_l$
cation exchange capacity	$CEC_1, .., CEC_n$	*CEC*	keq kg^{-1} → meq kg^{-1}	$= 10^{6} \frac{1}{z\rho} \sum_{l=1}^{n} z_l \rho_l CEC_l$
fraction of exchangeable base cations	$feCa_1, .., feK_n$ *(usually for one calibration year)*	*bsatobs)*	-	$= \frac{1}{z\rho CEC} \sum_{j=1}^{3} \sum_{l=1}^{n} z_l \rho_l CEC_l f_{ej,l}$
soil carbon content	$Corg_1, .., Corg_n$ *(usually for one calibration year)*	*Cpoolobs*	g m^{-2}	$= \sum_{l=1}^{n} z_{bulk,l} \left(\rho_{bulk,l} - 2650 \overline{X}_{coarse,l} \right) C_{org,l}$
soil nitrogen content	$Norg_1, .., Norg_n$ *(usually for one calibration year)*	*Npoolobs*	g m^{-2}	$= \sum_{l=1}^{n} z_{bulk,l} \left(\rho_{bulk,l} - 2650 \overline{X}_{coarse,l} \right) N_{org,l}$
partial pressure of CO_2	$p_{CO2,1}, .., p_{CO2,n}$	p_{CO2}	multiple of $p_{CO2,air}$	**
gibbsite constant	$K_{gibb,1}, .., K_{gibb,n}$	K_{Alox}	logarithm	**
DOC	$DOC_1, .., DOC_n$	*RCOO*	gC m^{-3} → mol m^{-3}	**
outflow	$p_{Q,out,n}$	$f_{Q,out}$	% → fraction	$= \frac{p_{Qout,n}}{100}$

[1] "u_1®u_2" means that SAFE-unit u_1 is converted to VSD-unit u_2;
[2] subscript l: layer; subscript j: Ca, Mg, K; in the C and N pool calculations z_{max} = 0.2 m; n in ;
[3] eqn used with all water contents including input for MetHyd (FS, FC and WP).

**For the gibbsite equilibrium constants (K_{gibb}), the layer specific partial CO_2 pressures (P_{CO_2}) and the dissolved organic carbon concentration (DOC), the input to the originally used equations rather than the values itself were averaged:

$$K_{gibb} = 9.8602 - 1.6755 \log(OM') \quad for\ 1.25 < OM' < 100\ wt.\%$$

$$P_{CO_2} = \left(\frac{398.26 + 23719 z' - 28856 z'^2 + 25882 z'^3 - 15693 z'^4 + 5722 z'^5 - 1114.6 z'^6 + 88.817 z'^7}{398.26} \right)$$

$$[DOC] = 0.007 \left(21.524 e^{(-7.2853 z')} \right)$$

where ..' is the respective layer mean.

Time-series data required by VSD+ are either also input to SAFE/ForSAFE (e.g. deposition) or calculated by the multi-layer model (e.g. weathering rate). ForSAFE climate data were annualized and rescaled to the climate input originally used with SAFE. Weathering rates were extracted from SAFE runs.

Table CH 4 Variables extracted from multi-layer models' time-series data:

Variable name	SAFE/ForSAFE variable(s)	VSD variable	Units*	Eqn
temperature	*T*	*TempC*	K → °C	$= T - 273.15$
percolation	*P*	*percol*	m a^{-1}	$= f_{Qout} P$
deposition	TD_j	*j_dep*	meq m^{-2} a^{-1} → eq m^{-2} a^{-1}	$= 0.001 TD_j$
weathering	$W_{i,1}$ .., $W_{i,n}$	*i_we*	keq ha^{-1} a^{-1} → eq m^{-3} a^{-1}	$= \frac{0.1}{z} \sum_{l=1}^{n} W_{j,l}$

subscript j: SO_4, NO_3, NH_4, Ca, Mg, K, Na, Cl; subscript i: Ca, Mg, K, Na;

Input required from VSD+ regarding growing biomass and nutrient contents of different compartments of the biomass can also be extracted from SAFE runs since SAFE relies on PRESAFE model runs regarding nutrient flux input. The above ground wood biomass (*m*) in a given year (t) is the sum of the modelled compartment masses (m_b, where *b* is stem, bark, branch) in t plus the annually harvested compartment masses ($h_{b,a}$) for the simulation period up to t:

$$m(t) = \sum_{b=1}^{3} m_b(t) + \sum_{b=1}^{3} \sum_{a=1}^{t} h_{b,a}$$

the growth increment in t finally is:

$$i = m(t) - m(t-1)$$

In MAKEDEP we have assumed 0.129 of the coniferous (*c*) and 0.7 of the deciduous (*d*) canopy (*C*) to fall every year and each site has a specific deciduous canopy (to total canopy mass) fraction (C_d). Therefore

$$f_{LF} = f_{C_d} f_{LF_d} + \left(1 - f_{C_d}\right) f$$

which is applied to the standing canopy

$$LF(t) = f_{LF} m_C(t)$$

Nutrient contents of the compartments input are also estimated from MAKEDEP output (i.e. SAFE runs input). In general, the values are averages or min/max values of the whole period modelled by MAKEDEP. To get e.g. "ctCast", the nutrient pools of the wood compartments in every time step (t) are summed up

$$Ca(t) = \sum_{c=1}^{3} Ca_c(t)$$

and then divided by the respective biomass to get the nutrient concentration in the biomass in t

$$c_{Ca}(t) = \frac{Ca(t)}{m(t)}$$

which finally is averaged over the whole simulation period according to

$$c_{Ca} = avg\left(c_{Ca}1500, \ldots, c_{Ca}2500\right)$$

As suggested by the model authors, the supplied model MethHyd 1.0 was used for the assessment of site-specific reduction factors for mineralization, nitrification and denitrification. Since the ForSAFE climate database slightly differs from the required climate input, for now the provided background meteorological data was used. Soil hydrological input, however, was drawn from the layered input as described in Table CH1.3.

Each directory (1 per site) also contains a file "sol.dat", which lists the annual averages (and standard deviations) of the measured (bi-weekly to monthly) concentrations of the considered ions in the soil solution (Source: IAP, Schönenbuch, Dr. S. Braun).

Results

In this particular exercise, VSD+ Studio Version 3.1.8.1 was used under MACOS X 10.4.11/parallels 3.2.14/Windows XP. We assume that some of the model's instability is due to the complexity of the platform. Most of the errors occasionally reported by VSD+, e.g. "pow: OVERFLOW error", were difficult to reproduce.

Nine out of 32 sites were up to now calibrated acceptably well. Figure CH.2 compares modelled and measured soil solution chemistry. Ignoring the outliers which all belong to one site, measured base cation concentrations (Bc^{2+}) are satisfactorily reproduced by the model. Measured hydrogen ion (H^+) concentrations are generally difficult to reproduce and in spite of more scatter, the modelled H^+

concentrations reasonably match the measurements. Again, the outliers along the y-axis are caused by only one site. So far the soil chemistry models (e.g. VSD, SAFE) tended to overestimate nitrogen (N) concentrations in the soil solution, even if immobilization and denitrification of N were considered (Figure CH.2D). The more complex and integrated N processes of VSD+ help to overcome this shortcoming. Although there is an only broad correlation of modelled and measured N concentrations (Figure CH.2C), the bias of earlier predictions disappeared.

The advanced modelling of carbon (C) and N dynamics in VSD+, increases on the other hand the complexity of the model employment. We observed particular difficulties in the calibration of sites with C and N pools substantially deviating from default model predictions. Such set-ups often resulted not only in the impossibility to reproduce the observed pools, but also in peculiar estimates of e.g. Gapon exchange coefficients. Reasons for this setback may be the uncertainty of measured C and N pools and the use of default values of a series of parameters driving the organic matter model. Generally, given the limited information in the manual, the calibration procedure is rather difficult to perform and some outcomes are not easy to interpret.

The managed forest is difficult to consider adequately in the current version of VSD+ since:
- the integrated growth model appears not to be applicable to managed stands,
- and the model does for good reasons not accept input nutrient fluxes as earlier VSD versions did.

Figure CH.2 Modelled ion solution concentrations compared with annual average measured ion concentrations. Time period usually is 1998 to 2008.

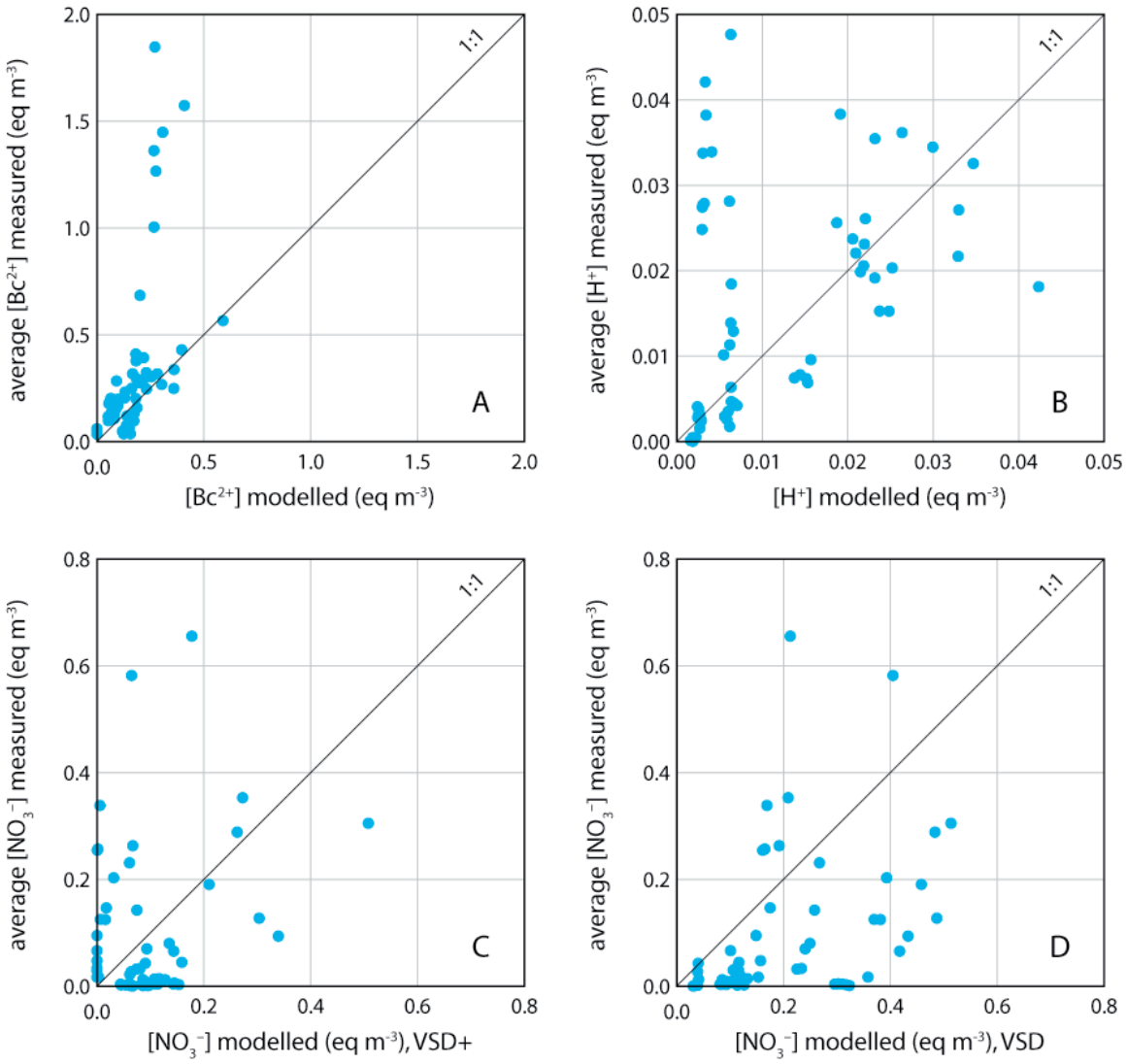

With the currently adopted "growth-file" approach, i.e. giving growth increment and litterfall per year, it is not clear how other management practices than whole tree harvesting can be considered properly. Additionally in this context, it remains indistinct how the canopy particularly in terms of cation pools should be input correctly.

Given the promising results, any further development of VSD+ appears worthwhile with the objective of fully integrating C and N dynamics and thereby improving soil chemistry predictions.

United Kingdom

National Focal Centre

Jane Hall, Chris Evans, Ed Rowe, Filip Oulehle
Centre for Ecology and Hydrology
Environment Centre Wales
Deiniol Road, Bangor
Gwynedd LL57 2UW
Tel: +44 1248 374500
Fax: +44 1248 355365
jrha@ceh.ac.uk
cev@ceh.ac.uk
ecro@ceh.ac.uk
http://critloads.ceh.ac.uk
(migrating to: http://cldm.defra.gov.uk)

Collaborating institutions

Chris Curtis
Environmental Change Research Centre
Department of Geography
University College London
Pearson Building, Gower Street
London WC1E 6BT
Tel: +44 20 7679 0547
c.curtis@ucl.ac.uk

Rachel Helliwell, Malcolm Coull
Macaulay Institute
Craigiebuckler
Aberdeen AB15 8QH
Tel: +44 1224 395000
r.helliwell@macaulay.ac.uk
m.coull@macaulay.ac.uk

Introduction

In response to this call for data the UK are re-submitting steady-state critical loads for acidity and empirical critical loads of nitrogen for the bog broad habitat (EUNIS class D1). The nutrient nitrogen critical loads remain unchanged from the 2008 submission. The critical loads of acidity have been revised as described below. Updated VSD outputs for this habitat (D1) have also been submitted. In addition steady-state critical loads for 1752 UK surface waters have been re-submitted (unchanged) together with updated dynamic modelling (MAGIC) outputs for 1438 of these sites.

This submission also asked countries to provide:

i. Test data for VSD+
ii. Species parameters for future vegetation modelling activities
iii. Contributions to the European database of releves with measured soil parameters.

The UK has submitted test data for a single site for VSD+. This is an upland acid grassland site on peaty podzol soils in mid-Wales, Pwllpeiran, which has been the location of a nitrogen addition and grazing manipulation experiment since the late 1990s. Data from the different treatment

regimes provide scope for detailed model testing The default values were used for most of the input parameters, except those for which site data were available (eg, soil chemistry). The deposition scaling factors used were the same as those used for MAGIC applications for this site. Other parameters altered were:

- N fixation: the default of zero resulted in the error of "VSD+ can't run as too little available N" and so this was set to 0.2.
- CN_hu (CN ratio of humified soil organic matter) was changed from the default of 10 to a more realistic value of 15 for this site.
- frhu_fs (fraction recalcitrant fresh litter transferred to microbial biomass) was set to 0.6.
- frhu_mb (fraction microbial transferred to humified soil organic matter) was set to 0.9.
- rf_nit (reduction of nitrification because of moisture and temperature) was set to 0.6.
- rf_denit (reduction of denitrification because of moisture and temperature) was set to 0.3.
- The growth function was defined by 3 parameters: stem growth = 0, yearly vegetation growth = 0.3 kg/m^2/year, yearly harvest (via sheep grazing) = 0.2 kg/m^2/year. These values are not well constrained and introduce significant uncertainties in the model parameterisation, since they determine the net annual carbon input to the system from primary production.

Results of running VSD+ with the data for this site also show a high sensitivity of modelled N leaching to the parameters rf_min, rf_nit and rf_denit. An attempted simulation of the response of the site to experimental $NaNO_3$ fertilisation failed to reproduce the observed response in N leaching. It is expected that model performance might be improved given more accurate representation of key parameters, but clearly there is a need for continued model testing at data-rich sites (particularly non-forest ecosystems) to ensure robust model performance at larger scales.

The UK has not been able to contribute to items (ii) and (iii) above in time for the deadline for the CCE submission in 2010. However, the UK intends to build this into their work program over the next year to aid further development of the methods and contribute to future Calls for Data. Specifically:

i. Data from other experimental sites on changes in soil N and C, and soil solution N and dissolved organic C and N, are being collated to test several alternative soil organic matter models. This testing will be done in coordination with the CCE and the models tested will include VSD+ where input parameters are available.
ii. Parameters for the VEG species competition model are being derived from observed responses to environmental conditions as represented by the empirical model GBMOVE. The method for transforming parameters is being assessed in a current study applying FORSAFE-VEG to simulate species change on experimental sites. If the results of this trial are promising, the method could be extended to derive VEG models for around 1150 UK plant species.
iii. The UK holds several datasets useful for the proposed European database, notably those from repeated surveys in the Countryside Survey of Great Britain. Enquiries should go to Simon Smart, Centre for Ecology and Hydrology, Lancaster, Lancaster Environment Centre, Library Avenue, Bailrigg, Lancaster, LA1 4AP, email: ssma@ceh.ac.uk

Critical loads and dynamic modelling for the bog broad habitat

The methods and data used to calculate critical loads for different broad habitats in the UK are described in detail in Hall et al (2003a,b & 2004a,b) and will not be repeated here. However, for this data submission the following changes have been made to the critical loads for the bog broad habitat:

- Previous critical loads for the bog broad habitat (like the other terrestrial habitats in the UK) were based on the dominant soil type in each 1x1 km grid square; due to the scale and resolution of the soil data this meant that the bog habitat was mapped as occurring on a range of different soil types. This update is based upon the premise that bog habitat should occur on peat soils only and the critical loads based on methods/data appropriate for peat soils. Values of CLmaxS have been updated incorporating new values of acidity critical loads for peat soils (Hall et al, 2009) for all 1x1 km grid squares mapped as bog. CLminN has been updated using values of nitrogen immobilisation and denitrification appropriate for peat soils (Nimacc = 3 kg N ha^{-1} year^{-1}, Nde = 1 kg N ha^{-1} year^{-1}). CLmaxN has been updated to incorporate the new CLmaxS and CLminN values.
- The inputs to the VSD model have been updated for the bog habitat to set parameters appropriate for bog habitat on peat soil and the VSD scenarios for 2008 re-run using the updated input data.

Critical loads and Dynamic Modelling of surface water habitats

The previous submission included acidity critical loads for 1752 freshwaters (EUNIS classes C1 and C2) calculated using the FAB model; for this submission these data are re-submitted but have not been changed. The dynamic model MAGIC has now been calibrated for 1438 of these freshwater sites and the model outputs for these included in the database submitted. The methods and data sources

used to calibrate the model are described in Hall et al, 2005. For this submission MAGIC has been run using a set of deposition scenarios defined by the CCE for the 2008 Call for Data.

References

Hall J, Ullyett J, Heywood L, Broughton R, Fawehinmi J & 31 UK experts, 2003a. Status of UK Critical Loads: Critical Loads Methods, Data and Maps. February 2003, Report to Defra (Contract EPG 1/3/185); critloads.ceh.ac.uk

Hall J, Ullyett J, Heywood L, Broughton R, Fawehinmi J, 2003b. UK National Focal Centre report. In: Posch et al. (eds): Modelling and Mapping of Critical Thresholds in Europe. Status Report 2003, Report 259101013, RIVM, Bilthoven, Netherlands, pp114–124; www.rivm.nl/cce/publ

Hall J, Ullyett J, Heywood L, Broughton R &12 UK experts. 2004a. Update to: The Status of UK Critical Loads – Critical Loads Methods, Data and Maps. February 2004, Report to Defra (Contract EPG 1/3/185); critloads.ceh.ac.uk

Hall J, Ullyett J, Heywood L, Broughton R, Fawehinmi J, 2004b. UK National Focal Centre report. In: Hettelingh et al (eds): Critical Loads and Dynamic Modelling results. CCE Progress Report 2004, Report 259101014, RIVM, Bilthoven, Netherlands, pp114–134; www.rivm.nl/cce/publ

Hall J, Ullyett J, Evans C, Rowe E, Aherne J, Helliwell R, Ferrier R, Jenkins A, Hutchins M, 2005. UK National Focal Centre report. In: Posch et al. (eds): European Critical Loads and Dynamic Modelling. CCE Status Report 2005, Report 259101016, Netherlands Environmental Assessment Agency, Bilthoven, Netherlands, pp158–160; www.rivm.nl/cce/publ

Hall J, 2009. Updates to UK Critical Loads and Exceedances. September 2009. Report to Defra; critloads.ceh.ac.uk

Part 5
Appendices

Appendix A Instructions for the 2009 CCE Call for data

This appendix is a reprint of the instructions as it was sent to the National Focal Centres with the call for data.

This document contains the instructions for the response to the 2009 CCE Call for Data. The deadline for submission is **15 March 2010.** Please mail your data to jaap.slootweg@pbl.nl.

The call for data consists of three parts, which are described below.
You are invited to download the material that is relevant to this call from the CCE website (http://www.pbl.nl/en/themasites/cce/news) where you can find the VSD+ model executable (under 'setup.exe' in 'VSDp.zip'), the VSD+ manual ('VSD+Man.pdf) and the file 'TemplateCall.mdb' containing data tables 'VEGpars' and 'relcontact'. You are also invited to present and discuss your work at the 20th CCE workshop (Paris, 19-21 April 2010) and prepare documentation following the known format enabling inclusion in the CCE Status report 2010.

Your submission should contain contributions to the following 3 issues/questions:

1. Test results for VSD+, with a document discussing the model results.
You are invited to participate in the trial of new VSD+ model with its improved and connected nitrogen and carbon cycles. Upon executing VSD+, a self explanatory 'help' feature becomes available including 'getting started' instructions. For you convenience also a user manual (VSD+Man.pdf) can be consulted.

The CCE suggests that National Focal Centres apply VSD+ to selected sites in their country and send us the results accompanied with a discussion of their experience with the model and their results.
The single-site version with a General User Interface of the VSD+ model (VSDp-Studio) is available from our website together with documentation. Use 'setup.exe' in VSDp.zip to download the setup for VSD+. Further information can be found in the extensive helpfile of VSDp-Studio. We suggest to run VSD+ for (a few) typical sites in your country, for which good input data are available. Please send to the CCE an archive (zip-file) of the VSD+ input files you created together with a documentation following a format you are used to apply for CCE Status Reports. A possible way to proceed is as follows

- Select sites with combinations of
  - low, median and high C:N ratios
  - (expected) low, median and high C:N ratios (decrease)
  - low, median and high N depositions
- If you select the sites from an existing VSD-Access version, you can export the site from there and add the missing, new parameters (..., defaults)
- Calibrate, run and save the VSD+ input file.
- Collect all input-files into an zip-file

2. Vegetation species for (future) soil-vegetation model chain, potentially with VEG-parameters.

NFCs are asked to extend the list of species that should be modelled by a vegetation model in a soil-vegetation model chain to study the relationship between nitrogen deposition and biodiversity. Your response (in 'VegPars') will enable first runs at the CCE of the VSD-VEG model for the sites that you report.

For the VEG model (Sverdrup et al. 2007) a list of parameters has been made available and the CCE strongly suggests (the initialization of) entering data for species not present in the list already. The steps below are the chrono-logical steps. It is possible that not all steps can be finished before the deadline of this call. It is important to realize that you can report if step 3, or even step 2, has not been finalized.

- Extend the list of species for which response functions should be derived for plant species in your country.
- Determine the parameters of the response function for these species.
- If you can, run ForSAFE-VEG and report results.

You can find a combined list of the Swedish, Swiss and French species in the table '*VegPars*' in the template database prepared for this call. Please add the species relevant to your country in the table, preferably with estimates of the parameters. See Table 1 and Sverdrup et al. (2007; Table 2) for more information. For the VEG model see also De Vries et al. (2007; Annex 6).

Table 1 Database table '*VegPars*' (Figure and equation numbers refer to Sverdrup et al. (2007).

Latinname	Latin name of species
tau	specific generation time (yr) (eq 1)
a0	Nitrogen: factor a0 (eq. 5)
kp	Nitrogen: parameter k+ (eq. 5)
wp	Nitrogen: exponent w+ (eq. 5)
km	Nitrogen: parameter k- (eq. 5)
wm	Nitrogen: exponent w- (eq. 5)
kBc	f([Bc])=1/(1+kBc*[Bc]^2)
kpH	f(pH)=1/(1+kpH*[H]) (eq. 8)
Wmin	Water availability: see Fig. 2
Wtop	Water availability: see Fig. 2
Wmax	Water availability: see Fig. 2 [Wend=1]
Tmin	Temperature: see Fig. 2
Ttop	Temperature: see Fig. 2
Tmax	Temperature: see Fig. 2
Lmin	Light: see Fig. 2
Lmax	Light: see Fig. 2 [Ltop=Lmax, Lend=infinity]
h	effective plant height (m) (eq.10)
rootclass	root class (not needed in VSD-Veg)
kG	grazing parameter (eq. 11)

3. Contribution to the European database of relevés with measured soil parameters.

The intention is to (a) extend the ICP-M&M network with habitat experts that can assist in improving site specific biotic and a-biotic information in databases relevant to European critical loads, dynamic modelling assessments, and (b) strengthen collaboration to the extent that such data can be considered for inclusion in a European data base for future vegetation modelling. More specifically, it is proposed that vegetation soil data also be included in a database constructed by Wieger Wamelink to relate plant species occurrence with soil parameters (see www.abiotic.wur.nl). The resulting model en responses per species will be made freely available through the same website.

For this, you are invited to provide contacts to persons who have information on vegetation relevés/species lists which have been collected together with measured soil parameters. in your country. They should fulfil the following criteria:

Vegetation relevés/species lists made on a limited surface area (e.g. ranging from 1–200 m^2), preferably, but not necessarily, made in the sense of Braun-Blanquet. The relevés have to be accompanied at least with: the coordinates, an estimate of the altitude, the species present in the plot (surface area cover is not necessary), and at least one measured soil parameter, e.g. soil pH, nitrate concentration in the soil, potassium concentration, base cations, total N content, C/N, moisture content etc.; meteorological data are also welcomed. For each measurement the analysis method (especially the extraction method) is also necessary, as well as the sample depth. Please enter the person and his/her coordinates into the access table '*relcontact*'.

References

De Vries W, Kros H, Reinds GJ, Wamelink W, Mol J, Van Dobben H, Bobbink R, Emmett B, Smart S, Evans C, Schlutow A, Kraft P, Belyazid S, Sverdrup H, Van Hinsberg A, Posch M, Hettelingh J-P, 2007. Developments in deriving critical limits and modeling critical loads of nitrogen for terrestrial ecosystems in Europe. Alterra Report 1382, Alterra WUR, Wageningen, The Netherlands, 206 pp
www.pbl.nl/cce

Sverdrup H, Belyazid S, Nihlgård B, Ericson L, 2007. Modelling change in ground vegetation response to acid and nitrogen pollution, climate change and forest management at in Sweden 1500–2100 A.D. *Water, Air and Soil Pollution: Focus*, 7: 163–179, DOI: 10.1007/s11267-006-9067-9

Appendix B
From VSD to VSD+

In this Appendix we summarise the mathematical formulations of those processes in VSD+ that constitute its upgrade from VSD (Posch and Reinds 2009). A complete description of the processes modelled in VSD+ can be found in Bonten et al. (2010). What distinguishes VSD+ from the VSD model is the much more detailed modelling of carbon (C) and nitrogen (N) pools and fluxes; and in the following we give a description of the processes modelled as well as the new input variables needed.

Organic carbon model:

For modelling carbon dynamics, VSD+ uses a 4-compartment model consisting of the following C-pools (in g/m^2):
easily degradable fresh litter (C_{fe});
slowly degradable (recalcitrant) fresh litter (C_{fs});
microbial biomass (C_{mb});
slowly degradable humic material (C_{hm}).
Each C-pool has its own first-order turnover rate k_x (in yr^{-1}) and its own fixed C/N ratio CN_x (in g/g). The first three C-pools can be converted to a different C-pool according to the scheme in Figure B.1; and all four pools loose C in the form of CO_2.

Figure B.1 The four C-pools used in VSD+, their interactions as well as input (litterfall and root turnover) and output (CO_2) fluxes.

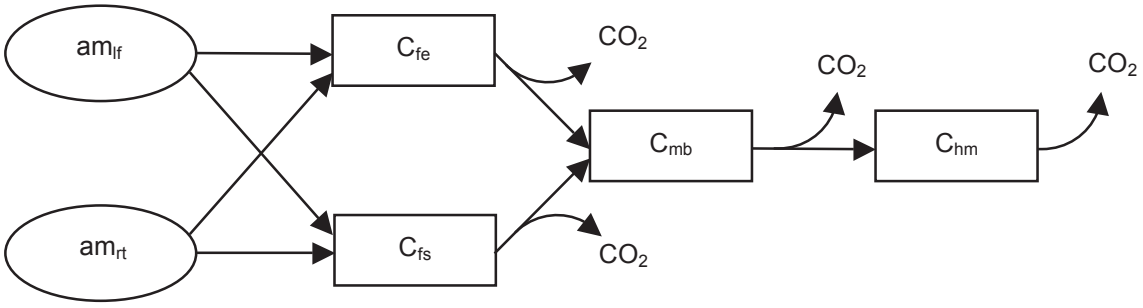

$$\frac{d}{dt}C_{fe} = (am_{lf} \cdot fr_{fe,lf} + am_{rt} \cdot fr_{fe,rt}) \cdot 500 - k_{fe} \cdot C_{fe}$$

The change in the four C-pools are given by:

(B-1) $$\frac{d}{dt}C_{fe} = (am_{lf} \cdot fr_{fe,lf} + am_{rt} \cdot fr_{fe,rt}) \cdot 500 - k_{fe} \cdot C_{fe}$$

(B-2) $$\frac{d}{dt}C_{fs} = (am_{lf} \cdot fr_{fs,lf} + am_{rt} \cdot fr_{fs,rt}) \cdot 500 - k_{fs} \cdot C_{fs}$$

(B-3) $$\frac{d}{dt}C_{mb} = k_{fe} \cdot fr_{hu,fe} \cdot C_{fe} + k_{fs} \cdot fr_{hu,fs} \cdot C_{fs} - k_{mb} \cdot C_{mb}$$

(B-4) $$\frac{d}{dt}C_{hm} = k_{mb} \cdot fr_{hu,mb} \cdot C_{mb} - k_{hm} \cdot C_{hm}$$

where am_{lf} is the litterfall and am_{rt} is the root turnover flux (both in kg/m²/yr); $fr_{fe,lf}$ and $fr_{fs,lf}$ are the easily degradable and recalcitrant fraction of the litterfall, respectively; analogously $fr_{fe,rt}$ and $fr_{fs,rt}$ for roots. The factor 500 converts from kg litterfall to g C (assuming a C-content of 50%). k_x is the turnover rate of pool *x=fe,fs,mb,hm*, and $fr_{hu,x}$ (*x=fe,fs,mb*) is the fraction of the total turnover of a C-pool converted to another C-pool (and $(1-fr_{hu,x}) \cdot k_x \cdot C_x$ is released as CO_2).

Litterfall and root turnover are distributed over the easily degradable and recalcitrant fractions depending on the C:N ratios of litterfall (CN_{lf}) and root turnover (CN_{rt}) according to:

(B-5) $$\left.\begin{array}{l} fr_{fe,lf} \cdot CN_{fe} + fr_{fs,lf} \cdot CN_{fs} = CN_{lf} \\ fr_{fe,lf} + fr_{fs,lf} = 1 \end{array}\right\}$$

(B-6) $$\left.\begin{array}{l} fr_{fe,lf} \cdot CN_{fe} + fr_{fs,lf} \cdot CN_{fs} = CN_{lf} \\ fr_{fe,lf} + fr_{fs,lf} = 1 \end{array}\right\}$$

The turnover rates k_x are calculated from maximum turnover rates $k_{x,max}$ by correcting for pH, temperature, wetness and drought according to:

(B-7) $$k_x = k_{x,max} \cdot rf_{mi,pH} \cdot rf_{mi}$$

where the modifying functions $rf_{mi,pH}$ and rf_{mi} (dependent on temperature, wetness and drought) are described below (see section 'Correction of mineralization and (de) nitrification for environmental conditions'; note that earlier these functions were called 'reduction functions').

N processes:

Nitrogen processes implemented in VSD+ are depicted in Figure B.2; and the numbers indicate the calculation sequence.

Inputs of N in VSD+ are NH_4 and NO_3 deposition, litterfall, root turnover and N fixation. N input by in litterfall, N_{lf} (eq/m²/yr), is dependent on the deposition of N, $N_{dep}=NH_{4,dep}+NO_{3,dep}$ (eq/m²/yr):

(B-8) $$N_{lf} = \frac{am_{lf}}{1.4} \cdot \left(ctN_{lf,min} + (ctN_{lf,max} - ctN_{lf,min}) \cdot (1 - e^{-expNlfdep \cdot N_{dep}}) \right)$$

where am_{lf} (kg/m²/yr) is the amount of litterfall (see below), $ctN_{lf,min}$/$ctN_{lf,max}$ (%) are the minimum/maximum N content of litterfall, *expNlfdep* (m²yr/eq) is an exponent relating N deposition to N in litterfall, and the division by 1.4 converts from % to moles (=eq) of N. N input by root turnover, N_{rt} (eq/m²/yr), is computed as:

Figure B.2 Nitrogen processes implemented in VSD+. The numbers indicate the calculation sequence.

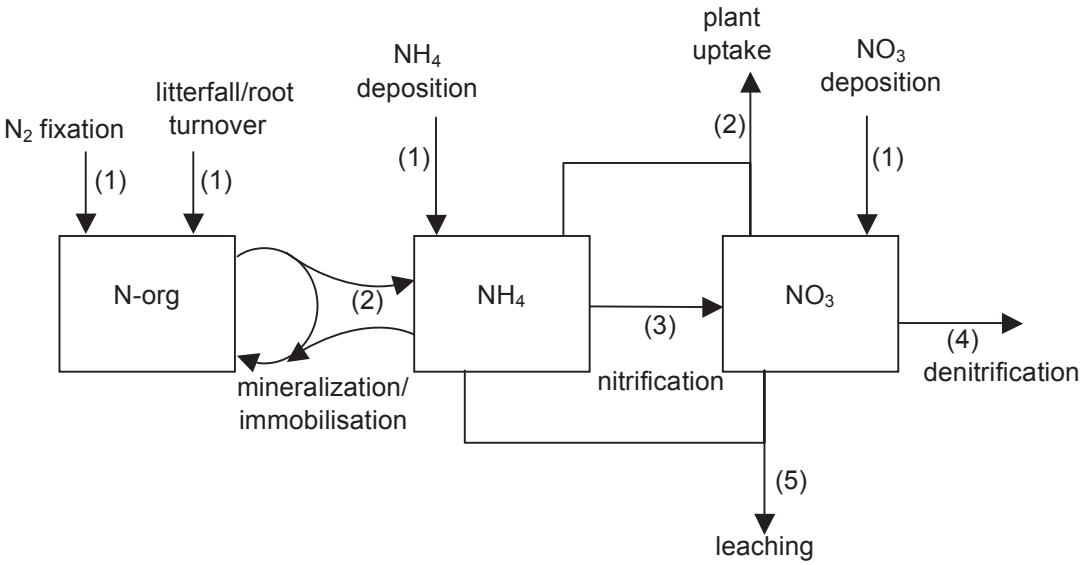

(B-9) $$N_{rt} = \frac{am_{rt} \cdot 500}{14 \cdot CN_{rt}}$$

where am_{rt} (kg/m²/yr) is the amount of root turnover (see below), CN_{rt} is the C:N-ratio (g/g) of the roots, the factor 500 converts from kg biomass to g C (assuming a C-content of 50%) and the division by 14 from g N to moles (=eq) of N.

N fixation, N_{fix}, is assumed constant (input). The immobilisation/mineralization of N depends on the turnover of the C-pools:

(B-10) $$N_{im,x} = \frac{1}{14 \cdot CN_x} \Delta C_{x,t} \quad \text{with} \quad x = fe, fs, mb, hm$$

where $N_{im,x}$ (eq/m²/yr) is the immobilisation of N in pool x, and $\Delta C_{x,t} = C_{x,t} - C_{x,t-\Delta t}$ (see eqs.B1-4). The total net N immobilisation is:

(B-11) $$N_{im} = N_{im,fe} + N_{im,fs} + N_{im,mb} + N_{im,hm} - N_{fix} - N_{lf} - N_{rt}$$

If $N_{im} > 0$, there is net N immobilization, otherwise net mineralization. The uptake of N by vegetation, N_u (eq/m²/yr), is computed as:

(B-12) $$N_u = \frac{\Delta Am_t}{14} \cdot ctN_{st}$$

where $\Delta Am_t = Am_{st,t} - Am_{st,t-\Delta t}$ is the growth increment at time-step t (in kg/m²/yr, see below) and ctN_{st} (%) is the N content of stems. If $N_{dep} - N_{im} - N_u < 0$, there is not enough N available for both immobilisation and uptake. In this case the turnover rate of the recalcitrant C-pool (k_{fs}) is reduced such that $N_{dep} - N_{im} - N_{up} = 0$. Total N uptake N_u is split into $NH_{4,u}$ and $NO_{3,u}$ – with preferential uptake of NH_4 – according to:

(B-13) $$NH_{4,u} = \min\left\{ NH_{4,dep} - N_{im}, N_u \right\}$$

(B-14) $$NO_{3,u} = N_u - NH_{4,u}$$

where it is assumed that all N_{im} is in the form of ammonium. The next step in the fate of N is nitrification, N_{ni} (eq/m²/yr):

(B-15) $$N_{ni} = fr_{ni} \cdot \left(NH_{4,dep} - N_{im} - NH_{4,u} \right)$$

where fr_{ni} is the fraction of available NH_4 that is nitrified in a year. Denitrification, N_{de} (eq/m²/yr), is then calculated as:

(B-16) $$N_{de} = fr_{de} \cdot \left(NO_{3,dep} + N_{ni} - NO_{3,u} \right)$$

where fr_{de} is the fraction of available NO_3 that is denitrified on an annual basis. The annual nitrification/denitrification fractions are calculated as:

(B-17) $$fr_y = 1 - \exp\left(-k_y \cdot rf_{y,pH} \cdot rf_y \right) \quad \text{with} \quad y = ni, de$$

where k_y are user-supplied constants, and rf_y and $rf_{y,pH}$ are modifying functions (see below).

The residual NH_4 and NO_3 will leach from the root zone ($NH_{4,le}$ and $NO_{3,le}$ in eq/m²/yr):

(B-18) $$NH_{4,le} = NH_{4,dep} - N_{im} - NH_{4,u} - N_{ni}$$

(B-19) $$NO_{3,le} = NO_{3,dep} - NO_{3,u} + N_{ni} - N_{de}$$

Vegetation growth:

For vegetation growth, VSD+ uses either a logistic growth-curve or user-prescribed growth and litterfall time series. In case of logistic growth, the amount of woody biomass (stems plus branches) in simulation year t, $Am_{st,t}$ (kg/m²), is calculated as:

(B-20) $$Am_{st,t} = \frac{Am_{st,mx}}{1 + \exp(-k_{gl} \cdot (age_{vg} + t - t_{1/2}))}$$

where $Am_{st,mx}$ is the maximum woody biomass (kg/m²), age_{vg} (yr) the initial age of the vegetation, $t_{1/2}$ (yr) the half life-time, and k_{gl} (yr⁻¹) the logistic growth rate constant.

The litterfall in year t, $am_{lf,t}$ (in kg/m²/yr), approaches its maximum value faster and is calculated as:

(B-21) $$am_{lf,t} = \frac{am_{lf,mx}}{1 + \exp(-3 \cdot k_{gl} \cdot (age_{vg} + t - t_{1/2}/3))}$$

where $am_{lf,mx}$ is the maximum amount of annual litterfall. The generic shapes of $Am_{st,t}/Am_{st,mx}$ and $am_{lf,t}/am_{lf,mx}$ are shown in Figure B.3; it shows that maximum litterfall is already reached with about 10% of the biomass.

Figure B-3: Generic shapes of the (relative) amount of woody biomass $Am_{st,t}/Am_{st,mx}$ (brown curve) and the amount of litterfall $am_{lf,t}/am_{lf,mx}$ (green curve) as given be eqs.B-20,21.

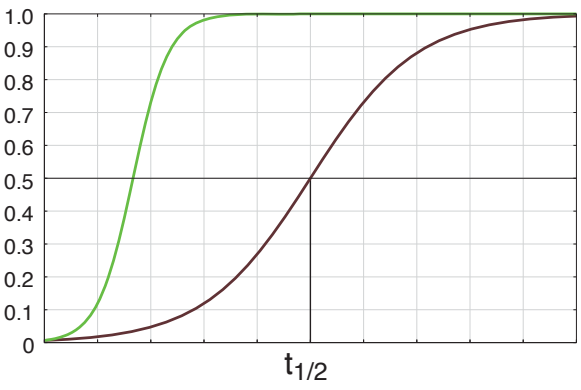

Root turnover, $am_{rt,t}$ (kg/m²/yr), is computed from litterfall by a vegetation-dependent – but time-independent – ratio *ncf*:

(B-22) $am_{rt,t} = ncf \cdot am_{lf,t}$

Correction of mineralization and (de)nitrification for environmental conditions:

Mineralization and (de)nitrification rates (called 'turn-over rates' above) depend on soil pH, temperature, wetness and drought, and are computed as follows:

pH: The modifying functions for mineralization and (de) nitrification due to pH, $rf_{mi,pH}$, are modelled as:

(B-23) $rf_{mi,pH} = \frac{1}{1+\exp(2\cdot(3.8-pH))}$

(B-24) $rf_{ni,pH} = \frac{1}{1+\exp(4\cdot(2.75-pH))}$

(B-25) $rf_{de,pH} = \frac{1}{1+\exp(2.5\cdot(5-pH))}$

where *pH* is the soil solution pH.

Temperature: The modifying function of mineralization due to temperature, $rf_{mi,T}$, is modelled as:

(B-26) $rf_{mi,T} = \exp\left[3.36\left(\frac{T-40}{T+31.79} - \frac{T_0-40}{T_0+31.79}\right)\right], \quad T_0 = 10^{\circ}\mathrm{C}$

where *T* (°C) is the soil temperature. For nitrification and denitrification VSD+ uses the same modifying function as for mineralization:

(B-27) $rf_{ni,T} = rf_{de,T} = rf_{mi,T}$

Wetness: The dependence of the decomposition rates on wetness is based on the aerobic/anaerobic zone concept. Mineralization is proportional to the relative size of the aerobic zone in a soil. This size can be estimated from the dependency of denitrification on the water-filled pore space (= θ/θ_{sat}), under the assumption that denitrification only takes place under anaerobic conditions. The modifying function of denitrification due to wetness, $rf_{de,\theta}$, is modelled as:

(B-28) $rf_{de,\theta} = \begin{cases} 0 & \text{for} \quad \frac{\theta}{\theta_{sat}} < 0.62 \\ \left(\frac{\theta/\theta_{sat} - 0.62}{1-0.62}\right)^{1.74} & \text{for} \quad 0.62 \le \frac{\theta}{\theta_{sat}} \le 1 \end{cases}$

where θ (m³/m³) is the soil water content and θ_{sat} (m³/m³) is the total pore space (soil moisture at saturation). In VSD+, the modifying function of mineralization and nitrification due to wetness is defined as one minus the correction for denitrification (i.e. the size of the aerobic zone):

(B-29) $rf_{mi,\theta} = 1 - rf_{de,\theta}$

(B-30) $rf_{ni,\theta} = 1 - rf_{de,\theta}$

Drought: The correction of mineralization due to drought stress, $rf_{mi,dr}$, is modelled as (Vleeshouwers and Verhagen 2002):

(B-31) $rf_{mi,dr} = \begin{cases} 0 & \text{for} \quad \theta \le \theta_{wp} \\ 2\cdot\frac{\theta-\theta_{wp}}{\theta_{fc}-\theta_{wp}} & \text{for} \quad \theta_{wp} < \theta < \frac{\theta_{fc}+\theta_{wp}}{2} \\ 1 & \text{for} \quad \theta \ge \frac{\theta_{fc}+\theta_{wp}}{2} \end{cases}$

where θ_{fc} (m³/m³) is the moisture fraction at field capacity and θ_{wp} (m³/m³) the moisture fraction at wilting point. For nitrification and denitrification VSD+ uses the same modifying functions as for mineralization:

(B-32) $rf_{ni,dr} = rf_{de,dr} = rf_{mi,dr}$

Since soil temperature and moisture can be highly variable within a year, average modifying factors are calculated from daily (or weekly) values as follows:

(B-33) $rf_x = \sum_{t=o}^{T} rf_{x,\theta} \cdot rf_{x,T} \cdot rf_{x,dr} \cdot \Delta t \Big/ \sum_{t=o}^{T} \Delta t \quad , \quad x = mi, ni, de$

In this way also coinciding events, such as high temperature and low moisture, are incorporated properly. And the program MetHyd (see Appendix C) does exactly that and can thus be used as a pre-processor for VSD+.

Model Input

The input data are provided in a single file (which, in turn, may refer to other files) and every input parameter is preceded by a keyword. After the keyword, on the same line, one (or more) parameters are expected. These can be numbers or character strings (e.g. filenames). The order of the keywords (i.e. records) is irrelevant; in addition, there can be comment lines, i.e. lines starting with an exclamation mark ('!'), anywhere in the file that are ignored when reading the input data.

Table 1 summarises those input parameters that are new to VSD+; parameters that are also needed in VSD are not listed. Some of them are optional, and if they are not specified (e.g. commented out), default values are used (given in column 4). A question mark ('?') in that column means that the value(s) are mandatory and that the model will not run if they are not provided.

Table 1 Input parameters specific for the VSD+ model. Note: Keywords are case sensitive.

Keyword	Description	Unit	Default
kmin_fe	mineralization rate of easily degradable fresh litter	yr^{-1}	8.7
kmin_fs	mineralization rate of recalcitrant fresh litter	yr^{-1}	0.06
kmin_mb	mineralization rate of microbial soil organic matter	yr^{-1}	1.0
kmin_hu	mineralization rate of humified soil organic matter	yr^{-1}	0.0013
frhu_fe	fraction easily degradable fresh litter transferred to microbial soil organic matter	–	0.0002
frhu_fs	fraction recalcitrant fresh litter transferred to microbial biomass	–	0.28
frhu_mb	fraction microbial transferred to humified soil organic matter	–	0.95
CN_fe	C:N ratio of easily degradable fresh litter	g/g	17
CN_fs	C:N ratio of recalcitrant fresh litter	g/g	295
CN_mb	C:N ratio of microbial soil organic matter	g/g	9.5
CN_hu	C:N ratio of humified soil organic matter	g/g	9.5
CN_rt	C:N ratio of root turnover	g/g	40
Nst	N content of stems	%	j)
knit	maximum nitrification rate	yr^{-1}	4
kdenit	maximum denitrification rate	yr^{-1}	4
Nfix	N fixation	$eq/m^2/yr$	0
ctCast	Ca content of stems	%	0
ctMgst	Mg content of stems	%	0
ctKst	K content of stems	%	0
rf_min	modifying factor of mineralization due to moisture and temperature	–	1
rf_nit	modifying factor of nitrification due to moisture and temperature	–	1
rf_denit	modifying factor of denitrification due to moisture and temperature	–	0.1
age_veg	age of the vegetation at the start of the simulation period	yr	?
growthfunc	growth function for the vegetation (2, 3 or 4 parameters) (V/F, if 2 or 3)	i)	?
veg_type	vegetation type (integer) (see Table 2)	–	?
Nlfmin	minimum N content of litterfall	%	j)
Nlfmax	maximum N content of litterfall	%	j)
expNlfdep	exponent for relation between N in litterfall and N deposition	m^2yr/eq	j)
ncf	ratio between root turnover and litterfall	–	j)

i) 4 parameters: maximum amount of stems (kg/m^2), logistic growth rate constant (yr^{-1}), half life time (yr) and maximum litterfall ($kg/m^2/yr$); 2 (3) parameters: yearly vegetation growth, yearly litter production (, yearly non-stem harvest) (all in $kg/m^2/yr$) [VSD+ subtracts the harvest from the litter production to obtain litterfall!]
j) Default values depend on veg_type (see Table 2)

Table 2 Vegetation types defining default values for Nlfmin, Nlfmax, expNlfdep, ncf and Nst.

veg_type	Vegetation type	Nlfmin	Nlfmax	expNlfdep	ncf	Nst
		%	%	m^2yr/eq	-	%
1	spruce	1.01	2.13	7.4	0.8	0.11
2	pine	1.07	1.51	10.8	0.6	0.11
3	broadleaf softwood (e.g. willow, poplar)	1.52	2.90	8.2	0.5	0.13
4	broadleaf hardwood (e.g. oak, beech)	1.52	2.90	8.2	0.5	0.13
5	evergreen broadleaf	1.52	2.90	8.2	0.5	0.13
6	shrubs	1.52	2.90	8.2	0.5	0.13
7	grassland	0.85	2.30	9.0	0.5	0.11
8	tundra/peat/heather	0.85	1.80	9.0	0.5	0.11

References:

Bonten L, Posch M, Reinds GJ, 2010. The VSD+ Soil Acidification Model – Model Description and User Manual. Alterra and CCE, Wageningen and Bilthoven.

Posch M, Reinds GJ, 2009. A very simple dynamic soil acidification model for scenario analyses and target load calculations. *Environmental Modelling & Software* 24: 329-340

Vleeshouwers LM, Verhagen A, 2002. Carbon emission and sequestration by agricultural land use: a model study for Europe. *Global Change Biology* 8: 519–530

Appendix C MetHyd – A meteo-hydrological pre-processor for VSD+

The VSD+ model requires as input annual average parameters related to mineralization and (de)nitrification (rf_{mi}, rf_{ni}, rf_{de}; see eq.B-33 in Appendix B). These parameters are dependent of meteorological (temperature) and hydrological (soil moisture) variables. It is highly recommended to compute these parameters from daily meteo-hydrology and then average over a year instead of simply using annual average meteo-hydrology in order to better capture the (correlation in) daily extremes. To assist model users in this task, the model MetHyd has been developed as a pre-processor for the VSD+ model (Bonten et al. 2010), but some of the output from MetHyd can also be used with other models, such as VSD (Posch and Reinds 2009).

MetHyd employs user-provided daily or monthly meteorological (i.e. temperature, precipitation and sunshine) time series and basic soil properties (see Figure C.1) to compute daily evapotranspiration, soil moisture and percolation (runoff), and from these the three parameters required by VSD+. It also computes annual averages of the meteo-hydrological quantities, which can be (and should be, for consistency reasons) used by VSD(+); in fact, all annual averages can be directly incorporated into an (existing) VSD(+) input data file. The computed daily time series can be easily viewed in and exported from MetHyd.

If only monthly meteorological time series are provided, MetHyd derives daily data with a simple downscaling procedure. Meteorological data are also available from a high-resolution data base (New et al. 2002), from which MetHyd extracts them at a user's request (by default for Europe only).

Input Data

The input data for MetHyd are provided interactively or in a single file, which, in turn, may refer to other files holding time series of data (see below). In case of a file, every input parameter is entered on a separate line, starting with a unique keyword. After the keyword, on the same line, one (or more) parameters are expected. These can be numbers or character strings (e.g. filenames). The order of the keywords (i.e. records) is irrelevant. In addition, there can be comment lines, i.e. lines starting with an exclamation mark ('!'), anywhere in the file; they are ignored when reading the input data.

Table C.1 summarises the input parameters. Some of them are optional, and if they are not specified, default values are used (given in column 4). A question mark ('?') in that column means that the value(s) are mandatory, and that the program terminates (or asks interactively), if they are not provided in the parameter file.

Figure C.1 A screen of MetHyd illustrating the assistance provided for computing soil properties such as bulk density and water holding capacities from basic soil characteristics.

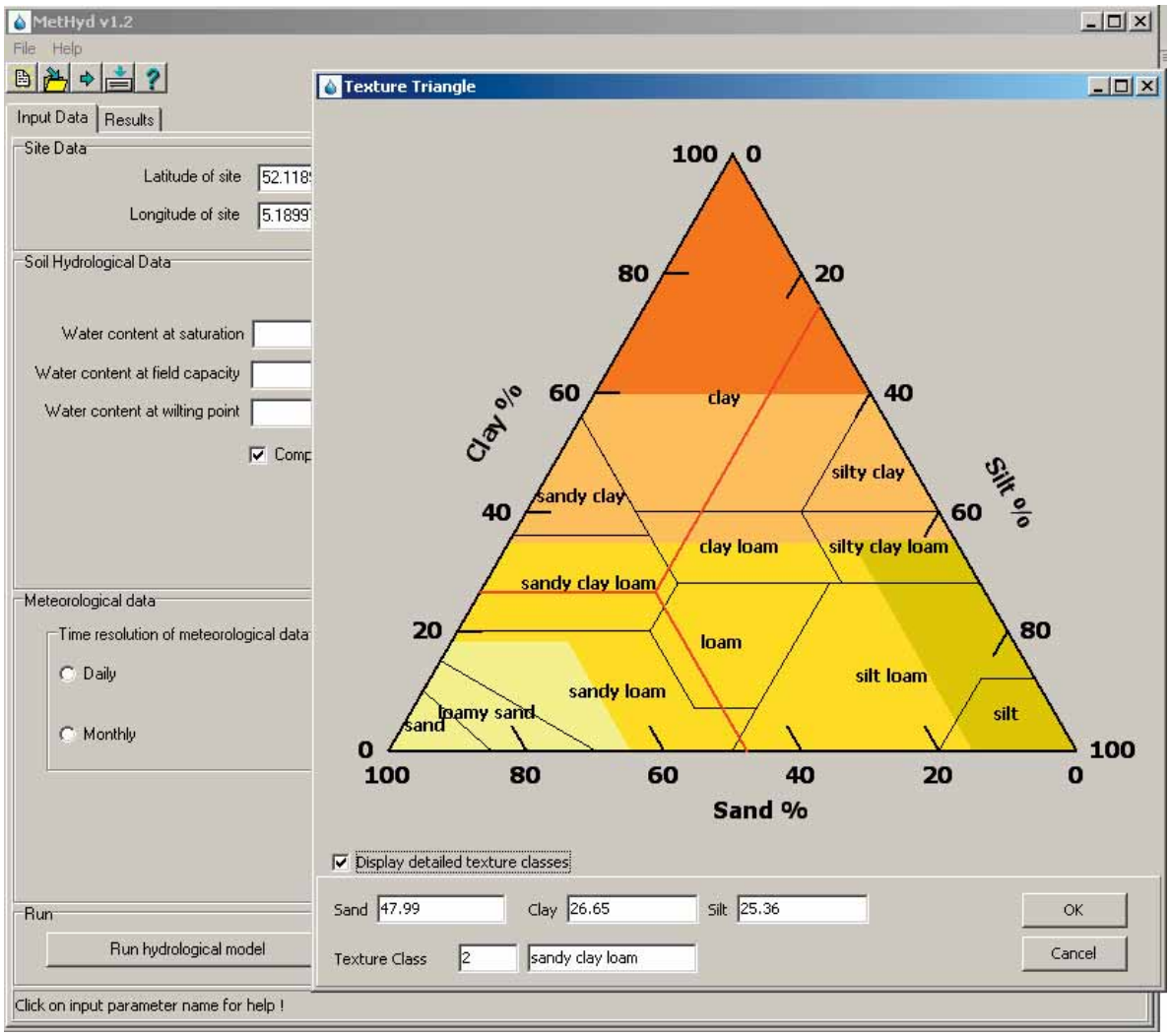

Table C.1 Input parameters for MetHyd. Note: Keywords are case sensitive.

Keyword	Description	Unit	Default
SiteInfo	text describing the site (max. 128 chars)	-	(blank)
Longitude	longitude of the site (<0 for west of Greenwich)	°	?
Latitude	latitude of the site (<0 for south of the equator)	°	?
MetYears	number of years of meteorological data to be considered	-	1
DefMetFile	name of file (incl. path) with default meteorological data	-	a)
TimeResolution	time resolution of the meteorological data (0=daily, 1=monthly)	-	?[b)]
TempFile	name of file with temperature data	°C	c)
PrecFile	name of file with precipitation data	mm	c)
SunFile	name of file with sunshine percent data	%	c)
Albedo	albedo of the (vegetation at the) site	-	?
ThetaSat	soil water content at saturation	m/m	d)
ThetaFC	soil water content at field capacity	m/m	d)
ThetaWP	soil water content at wilting point	m/m	d)
Clay_ct	clay content of the soil	%	?[e)]
Sand_ct	sand content of the soil	%	?[e)]
OrgC_ct	organic C content of the soil	%	?[e)]
bulkdens	bulk density of the soil	g/cm^3	?[e)f)]

[a)] Default file for Europe provided with MetHyd.
[b)] Not read, if met data are from DefMetFile (which are monthly).
[c)] Either all 3 files are specified or DefMetFile is used.
[d)] If one of them is not given, they are all computed from Clay_ct, Sand_ct, OrgC_ct and bulkdens.
[e)] Not read, if ThetaSat, ThetaFC and ThetaWP are given.
[f)] If not given, computed from OrgC_ct (and Clay_ct and Sand_ct).

A complete description of the procedures used in MetHyd can be found in Posch and Reinds (2010), and this document can also be viewed under the 'Help'-function of MetHyd. The model MetHyd itself and an instruction video explaining its use are available from the CCE website.

References

Bonten L, Posch M, Reinds GJ, 2010. The VSD+ Soil Acidification Model – Model Description and User Manual. Alterra and CCE, Wageningen and Bilthoven

New M, Lister D, Hulme M, Makin I, 2002. A high-resolution data set of surface climate over global land areas. *Climate Research* 21: 1–25

Posch M, Reinds GJ, 2009. A very simple dynamic soil acidification model for scenario analyses and target load calculations. *Environmental Modelling & Software* 24: 329-340

Posch M, Reinds GJ, 2010. MetHyd – A Meteo-Hydrological Pre-processor – Description and User Manual. CCE and Alterra, Bilthoven and Wageningen

Appendix D
The polar stereographic projection (EMEP grid)

EMEP provides depositions and other results of atmospheric dispersion modelling on the so-called EMEP grid (see http://www.emep.int/grid/griddescr.html). The EMEP grid is a special case of the so-called polar stereographic projection. Here we describe this projection for various grid sizes, and also how to calculate the area of a grid cell.

The polar stereographic projection:

In the polar stereographic projection each point on the Earth (assumed to be a sphere) is projected from the South Pole onto a plane perpendicular to the Earth's axis and intersecting the Earth at a fixed latitude f_o (see Figure D-1, top). Consequently, the coordinates *x* and *y* are obtained from the geographical longitude l and latitude f (in radians) by the following equations (see Figure D-1, bottom):

(D-1) $$x = x_p + M \tan\left(\frac{\pi}{4} - \frac{\phi}{2}\right)\sin(\lambda - \lambda_0)$$

and

(D-2) $$y = y_p - M \tan\left(\frac{\pi}{4} - \frac{\phi}{2}\right)\cos(\lambda - \lambda_0)$$

where (x_p, y_p) are the coordinates of the North Pole; l_o is a rotation angle, i.e. the longitude parallel to the *y*-axis; and *M* is the scaling of the *x*-*y* coordinates. In the above definition the *x*-values increase and the *y*-values decrease when moving towards the equator. For a given *M*, the unit length (grid size) *d* in the *x*-*y* plane is given by:

(D-3) $$d = \frac{R}{M}(1 + \sin\phi_0)$$

where *R* is the radius of the Earth. The inverse transformation – i.e. longitude and latitude as function of *x* and *y* – is given by:

(D-4) $$\lambda = \lambda_0 + \arctan\left(\frac{x - x_p}{y_p - y}\right)$$

and

(D-5) $$\phi = \frac{\pi}{2} - 2\arctan(r/M) \quad \text{with} \quad r = \sqrt{(x - x_p)^2 + (y - y_p)^2}$$

The *arctan* in eq.D-5 gives the correct longitude for quadrant 4 ($x > x_p$ and $y < y_p$) and quadrant 3 ($x < x_p$ and $y < y_p$); p (=180°) has to be added for quadrant 1 ($x > x_p$ and $y > y_p$) and subtracted for quadrant 2 ($x < x_p$ and $y > y_p$). Note that quadrant 4 is the one covering (most of) Europe.

Every stereographic projection is a so-called conformal projection, i.e. an angle on the sphere remains the same in the projection plane, and vice versa. However, the stereographic projection distorts areas (even locally), i.e. it is not an equal-area projection.

Figure D.1 Polar stereographic projection from the South Pole onto a plane cutting the Earth at a given latitude (top); and geometric relationships in a plane cutting the Earth vertically at a given longitude used to derive the projection equations (bottom).

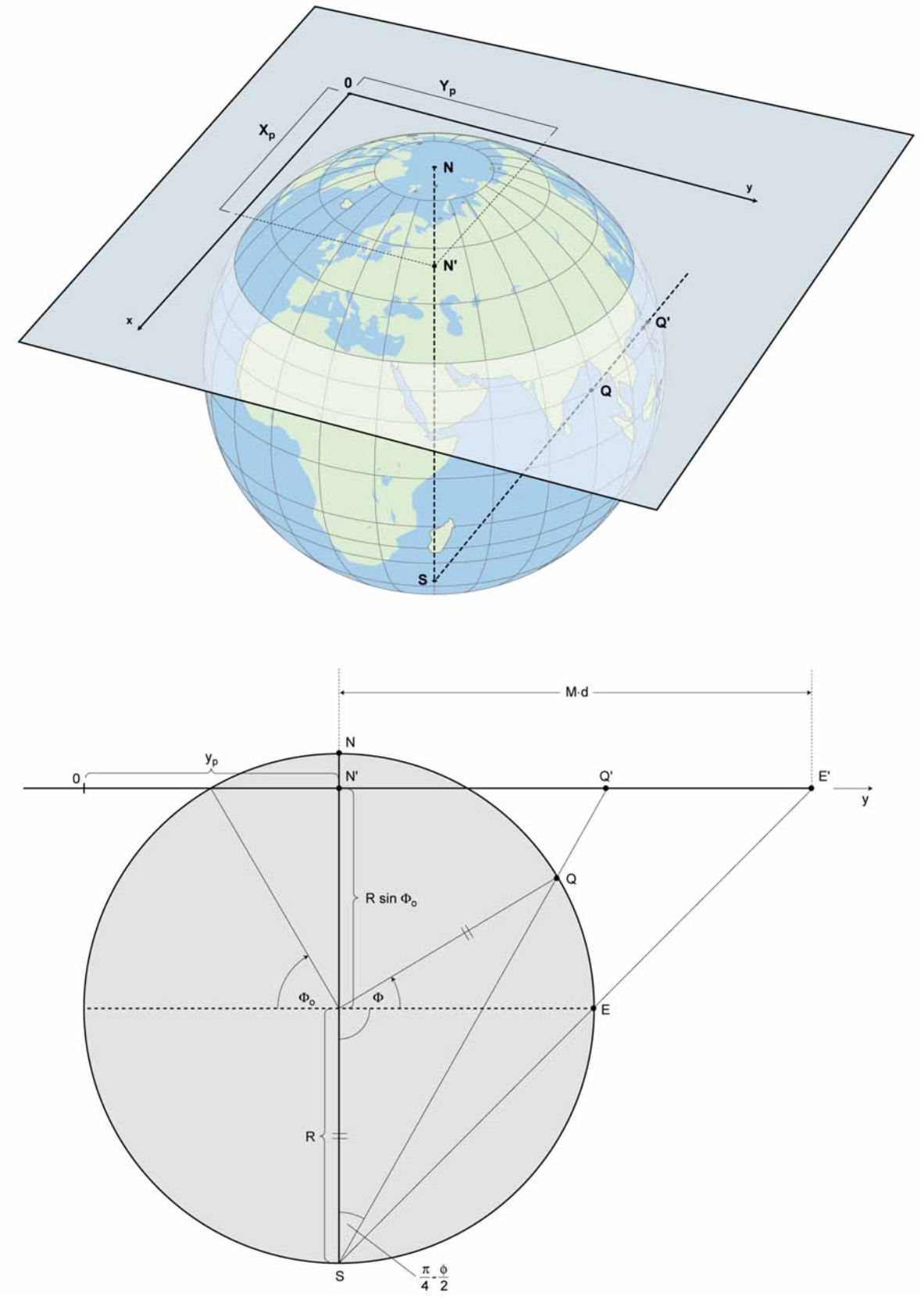

EMEP grid cells:

We define an EMEP **grid cell** (*i, j*) as a square in the *x*-*y* plane with side length *d* (see eq.D-3) and with its centre point as the integral part of *x* and *y*, i.e.

(D-6) $i = \mathrm{nint}(x) \quad \text{and} \quad j = \mathrm{nint}(y)$

where 'nint' is the nearest integer (rounding function). Consequently, the four corners of the grid cell have coordinates ($i \pm ½, j \pm ½$).

The EMEP projection uses the parameter values f_o = 60°N, λ_o = −32° (i.e. 32°W), and *R* = 6370 km for the radius of the Earth. A specific 'EMEP grid' is defined by the size *d* (in km) of the grid cell (which also determines the parameter *M* in eq.D-3); e.g. *d*=50 defines the 'EMEP50 grid', etc. An EMEP grid is uniquely defined by specifying the coordinates of the North Pole (x_p,y_p). For EMEP grids used in the past, at present, and in the (near) future the North Pole coordinates are listed in Table D.1.

Table D.1 EMEP coordinates (x_p,y_p) of the North Pole for different grid cell sizes *d* (in km).

d	150*	50	25	10	5**
x_p	3	8	15.5	38	75.5
y_p	37	110	219.5	548	1095.5

*Used in the past in the lagrangian EMEP model (Saltbones and Dovland 1986).
**Not (yet) used by EMEP, but used by the CCE for reporting critical loads.

Note that the ratio $(x_p - ½)/(y_p - ½)$ is constant for all EMEP grids listed in Table D-1, and equal to 5/73=0.068493. This shows that the lower-left corner of EMEP grid cell (1,1), i.e. the EMEP coordinates of the point (½,½), has the same latitude and longitude in all these EMEP grids, namely f = 40.43611°N and λ = 35.91825°W (somewhere in the Atlantic west of the Azores; computed by inserting *x*=½ and *y*=½ into eqs.D-4 and D-5). In contrast, the origin (0,0) does *not* have the same latitude and longitude in all grid systems (see Table D.2; '½' is of different size in the different grid systems!).

Table D.2 (Rounded) latitude f_{ori} and longitude λ_{ori} of the origin (0,0) of the different EMEP grid systems.

d (km)	150	50	25	10	5
ϕ_{ori} (°N)	39.80	40.22	40.33	40.39	40.41
λ_{ori} (°W)	36.64	36.16	36.04	35.97	35.94

An EMEP*d* grid cell (*i,j*) contains *k*´*k* EMEP(*d*/*k*) grid cells (*m,n*) with all combinations of the indices *m*=*k*·*i*−*k*+1, ..., *k*·*i* and *n*=*k*·*j*−*k* +1, ..., *k*·*j*. For example, the EMEP50 grid cell (2,7) contains 25 EMEP10 grid cells (*m,n*) with all combinations of indices *m*=6,7,8,9,10 and *n*=31,32,33,34,35.

In general, a point with coordinates (*x,y*) in the EMEPd_1 system has the coordinates (r·(x−½)+½, r·(y−½)+½) in the EMEPd_2 system, where $r = d_1/d_2$.

Figure D-2 illustrates the four EMEP grids listed in Table D-1 covering the Netherlands, mapped in the Dutch RD-coordinate system.

Figure D.2 EMEP10 and EMEP50 grids (left) as well as EMEP5 and EMEP25 grid (right) covering the Netherlands, mapped in the Dutch RD-coordinate system. The centre of the black dot marks the location of the CCE and has grid indices (57,45), (114,90), (285,223) and (569,446) in the EMEP50, -25, -10 and -5 grid , resp.

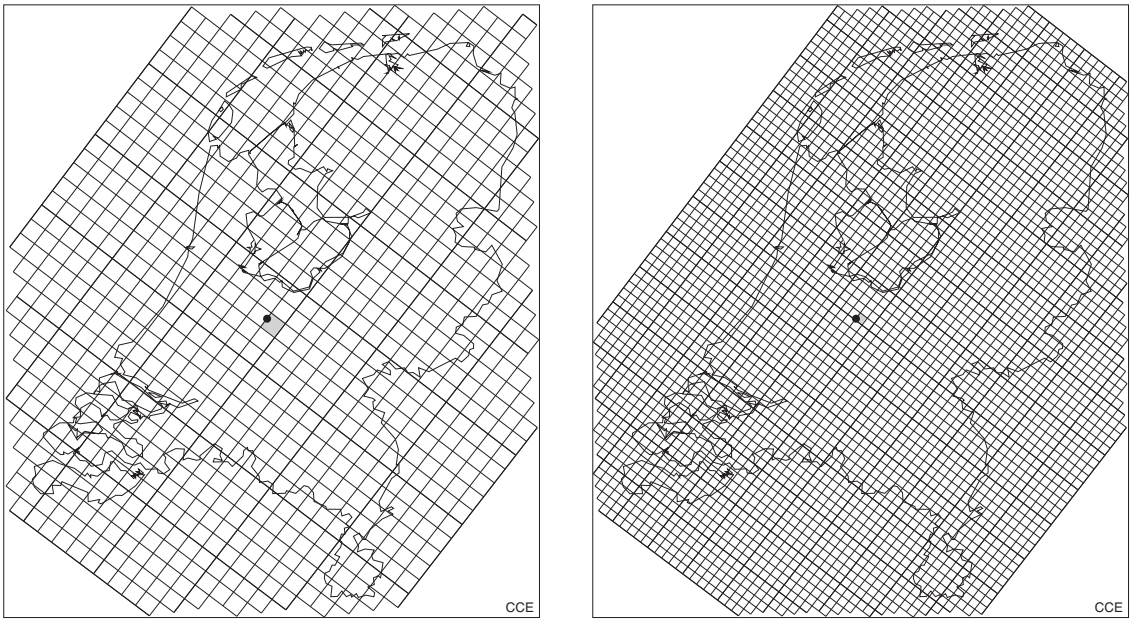

Area of an EMEP grid cell:

As mentioned above, the stereographic projection does not preserve areas, e.g. a 50×50 km² EMEP grid cell is 2500 km² only in the projection plane, but never on the globe. The area of an EMEP grid cell (axes-parallel rectangle) with lower-left corner (x_1, y_1) and upper-right corner (x_2, y_2) on the (spherical) globe is given by (for a derivation, see Appendix A in Posch et al. 1997):

$$(D\text{-}7)\quad A(x_1,y_1,x_2,y_2) = 2R^2\{I(u_2,v_2) - I(u_1,v_2) - I(u_2,v_1) + I(u_1,v_1)\}$$

where $u_1=(x_1-x_p)/M$, etc.; and $I(u,v)$ is the double integral:

$$(D\text{-}8)\quad I(u,v) = \iint \frac{2dudv}{(1+u^2+v^2)^2} = \frac{v}{\sqrt{1+v^2}}\arctan\frac{u}{\sqrt{1+v^2}} + \frac{u}{\sqrt{1+u^2}}\arctan\frac{v}{\sqrt{1+u^2}}$$

These two equations allow the calculation of the area of the EMEP grid cell (i, j) by setting (x_1, y_1) = (i–½, j–½) and (x_2, y_2) = (i+½, j+½).

The area distortion ratio α – i.e. the ratio between the area of a small rectangle in the EMEP grid and its corresponding area on the globe – is obtained by the following limit operation:

$$(D\text{-}9)\quad \alpha = \lim_{h,k\to 0}\frac{A(x,y,x+h,y+k)}{hkd^2} = \frac{R^2}{d^2M^2}\,\frac{4}{\left(1+(r/M)^2\right)^2}$$

where R, M, d and r are defined in eqs.D-1–D-5. Using eqs.D-3 and D-5, and the identities $1/(1+\tan^2 z) = \cos^2 z$ and $2\cos^2(\pi/4-z/2) = 1+\sin z$, one arrives at the following expression for the area distortion ratio:

$$(D\text{-}10)\quad \alpha = \left(\frac{1+\sin\phi}{1+\sin\phi_0}\right)^2$$

This shows that the distortion ratio depends on the latitude f only, and areas are (almost) undistorted, i.e. α =1, only at f=f_o=60° (co-incidentally the approximate latitude of Oslo; see Fig.D.3; see also Figure A.3 in Posch et al. 1999).

Figure D-3. Area-distortion ratio of the EMEP projection as a function of the latitude. An estimate of the size of a d×d grid cell at latitude f is obtained by multiplying d^2 by the distortion ratio for that f (the exact area is, of course, obtained by using eqs.D-7 and D-8).

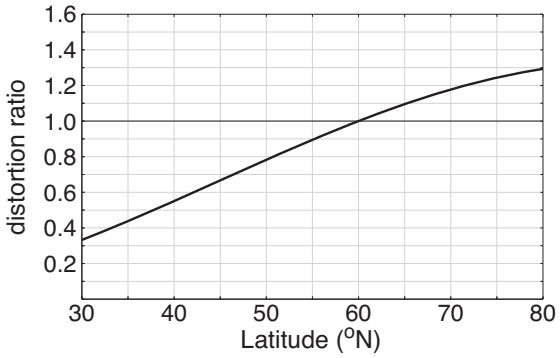

References

Posch M, Hettelingh J-P, De Smet PAM, Downing RJ (eds), 1997. Calculation and mapping of critical thresholds in Europe: Status Report 1997. RIVM Report 259101007, Coordination Centre for Effects, Bilthoven, Netherlands, iv+163 pp www.rivm.nl/cce

Posch M, De Smet PAM, Hettelingh J-P, Downing RJ (eds), 1999. Calculation and mapping of critical thresholds in Europe: Status Report 1999. RIVM Report 259101009, Coordination Centre for Effects, Bilthoven, Netherlands, iv+165 pp www.rivm.nl/cce

Saltbones J, Dovland H, 1986. Emissions of sulphur dioxide in Europe in 1980 and 1983. EMEP/CCC Report 1/86, Norwegian Institute for Air Research (NILU), Lillestrøm (now Kjeller), Norway

J. Slootweg | M. Posch | J-P. Hettelingh (eds)

Report 680359001/2011

What are the environmental effects of the current international protocols to abate eutrophication, acidification and heavy metals, and what improvements can be made with the revision of these protocols? These questions are addressed this CCE-report. The report also presents recent findings in modelling the relation between nitrogen and carbon in the soil and the diversity of plant species.

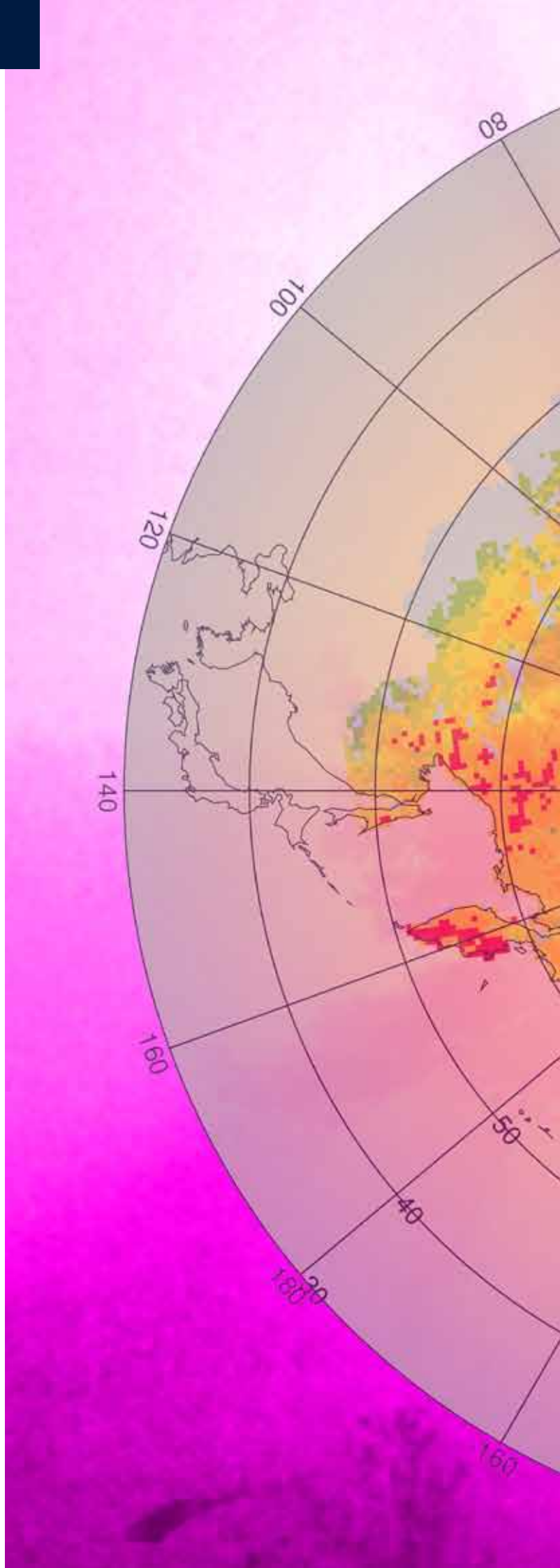

National Institute for Public Health
and the Environment
Ministry of Health, Welfare and Sport

This is a publication of:

**National Institute for Public Health
and the Environment**
P.O. Box 1 | 3720 BA Bilthoven
The Netherlands
www.rivm.nl

Februari 2011